Imperial College London

Mechanisms of T Cell Dysfunction During Human T Cell Leukemia Virus Type 1 Infection

Submitted in partial fulfillment of the requirements for the degree of
Doctor of Philosophy

Allison Katherine Maher

June 2024

Department of Infectious Disease
Imperial College London

Supervisors:
Dr. Margarita Dominguez-Villar
Professor Graham Taylor

Abstract

Human T cell leukemia virus type 1 (HTLV-1) is a retrovirus that infects 10-20 million people worldwide. While most infected people remain asymptomatic carriers (ACs), 2-5% of HTLV-1 carriers develop adult T-cell leukemia, and another 2-5% develop inflammatory diseases including HTLV-1-associated myelopathy (HAM). HAM is an inflammatory disease of the central nervous system (CNS) with no available curative treatments. Individuals with higher HTLV-1 proviral loads (PVLs) are at an increased risk for HAM development. While $CD4^+$ T cells predominate in early CNS lesions, suggesting their involvement in early HAM pathogenesis, and $CD8^+$ T cells predominate in chronic lesions, much remains to be uncovered about the mechanism of HAM pathogenesis and CNS damage. The overall aims of this work were to study mechanisms of T cell dysfunction during HTLV-1 infection to gain insights into T cell responses associated with effective viral control and the mechanisms by which T cells contribute to HAM pathogenesis.

Here, I show that HTLV-1-specific $CD4^+$ and $CD8^+$ T cells from patients with HAM have an enhanced capacity to migrate to the CNS and can induce proinflammatory astrocytes and microglia. Through in-depth phenotypic, functional, and/or transcriptional characterization of HTLV-1-specific $CD4^+$ and $CD8^+$ T cells, I show that HTLV-1-specific T helper (Th) 17 responses are associated with a low PVL, while an unfocused HTLV-1-specific Th1 response, in addition to a strong HTLV-1-specific T cytotoxic 17 response, are associated with HAM. Finally, I show that $CD4^+CD8^+$ double-positive T cells are more abundant in patients with HAM, highly HTLV-1-infected, proinflammatory, have an enhanced capacity to migrate to the CNS and induce inflammatory astrocytes. Taken together, this thesis provides a deeper understanding of the contribution of T cells to CNS inflammation and HAM pathogenesis.

Declaration of Originality

All the work presented in this thesis including data collection, experimental work, data analysis, and literature review, is my own. The data presented in the $CD4^+CD8^+$ double-positive T cell chapter has been published in JCI insight [1]. For this publication, I collected all the data, prepared all the figures, and wrote the manuscript. The text and figures in this chapter have been adapted from my publication for this thesis. Throughout this thesis, work that is not my own has been appropriately referenced.

Copyright Declaration

The copyright of this thesis rests with the author. Unless otherwise indicated, its contents are licensed under a Creative Commons Attribution-Non Commercial 4.0 International license (CC BY-NC). Under this license, you may copy and redistribute the material in any medium or format. You may also create and distribute modified versions of the work. This is on the condition that: you credit the author and do not use it, or any derivative works, for a commercial purpose. When reusing or sharing this work, ensure you make the license terms clear to others by naming the license and linking to the license text. Where a work has been adapted, you should indicate that the work has been changed and describe those changes. Please seek permission from the copyright holder for uses of this work that are not included in this license or permitted under UK Copyright Law.

Acknowledgments

First and foremost, I would like to express my deepest gratitude to my supervisor, Dr. Margarita Dominguez-Villar. Marga, you have made the last 3.5 years wonderful. I am so thankful for the opportunity to have learned from such an incredibly strong scientist and to be mentored by such a wonderful boss. I appreciate all the time you took to train me, both in and out of the lab, to teach me to think critically and scientifically and to help mold me into the scientist I am today. In addition to your exceptional scientific training and support, I am grateful for the genuine care and mentorship you extended to me on a personal level. I am incredibly grateful for the last 3.5 wonderful years - thank you!

I would like to thank my co-supervisor, Prof. Graham Taylor, for his support and insight throughout this project. Graham, your clinical perspective and HTLV-1 expertise were highly appreciated, and thank you for allowing me to engage so much with the HTLV-1 clinic. Working with the HTLV-1 clinic staff and getting to meet the people living with HTLV-1 who were donating blood to research has been an incredibly enriching experience. I am extremely grateful to the HTLV-1 clinic staff who have made this research possible, in particular, Jana Haddow and Hollie Mortimer. Thank you, Dominic Smith, for being the best lab manager, and Parisa Amjadi for all your help with Cat3 sorting.

I would also like to thank fellow members of the group who have come and gone over the years, especially Dr. Claudia Selck, Dr. Nicolas Giang, Emma Jones, and Rachel Coulombeau for their incredible support. I would like to thank Dr. Danai Koftori and Dr. Aris Aristodemou for being the most brilliant, kind, and supportive friends both inside and outside the lab. You helped make my time at St. Mary's so special.

I would like to thank my family for their unwavering support, encouragement, and love. Mama and Papa, thank you for always supporting me in all my endeavors, and for making me feel like I can take on any challenge. Thank you to my grandparents, Lena and Erik, and Tante Hilde and Franz for having supported me throughout my education and beyond. Alex and Thomas, thank you for being the most wonderful siblings anyone could have asked for.

Finally, I would like to thank my partner (and fiancé), Gilles. You've seen the whole range of emotions through these last 3.5 years. Thank you for letting me talk at you excitedly for hours on end about HTLV-1-specific T cells and for looking at every single one of my chaotically plotted graphs. I'm sorry that I don't understand half as much about your PhD as you do mine. Thank you for your patience and love when I was deep down the science rabbit hole. Thank you for picking me up when I was tired and supporting me when I was stressed. Thank you for the joy you took in sharing the many highs of my PhD journey. I am so grateful that we were able to share this unique experience.

Contents

List of Figures **10**

List of Tables **12**

1 Introduction **13**
1.1 The immune system . . . 13
1.1.1 Innate immune pathogen detection . . . 14
1.1.2 The adaptive immune system . . . 15
1.2 Immune cells . . . 15
1.2.1 Innate immune cells . . . 16
1.2.2 Adaptive immune cells . . . 16
1.3 T cells . . . 17
1.3.1 Development . . . 17
1.3.2 Antigen presentation to T cells . . . 19
1.3.3 T cell activation . . . 20
1.3.4 T cell memory . . . 21
1.3.5 $CD4^+$ T cells . . . 22
1.3.6 $CD8^+$ T cells . . . 27
1.3.7 Double Positive (DP) T cells . . . 27
1.4 Immune tolerance and autoimmunity . . . 30
1.5 Human T Cell Leukemia Virus Type 1 . . . 32
1.5.1 HTLV-1 infection and propagation . . . 32
1.5.2 HTLV-1 proteins . . . 34
1.5.3 HTLV-1-associated diseases other than HAM . . . 35
1.6 HTLV-1-Associated Myelopathy . . . 36
1.6.1 HAM risk factors . . . 37
1.6.2 Mechanisms of pathogenesis . . . 39
1.7 Immune responses to HTLV-1 . . . 41
1.7.1 Innate immune response . . . 41
1.7.2 Adaptive immune response . . . 42
1.8 Antigen-specific T cells . . . 45
1.8.1 Identifying antigen-specific T cells . . . 45
1.9 Hypothesis and Aims of the PhD . . . 47

2 Materials and Methods **49**
2.1 Participants, study design, and clinical data collection . . . 49
2.2 Cell isolation, storage, and thawing . . . 50
2.3 Generation of virus stocks . . . 51

2.4 *Ex vivo* stimulation assays . . . 51
2.5 Cell staining for flow cytometry . . . 52
2.6 Flow cytometry data analysis, dimensionality reduction, and clustering . . 55
2.6.1 Chapter 4: $CD8^+$ T cells in HTLV-1- Infection . . . 55
2.6.2 Chapter 5: $CD4^+CD8^+$ T cells in HTLV-1- Infection . . . 55
2.7 Glial-T cell co-cultures . . . 56
2.7.1 Astrocyte and microglia cell line cultures . . . 56
2.7.2 Sorting HTLV-1-specific and non-specific T cells . . . 56
2.7.3 Expansion of primary T cell lines . . . 57
2.7.4 Glial cell-T cell co-cultures . . . 57
2.7.5 Glial cell staining for flow . . . 58
2.8 HTLV-1 infection of sorted T cell populations . . . 58
2.8.1 Sorting $CD4^+$, $CD8^+$, DP, and DN T cells for HTLV-1-infection . . 58
2.8.2 HTLV-1-infection of primary T cells . . . 59
2.9 Astrocyte-DP T cell co-culture . . . 60
2.10 RNA-Seq analysis . . . 60
2.10.1 Stimulation, magnetic enrichment, and staining of HTLV-1-specific $CD4^+$ T cells . . . 60
2.10.2 Sorting HTLV-1-specific $CD4^+$ T cells . . . 61
2.10.3 RNA isolation and quantification . . . 61
2.10.4 RNA sequencing . . . 61
2.10.5 Processing RNA data . . . 62
2.10.6 Differential gene expression analysis . . . 62
2.11 Quantification of mRNA expression by real-time PCR . . . 63
2.12 Determining PVL by digital droplet PCR . . . 63
2.12.1 Sorting of fixed cells for digital droplet PCR (ddPCR) . . . 63
2.12.2 DNA isolation . . . 65
2.12.3 PVL quantification by ddPCR . . . 65
2.13 Statistics and data presentation . . . 67
2.14 Diagrams . . . 67

3 $CD4^+$ T cells in HTLV-1 infection 68
3.1 Introduction . . . 68
3.2 Results . . . 70
3.2.1 Identification and initial characterization of HTLV-1-specific $CD4^+$ T cells . . . 70
3.2.2 HTLV-1-specific $CD4^+$ T cells from patients with HAM induce proinflammatory astrocytes . . . 74
3.2.3 HTLV-1-specific $CD4^+$ T cells from all HTLV-1-infected groups activate microglia . . . 78
3.2.4 Non-HTLV-1-specific $CD4^+$ T cells from patients with HAM induce moderate astrocytes and microglia activation . . . 82
3.2.5 Sorting and RNA sequencing of HTLV-1-specific $CD4^+$ T cells from different HTLV-1-infected groups . . . 86
3.2.6 Transcriptional analysis of HTLV-1-specific $CD4^+$ T cells in HTLV-1-infected groups relative to UCs . . . 88

3.2.7 Transcriptional analysis of HTLV-1-specific CD4$^+$ T cells in HTLV-1-infected groups . . . 92
3.2.8 HTLV-1-specific CD4$^+$ T cells in patients with HAM have an unfocused Th1 response . . . 98
3.2.9 Pathway enrichment analysis of HTLV-1-specific CD4$^+$ T cells in different HTLV-1-infected groups . . . 101
3.2.10 Characterization of bulk CD4$^+$ T cells . . . 105
3.3 Discussion . . . 109
3.4 Appendix . . . 118
3.4.1 Pathway enrichment in HTLV-1 infected groups relative to UC . . . 118
3.4.2 Pathway enrichment in HTLV-1 infected groups . . . 122

4 CD8$^+$ T cells in HTLV-1 infection 125
4.1 Introduction . . . 125
4.2 Results . . . 127
4.2.1 Identification and characterization of HTLV-1-specific CD8$^+$ T cells 127
4.2.2 Phenotypic characterization of HTLV-1-specific CD8$^+$ T cells . . . 130
4.2.3 HTLV-1-specific CD8$^+$ T cells from patients with HAM induce inflammatory astrocytes . . . 132
4.2.4 HTLV-1-specific CD8$^+$ T cells from all HTLV-1-infected groups activate microglia . . . 137
4.2.5 Non-HTLV-1-specific CD8$^+$ T cells from patients with HAM induce astrocyte and microglia activation . . . 140
4.2.6 Characterization of bulk CD8$^+$ T cells . . . 142
4.3 Discussion . . . 145

5 CD4$^+$CD8$^+$ T cells in HTLV-1 infection 148
5.1 Introduction . . . 148
5.2 Results . . . 150
5.2.1 Patients with HAM have an increased frequency of DP T cells . . . 150
5.2.2 DP T cells are a distinct T cell population in ACs . . . 153
5.2.3 Contribution of DP T cells to anti-HTLV-1 immune response . . . 158
5.2.4 HTLV-1-specific DP T cells are phenotypically distinct in ACs and patients with HAM . . . 160
5.2.5 DP T cells induce proinflammatory astrocytes . . . 164
5.2.6 HTLV-1 infection of SP T cells gives rise to a DP T cells population 165
5.2.7 Involvement of ThPOK and RunX3 in DP T cell generation and stability . . . 169
5.3 Discussion . . . 172

6 Discussion and Conclusion 176

7 Final Words and Future Directions 182

8 List of Acronyms 185

Bibliography 191

Publications

1. Maher, A.K., Aristodemou A., Giang N., Tanaka, Y., Taylor G.P., Bangham R.M C., Dominguez-Villar M. HTLV-1 induces an inflammatory $CD4^+$ $CD8^+$ T cell population in HTLV-1-Associated Myelopathy. *JCI Insight*. 2024;9(1):e173738. https://doi.org/10.1172/jci.insight.173738.

2. Kalemera, D.M., Maher, A.K., Dominguez-Villar M., Maertens, G.N. Cell culture evaluation hints widely available HIV drugs are primed for success if repurposed for HTLV-1 prevention. (Paper re-submitted after reviews)

3. Maher, A.K., Burnham, K.L., Tanaka, Y., Taylor G.P., Dominguez-Villar M. HTLV-1-specific $CD4^+$ T cell contribute to neuroinflammation in HTLV-1-Associated Myelopathy (manuscript in preparation)

Other publications:

During the COVID-19 pandemic, I contributed to research on the dysfunction of monocytes during COVID-19, and we published our findings in *Nature Communications*.

4. Maher, A.K., Burnham, K.L., Jones, E.M. Tan M.M.H., Saputil R.C., Baillon L., Selck C., Giang N., Arguello R., Pillay C., Thorley E., Short C.E., Quinlan R., Barclay W.S., Cooper N., Taylor G.P., Davenport E.E., Dominguez-Villar M. Transcriptional reprogramming from innate immune functions to a pro-thrombotic signature by monocytes in COVID-19. *Nature Communications* **13**, 7947 (2022). https://doi.org/10.1038/s41467-022-35638-y

List of Figures

1.1 Timeline of innate and adaptive immune responses after an infection 14
1.2 Immune cell lineages 15
1.3 T cell development in the thymus 18
1.4 T cell activation 20
1.5 $CD4^+$ T cell differentiation 22
1.6 The establishment of the HTLV-1 PVL 33
1.7 HTLV-1 genome 34
1.8 Hypothesized mechanism of HAM pathogenesis 39

2.1 Gating strategy for sorting HTLV-1-specific and non-specific T cells 57
2.2 Gating strategy for identifying glial cells 58
2.3 Gating strategy for sorting $CD4^+$ SP, $CD8^+$ SP, DP, and DN T cells from total PBMCs. 59
2.4 Gating strategy for sorting HTLV-1-specific $CD4^+$ T cells 61

3.1 Gating strategy to identify $CD4^+$ T cells. 71
3.2 HTLV-1-specific $CD4^+$ T cell *ex vivo* identification and characterization . . 72
3.3 The effect of HTLV-1-specific $CD4^+$ T cells on the viability and iNOS expression of astrocytes 74
3.4 Representative flow staining of astrocytes 76
3.5 The effect of HTLV-1-specific $CD4^+$ T cells on astrocyte activation 77
3.6 The effect of HTLV-1-specific $CD4^+$ T cells on microglia viability and iNOS expression 78
3.7 Representative flow staining of microglia 80
3.8 The effect of HTLV-1-specific $CD4^+$ T cells on microglia activation 81
3.9 The effect of non-HTLV-1-specific $CD4^+$ T cells on astrocytes 82
3.10 The effect of non-HTLV-1-specific $CD4^+$ T cell co-culture on microglia . . 84
3.11 Gating strategy and sorting of HTLV-1-specific $CD4^+$ T cells for RNA-seq analysis 86
3.12 RNA sequencing of HTLV-1-specific $CD4^+$ T cells 87
3.13 Transcriptional analysis of HTLV-1-specific $CD4^+$ T cells from AC lPVL, AC hPVL, and patients with HAM relative to UCs 89
3.14 Venn diagram of differentially expressed genes and principal component analysis of HTLV-1-specific $CD4^+$ T cells 93
3.15 Transcriptional analysis of HTLV-1-specific $CD4^+$ T cells in HTLV-1- infected groups 96
3.16 T helper phenotype of HTLV-1-specific $CD4^+$ T cells in AC lPVL, AC hPVL, and patients with HAM 99

3.17 Pathway enrichment analysis in HTLV-1-specific CD4$^+$ T cells in different HTLV-1-infected groups . . . 102
3.18 Characterization of bulk CD4$^+$ T cells in UCs, ACs, and patients with HAM. 106
3.19 Characterization of surface markers on bulk CD4$^+$ T cells in UCs, ACs, and patients with HAM . . . 107

4.1 Gating strategy for the identification of CD8$^+$ T cells. . . . 127
4.2 *Ex vivo* HTLV-1-specific CD8$^+$ T cell identification and characterization . 128
4.3 Characterization of HTLV-1-specific CD8$^+$ T cells . . . 131
4.4 The effect of HTLV-1-specific CD8$^+$ T cells on astrocytes viability, and CXCL10 and iNOS expression . . . 133
4.5 Representative flow staining of astrocytes . . . 135
4.6 The effect of HTLV-1-specific CD8$^+$ T cells on astrocytes . . . 136
4.7 The effect of HTLV-1-specific CD8$^+$ T cells on the microglia viability, and iNOS and CXCL10 expression . . . 137
4.8 Representative flow staining of microglia . . . 138
4.9 The effect of HTLV-1-specific CD8$^+$ T cells on microglia . . . 139
4.10 The effect of non-HTLV-1-specific CD8$^+$ T cells on astrocytes . . . 140
4.11 The effect of non-HTLV-1-specific CD8$^+$ T cells on microglia . . . 141
4.12 Characterization of bulk CD8$^+$ T cells in UCs, ACs, and patients with HAM. 143

5.1 Frequency and HTLV-1 infection of DP T cells. . . . 151
5.2 DP T cells *ex vivo* phenotyping flow staining . . . 154
5.3 Characterization of DP T cells in HTLV-1 ACs . . . 155
5.4 Characterization of DP T cells antigen experience and cytokine expression in HTLV-1 ACs . . . 156
5.5 DP Cytokine phenotyping in AC hPVL . . . 157
5.6 Contribution of DP T cells to HTLV-1-specific immunity . . . 159
5.7 Phenotype of DP T cells in UCs, ACs, and patients with HAM . . . 161
5.8 Astrocyte co-cultured with HTLV-1-stimulated DP cells . . . 164
5.9 Origin of DP T cells in HTLV-1 infection . . . 167
5.10 Mechanism of CD4 and CD8 co-expression . . . 170
5.11 Hypothesized contribution of DP T cells neuroinflammation in HAM . . . 172

6.1 Summary of new insights into the hypothesized mechanism of HAM pathogenesis . . . 180

List of Tables

2.1 Participant Characteristics 50
2.2 Cell Surface Antibodies 53
2.3 Intracellular Antibodies 54
2.4 RT-PCR Probes 64

3.1 Enriched pathways from upregulated genes in all HTLV-1-infected groups relative to UCs 118
3.2 Enriched pathways from downregulated genes in all HTLV-1-infected groups relative to UCs 118
3.3 Upregulated pathways in AC lPVL relative to UC 118
3.4 Upregulated pathways in AC hPVL relative to UC 119
3.5 Upregulated pathways in HAM pelative to UC 120
3.6 Downregulated pathways in AC lPVL Relative to UC 121
3.7 Downregulated pathways in AC hPVL relative to UC 121
3.8 Upregulated pathways in HAM relative to AC hPVL 122
3.9 Upregulated pathways in AC hPVL relative to AC lPVL 122
3.10 Upregulated pathways in HAM relative to AC lPVL 123
3.11 Downregulated pathways in HAM relative to AC hPVL 124
3.12 Downregulated pathways in HAM relative to AC lPVL 124

1

Introduction

1.1 The immune system

Nearly all organisms have some kind of an immune system to protect themselves against pathogens. Humans have evolved a complex immune system composed of barriers, chemicals, proteins, and cells to fend off pathogens such as bacteria, fungi, parasites, viruses, and toxins. This vast network of cells and tissues is constantly surveying the body for invaders, in addition to being strongly involved in cancer surveillance. The immune system is composed of two main branches: the innate immune system and the adaptive immune system [2]. The innate immune system is the body's first line of defense against pathogens and can be further broken down into two levels. The first level includes physical barriers such as the skin, mucosal barriers, the blood-brain barrier (BBB), and chemical barriers including pH and enzymes, while the second level is made up of innate immune cells. When triggered, the innate immune system provides a rapid non-specific response within hours of infection [3]. Following this, the innate immune system activates the adaptive immune system which launches a response within a few days of infection (Figure 1.1) [4].

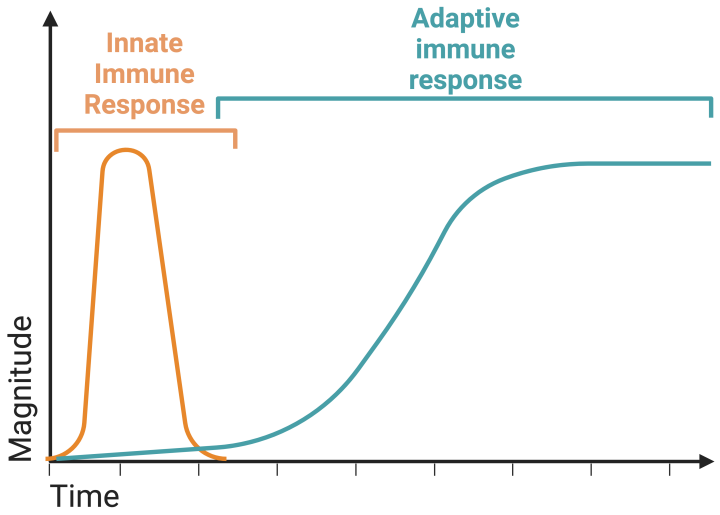


Figure 1.1: Timeline of innate and adaptive immune responses after an infection. After infection by a pathogen, the innate immune system mounts a rapid non-specific response within hours of infection. The innate immune system then activates the adaptive immune system which can mount an antigen-specific response within a few days of infection. Figure created using BioRender.

1.1.1 Innate immune pathogen detection

Invading pathogens are first detected by the innate immune system. Pathogen-associated molecular patterns (PAMPs) are recognized by pattern recognition receptors (PRRs) [5]. These PRRs are expressed in both immune and non-immune cells and recognize the nucleic acids, carbohydrates, proteins, and lipids of invading pathogens [5, 6]. PRRs must distinguish host molecules from PAMPs by binding exclusively to molecules associated with pathogens. Examples of PAMPs include cytoplasmic deoxyribonucleic acid (DNA), since host DNA is confined to the nucleus, and cytoplasmic 5-triphosphate ribonucleic acid (RNA), as host messenger ribonucleic acid (mRNA) is capped at the 5' end before nuclear export [7]. This ability to differentiate host molecules from PAMPs is crucial to prevent inappropriate inflammation and to preserve self-tolerance [5]. Once PAMPs are detected, signaling pathways result in the production of type I and III interferons (IFNs-I/III) and other early pro-inflammatory cytokines including tumour necrosis factor (TNF), interleukin (IL)-1, and IL-6 [5]. IFN-I/III activate the transcription, in both an autocrine and paracrine manner, of a wide range of pro-inflammatory genes termed interferon-stimulated genes (ISGs) which act to limit the spread of the infection by a variety of mechanisms including the upregulation of nucleases to digest foreign nucleic acids, limiting translation of viral proteins, shifting cell metabolism, signaling to other

cells to activate their innate immune defenses, and the activation and recruitment of both innate and adaptive immune cells [8]. TNF, IL-1, and IL-6 also drive inflammation which activates and recruits innate and adaptive immune cells to the sites of infection and inflammation [9, 10, 11].

1.1.2 The adaptive immune system

The innate immune system triggers an adaptive immune response, which comprises two main branches: cellular immunity, mediated by T lymphocytes, and humoral immunity, mediated by B lymphocytes [3, 12, 13]. The adaptive immune system mounts an antigen-specific immune response and develops immunological memory that serves to protect the host more efficiently and effectively when re-infected with the same or a similar pathogen in the future [3, 12, 13]. I will discuss the types of adaptive immune cells and adaptive immune activation and function in later sections.

1.2 Immune cells

Immune cells can be broadly divided into 2 lineages: the lymphoid lineage and the myeloid lineage (Figure 1.2). Generally, the myeloid lineage and natural killer (NK) cells are considered innate immune cells while the lymphoid lineage, except NK cells, are adaptive immune cells [3].

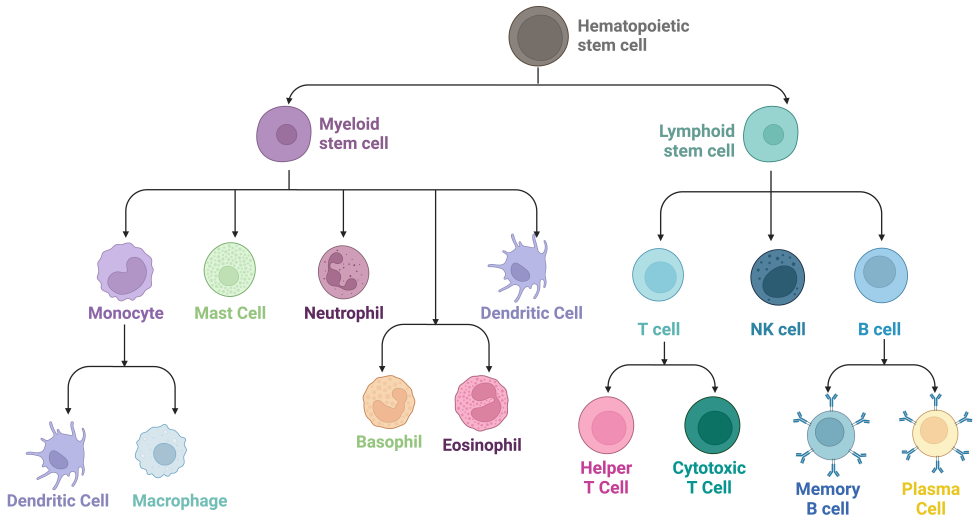


Figure 1.2: Immune cell lineages. Figure created using BioRender.

1.2.1 Innate immune cells

An important function of the innate immune system is the early detection of pathogens and rapid recruitment of immune cells to sites of infection and inflammation through the production of chemokines and cytokines [8]. Key early cytokines released by innate immune cells include IFNs-I/III, TNF, IL-1, and IL-6 [9, 10]. Professional phagocytes such as neutrophils, monocytes, macrophages, and dendritic cells engulf pathogens, dead cells, or other debris [2]. NK cells are innate cytotoxic lymphocytes that recognize and kill stressed cells in the absence of antibodies or major histocompatibility complex (MHC) molecules [14, 15]. Other innate immune cells including eosinophils, basophils, and mast cells in addition to non-immune cells such as epithelial cells and fibroblasts, express PRRs and are essential for early pathogen detection [6, 16]. While the innate immune system does not form immunological memory in the same way as the adaptive immune system, it can form trained immunity, which occurs when recent activation of the innate immune system results in enhanced responsiveness to subsequent infection with either the same pathogen (homologous re-challenge) or exposure to different pathogens (heterologous re-challenge) driven by metabolic and epigenetic re-programming [17].

1.2.2 Adaptive immune cells

Unlike the innate immune response, the adaptive immune response is antigen-specific, and results in the formation of antigen-specific immunological memory [18, 19]. There are two main branches of adaptive immune responses: an antibody-mediated response and a cell-mediated response carried out by B and T lymphocytes respectively. Each naïve B and T cell carry a unique B cell receptor (BCR) or T cell receptor (TCR) [20]. BCRs and TCRs are specialized protein complexes found on the surface of B cells and T cells, respectively, playing pivotal roles in antigen recognition and adaptive immune response initiation [21, 22]. TCRs are composed of alpha and beta chains, forming a heterodimeric complex, while BCRs are composed of two protein chains referred to as heavy and light chains [19, 23]. The huge diversity of BCR and TCR receptors enables the adaptive immune system to respond to virtually any pathogen [21, 22]. Lymphocytes that recognize a pathogen become activated, proliferate, and eventually produce memory cells that will recognize the pathogen if it is re-encountered [18, 19].

1.3 T cells

While T cells populate virtually every organ and tissue, the majority of T cells are found within lymphoid tissues such as bone marrow, spleen, tonsils, and an estimated 500–700 lymph nodes, while 2%–3% of T cells are found in peripheral blood [24, 25, 26, 27]. T cells constantly circulate between peripheral blood and secondary lymphoid organs, spending approximately 6-12 hours (h) surveying a lymph node for their cognate antigen before re-entering circulation [28, 29]. Conventional T cells, also known as $\alpha\beta$ T cells, comprise different cell populations including naïve, effector, memory, and regulatory T cells (Tregs) [24]. Naïve T cells can respond to new antigens and once activated they become effector cells that execute immune functions including cytokine secretion, immune regulation, and cytotoxicity [18]. Memory T cells derive from previously antigen-activated T cells and maintain long-term immunity [30]. Tregs suppress excessive immune responses to self-antigens and foreign antigens, thereby preventing autoimmune diseases, maintaining immune tolerance, and promoting immune homeostasis through various mechanisms such as cytokine secretion, direct cell-cell contact, and inhibition of effector T cell function [31]. Conventional T cells are made up of helper $CD4^+$, cluster of differentiation (CD), T cells and cytotoxic $CD8^+$ T cells, which can be broken down into further subsets which will be discussed later [3].

1.3.1 Development

All T cells originate from hematopoietic stem cells (HSC) in the bone marrow before differentiating into lymphoid progenitors that migrate from the bone marrow through the blood to the thymus. Once in the thymus, they are referred to as thymocytes, and undergo maturation, selection, and export to the periphery (Figure 1.3) [21]. Most models of T cell development in the thymus are based on mouse models which have shown thymocytes pass through 3 main developmental stages: the double negative, $CD4^-CD8^-$ (DN), double positive, $CD4^+CD8^+$ (DP), and the single positive, $CD4^+CD8^-$ or $CD4^-CD8^+$ (SP) stages [24, 32]. Thymocytes in the DN phase develop a functional TCR which consists of highly variable alpha and beta chains designed to produce a huge diversity of different TCRs [33, 34, 35]. DN thymocytes re-arrange their TCRβ chain by variability, diversity, and joining

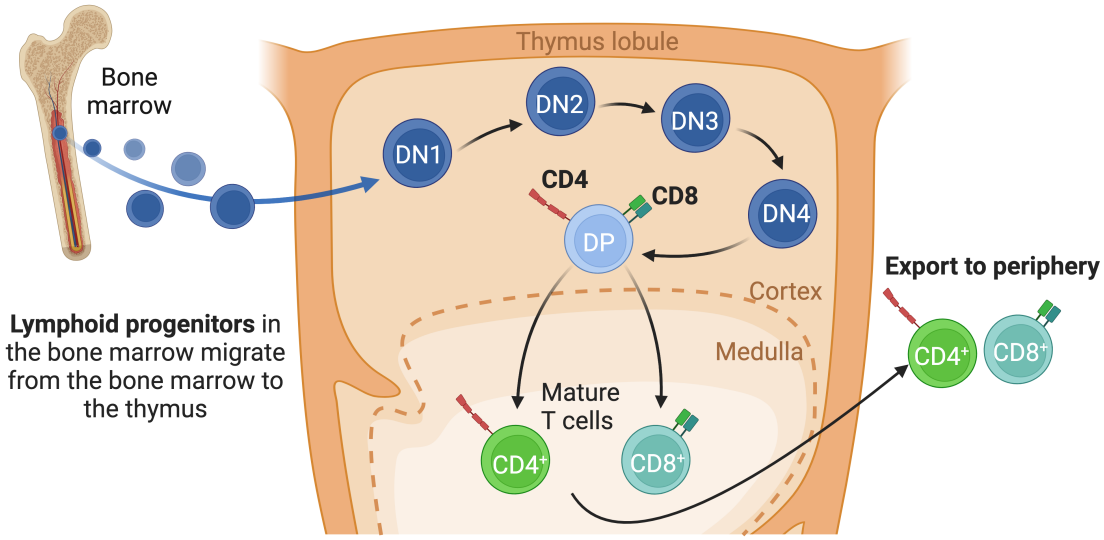


Figure 1.3: T cell development in the thymus. Lymphoid progenitors from the bone marrow migrate to the thymus where they go through several double negative (DN) phases, and a double positive (DP) phase and undergo negative selection and positive selection, respectively, and exit the thymus as mature naïve T cells [21]. Figure created using BioRender.

(VDJ) recombination; a process by which T cells, and B cells, randomly assemble different gene segments, known as variable (V), diversity (D), and joining (J) genes, to generate millions of unique antigen receptors from a small number of genes [21, 36]. Once the TCRβ chain has been produced, the thymocytes enter the DP stage. During the DP stage, the TCRα chain is rearranged by V-J recombination [21, 36]. Once DP thymocytes have acquired a unique functional TCR, they undergo positive selection [37]. Here thymocytes are presented with self-antigens expressed on MHC molecules by thymic epithelial cells, and only thymocytes that interact strongly with either major histocompatibility complex class I (MHC-I) or major histocompatibility complex class II (MHC-II) receive a survival signal, while over 90% of the remaining thymocytes die from neglect [38, 39, 40, 41]. DP thymocytes that interact strongly with MHC-II downregulate CD8 and DP thymocytes that interact strongly with MHC-I downregulate CD4 to become either $CD4^+$ or $CD8^+$ SP T cells, respectively [42, 43, 44, 45]. The final stage of thymocyte maturation is negative selection where the majority of SP cells with strongly auto-reactive TCRs receive an apoptotic signal [46]. However, a minority of auto-reactive SP cells are selected to become thymic Tregs, also known as natural Tregs (nTregs), whose function is to downregulate and inhibit immune responses to auto-antigens [47]. The surviving thymocytes exit the thymus as mature naïve T cells.

1.3.2 Antigen presentation to T cells

Antigen is presented on the surface of cells by MHC molecules and this process is essential for T cell activation. As previously mentioned, there are two classes of MHC molecules: MHC-I and MHC-II [3]. All nucleated cells express MHC-I, and expression of MHC-I is upregulated upon the detection of PAMPs during infection, although some viruses have developed sophisticated immune evasion strategies to prevent MHC-I upregulation [48]. Proteins from within the cell are degraded and peptides of 8-11 amino acids are bound by MHC-I and presented on the surface of the cell [23, 49, 50, 51]. The TCRs of $CD8^+$ T cells interact with the MHC-I molecules, stabilized by the CD8 co-receptor, and scan the presented peptide [52]. Once the TCR detects its cognate antigen, the activated $CD8^+$ T cell can induce apoptosis of the cell displaying antigen [53, 54]. This will be discussed further in later sections.

Antigen presentation to $CD4^+$ T cells is done by professional antigen presenting cells (APCs) including B cells, monocytes, macrophages, and dendritic cells which express MHC-II in addition to MHC-I [55]. Phagocytic monocytes, macrophages, and dendritic cells engulf extracellular pathogens, viruses, and dead cells, while B cells endocytose smaller soluble extracellular material. APCs digest exogenously derived proteins and present peptides of 13-25 residues on MHC-II molecules on their cell surface [55, 56, 57]. MHC-II molecules are scanned by the TCRs of $CD4^+$ T cells, and recognition of an antigen by the TCR of a $CD4^+$ T cell provides the first signal for $CD4^+$ T cell activation [58, 59, 60].

1.3.3 T cell activation

Naïve T cells circulate between peripheral blood and secondary lymphoid organs looking for their cognate antigen [61]. However, before T cells can carry out effector functions, they need to be activated by two activation signals (Figure 1.4) [59]. The first activation signal is provided when a TCR binds its cognate antigen presented by an APC on MHC-II or I molecules for $CD4^+$ and $CD8^+$ T cells respectively (Figure 1.4) [23]. Both naïve $CD4^+$ and $CD8^+$ T cells have to be activated by APCs, and naïve $CD8^+$ T cells cannot directly eliminate malignantly transformed or infected cells before being activated by an APC [62, 63, 64]. Unlike other nucleated cells, APCs can cross-present exogenously derived peptides on MHC-I allowing the APCs to activate $CD8^+$ T cells without necessarily being infected themselves [65, 66, 67].

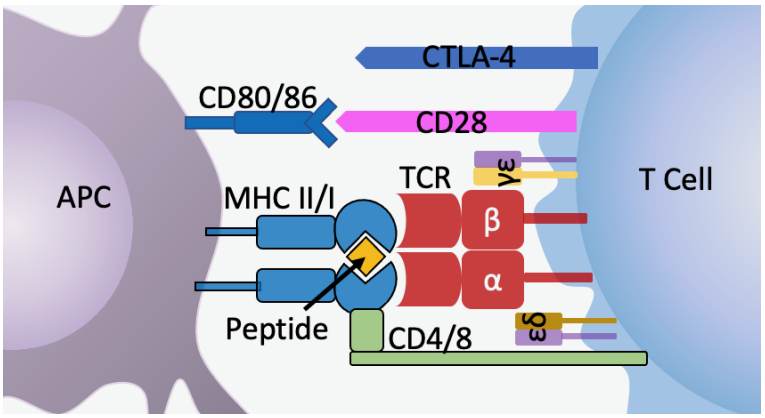


Figure 1.4: T cell activation. The TCR is flanked by the co-receptor CD3 (γ, δ, and ϵ chains). TCRs recognize their cognate antigen presented on MHC-I for $CD8^+$ T cells and MHC-II for $CD4^+$ T cells. T cells require a second signal for activation which is provided by the binding of CD28 to CD80/86 [23, 58, 59, 68, 69, 70].

For $CD4^+$ T cells, the second activation signal is provided by the binding of CD28 on the surface of the $CD4^+$ T cell to CD80 or CD86 on the surface of the APC (Figure 1.4) [68]. $CD8^+$ T cells can also be activated by CD28-CD80/86 interactions, but this second signal can be replaced with other co-stimulatory signals such as the cytokines secreted by activated $CD4^+$ T cells [71, 72, 73]. Other important co-stimulatory molecules include inducible T-cell COStimulator (ICOS), CD137, OX40, CD27, and members of the TNF receptor (TNFR) family [72, 73, 74]. These molecules are found on the T cell surface, but unlike CD28, they are not constitutively expressed [72, 75, 76]. These receptors can be stimulated by their ligands which are only expressed on the surface of APCs following

pathogen recognition. Depending on the PRR that detected the pathogen in the APC, the APCs will be polarized in their response and thereby polarize the T cell response [77]. Furthermore, the cytokine milieu created by both innate and adaptive immune cells will further polarize the T cell response into the desired T helper (Th) or T cytotoxic (Tc) phenotypes and is often described as the third activation signal [78]. T cell polarization allows for a specific T cell response tailored to the type of antigen. Once activated, T cells produce high levels of IL-2 which drives T cell proliferation and differentiation into different effector and memory phenotypes which will be discussed in later sections [79].

1.3.4 T cell memory

Once $CD4^+$ and $CD8^+$ T cells are activated, they differentiate into effector T cells which are believed to be the precursors of antigen-specific long-lived memory T cells which coordinate the T cell response during pathogen re-exposure [80]. The lineage relationships of memory T cells remain unresolved and most of our current understanding comes from mouse models. However, these models do not capture the changes in T cell populations that occur over decades of human life [81]. In humans, the markers C-C chemokine recptor (CCR) 7 and CD45RA are often used classify T cell populations into central memory (CM, $CCR7^+CD45RA^-$), naïve ($CCR7^+CD45RA^+$), terminally differentiated effector (TDE, $CCR7^-CD45RA^+$), and effector memory (EM, $CCR7^-CD45RA^-$) cells [18, 82, 83]. Additionally, there are other memory sub-populations including tissue resident memory (TRM) which reside within tissues, and stem cell-like memory (TSCM) which are a long-lived population that can rapidly differentiate into effector cells [84, 85]. In humans, the dynamics and lineages of memory T cell fate determination remain poorly defined.

1.3.5 CD4$^+$ T cells

CD4$^+$ T cells are the largest lymphocyte population and are essential for effective humoral and cellular immune responses [59]. CD4$^+$ T cells polarize and regulate immune responses through the secretion of cytokines and cell-to-cell interactions [78]. They are essential for B cell antibody class switching, the activation and growth of CD8$^+$ T cells, maximizing the bactericidal activity of phagocytes, and for the suppression of aberrant inflammation [71, 86, 87]. Once activated, CD4$^+$ T cells have the potential to differentiate into several functionally distinct effector phenotypes which produces a tailored immune response to the specific pathogens [88].

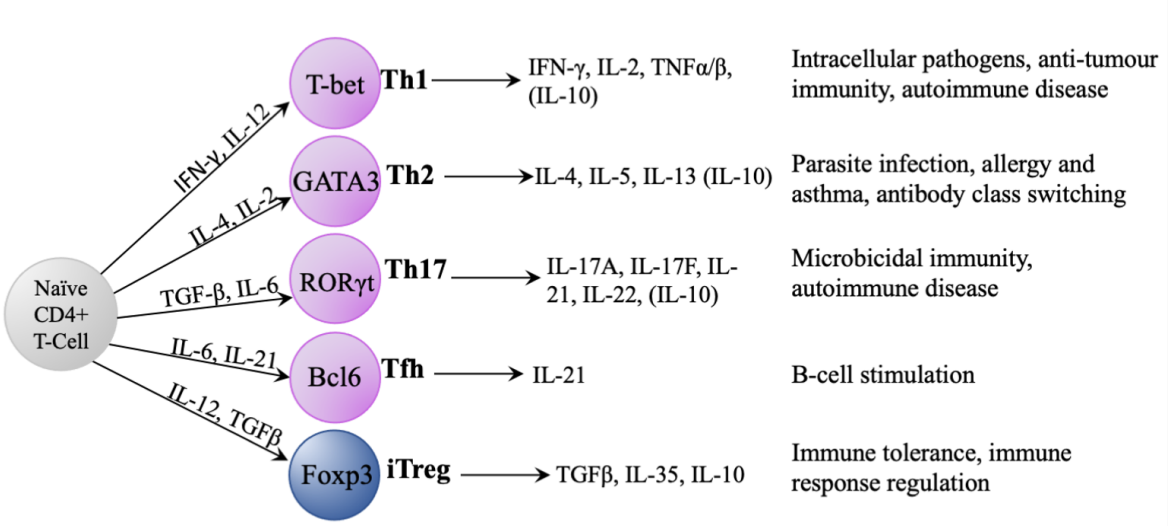


Figure 1.5: CD4$^+$ T cell differentiation. Naïve CD4$^+$ T cells skew towards different effector phenotypes based on the cytokines they are exposed to and the nature of the co-stimulatory signals they receive [78]. The transcription factors T-bet, GATA3, ROR-γt, Bcl-6, or Foxp3 are required for differentiation into Th1, Th2, Th17, Tfh, or iTreg respectively. Different CD4$^+$ T cell phenotypes are associated with different effector functions [59].

CD4$^+$ T cell differentiation and effector function

Lineage-specific CD4$^+$ T cell differentiation depends on the cytokine milieu, the concentration of activating antigens, the strength of the TCR signal, the type of activating APC, and the co-stimulatory signals received [59]. Dendritic cells play the most important role in CD4$^+$ T cell activation due to their enhanced capacity to activate naïve CD4$^+$ T cells [89]. Innate immune cells release the cytokines that initially help polarize the early T cells response [59, 60, 77]. Polarized T cells secrete more polarizing cytokines es-

tablishing a positive feedback loop driving more T cell differentiation [59, 60, 77]. These distinct $CD4^+$ T cell phenotypes include Th 1, Th2, Th17, Th22, Th9, follicular helper T cell (Tfh), induced Treg (iTreg), and regulatory type 1 cells (Tr1) [88, 89]. Figure 1.5 summarizes the main $CD4^+$ T cell subsets, the cytokines that drive their differentiation, the primary transcription factors (TFs) associated with each subset, and the cytokines the subsets express. However, differentiated effector $CD4^+$ T cells do retain an element of plasticity, especially in humans [90].

Th1 cells

IL-12 and interferon (IFN)-γ are essential for the differentiation of Th1 cells [59]. IL-12 is secreted in large amounts by activated APCs, specifically dendritic cells, monocytes, and macrophages, which induces NK cells to produce IFN-γ [59, 90, 91]. IFN-γ activates signal and transducer of activation 1 (STAT1) which results in the expression of T-box expressed in T cells (T-bet) [92, 93]. T-bet is the master TF driving Th1 differentiation and activates genes that promote Th1 development and suppress the development of other lineages [92, 94]. T-bet expression drives more IFN-γ secretion, causing a positive feedback loop of Th1 differentiation. T-bet suppresses the expression of the master TF of Th2 cells, GATA-binding protein 3 (GATA3), and inhibits IL-4 production which is essential for Th2 differentiation [95, 96]. Th17 differentiation is prevented by the interaction of T-bet with the *RORC* promoter, which encodes the Th17 master TF retinoic acid-related orphan receptor γt (ROR-γt) [94].

Th1 cells are essential for the elimination of intracellular pathogens, such as viruses, but have also been implicated in autoimmunity [97]. Th1 cells mainly secrete IFN-γ, TNF-α, TNF-β, and IL-2 [59]. IFN-γ activates phagocytes such as macrophages, monocytes, and microglial cells resulting in enhanced phagocytic activity, antigen presentation, and cytokine expression [98, 99, 100]. There are over 200 IFN-γ-responsive genes including genes involved with pathogen recognition, antigen processing and presentation, the antiviral state, inhibition of cellular proliferation, apoptosis, activation of microbicidal effector functions, and leukocyte trafficking [98, 99, 100, 101, 102]. TNF also has over 700 responsive genes with a wide range of downstream immune effects [103]. High levels of IFN-γ and TNF expression have been implicated in autoimmune diseases including multiple sclerosis (MS) and inflammatory bowel disease (IBD) [101, 103].

Th2 and Th9 cells

IL-4 and IL-2 are essential for Th2 differentiation, and IL-4 is secreted in large quantities by activated mast cells, eosinophils, and basophils [104, 105]. IL-4 induces STAT6 and results in the upregulation of the Th2 master TF GATA3 which drives more IL-4 production [105, 106, 107, 108]. GATA3 inhibits Th1 differentiation by downregulating STAT4 [106]. As with Th1 cells and IFN-γ, Th2 cells produce high levels of IL-4 which drives further Th2 differentiation.

Th9 cells were initially characterized as a subset of Th2 cells, but IL-9 secreting-Th9 cells are now seen as a distinct subset [109, 110]. Transforming growth factor-β (TGF-β) and IL-4 induce Th9 differentiation, and interferon regulatory factor 4 (IRF4) binds directly to the IL-9 promoter and induces IL-9 expression [110].

Activated Th2 cells mainly secrete IL-4, IL-5, IL-13, and IL-31 [59]. Th2 cells are essential for immune responses to parasites such as helmiths, but also play a key role in allergy and asthma [97, 111]. IL-4 is involved in immunoglobulin (Ig) E antibody class switching and secretion by B cells and upregulates the expression of low-affinity IgE receptor (FcϵRI) on B lymphocytes and phagocytes [111, 112, 113]. It induces the upregulation of high-affinity IgE receptor (FcϵRII) on mast cells and basophils, which when bound results in the degranulation of these cells and the release of histamine [113, 114]. IL-13 is essential in controlling gastrointestinal helminths and for the elimination of intracellular pathogens, such as Leishmania [115, 116]. It also plays a major role in the induction of allergic asthma, through activation of eosinophils, enhanced mucus secretion, and airway hyper-responsiveness [113]. The IL-9 secreted by Th9 cells also contributes strongly to allergic asthma and airway inflammation [117].

Th17 cells

Th17 differentiation involves 3 stages: the differentiation stage mediated by TGF-β and IL-6, the self-amplification stage mediated by IL-21, and the stabilization stage mediated by IL-23 [59]. IL-6 and low concentrations of TGF-β induced Th17 differentiation, IL-21 production, and the upregulation of the IL-23 receptor [118, 119, 120]. TGF-β activates STAT3 which induces RORγt, the Th17 master TF, which binds to the IL-17A and IL-17F promoters [121, 122]. Unlike Th1 and Th2 cells, the main cytokines produced

by Th17 cells do not drive self-amplification. IL-21 and TGF-β amplify Th17 differentiation [123, 124]. The stabilization of Th17 differentiation is induced by IL-23, which is mainly produced by activated macrophages and dendritic cells and is required for the expansion and maintenance of the Th17 population [125].

Th17 cells drive the $CD4^+$ T cell response against extracellular bacteria and fungi but have also been implicated in autoimmune diseases [122, 126, 127]. The main Th17 effector cytokines include IL-17A, IL-17F, IL-21, and IL-22 [128]. IL17A and IL17F signal through the same receptor to induce proinflammatory cytokine expression by other immune cells including IL-6, IL-1, and TNF, and induce the secretion of chemokines that recruit more inflammatory cells to sites on infection and inflammation [128, 129]. IL-21 promotes activation, and differentiation, enhances survival and enhanced anti-viral activities in $CD8^+$ T cells, induces B cells to differentiate into plasmacytes and memory cells, and activates NK cells [130]. IL-22 contributes to mucosal host defense against bacterial pathogens, by inducing antimicrobial peptides and increasing cell proliferation [131, 132].

Th22 cells

Recently Th22 cells have been identified as a distinct subset of $CD4^+$ T cells. They are induced by IL-6, TNF-α, IL-23, and IL-1β, express the TFs aryl hydrocarbon receptor (AhR), STAT3, and RORγt, and primarily express IL-22 in addition to IL-13, IL26, and TNF-α [133]. They are distinct from Th17 cells, due to their low production of IL-17. Th22 cells were initially found to play a role in skin inflammatory diseases, but recent studies have demonstrated their involvement in the development of various autoimmune diseases [133].

Tfh cells

Tfh cell differentiation is mainly driven by IL-21 and IL-6 [134]. Both cytokines activate STAT3, but without TGF-β Th17 cells are not induced [135]. ICOS co-stimulation is required for Tfh development [135]. B-cell lymphoma 6 (Bcl-6) is the master TF expressed in Tfh cells and is activated downstream of IL-6 and IL-21 [136].

Tfh cells play a significant role in mediating humoral immunity through interactions

with B cells [137]. Activated Tfh cells upregulate C-X-C motif receptor (CXCR) 5 which allows them to enter the pre-germinal center in secondary lymphoid tissues for initial interaction with antigen-primed B cell resulting in the differentiation of B cells into Ig-producing plasma cells [138, 139]. Tfh cells also contribute to the development of long-lived memory B cells [139]. Activated $CD4^+$ T cells express CD154, also known as CD40 ligand (CD40L), on their cell surface which can bind CD40 on the surface of B cells providing a co-stimulatory signal for B cell activation [137]. CD154-CD40 interactions in addition to IL-21 and other cytokines secreted by the activated Tfh induce B cell proliferation and Ig class switching [137]. B cell responses that involve $CD4^+$ T cell interactions can take multiple days, however, the antibodies generated with $CD4^+$ T cell help have a higher affinity for the antigen and are more functionally versatile than those generated from T cell-independent activation [12].

Tregs

Tregs are essential for suppressing excessive inflammation, thereby maintaining homeostasis and self-tolerance [31, 140]. There are 2 main Treg populations: nTregs which are produced in the thymus and iTregs which develop in peripheral lymphoid organs after antigen priming [31]. Both express the master TF forkhead box P3 (Foxp3) and secrete high levels of IL-10 [141]. TGF-β in addition to driving Th17 differentiation, is also critical in the differentiation of iTregs [142]. TGF-β alone at high concentrations can induce the expression of Foxp3 [143, 144]. Tregs are a heterogeneous population that express a wide variety of cell surface receptors [31].

Tregs can inhibit T cell proliferation and cytokine production and play a critical role in preventing dysregulated inflammation and autoimmunity [31]. After clearance of pathogens, Tregs negatively regulate the immune response, thereby protecting against immunopathology. Their main effector cytokines include IL-10, TGF-β, and IL-35 [145]. IL-10 is a potent inhibitory cytokine and is essential in limiting the damage caused by inflammation [146, 147]. IL-10 and TGF-β reduce allergic inflammation through the suppression of IgE production [148]. Tregs can induce cell death in auto-reactive T cells, induce anergy, downregulate CD80/86 in APCs, and upregulate the inhibitory receptor cytotoxic T-lymphocyte associated protein 4 (CTLA-4) on T cells [148]. CTLA-4 inhibits $CD4^+$ T cell activation by competing with CD28 for CD80/86 binding thereby preventing

the second CD4$^+$ T cell activation signal [148]. High levels of IL-10 and TGF-β also induce the differentiation of more Tregs [59].

1.3.6 CD8$^+$ T cells

CD8$^+$ T cells are essential for the removal of infected or malignantly transformed cells. As previously discussed, naïve CD8$^+$ T cells can only be activated by APCs [66, 149]. Dendritic cells that have interacted with activated CD4$^+$ T cells are required to generate long-lasting CD8$^+$ T cell memory [71, 150]. Activated CD4$^+$ T cells interact with dendritic cells through CD154-CD40 interactions and license the dendritic cells to mature, increase their cytokine production, induce the expression of co-stimulatory molecules on their cell surface, and induce cross-presentation of exogenously derived peptides on MHC-I molecules [151]. This allows activated dendritic cells to potently activate naïve CD8$^+$ T cell which then differentiate into different effector phenotypes [152].

Activated CD8$^+$ T cells scan the MHC-I molecules on the surface of all nucleated cells for their cognate antigen. When their TCR binds the peptide presented on a MHC-I molecule of an infected or malignantly transformed cell, the CD8$^+$ T cell releases the cytotoxins perforin, granzymes, and granulysin [153]. Perforin makes pores in the cell membrane which allows granzymes to enter the target cell which triggers the caspase cascade and apoptosis [154]. CD8$^+$ T cells can also induce cell death through cell-to-cell interactions. Activated CD8$^+$ T cells express Fas ligand (FasL) which can bind Fas on the target cell, triggering apoptosis through the caspase cascade [153, 155]. Cytokines such as IFNs and TNF can also be cytotoxic in high concentrations [156, 157, 158]. CD8$^+$ T cells can be broken down into similar subsets as CD4$^+$ T cells including Tc1, Tc2, Tc17, and Tc9. Tc1 CD8$^+$ T cells secrete many of the Th1 cytokines including IFN-γ and TNF-α while Tc2 cells secrete Th2 cytokines including IL-4 and IL-5 [159]. Recently Tc9 and Tc17 cells have also been identified, with Tc17 cells being implicated with contributing to experimental autoimmune encephalomyelitis (EAE), a mouse model of MS [160, 161]

1.3.7 Double Positive (DP) T cells

Mature DP T cells, expressing both CD4 and CD8, account for approximately 1-3% of peripheral T cells in healthy individuals [61, 162, 163]. While the DP T cell stage

is well characterized in T cell development, it is unclear how mature peripheral DP T cells emerge given that the principal pathway of thymic selection leads to mature SP cells expressing either CD4 or CD8 [164]. Two models explain the presence of DP T cells in the periphery: either a small number of DP T cells can egress from the thymus as mature DP T cells or SP T cells manage to re-acquire the co-expression of CD4 and CD8 in the periphery [165]. The TFs T-helper-inducing POZ/Krüppel-like factor (ThPOK) and runt-related transcription factor 3 (RunX3) tightly regular CD4 and CD8 expression, respectively, during the DP thymocyte stage of T cell development [162]. RunX3 and ThPOK expression was once believed to be mutually exclusive outside the thymus, however, DP T cells can be generated from SP T cells *in vitro* under certain activation and/or cytokine conditions indicating that differentiated T cells retain an element of plasticity [162].

In the periphery, DP T cells appear antigen-experienced and increased frequencies of DP T cells have been reported in autoimmune diseases such as MS, systemic sclerosis (SS), rheumatoid arthritis (RA) as well as in viral infections such as human immunodeficiency viruse (HIV), hepatitis C virus (HCV), and Epstein-Barr virus (EBV), and in some cancers [166, 167, 168, 169, 170, 171]. DP T cells are phenotypically heterogeneous and have been scarcely studied, with contrasting results regarding their function in different disease settings [172, 173, 174, 175, 176, 177, 178]. In HIV and human cytomegalovirus (HCMV) infection, DP T cells appear to be cytotoxic, have a high proportion of virus-specificity, and have a high proliferative capacity and cytolytic activity [179, 180]. In dengue virus (DENV) infection, increased DP T cell frequency is associated with plasma leakage and the DP T cells are transcriptionally similar to $CD8^+$ SP T cells [181]. In contrast, DP T cells in the autoimmune conditions SS and IBD appear to be regulatory/suppressive by secreting high levels of IL-10 [182, 183]. In RA, DP T cells are more proinflammatory, secreting high levels of IFN-γ and IL-21, but not IL-17A relative to $CD4^+$ SP T cells [171]. DP T cells are enriched in the synovial fluid of RA patients and DP T cell frequency is also increased in HCMV-positive RA patients [171]. In MS and non-inflammatory neurological diseases, DP T cells are enriched in the CSF of patients relative to peripheral blood, but their phenotype has not been characterized in depth [184]. DP T cells have also been reported to be enriched in different cancers, where again they have heterogeneous functionalities. In melanoma, colorectal, and urological cancers, DP T cells have a more

suppressive phenotype, while in cutaneous T cell lymphoma, DP T cells appear more cytotoxic [174, 175, 176, 177, 178]. Overall, DP T cells appear to be cytotoxic in most viral infections that have been studied, suppressive in the autoimmune disease SS and IBD but not RA, and suppressive in most of the cancers studied, except for cutaneous T cell lymphoma. While there have been some previous studies that have started to uncover some of the potential functionalities, phenotypes, and pathologies of DP T cells, more work needs to be done to understand this extremely variable population in the context of different diseases.

1.4 Immune tolerance and autoimmunity

Immune tolerance is a state of immune unresponsiveness to an antigen that would otherwise elicit an immune response and is essential for homeostasis [31]. There are two types of tolerance: central and peripheral tolerance. Central tolerance is established in the thymus during T cell development by the removal of the majority of strongly auto-reactive TCR clones [31]. The remaining weakly auto-reactive T cell clones differentiate into nTregs and help maintain tolerance in the periphery. However, deletion of auto-reactive T cell clones is only 60-70% effective, because not all self-antigens are expressed in the thymus, such asantigens from islets of Langerhans, brain, or spinal cord, and some self-antigens are expressed at much higher concentrations in the periphery resulting in the activation of weakly-interacting TCRs [185, 186]. These auto-reactive T cells can cause pathology if peripheral tolerance is not induced. Peripheral tolerance occurs through a variety of mechanisms including inducing T cell quiescence, clonal deletion, and conversion to iTregs [186]. In addition to preventing autoimmunity, peripheral tolerance is essential in preventing over-reactivity to environmental antigens such as allergens and gut microbes. Dysfunction in central or peripheral tolerance can result in severe allergies and autoimmunity. However, tolerance can also be pathogenic, such as during malignancies and chronic infections, and homeostasis requires a careful balance between tolerance and responsiveness [187].

A breakdown of tolerance can result in autoimmunity, and the symptoms of autoimmune diseases often present long after the initial break in tolerance making it difficult to identify the factors responsible for the initiation of the disease. Autoimmune conditions can often be triggered by viral infections, and there are two main hypothesized mechanisms to explain the breakdown of self-tolerance [188]. The first proposed mechanism is by molecular mimicry, where viruses carry structurally similar antigens to self-antigens which activate lymphocytes and cause a cross-reactive response to both self and viral antigens [188]. The second proposed mechanism is bystander activation, where an over-reactive antiviral response creates a localized pro-inflammatory environment along with the release of self-antigens from the damaged tissue [188]. High concentrations of self-antigens activate autoreactive T cells which drive further autoimmunity. Both bystander activation and molecular mimicry have been observed in EAE [188]. Furthermore, infection of

lymphocytes by chronic viruses may result in the immortalization of autoreactive effector cells as was observed in EBV infected B cells [188]. While viral infections, genetics, and environmental factors may contribute to autoimmunity, the mechanisms of the breakdown of tolerance and autoimmunity are not fully understood.

1.5 Human T Cell Leukemia Virus Type 1

Human T Cell Leukemia Virus Type 1 (HTLV-1) is a retrovirus that is estimated to infect 10-20 million people worldwide, however, the actual number of people infected is likely higher as no systematic epidemiological studies have been carried out [189, 190]. HTLV-1 has a wide geographical spread and is mainly found in the tropics and sub-tropics in Sub-Sahara Africa, South America, the Caribbean, southern Japan, central Australia, and Melanesia [189]. HTLV-1 is transmitted by the transfusion of infected cellular blood products, unprotected sexual intercourse, and breastfeeding, which often results in the clustering of HTLV-1 infections within families [191, 192]. Most HTLV-1-infected people remain asymptomatic carriers (ACs), while 2-5% of HTLV-1 carriers develop adult T-cell leukemia/lymphoma (ATL) and another 2-5% develop chronic inflammatory conditions [193]. The most well-characterized HLTV-1-associated inflammatory condition is an inflammatory demyelinating disease of the central nervous system (CNS) termed HTLV-1-associated myelopathy/tropic spastic paraparesis (HAM/TSP), hereafter abbreviated to HAM [193]. Treatments for HTLV-1-associated diseases are limited, and none are curative.

1.5.1 HTLV-1 infection and propagation

Despite producing enveloped virions, HTLV-1 does not release cell-free virions *in vivo* and HTLV-1 is spread by direct cell-to-cell contact [193]. During contact between an infected cell and an uninfected cell, the HTLV-1 transactivator protein Tax causes polarization of the microtubule cytoskeleton towards the cell junction forming a virological synapse [194]. Microtubules direct the budding HTLV-1 virions towards the synapse and the virions travel across the synapse or around the periphery of the synapse towards the plasma membrane of the new host cell [194]. Glucose transporter 1 (GLUT-1), neuropilin-1 (NRP-1) and heparan sulfate proteoglycans (HSPGs) are involved in HTLV-1 binding and cell entry, but the precise mechanism of HTLV-1 cell entry is unclear [193]. *In vitro* cell-free HTLV-1 virions have been shown to infect dendritic cells which are then able to infect T cells, but the physiological relevance of these observations is unclear [195]. To stably infect a new host cell, HTLV-1 integrates its provirus into the host cell genome

[193]. The term clone is used to describe each unique integration of the HTLV-1 provirus [193]. The provial load (PVL) is a measure of the number of copies of the integrated provirus per periphreal blood mononuclear cell (PBMC) and is usually described as a percentage. Generally, an infected cell will only carry one integrated proviral copy [193]. The main targets of HTLV-1-infection are T cells with $CD4^+$ T cells carrying 95% of the HTLV-1 PVL and $CD8^+$ T cells carrying the remaining 5% [196]. The PVL varies widely between individuals ranging from less than $1x10^{-4}$% to over 100% [197].

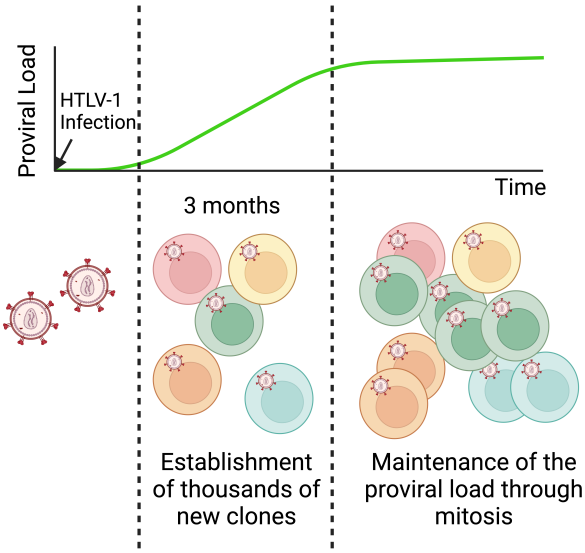


Figure 1.6: The establishment of the HTLV-1 PVL. During early infection, HTLV-1 infects many new cells establishing thousands of new clones resulting in a rapid rise in the PVL. During the chronic phase of infection, the PVL plateaus and is mainly maintained through mitosis [193]. The figure was created used BioRender.

During initial HTLV-1 infection, there is a rapid rise in the PVL as HTLV-1 infects many new T cells resulting in the establishment of thousands of new clones [193]. Eventually, the PVL plateaus as an equilibrium between the virus and the immune system is established (Figure 1.6) [193]. The height of the PVL plateau is dependent on the efficiency of the host immune response in controlling the infection [193]. During the chronic phase of infection, anti-retroviral therapy is ineffective at reducing the PVL as the primary method for PVL maintenance is through the mitosis of infected cells [198, 199]. A typical HTLV-1 AC carries between 10^4-10^5 distinct HTLV-1-infected T cell clones, and the majority of the PVL is made up of low abundance clones [200].

1.5.2 HTLV-1 proteins

HTLV-1 has a 9-kilobase genome including *gag, pol*, and *env* genes present in other retroviruses (Figure 1.7) [201]. There are several regulatory genes at the *3'* end of the genome in the pX region that regulate the expression, splicing, and transport of viral mRNAs [202, 203]. The pX region of the HTLV-1 provirus has six open reading frames: five on the plus-strand and one on the minus-strand (Figure 1.7). Tax and HTLV-1 basic leucine zipper factor (HBZ) have essential roles in viral expression and replication, while p12, p13, and p30 are not essential proteins, and are absent in some naturally occurring HTLV-1 strains [193].

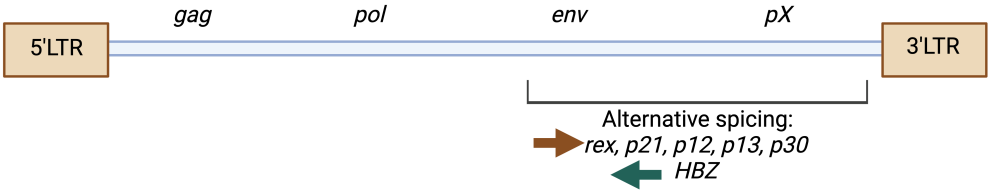


Figure 1.7: HTLV-1 genome [193]. Figure created using BioRender.

Tax

In addition to playing a key role in HTLV-1 cell-to-cell spread, Tax is a nuclear transcriptional transactivator and is responsible for the transactivation of the proviral plus strand by recruiting cyclic adenosine monophosphate cAMP response element binding protein (CREB), transcriptional co-activators CREB binding protein (CBP)/p300, and chromatic assembly factor 1 to the three Tax response elements in the 5' long terminal repeat (LTR) of the HTLV-1 provirus [193]. Tax can activate nuclear factor kappa-light-chain-enhancer of activated B cells (NF-κB), and Tax expression correlates with the upregulation of several genes including IFN-γ, IL-6, IL-15, granulocyte-macrophage colony-stimulating factor (GM-CSF), and CC motif chemokine ligand (CCL) 22 [204, 205]. Tax has been shown to inhibit DNA repair factors, DNA damage responses, and the chromosome instability checkpoint resulting in genomic instability [193, 206, 207]. Tax is not persistently expressed, but is expressed in transcriptional bursts [206, 208]. The Tax transcriptional burst has been shown to have far-reaching effects on the infected host cell transcriptome, including oncogenic effects, and the impacts on the transcriptome appear

to vary between clones, indicating that proviral integration site loci may impact the effect of Tax [209].

HBZ

HBZ is persistently expressed at low levels and acts in the nucleus to downregulate HTLV-1 transcription [193]. However, the deletion of HBZ in HTLV-1 clones resulted in lower PVLs in rabbits [210]. Additionally, HBZ is not present in HTLV-2, a closely related retrovirus, which is associated with lower PVLs than HTLV-1 and no recognized associated diseases [193]. Both the HBZ protein and mRNA induce cellular proliferation by an unknown mechanism. HBZ binds and sequesters CREB and CBP/p300 which is thought to contribute to the downregulation of Tax by HBZ [193]. HBZ promotes cell immortalizing of HTLV-1-infected cells by stimulating telomerase [211]. Many of the functions of HBZ oppose the effects of Tax suggesting that HTLV-1 persistence *in vivo* depends on a balance between the opposing functions of these two proteins [193].

1.5.3 HTLV-1-associated diseases other than HAM

While the majority of HTLV-1-infected people remain overtly asymptomatic, 2-5% of HTLV-1 carriers develop ATL and another 2-5% develop chronic inflammatory conditions. However, even in overtly asymptomatic HTLV-1 carriers, HTLV-1-infection results in a 57% increase in adjusted mortality [212, 213]. Overall, HTLV-1-infected individuals with higher PVLs are more likely to develop symptomatic disease [193]. In addition to HAM, HTLV-1 can cause symptomatic inflammatory syndromes such as uveitis, polymyositis, infective dermatitis, sicca syndrome, polyneuropathy, dysautonomia, chronic diffuse encephalomyelopathy, encephalitis, and cognitive deficits [214]. HTLV-1-infected T cells have been also shown to invade the lung causing bronchiectasis, bronchitis, or bronchiolitis [215]. HTLV-1 infection predisposes individuals to certain pathogens such as *Mycobacterium tuberculosis*, *Strongyloides stercoralis*, *Staphylococcus aureus* caused dermatitis, and *Sarcoptes scabiei* [193]. There are no systematic differences in the genotypes of HTLV-1 in patients with HAM, ATL, or other HTLV-1-associated diseases and infected individuals who remain asymptomatic [216, 217], therefore difference in infection outcome is due to a combination of host and environmental factors [212].

Adult T cell leukemia

ATL is a malignant disease of the T cells, typically $CD4^+$ T cells, and has four subtypes: smoldering, chronic, lymphoma, and acute [218]. ATL usually develops in individuals that were infected in early childhood and presents between 50-60 years of age [193]. Individuals with PVLs above 4% are far more likely to develop ATL than individuals with lower PVLs, and have a 20% lifetime risk of ATL [204, 219]. Certain Human leukocyte antigens class I (HLA-I) and killer immunoglobulin-like receptor (KIR) alleles are associated with ATL development [220]. However, it is likely that these genes predispose HTLV-1 carriers to a higher HTLV-1 PVL rather than contribute to ATL pathogenesis as they are also associated with HAM and other HTLV-1-associated diseases. Males are 1.2 fold more likely to develop ATL than females [193]. The prognosis for aggressive ATL is very poor with an overall survival rate of less than one year [221]. Favorable chronic and smoldering sub-types still carry poor long-term prognosis.

Neither HBZ nor Tax are classical oncogenes, however, both are oncogenic and their proteins cooperate to balance infectivity, proliferation, longevity, and immune evasion [221]. Tax causes cells to bypass cell-cycle checkpoints, affects DNA damage and repair responses, and affects the apoptosis pathway, and HBZ alone can cause tumors in transgenic mice [222]. HBZ has been also shown to drive host cell proliferation, increase human telomerase reverse transcriptase (hTERT) transcription, increase genomic instability, and inhibit apoptosis [223, 224]. The inhibition of DNA damage checkpoints and T cell proliferation may result in the accumulation of mutations with the potential to result in a malignant transformation after many years. The bulk of the PVL in ACs is made up of low abundance clones, but at the stage of clinic presentation in ATL, there tends to be a single dominant clone [89, 225]. Every infected clone has the potential to undergo malignant transformation, and therefore higher PVLs, in combination with other risk factors, increase the risk of ATL [193].

1.6 HTLV-1-Associated Myelopathy

HAM is an inflammatory disease of the CNS characterized by chronic inflammatory demyelination that resembles progressive spinal forms of MS. HAM presents with a wide

range of symptoms but is defined by progressive weakness of lower limbs, lower back pain, urinary incontinence, bowel dysfunction, and sexual dysfunction [226]. There are limited treatments that aim to reduce HAM symptoms, but there are no satisfactory treatments to prevent or reverse disease progression [227]. Immuno-suppressive therapies are often initiated with variable outcomes and over 50% of patients with HAM are wheelchair-bound within a decade of disease onset [227, 228, 229]. While not directly life-threatening, HAM can cause severe disability and life expectancy is significantly reduced [230]. Despite the higher risk of developing ATL than HAM, the disease burden of HAM is higher due to its long and progressive course.

1.6.1 HAM risk factors

Age, sex, ethnic background, route of HTLV-1 infection, and PVL have been shown to influence the risk of developing HAM [193]. The median age of onset is between 50 to 60 years and females are more likely to develop HAM with a 4:1 female to male ratio in the UK [212, 229, 231]. The disease also seems to progress faster in females than males [232]. Individuals infected with HTLV-1 through organ donation or blood transfusion seem to be at an increased risk of developing HAM, and HAM symptoms have a rapid onset [233, 234].

Different ethnic backgrounds are more predisposed to developing HAM. Individuals from Afro-Caribbean backgrounds are more likely to develop HAM than individuals from Japanese backgrounds [231, 235]. A Japanese study found that the lifetime risk of developing HAM was around 0.25% [235], while North American studies reported a lifetime risk of 2.4-3.7% [236, 237].

The HTLV-1 PVL is the strongest predictor of developing HTLV-1-associated diseases, with high PVLs associated with HAM [238, 239, 240, 241]. As previously discussed, an individual's PVL remains relatively constant during the chronic phase of infection with only minor fluctuations. The height of the PVL plateau is determined by the efficacy of the immune response to HTLV-1, which is affected by host genetics and previous immune system priming [242]. HAM is rarely diagnosed in individuals with PVLs below 1%, and the higher the PVL, the higher the incidence of HAM [239, 243]. However, over 50% of ACs also have PVLs above 1%, therefore only a minority of high PVL ACs go on

to develop HAM, and patients who go on to develop HAM have high PVLs for decades before the onset of HAM symptoms [197, 212]. Therefore it is apparent that a high PVL in isolation is not enough to drive HAM pathogenesis. A HAM-like phenotype has recently been described in a subset of high PVL ACs which expressed markers of T cell activation, beta-2 microglobulin (*B2M*), and neuronal damage in blood analysis which identified 88% of patients with HAM and 6% of ACs [244]. These ACs were considered to have a HAM-like or pre-HAM phenotype, and 10% of these HAM-like ACs went on to develop HAM within 60 months [244].

The immune response to HTLV-1 helps determine the height of the PVL plateau, and therefore, in turn, contributes to the risk of developing HAM [243]. HLA-I and II alleles contribute to the efficacy and efficiency of the T cell response. HLA-A*02 has been shown to be protective in studies in southern Japan and Brazil [243, 245, 246], however this was not observed in Peru [247] or in French Afro-Caribbean populations [248]. A Spanish study found an association between HLA-DRB1*0101 and HLA-B*07 and higher PVLs [249]. In addition to HLA variations, certain single nucleotide polymorphisms (SNPs) have been associated with HAM. SNPs in the IL-6 promoter (IL6-634C) and TNF promoter(TNF-963A) were enriched in HTLV-1 carriers with high PVLs [250, 240]. SNPs in the 3' untranslated region (UTR) of the chemokine stromal cell-derived factor (SDF1+801A) and IL-15 (IL-15-191C) were found to be protective against high PVLs and HAM [240]. HAM cases have been shown to cluster within families, however, the contribution of individual genes to this clustering has not been quantified [251]. HAM risk increases due to a range of complex and interwoven genetic, immunological, and environmental factors.

1.6.2 Mechanisms of pathogenesis

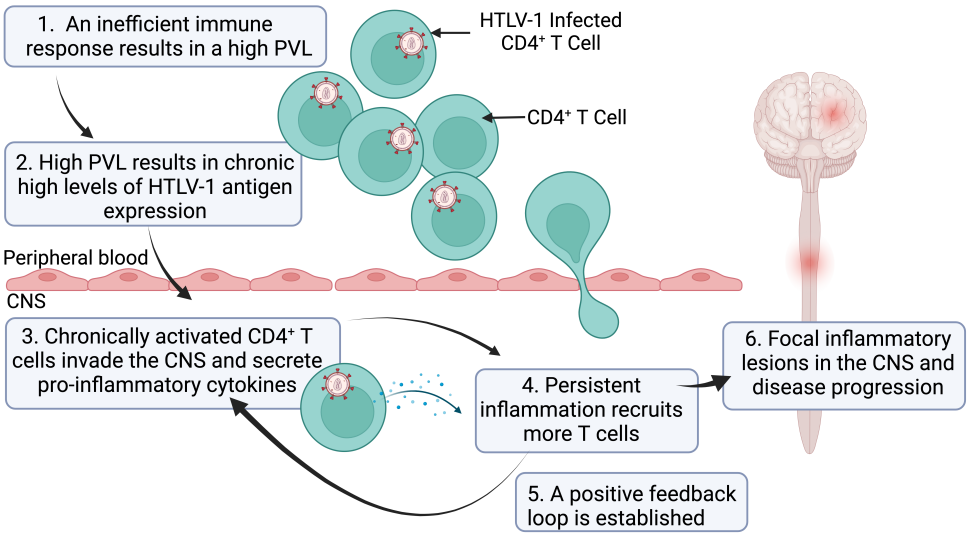


Figure 1.8: Hypothesized mechanism of HAM pathogenesis. Figured created using BioRender.

The exact mechanism of HAM pathogenesis is not understood. HAM symptoms are caused by focal inflammatory lesions in the CNS, both in the spinal cord and cerebrum (Figure 1.8) [252]. It is currently hypothesized that an inefficient initial immune response to HTLV-1, due in part to certain HLA alleles, results in a high PVL and chronic high levels of HTLV-1 antigen expression [212, 242, 243]. This results in chronically activated $CD4^+$ T cells that can invade the CNS more readily than resting T cells as they express high levels of adhesion molecules, chemokine receptors, and integrins that allow them to cross the BBB [253, 254, 255, 256, 257, 258]. It has been shown that $CD4^+$ T cells predominate in early HAM lesions, while $CD8^+$ T cells predominate in older HAM lesions [158, 259]. $CD4^+$ T cells are thought to enter the CNS from areas of circulation where the blood flow rate is low [260]. Tax and HBZ upregulate activated leukocyte cell adhesion molecule (ALCAM) and intercellular adhesion molecule 1 (ICAM-1), respectively, which may also facilitate the entry of HTLV-1-infected cells into the CNS [261, 262, 263]. Activated and/or infected $CD4^+$ T cells in the CNS persistently secrete pro-inflammatory cytokines such as IFN-γ and TNF-α which are neurotoxic at high concentrations and can cause bystander damage [156, 157, 158, 264, 265]. IFN-γ also regulates the passage of leukocytes into the CNS and there is a strong upregulation of ISGs in the PBMCs of patients with HAM, with the intensity of the IFN signature correlated with disease severity

[266, 267]. A positive inflammatory feedback loop recruits more $CD4^+$ and $CD8^+$ T cells to the CNS resulting in the loss of surrounding neurons and demyelination, eventually resulting in focal inflammatory lesions in the CNS [158, 252, 268, 269]. Over time the inflammation results in the loss of spinal cord volume and disease progression [270].

It is currently hypothesized that the majority of the damage to the CNS is caused by bystander damage as there currently is no evidence for direct T cell or antibody-mediated damage to the CNS. Anti-Tax antibodies are not present in all individuals with HAM, and anti-heterogeneous nuclear ribonuclear protein A1 (hnRNP-A1) antibodies, which are elevated in the cerebrospinal fluid (CSF) of patients with MS, are not elevated in patients with HAM [271]. However, cross-reactive T cells or antibodies specific for proteins other than Tax have not been thoroughly investigated.

There is no *in vivo* evidence that CNS cells are readily infected with HTLV-1 and the majority of the infected cells in the CNS of patients with HAM are invading lymphocytes [193, 272]. However, cells of the CNS are still likely to be involved in HAM pathogenesis. Microglia are the macrophages of the CNS and play essential roles in immune surveillance, maintaining tissue homeostasis, synaptic pruning, neuroinflammation regulation, and response to injury or infection in the CNS [273]. Very little work has been done to elucidate the potential role of microglia in HAM pathogenesis, however, as the main APC in the brain, they would play a key role in re-activating HTLV-1-specific T cells in the CNS. Furthermore, Th1 cytokines have been shown to activate and induce proinflammatory microglia in EAE with the capacity to drive further neuroinflammation [274, 275]. Activated proinflammatory microglia induce neurotoxic reactive A1 astrocytes by secreting IL-1α, TNF, and complement component 1q (C1q) [276]. Astrocytes are the most abundant glial cells in the CNS, and support and regulate the activities of neurons including synaptic signaling, neurotransmitter uptake, and maintenance of the BBB [277]. HTLV-1 infected $CD4^+$ T cells, soluble recombinant TNF, and Tax, each have been shown to impair the catabolism and uptake of the neurotransmitter glutamate in astrocytes by decreasing the expression of glutamate aspartate transporter (GLAST) and glutamate transporter 1 (GLT-1) [278]. Impairing the ability of astrocytes to regulate CNS glutamate levels heavily impacts neuronal and oligodendrocytic functions and survival [278]. Inflammatory astrocytes have also been shown to be key players in amplifying CNS inflammation in MS [277]. Highly proinflammatory and neurotoxic astrocytes, char-

acterized by increased GM-CSF signaling, NF-κB activation, and inducible nitric oxide synthase (iNOS) expression have been identified in EAE and post-mortem brain samples from MS patients [279]. Astrocytes also have the potential to recruit more T cells to the CNS by expressing high levels of chemokine IFN-γ inducible protein 10 kDa (CXCL10) in response to IFN-γ secreted by $CD4^+$ T cells [280]. CXCL9, CXCL10, and CXCL11 bind CXCR3 to elicit migration of CXCR3-expressing cells, such as activated Th1 $CD4^+$ T cells and $CD8^+$ T cells, and have been shown to activate peripheral immune cells, microglia and CNS resident macrophages during brain injury to direct them to the lesion site [281, 282, 283, 284, 285, 286]. CXCL9 and CXCL10 are upregulated in the CSF of patients with HAM relative to MS patients who have significantly higher levels relative to healthy controls, however, the source of the CXCL10 in patients with HAM has not been identified [287]. While microglia, astrocytes, and other glial cells can drive neuroinflammation, to date, very few studies have explored the contribution of glial cells and/or T cell-glial interactions to HAM pathogenesis [288]. While many factors contributing to HAM pathology have been identified, including PVL and HLA genotypes, the underlying mechanisms of HAM pathogenesis driven by both T cells and glial cells are still not understood.

1.7 Immune responses to HTLV-1

1.7.1 Innate immune response

There has been relatively little work done on the innate immune response to HTLV-1. It has been suggested that dendritic cells are important in the early stages of infection due to their ability to endocytose infected cells and viruses [195]. HTLV-1 DNA has been detected in myeloid cells such as monocytes and dendritic cells *in vitro* and *in vivo*, however the HTLV-1 DNA may simply be present due to the phagocytosis of infected cell debris [195, 289, 290]. Proviral DNA detected in non-T cell populations is very low [193]. HTLV-1 has been shown to infect HSCs, and more than 40% of HTLV-1-infected B cells, monocytes, and neutrophils shared an integration site with a T cell [291].

IFN-I plays an important role in the HTLV-1 immune response and there is impaired IFN-I production in the dendritic cells of ATL patients [292, 293, 294]. IFN-I has been

shown to reduce HTLV-1 replication, and the addition of IFN-I may overcome some of the effects induced by Tax expression [295]. Tax has been shown to inhibit TANK-binding kinase 1 (TBK1) phosphorylation of interferon regulatory factor 3 (IRF3) which is required for the transcription of ISGs and blunting the innate immune response [296].

The role of other innate immune cells such as NK cells or monocytes in HTLV-1 infection is unclear [193]. Several groups have reported decreased circulation of NK T-like cells in HTLV-1 carriers and the reduction was more severe with increased PVLs [296, 297]. Increased frequencies of aggregated monocytes have been reported in patients with HAM relative to ACs which may indicate more monocyte activation, however, the physiological significance of this is not clear [298]. Overall, the innate immune response to HTLV-1 remains relatively poorly characterized.

1.7.2 Adaptive immune response

The majority of the work studying the adaptive immune response to HTLV-1 has focused on $CD8^+$ T cells [193]. Given the chronic and dynamic nature of HTLV-1 infection, the efficacy of the T cell response cannot be inferred from the frequency of HTLV-1-specific T cells, as a highly efficient T cell response may be carried out by a small number of highly effective T cells [242, 299].

$CD4^+$ T Cell Response

Despite carrying 95% of the HTLV-1 PVL and playing a central role in effective cellular and humoral immune responses, our understanding of the $CD4^+$ T cell response to HTLV-1 remains limited as it has been a major challenge to study HTLV-1-specific $CD4^+$ T cells. The two main studies that have started characterizing HTLV-1-specific $CD4^+$ T cells used IFN-γ expression after stimulation with an HTLV-1 peptide library as a marker for HTLV-1-specificity [300, 301]. Given that HTLV-1-infected cells spontaneously secrete proinflammatory cytokines including IFN-γ and TNF after 6 h in culture, *ex vivo* $CD4^+$ T cell stimulation experiments were limited to under 6 h [294, 302, 303]. The majority of HTLV-1-specific IFN-γ^+ $CD4^+$ T cells were not infected with HTLV-1, but HTLV-1-specific $CD4^+$ T cells were infected at higher rates than non-HTLV-1-specific $CD4^+$ T cells [301]. Patients with HAM had on average a 25-fold greater frequency of HTLV-1-specific

IFN-γ^+ $CD4^+$ T relative to ACs, however, the ACs in the study had a significantly lower PVL than patients with HAM [301]. Most of the HTLV-1 immunodominant antigens for $CD4^+$ T cells are within the HTLV-1 envelope protein [301]. These studies also showed that $CD4^+$ T cells from ACs secreted more IL-4 indicating more of a Th2 phenotype and patients with HAM secreted more IFN-γ indicating more of a Th1 phenotype [300, 301]. However, the ACs and patients with HAM in these studies were not matched by PVL, and therefore the Th1 phenotype could simply be associated with an increased PVL and Th2 with a lower PVL.

HTLV-1-infected individuals have a higher proportion of $Foxp3^+$ $CD4^+$ T cells relative to uninfected individuals [304]. It is unclear whether HTLV-1 preferentially infects $Foxp3^+$ cells or induces Foxp3 expression in infected cells [304]. It is also unclear whether these infected $Foxp3^+$ infected cells have suppressive Treg functions [305]. Furthermore, Tax induces $CD4^+$ T cells to produce CCL22 which maintains a high frequency of Tregs which may impair the quality of the HTLV-1 specific T cell response [306].

$CD4^+$ T cells are key drivers of neuroinflammation during HAM pathogenesis given that $CD4^+$ T cells carry 95% of the HTLV-1 PVL, predominate in early HAM lesions, and both HTLV-1-infected and HTLV-1-specific $CD4^+$ T cells secrete high levels of pro-inflammatory cytokines [212]. However, despite the clear involvement of $CD4^+$ T cells in HAM pathogenesis, their phenotype and functionality remain relatively uncharacterized.

$CD8^+$ T Cell Response

Most of the work characterizing the T cell response to HTLV-1 has focused on $CD8^+$ T cells [193]. The importance of $CD8^+$ T cells to the HTLV-1 immune response is demonstrated by protective HLA-I alleles [243, 245, 246]. HLA-I alleles determine the identity and number of HTLV-1 antigens presented to $CD8^+$ T cells, and therefore shape the speed and quality of the $CD8^+$ T cell response [307]. The HLA-A*02 allele was found to be protective as it binds several Tax epitopes unusually strongly [243]. This is thought to be protective because Tax is one of the first viral proteins to be expressed after *de novo* infection, allowing individuals with this allele to induce a $CD8^+$ T cell response more quickly [243]. The majority of immunodominant antigens for HTLV-1-specific $CD8^+$ T cells are within the Tax sequence [308]. However, a robust HBZ-specific $CD8^+$ T cell response is required for efficient viral control [307, 309, 310]. This may be due to the per-

sistent expression of HBZ, while Tax is only expressed sporadically [311]. HLA-I alleles which present a high frequency and diversity of HBZ epitopes were found to be protective against the development of high PVLs [309]. In addition to HLA alleles, KIR genotypes have been also shown to influence the $CD8^+$ T cell immune response to HTLV-1. KIRs are found on around 50% of NK cells and 5% of $CD8^+$ T cells [193]. KIR2DL2 is an inhibitory KIR that has been shown to reduce activation-induced cell death possibly helping maintain $CD8^+$ T cell memory populations during chronic viral infections [312]. By increasing the lifespan of HTLV-1-specific $CD8^+$ T cells, KIR2DL2 is through to enhance both protective or dysfunctional $CD8^+$ T cells responses to chronic viral infections [311].

Previous studies reported an increased frequency of HTLV-1-specific $CD8^+$ T cells in patients with HAM and that their frequency was correlated with disease severity, leading to the suggestion that HTLV-1–specific $CD8^+$ T cells are the main subset of pathogenic lymphocytes in HAM [299, 313]. However, the correlation was not statistically significant and the patients with HAM in these studies had a significantly higher PVL relative to the AC group. Overall the frequency of HLTV-1-specific $CD8^+$ T cells increased with PVL, indicating a less efficient $CD8^+$ T cell response as PVL increased [299, 313]. Other than assessing the frequency and immunodominant antigens of HTLV-1-specific $CD8^+$ T cells, the HTLV-1-specific $CD8^+$ T cell population, like the HTLV-1-specific $CD4^+$ T cell population, remains relatively uncharacterized.

1.8 Antigen-specific T cells

Virus-specific $CD4^+$ and $CD8^+$ T cell responses are essential during acute and chronic viral infections. While the quality of the HTLV-1-$CD8^+$ T cell response has been shown to directly impact the HTLV-1 PVL, the impact of the HTLV-1-specific $CD4^+$ T cell response is less clear. During HCV infection, an early, robust, and multi-specific $CD4^+$ T cell response is associated with viral clearance, while a weak or absent response is associated with HCV establishment [314, 315]. In people with HIV that progress quickly to acquired immune deficiency syndrome (AIDS), chronic progressors, the HIV-specific $CD4^+$ T cells tend toward a Tfh cell profile [316], while in people spontaneously controlling the virus, elite controllers, HIV-specific $CD4^+$ T cells express diverse phenotypes [316, 317, 318]. As chronic HIV and HCV infection persists, the $CD4^+$ T cell repertoire shifts from Th1 to Tfh for both antigen-specific and non-specific $CD4^+$ T cells [319]. This may protect the host from Th1-driven immunopathology. Overall both $CD4^+$ and $CD8^+$ T cell dysfunction is common during chronic viral infections and includes T cell exhaustion, antigen-specific T cells lacking a range of phenotypes, cross-reactive or auto-reactive T cells, $CD4^+$ T cell dysfunction in B cell help or $CD8^+$ T cell help, differences in TCR avidity, and simply the inability to promote viral clearance [316, 319, 320, 321, 322].

1.8.1 Identifying antigen-specific T cells

Earlier methods used to study antigen-specific T cells included the isolation of cytokine-producing cells after stimulation with antigen or the use of peptide-MHC multimers [323]. MHC multimers are MHC oligomers that are known to present a specific antigen. Usable peptide MHC-multimers for HTLV-1 are rare as immunodominant peptides and MHC alleles first need to be characterized and then manufactured. Goon *et al.* 2004 and Goon *et al.* 2002 identified HTLV-1-specific $CD4^+$ T cells based on IFN-γ expression after stimulation with an HTLV-1 peptide library [300, 301]. These studies provided the first insights into HTLV-1-specific $CD4^+$ T cells. Previous studies on HTLV-1-specific $CD8^+$ T cells also IFN-γ secretion after stimulation or used HTLV-1 Tax11-19/HLA-A*0201 tetramers to identify HTLV-1-specific $CD8^+$ T cells. However, using IFN-γ as a marker for HTLV-1-specificity or using specific tetramers will have biased the population of cells

studied and is unlikely to have captured the diversity of HTLV-1 epitopes, TCR receptors, cytokines produced, frequency of cells, and T cell phenotypes.

More recent techniques rely on the upregulation of surface activation induced markers (AIMs) on antigen-specific $CD4^+$ and $CD8^+$ T cells after stimulation with the antigen [324]. Upregulated AIMs include CD25, CD69, CD27, and CD71, however, these AIMs lack specificity as they are sometimes expressed on some specialized T cell subsets independent of TCR activation [325, 326, 327]. CD154 is only expressed on the surface of activated $CD4^+$ T cells after direct TCR stimulation by antigen [69, 324]. CD154 is internalized after binding CD40 on the surface of APCs and B cells, but this can be inhibited with the addition of a CD40 antibody which prevents CD40-CD154 interactions [324, 328]. With the addition of this antibody, the expression of CD154 peaks 6 h after antigen stimulation and then remains expressed at high levels for 24 h [324]. Antigen-specific $CD8^+$ T cells upregulate CD137 after stimulation with antigen [329]. CD137 is often used in conjunction with CD69 to identify antigen-specific $CD8^+$ T cells [329]. The use of CD154 for $CD4^+$ T cells and CD137 and CD69 for $CD8^+$ T cells allows direct access to antigen-specific T cells from an unrestricted pool of epitopes, phenotypes and TCR sequences [127, 316, 320, 323, 329].

1.9 Hypothesis and Aims of the PhD

As outlined in the introduction, significant gaps persist in our understanding of the immune response to HTLV-1, particularly regarding T cell responses during HTLV-1 infection, as well as the role of T cells in driving neuroinflammation and the pathogenesis of HAM. T cells are the main target of HTLV-1 infection and predominante in the CNS lesions of patients with HAM, suggesting their involvement in driving HAM pathogenesis. Activated $CD4^+$ T cells appear to infiltrate the CNS first and recruit more $CD8^+$ T cells to the CNS lesions over time. The overarching hypothesis tested in this PhD is that HTLV-1-specific T cells in patients with HAM are phenotypically and functionally distinct relative to ACs, and T cell dysfunction drives HAM pathogenesis. T cell dysfunction includes the inability of T cells to maintain a low PVL during HTLV-1 infection, T cell exhaustion, an enhanced migratory capacity, and the direct contribution of T cells to CNS inflammation and pathology.

The overall aim of this work is to deeply characterize HTLV-1-specific T cell responses in different groups of HTLV-1 carriers and uninfected controls (UCs). The four main aims of this PhD are as follows:

1. Deep phenotypic and functional characterization of HTLV-1-specific $CD4^+$ and $CD8^+$ T cells from UCs, AC lPVL, AC hPVL, and patients with HAM to identify differences in phenotype associated with different HTLV-1 infection outcomes.

2. Analysis of the interaction of HTLV-1-specific $CD4^+$ T cells and $CD8^+$ T cells with cells from the CNS (*e.g.* astrocytes and microglia) to determine whether HTLV-1-specific cells from ACs and patients with HAM modulate the function, viability, and phenotype of glial cells differently.

3. Analysis of the whole genome transcriptional signature of HTLV-1-specific $CD4^+$ T cells from UCs, AC lPVL, AC hPVL, and patients with HAM to demonstrate distinct profiles associated with the different HTLV-1 infection outcomes.

4. Characterization of $CD4^+CD8^+$ DP T cells in HTLV-1-infected individuals to examine the role DP T cells may play in HTLV-1 infection, anti-HTLV-1 immunity, inflammation, and HAM pathogenesis.

This thesis has been organized into three results chapters with the first chapter focusing on $CD4^+$ T cells, the second on $CD8^+$ T cells, and the third chapter on $CD4^+CD8^+$ DP T cells in HTLV-1 infection.

2

Materials and Methods

2.1 Participants, study design, and clinical data collection

HTLV-1-infected individuals are ACs and patients with HAM attending the National Centre for Human Retrovirology, Imperial College Healthcare NHS Trust, at St Mary's Hospital. Blood samples were obtained through the Communicable Diseases Research Tissue Bank (NRES ID: 20/SC/0226). HTLV-1 infection was diagnosed using a commercially available enzyme-linked immunosorbent assay (ELISA) and confirmed using Western blot (Genelabs HTLV 2.4, Singapore) according to the manufacturer's instructions. This was undertaken by the Virus Reference Division of Public Health England. The diagnosis of HAM was made using the World Health Organization (WHO) criteria. Uninfected volunteers were Imperial College staff and all participants provided informed consent for blood donation. Patients with HAM had not been on HAM treatment for at least 3 months before blood donation.

In this work, HTLV-1 carriers were divided into 3 groups: ACs with a PVL below 3% (AC low PVL (AC lPVL)), ACs with a PVL above 3% (AC high PVL (AC hPVL)), and patients with HAM not on treatment (HAM). The 3% cut-off was chosen to match the

PVL of the AC hPVL to patients with HAM (Table 2.1). This allowed for comparisons of T cell responses based on disease status while controlling for differences in PVL. By making comparisons between AC lPVL and AC hPVL, I was able to gain insights into differences in the T cell responses between AC lPVL and AC hPVL, gaining a deeper understanding of the factors that allow for effective HTLV-1 control. Comparisons between AC hPVL and patients with HAM allowed me to identify T cell phenotypes, molecules, and signaling pathways that are associated with the transition from AC to HAM providing insight into the pathophysiology of the demyelinating disease and could allow for the identification of novel targets for HAM treatment. UCs, AC lPVL, AC hPVL, and HAM groups were matched on biological sex (Table 2.1). Patients with HAM were significantly older than ACs, however, the mean age of the AC hPVL group was 54.0 which is older than the mean age of HAM onset [193].

Table 2.1: Participant Characteristics

Category	**UC**	**AC lPVL**	**AC hPVL**	**HAM**
Participant Number	28	35	24	14
Age (years) - mean, range	43.6, 24-68	53.9, 24-79	54.0, 27-81	66.4, 52-88
Sex- Number, Percentage				
Male	7, 25%	8, 23%	6, 27%	3, 27%
Female	21, 75%	27, 77%	22, 73%	11, 73%
PVL (% of PBMCs) - mean, range	NA	0.65, Undetected-2.92	9.65, 3.16-22.89	12.62, 3.51-53.12

2.2 Cell isolation, storage, and thawing

Peripheral blood was collected in sodium heparin tubes and the PBMCs were isolated immediately after blood draw by Ficoll Hypaque gradient. The PBMC layer was collected, washed with phosphate buffered saline (PBS), and re-suspended at 20 million cells/mL in fetal calf serum (FBS) supplemented with 10% dimethyl sulfoxide (DMSO) and stored at -150°C. For PBMC thawing, vials were thawed in a pre-warmed water bath at 37°C and immediately transferred to a 15 mL falcon tube where 5 mL of warm RPMI 1640 media supplemented with 2 mM L-Glutamine (GIBCO, 25030-024), 5% human serum (HS), 100

μg/mL Penicillin and Streptomycin (GIBCO, 15140-122) at 37°C were added drop by drop. The PBMCs were subsequently centrifuged for 10 minutes (min) at 300 x g and resuspended in warm media at 20 million cells/mL.

2.3 Generation of virus stocks

The HTLV-1-producing MT-2 cell line was plated in complete T cell media (RPMI 1640 media (Gibco, 21875-034) supplemented with 5% HS, 10 mM Hepes buffer solution (GIBCO, 15630-056), 1 x nonessential amino acids (GIBCO, 11140), 1 mM sodium pyruvate (GIBCO, 11360-070), 2 mM L-Glutamine (GIBCO, 25030-024), and 100 μg/mL Penicillin and Streptomycin (GIBCO, 15140-122)) at 0.3 million cells/mL. The cells were incubated for 7 days at 37°C. The cell culture media containing the HTLV-1 virions was collected and centrifuged for 15 min at 400 x g to remove large debris. 3 volumes of supernatant were mixed with 1 volume of Lenti-X concentrator (TakaraBio, 631231) and incubated at 4°C for 24 h followed by centrifugation at 1500 x g for 45 min at 4°C. The pellet was resuspended in $1/100^{\text{th}}$ the initial volume of PBS and heat-inactivated by incubation at 56°C for 4 hours, aliquoted, and stored at -80°C. The concentration of HTLV-1 p19 was quantified before heat-inactivation using a p19 ELISA kit (ZeptoMetrix, 080116).

2.4 *Ex vivo* stimulation assays

PBMCs were thawed and rested for 2 h in complete T cell media. PBMCs were then stimulated for 12-20 h at 10 million cells/mL with a control or heat-inactivated HTLV-1 at a concentration of 0.92μg/mL p19, 1 μg/mL anti-CD40 (Miltenyi Biotec, 130-094-133) and 1 μg/mL anti-CD28 (Miltenyi Biotec, 130-093-975). The vehicle-stimulated control contained all the same reagents as the heat-inactivated HTLV-1, including complete T cell media that had been concentrated using the same method to produce the HTLV-1 viral stocks. For 12 h stimulations with intracellular stainings other than Tax, 3μg/mL GolgiStop$^{\text{TM}}$ (BD Biosciences, 554724) and 1μg/mL GolgiPlug$^{\text{TM}}$ (BD Biosciences, 555029) were added to the cultures 9 h after the start of the stimulation for an additional 3 h. For 20 h stimulations with intracellular stainings other than Tax,

3μg/mL GolgiStop^{TM} (BD Biosciences, 554724) and 1μg/mL GolgiPlug^{TM} (BD Biosciences, 555029) were added to the cultures 11 h after the start of the stimulation for an additional 9 h.

For phorbol 12-myristate 13-acetate (PMA) and ionomycin stimulation experiments, PBMCs were rested for 2 h and then stimulated with 50ng/mL PMA, 250ng/mL ionomycin, 3μg/mL GolgiStop^{TM} (BD Biosciences, 554724) and 1μg/mL GolgiPlug^{TM} (BD Biosciences, 555029) for 4 h.

2.5 Cell staining for flow cytometry

For *ex vivo* stainings, PBMCs were thawed and rested for 2 h at 37°C in antigen-specific T cell enrichment (ARTE) media (RPMI 1640 media supplemented with 2 mM L-Glutamine, 5% HS, 100 μg/mL Penicillin and Streptomycin (GIBCO, 15140-122)) at 20 million cells/mL. For *ex vivo* phenotypic characterization, 5x10^5-2x10^6 PBMCs were immediately stained after resting. For all stimulation experiments, cells were stained immediately after stimulation.

For all stainings, cells were stained with LIVE/DEAD Fixable Dead Cell Dyes (Thermo Fisher Scientific, L23105) according to the manufacturer's specifications. A Fc receptor (FcR) blocking step was performed using FcR Blocking Reagent Human (Miltenyi Biotec, 130-059-901) before cell surface antibody staining. The antibodies used in the cell surface staining are shown in Table 2.2. Cells were subsequently fixed using the Foxp3 staining buffer kit (Invitrogen, 00-5523-00) following the manufacturer's specifications. Cells were stained intracellularly after fixation. The antibodies used for intracellular staining are shown in Table 2.3. Intracellular staining was performed using the Foxp3 staining buffer kit. Following the staining, cells were resuspended in PBS for analysis on the flow cytometer. For samples where the number of cells were counted to determine absolute cell counts in a sample, the CountBright^{TM} Absolute Counting Beads (Invitrogen, C36950) were added to the sample before running on the Fortessa (BD Biosciences).

Table 2.2: Cell Surface Antibodies

Target	**Clone**	**Company**
CCR7	3D12	eBioscience
CD127	hIL-7R-M21	BD
CD137	4B4-1	Biolegend
CD154	24-31	Invitrogen
CD25	M-A251	Biolegend
CD27	0323	Biolegend
CD3	UCHT1	Biolegend
CD4	RPA-4	Biolegend and BD
CD40	5C3	Biolegend
CD45RA	HI100	BD
CD49d	9F10	Biolegend
CD69	FN50	Invitrogen
CD8	SK1	Biolegend and BD
CD80	2D10	Biolegend
CD86	BU63	Biolegend
CXCR3	1C6/CXCR3	BD
CXCR3	G025H7	Biolegend
HLA-DR	L243	Biolegend
IL17RA	BG/hIL17AR	Biolegend
LAG-3	11C3C65	Biolegend
NKG2A	131411	R&D Systems
NKG2D	1D11	Biolegend
panKIR	HP-MA4	Invitrogen
PD-1	MIH4	BD
PD-1	EG12.2H7	Biolegend
Tim-3	F38-2E2	Invitrogen
TIGIT	MBSA43	Invitrogen

Table 2.3: Intracellular Antibodies

Target	**Clone**	**Company**
BDNF	REA358	Miltenyi
C1q	JL-1	Invitrogen
C3	3E7/C3b	Biolegend
CXCL10	J034D6	Biolegend
EOMES	WD1928	eBioscience
Foxp3	PCH 101	Invitrogen
GATA3	TWAJ	Biolegend
GM-CSF	BVD2-21C11	Biolegend
Granzyme B	GB11	BD
IFN-γ	4S.B3	Biolegend
IL-10	JES3-19F1	Biolegend
IL-10	JES3-9DF	Biolegend
IL-1a	364-3B3-14	Biolegend
IL-13	JES10-5A2	Biolegend
IL-17A	TC11-18H10.1	Biolegend
IL-17A	BL168	Biolegend
IL-17F	SHLR17	eBioscience
IL-2	MQ1-17H12	BD
IL-21	eBio3A3-N2	Invitrogen
IL-22	22URTI	eBioscience
IL-6	MQ2-13A5	Biolegend
iNOS	REA451	Miltenyi
Ki67	B56	BD
ROR-γt	Q21-559	BD Pharmingen
SEMA4A	5E3	Invitrogen
T-bet	4B10	Invitrogen
Tax	LT-4	Prof. Tanaka, Ryukyus University
ThPOK	11H11A14	Biolegend
TNF	Mab11	Biolegend
RunX3	R3-5GH	Invitrogen

2.6 Flow cytometry data analysis, dimensionality reduction, and clustering

All samples were run on a Fortessa instrument (BD Biosciences) and analyzed using FlowJo v.10 (BD Biosciences).

2.6.1 Chapter 4: CD8$^+$ T cells in HTLV-1- Infection

To make comparisons between HTLV-1-specific CD8$^+$ T cells in AC hPVL and patients with HAM, dimensionality reduction and t-distributed Stochastic Neighbor Embedding (tSNE) plots were obtained by downsampling 10 AC hPVL and 10 patients with HAM samples to 145 HTLV-1-specific CD8$^+$ T cells per sample, and the concatenated sample was used to calculate tSNE axes using 1,000 iterations, perplexity of 30, and the default learning rate (203). The following compensated parameters were included in the tSNE analysis: T-cell immunoglobulin and mucin-domain containing-3 (Tim-3), Foxp3, CD127, programmed cell death protein 1 (PD-1), and CD25.

2.6.2 Chapter 5: CD4$^+$CD8$^+$ T cells in HTLV-1- Infection

To make comparisons between CD4$^+$, CD8$^+$ and DP T cells *ex vivo*, dimensionality reduction and tSNE plots were obtained by downsampling 14 AC lPVL and 14 AC hPVL samples to 416 events per T cell population per sample, and the concatenated sample was used to calculate tSNE axes using 1,000 iterations, perplexity of 30 and the default learning rate (2446). The following compensated parameters were included in the tSNE analysis: Tim-3, CD45RA, CD27, Foxp3, PD-1, CCR7, TIGIT, CD25, CD127. To make comparisons between the DP T cell populations in UCs and HTLV-1-infected groups, dimensionality reduction and tSNE plots were obtained by downsampling 11 samples per group (UC, AC lPVL, AC hPVL, HAM) to 523 events per sample, and the concatenated sample was used to calculate tSNE axes using 1,000 iterations, perplexity of 30 and the default learning rate (1610). To obtain cell clusters, I used the Phenograph plugin in FlowJo, with k=137 and the following compensated parameters: CD154, CD25, Tim-3, CD137, CD69, Foxp3, PD-1, and CD127.

2.7 Glial-T cell co-cultures

2.7.1 Astrocyte and microglia cell line cultures

The microglia cell line HMC3 (CRL-3304, ATCC) was cultured in complete microglia media (EMEM media (Sigma-Aldrich, M5650-500ML) supplemented with 10% FBS, 1 mM sodium pyruvate (GIBCO, 11360-070), 2 mM L-Glutamine (GIBCO, 25030-024), and 100 µg/mL Penicillin and Streptomycin (GIBCO, 15140-122)). Cultures were established between 1 x 10^4 and 4 x 10^4 cells/cm^2 and maintained between 1 x 10^4 and 2 x 10^5 cells/cm^2, split 1:4 when necessary, and the media renewed 2-3 times per week.

The astrocyte cell line CCF-STTG1 (CRL-1718, ATCC) was cultured in complete astrocyte media (RPMI 1640 media (Gibco, 21875034) supplemented with 10% FBS, 10 mM Hepes buffer solution (GIBCO, 15630-056), 1 mM sodium pyruvate (GIBCO, 11360-070), 2 mM L-Glutamine (GIBCO, 25030-024), and 100 µg/mL Penicillin and Streptomycin (GIBCO, 15140-122)). Cultures were established between 1 x 10^4 and 4 x 10^4 cells/cm^2 and maintained between 1 x 10^4 and 2 x 10^5 cells/cm^2, split 1:4 when necessary, and the media renewed 3 times per week.

Both cell lines were cultured at 37 °C and 5% CO_2. When splitting the cultures, 1-3 mL/ 75 cm^2 of Trypsin-EDTA (0.25%) (Gibco, 11570626) was added to the flasks for 15 min to detach the cells from the culture vessels when required.

2.7.2 Sorting HTLV-1-specific and non-specific T cells

Thawed PBMCs were rested and stimulated with heat-inactivated HTLV-1 for 12 h as previously described (section 2.4). PBMCs were stained as previously described, in Section 2.5, for CD3 (UCHT1, Biolegend), CD4 (RPA-4, Biolegend, BD), CD8 (SK1, Biolegend, BD), CD154 (32-31, Invitrogen), CD137 (4B4-1, Biolegend), and CD69 (FN50, Invitrogen). PBMCs were sorted in complete T cell media at 30 million cells/mL, and propidium iodide (PI) was added to samples before sorting to exclude dead cells. The following gating strategy was used to sort HTLV-1-specific and non-specific T cells: lymphocyte gating based on size and granularity based on FSC versus (vs.) SSC, single cells based on FSC-A vs. FSC-H, and live cells (cells negative for PI, Figure 2.1). HTLV-1-specific $CD4^+$ T cells were $CD3^+CD4^+CD8^-CD154^+$, HTLV-1-non specific $CD4^+$ T cells were

$CD3^+CD4^+CD8^-CD154^-$, HTLV-1-specific $CD8^+$ T cells were $CD3^+CD4^-CD8^+CD69^+CD137^+$, and non-HTLV-1-specific $CD8^+$ T cells were $CD3^+CD4^-CD8^+CD69^-CD137^-$ (Figure 2.1). Post-sort purity was determined in all samples by flow cytometry and was above 97% in all samples.

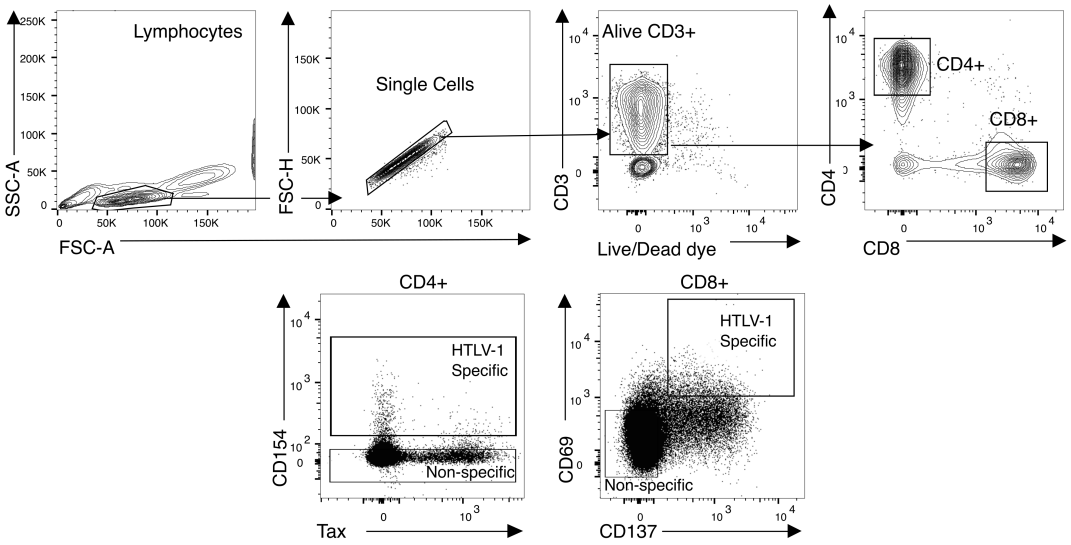


Figure 2.1: Gating strategy for sorting HTLV-1-specific and non-specific T cells. Total PBMCs were stimulated with heat-inactivated for 12 h and HTLV-1-specific T cells were identified as $CD154^+$ for $CD4^+$ T cells, and $CD69^+CD137^+$ for $CD8^+$ T cells [127, 316, 320, 323, 329].

2.7.3 Expansion of primary T cell lines

After the T cells were sorted, up to 100,000 T cells were plated in a 96-round bottom plate with 50,000 autologous irradiated PBMCs (30 gray), 20 U/mL IL-2, 30 ng/mL anti-CD3 (clone Hit3a, BD) and 30 ng/mL anti-CD28 (clone 28.2, BD) in CST media: CST™ OpTimizer™ T cell Expansion SFM (Gibco, A1048501) supplemented with 2 mM L-Glutamine and 1 x Penicillin and Streptomycin. T cell populations were expanded for 15 days, the media was changed every 2-3 days, and the cells split when necessary. After 15 days, T cell lines were washed to remove soluble anti-CD3 and IL-2 and left to rest for 48 h in 200 μL CST media.

2.7.4 Glial cell-T cell co-cultures

On day 16 of the T cell expansion, 24 h after the T cells were washed, astrocytes and microglia were plated at 10,000 cells per well in 100 μl in a flat-bottomed 96-well

plate (Corning, 10695951) in their respective media and left overnight to adhere to the plates. On day 17 of the T cell expansion, T cells were counted and 5000 cells were added per well to the astrocytes or microglia in the respective cell culture medias. T cells were stimulated with 1 μg/mL anti-CD3 (clone Hit3a) and 1 μg/mL anti-CD28 (clone 28.2) in a total volume of 200 μl per well. Cells were left in co-culture for 48 h.

2.7.5 Glial cell staining for flow

After 48 h, T cells were removed from the wells, and the adhesive glial cells were washed once with PBS. The T cells were stained and fixed for flow cytometry as previously described in Section 2.5. The glial cells were detached from the plate using 30 μl Accutase (Thermo, 00-4555-56) per well for 15 min. Astrocytes and microglia were stained with Annexin V (Biolegend, 640918) following the manufacturer's specifications. The glial cells were stained and fixed as previously described in Section 2.5. Astrocytes and microglia were identified by flow cytometry as CD3$^-$ cells (Figure 2.2).

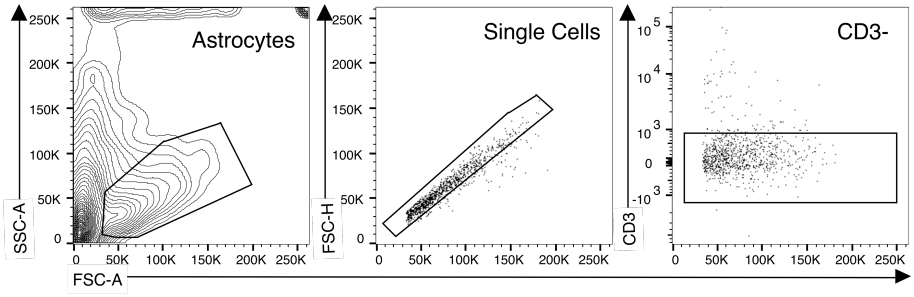


Figure 2.2: Gating strategy for identifying glial cells. After glial cells were co-cultured with T cells, the T cells were removed and the glial cells were washed with PBS and stained. Glial cells were identified as CD3$^-$.

2.8 HTLV-1 infection of sorted T cell populations

2.8.1 Sorting CD4$^+$, CD8$^+$, DP, and DN T cells for HTLV-1-infection

Fresh PBMCs were stained immediately after PBMCs isolation for CD3 (UCHT1, Biolegend), CD4 (RPA-4, Biolegend, BD), and CD8 (SK1, Biolegend, BD). Samples were kept on ice at 30 million cells/mL in complete T cell media and sorted cold. 1 μg/mL

PI was added to the cells before the start of the sort to identify dead and dying cells. The following gating strategy was used to sort $CD4^+$ SP, $CD8^+$ SP, DP, and DN T cells: lymphocyte gating based on size and granularity based on forward scatter (FSC) vs. side scatter (SSC), single cells based on FSC-A vs. FSC-H, and live cells (cells negative for PI, Figure 2.3). CD4 SP T cells were $CD3^+CD4^+CD8^-$, CD8 SP T cells were $CD3^+CD4^-CD8^+$, DP T cells were $CD3^+CD4^+CD8^+$, and DN cells were $CD3^+CD4^-CD8^-$ (Figure 2.3). Post-sort purity was determined in all samples by flow cytometry and was above 95% in all samples.

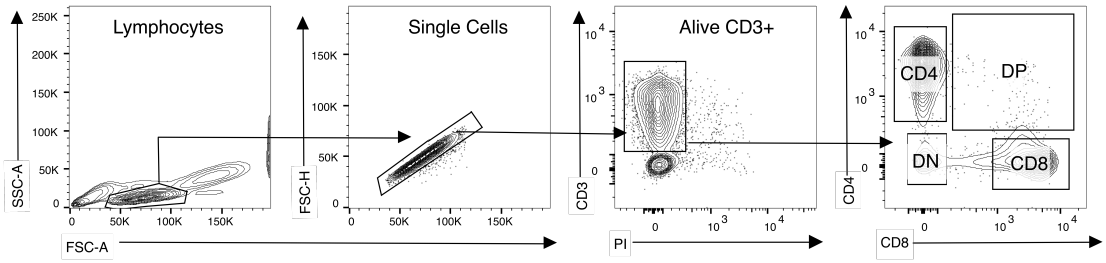


Figure 2.3: Gating strategy for sorting $CD4^+$ SP, $CD8^+$ SP, DP, and DN T cells from total PBMCs.

2.8.2 HTLV-1-infection of primary T cells

MT-2 and Jurkat cells (JKT) cells were cultured for at least 2 weeks before using them for experiments. MT-2 or JKT cells were plated at 0.3 million cells/mL in complete T cell media and split once a week until use. Fresh PBMCs from uninfected donors were sorted into $CD4^+$ SP, $CD8^+$ SP, DP, and DN T cell populations. For T cells co-cultured with MT-2 cells and the HIV integrase inhibitor raltegravir, the sorted T cells were pre-treated with 10 μM raltegravir in complete T cell media for 2 h before the addition of MT-2 cells. The sorted T cells were co-cultured with either MT-2 or JKT cells at a 5:1 ratio (T cell:MT-2/JKT) at 1 million cells/ mL in complete T cell media supplemented with 20 U IL-2, and for the raltegravir co-culture samples, with 10 μM raltegravir. MT-2 and JKT cells had been irradiated with 400 gray to inhibit proliferation and labeled with CellTace^{TM} carboxyfluorescein succinimidyl ester (CSFE) (ThermoFisher, C34554) or Violet (ThermoFisher, C34557) Cell Proliferation Kit following manufacturers instructions to distinguish them from the sorted T cell populations. Cells were stained on day 1, 4, 6, 8, 11, 13, 15, 18, 20, and 22 and the media was changed on those days and the cells split

when necessary.

2.9 Astrocyte-DP T cell co-culture

24 h before the start of the co-culture experiments, the astrocyte cell line (CRL-1718, ATCC) was plated in a flat bottom 96-well plate (Corning, 10695951) at 10,000 cells per well in 100 μl complete astrocyte media.

24 h before the start of the co-culture experiment, PBMCs were thawed, rested, and stimulated with heat-inactivated HTLV-1 for 12 h, as previously described (section 2.4). $CD4^+$ SP, $CD8^+$ SP, and DP T cells were sorted as previously described (section 2.8.1). 5000 T cells were resuspended in 100 μl astrocyte media and placed in co-culture with the astrocytes for 36 h. Subsequently, the media and non-adhesive T cells were removed from the wells, the wells were washed with PBS, and 50 μl Accutase (Invitrogen, 00-4555-56) was added to the wells for 15 minutes to detach the astrocytes. Astrocytes were stained with Annexin V (Biolegend, 640918) following the manufacturer's specifications. The astrocytes were stained and fixed as previously described in Section 2.5. Astrocytes were identified by flow cytometry as $CD3^-$ cells (Figure 2.2).

2.10 RNA-Seq analysis

2.10.1 Stimulation, magnetic enrichment, and staining of HTLV-1-specific $CD4^+$ T cells

10 million freshly isolated PBMCs were rested at 4°C for 3-5 h in ARTE media at 20 million cells/mL and then stimulated with heat-inactivated HTLV-1 or a control for 12 h, as previously described (section 2.4). $CD154^+$ cells were magnetically enriched using the protocol described in the human CD154 MicroBead Kit Miltenyi Biotec data sheet (130-092-658). Cells were stained for CD4 (RPA-4, Biolegend, BD), CD45RA (HI100, BD), and CD154 (24-31, Invitrogen) on the magnetic column. Antibodies targeting cell surface antigens were prepared in 60 μl PBS per sample and the cells were stained for 15 min. After magnetic enrichment, cells were resuspended in 300 μl PBS for sorting.

2.10.2 Sorting HTLV-1-specific CD4$^+$ T cells

1 μg/mL PI was added to the cells before the start of the sort to identify dead and dying cells. The following gating strategy was used to sort CD154$^+$ CD4$^+$ T cells: lymphocyte gating based on size and granularity based on FSC vs. SSC, single cells based on FSC-A vs. FSC-H, live cells (cells negative for PI), and CD4$^+$CD154$^+$ (Figure 2.4). Post-sort purity was determined in all samples by flow cytometry and was above 97% in all samples.

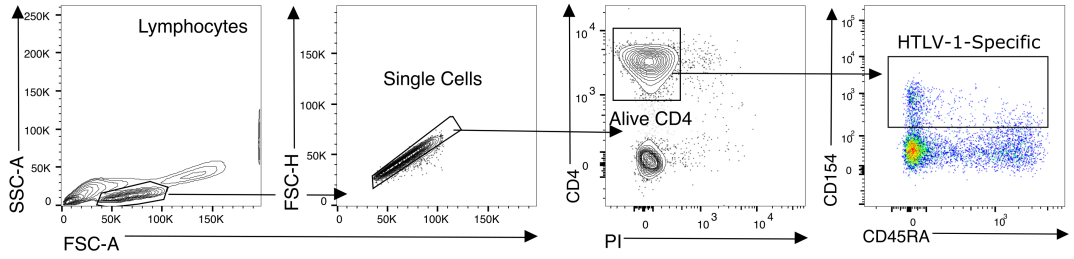


Figure 2.4: Gating strategy for sorting HTLV-1-specific CD4$^+$ T cells. Total PBMCs were stimulated with heat-inactivated HTLV-1 for 12 h before magnetic enrichment of CD154$^+$ cells and staining for sorting.

2.10.3 RNA isolation and quantification

RNA was isolated using the RNeasy Micro Plus Kit (Qiagen, 74004) following the manufacturer's guidelines in Appendix D of the Qiagen RNeasy handbook. RNA quality was quantified using the Agilent RNA 6000 Pico Kit (Agilent Technologies, 5067- 1513) following the manufacturer's guidelines. RNA samples were stored at -80°C until further processing.

2.10.4 RNA sequencing

RNA sequencing (RNA-seq) was performed by the Oxford Genomics Center where the RNA library was prepared using the RNA-Seq Ultra Low library prep (Illumina). All samples were pooled together and 150 bp paired-ends reads were sequenced on a Novaseq system, resulting in a median read count of 32 million reads per sample.

2.10.5 Processing RNA data

Raw data was processed using the Imperial College London Nextflow RNA-seq pipeline, version 3.5. The Imperial College London computing-compatible Nextflow profile was written by Dr. Combiz Khozoie. Using this Nextflow pipeline, reads were aligned to the reference genome (GRCh37) using STAR v2.7.10b [330], and gene counts were quantified using Salmon [331]. Mapping table and quality control metrics from FastQC indicated high data quality for all samples with no outliers detected [332].

Given that UCs had a much lower input number of HTLV-1-specific cells, 2 separate analyses were performed: the first analysis contained all groups including UCs, AC lPVL, AC hPVL, and patients with HAM, while the second group only contained the HTLV-1-infected groups including AC lPVL, AC hPVL, and patients with HAM. RNA-seq data analysis was performed using R v4.1.1 in Rstudio. Genes that did not have at least 5 reads in at least 7 samples (the size of the smallest biological subgroup) were filtered out using the genefilter package [333], resulting in a processed data set of 12,250 genes for the HTLV-1 patient analysis and 12,468 genes when UCs were included. Principal component analysis (PCA) with the prcomp function was used to explore the relationship between samples after the filtered gene counts were transformed using a regularized log transformation from the DESeq2 package [334].

2.10.6 Differential gene expression analysis

Differential gene expression analysis was performed using DESeq2 [334], comparing HTLV-1-specific $CD4^+$ cells from uninfected controls (UCs, n=9) with each of the HTLV-1-infected groups: asymptomatic carriers with low proviral load (AC lPVL, n=10), asymptomatic carriers with high proviral load (AC hPVL, n=7), and patients with HAM (HAM, n=9). A second differential gene expression analysis, limited to the HTLV-1-infected groups, compared each group to the others: AC lPVL vs. AC hPVL, AC lPVL vs. HAM, and AC hPVL vs. HAM. For clustering analysis in the PCA, k-means clustering was conducted using the first 19 principal components (PCs), which together accounted for 90% of the cumulative variance. The algorithm was set to identify 3 clusters, with a random seed of 123 to ensure reproducible results.

Genes with false discover rate (FDR)$\leq$0.05 and a fold change (FC)$\geq$1.5 were deemed

significantly differentially expressed [335]. Pathway enrichment analysis was performed using Fisher's exact test in XGR with annotations from Reactome, using all genes retained in the processed RNA-seq data as the background, and employing the xEnrichConciser options [336]. An adjusted p-value (p adj, FDR) threshold of 0.05 was used to identify significantly enriched pathways.

2.11 Quantification of mRNA expression by real-time PCR

Fresh PBMCs were stimulated with HTLV-1 and the HTLV-1-specific $CD4^+$ T cells were magnetically enriched and sorted as previously described in sections 2.10.1 and 2.10.2. RNA was isolated using the RNeasy Micro Plus Kit (Qiagen, 74004) following the manufacturer's guidelines in Appendix D of the Qiagen RNeasy handbook. Isolated RNA was converted to complementary DNA by reverse transcription (RT) with random hexamers and Multiscribe RT (TaqMan Reverse Transcription Reagents; Thermo Fisher Scientific, N8080234). For real-time reverse transcription–polymerase chain reaction (RT-PCR), Table 2.4 lists the probes from Thermo Fisher Scientific that were used.

The reactions were set up using the manufacturer's guidelines and run on a StepOnePlue RT-PCR Machine (Thermo Fisher Scientific). Values are represented as the difference in cycle threshold (Ct) values normalized to *B2M* expression for each sample as per the following formula: Relative RNA expression = (2-ΔCt) x 1000 [337].

2.12 Determining PVL by digital droplet PCR

2.12.1 Sorting of fixed cells for ddPCR

Total PBMCs were stimulated with heat-inactivated HTLV-1 for 12 h as previously described in section 2.4. PBMCs were stained with fixable viability dye, then stained for cell surface receptors, fixed, and stained intracellularly as described in section 2.5. The following cell surface antibodies were used: CD3 (UCHT1, Biolegend), CD4 (RPA-4, Biolegend, BD), CD8 (SK1, Biolegend, BD), CD69 (FN50, Invitrogen), CD137 (4B4-1, Biolegend), CD154 (24-31, Invitrogen); and the following intracellular antibody was

Table 2.4: RT-PCR Probes

Gene	Assay Identification Number
ABR	(Hs01077820_m1)
ARHGAP4	(Hs00155870_m1)
B2M	(Hs00187842_m1)
ECT2	(Hs00978168_m1)
FGD1	(Hs00171676_m1)
FDG3	(Hs00382004_m1)
PREX1	(Hs01031507_m1)
GNA12	(Hs04992528_s1)
GNA13	(Hs00183573_m1)
RIPK2	(Hs01572686_m1)
ADCY7	(Hs00181579_m1)
TICAM1	(Hs00706140_s1)
SEMA4A	(Hs00223617_m1)
EOMES	(Hs00172872_m1)

used: Tax (LTA-4, Prof. Tanaka Ryukyus University). Samples were kept on ice and sorted cold. As previously described, the following gating strategy was used to sort CD4 SP, CD8 SP, DP, and DN T cells: lymphocyte gating based on size and granularity-based on FSC vs. SSC, single cells based on FSC-A vs. FSC-H, and live cells (cells negative for the fixable viability dye). CD4 SP T cells were $CD3^{+}CD4^{+}CD8^{-}$, CD8 SP T cells were $CD3^{+}CD4^{-}CD8^{+}$, DP T cells were $CD3^{+}CD4^{+}CD8^{+}$, and DN cells were $CD3^{+}CD4^{-}CD8^{-}$ (Figure 2.3). DNA was isolated immediately after sorting. Post-sort purity was determined in all samples by flow cytometry and was above 95% in all samples.

2.12.2 DNA isolation

DNA was extracted from up to 5 million cells using an optimized protocol for fixed cells [337]. Briefly, sorted T cells were pelleted and resuspended in 0.6 mL lysis buffer (50 mM Tris, 50 mM EDTA, 1% SDS, pH 8). 3 μL Proteinase K (Qiagen, 19131) was added and the samples were incubated at 55°C overnight. RNase A (Qiagen, 19101) was diluted to 10 mg/mL in lysis buffer, and 3 μl was added to the samples and incubated at 37°C for 30 min. The samples were cooled down on ice for 30 min. 0.2 mL of pre-chilled 7.5 M ammonium acetate solution was added and the samples were centrifuged at 4000 x g for 10 min. The supernatant was transferred to a fresh tube, 0.6 mL of isopropanol was added and the samples were centrifuged at 4000 x g for 10 min. The supernatant was discarded and 0.6 mL of 70% ethanol was added and the sample was centrifuged at 4000 x g for 1 min. The supernatant was discarded and the tubes were left to air dry for 20 min. 50 μL Tris-EDTA buffer (Sigma, T9285) was added, incubated at 65°C for 1 h, and left at room temperature overnight. The DNA concentration was quantified using a Nanodrop instrument.

2.12.3 PVL quantification by ddPCR

The PVL in the sorted T cell populations was quantified using ddPCR. HTLV-1 primers and probes were designed to bind HTLV-1 *tax* and human *albumin*. The primers and probes were adapted from previous publications [338, 339]. Primers and probes were obtained from Integrated DNA Technologies (Coralville, IA). A reaction mixture with a final concentration of 2 ng/uL DNA, 900 nm *tax* forward and reverse primer,

600 nM *albumin* forward and reverse primer, 250 nM *tax* probe, 250 nM *albumin* probe, and 1 x ddPCR Supermix for Probes (no dUTP) (Bio-Rad, 186-3023) was prepared in a total volume of 22 μL. The primer and probes sequences are as follows: HTLV-1 *tax* forward primer: (5'-CGG ATA CCC AGT CTA CGT GTT-3')[339], HTLV-1 *tax* reverse primer: (5'-CAG TAG GGC GTG ACG ATG TA-3')[339], HTLV-1 *tax* double quencher probe: (5'-56-FAM/CTG TGT ACA/ZEN/AGG CGA CTG CC/3IABkFQ-3')[339], *albumin* forward primer: (5'-TGC ATG AGA AAA CGC CAG TAA-3') [338], *albumin* reverse primer: (5'-ATG GTC GCC TGT TCA CCA A-3') [338], *albumin* double quencher probe: (5'-/HEX/TGA CAG AGT / ZEN/ CAC CAA ATG CTG CAC AGA A/3lABkFQ/-3') [338].

The ddPCR reaction was prepared in a white/clear hard-shell 96-well PCR plate with samples and controls, mixed, and 20 μL were transferred to an 8 channel DG8^{TM} cartridge (Bio-Rad, 1864008) with 70 μL droplet generation oil (Bio-Rad, 1863005). A DG^{TM} Gasket (Bio-Rad, 1863009) is placed over the cartridge and the cartridge is placed in the QX200 droplet generator (Bio-Rad, 1864002) for droplet formation. 40 μL of droplets were transferred to a semi-skirted clear 96-well PCR plate (Bio-Rad, 12001925), sealed with a pierce-able foil heat seal (Bio-Rad 1814040) in the PX1 PCR Plate Sealer (Bio-Rad, 1814000), and placed into the C1000 Touch Thermal Cycler (Bio-Rad) for amplification. The cycling conditions were as follows: 10 min at 95°C, 40 cycles each of 30 seconds (sec) at 94°C followed by 1 min at 60°C, and 10 min at 98°°C. A 2°C/s ramp rate was set for each cycling step. Samples were transferred immediately to the QX200 Droplet Reader (Bio-Rad). Results from the QX200 droplet reader were recorded in Bio-Rad's QuantaSoft software (version 1.7) using absolute quantification. The software counts the number of positive and negative droplets and calculates the number of copies per μL. The HTLV-1 PVL was calculated by dividing the number of *tax* positive droplets by the number of *albumin* positive droplets divided by 2 (to account for the two copies of *albumin* in the genome). Each ddPCR experiment had non-template negative controls and a positive control with a known HTLV-1 PVL of 100%.

2.13 Statistics and data presentation

Graphs were drawn using R V2022.12.0+353. Data were tested for normality using the Shapiro-Wilk normality test. Statistical significance for normally distributed data was calculated using a T test and non-parametric data were tested using the Wilcoxon signed-rank test. Significance was corrected for multiple comparisons using the Holm method. For data where I only made pre-defined comparisons rather than all possible comparisons between groups, I did not correct for multiple comparisons to avoid false negatives [340].

2.14 Diagrams

Diagrams were drawn using BioRender.

3

$CD4^+$ T cells in HTLV-1 infection

3.1 Introduction

Despite affecting up to 3% of HTLV-1 carriers and causing decades of serious disability and morbidity, the pathogenesis of HAM is not well understood and treatment options remain extremely limited. The current hypothesis of HAM pathogenesis is that an inefficient immune response results in a high PVL and chronic high level of HTLV-1 antigen expression, which persistently activate HTLV-1-specific T cells [243, 341]. During early HAM pathogenesis, activated $CD4^+$ T cells appear to first infiltrate and accumulate in the CNS, and then recruit $CD8^+$ T cells to the CNS lesions over time [158, 251, 259]. Despite $CD4^+$ T cells predominating in early HAM lesions [259], very little work has been done to characterize HTLV-1-specific $CD4^+$ T cell responses. Previous studies have used IFN-γ secretion after stimulation with an HTLV-1 peptide library to identify HTLV-1-specific $CD4^+$ T cells and showed that patients with HAM had a 25-fold greater frequency of IFN-γ^+ HTLV-1-specific $CD4^+$ T cells relative to ACs [300, 301]. These studies also showed that these IFN-γ^+ HTLV-1-specific $CD4^+$ T cells were infected with HTLV-1 at higher rates relative to non-HTLV-1-specific $CD4^+$ T cells [300, 301]. Outside of these studies, very little work has been done to characterize HTLV-1-specific $CD4^+$ T cell responses

or explore how HTLV-1-specific CD4$^+$ T cell dysfunction contributes to the inability to maintain a low PVL or drive neuroinflammation in HAM.

This chapter aimed to deeply phenotypically and functionally characterize HTLV-1-specific CD4$^+$ T cells in UCs, AC lPVL, AC hPVL, and patients with HAM to gain insight into how HTLV-1-specific CD4$^+$ T cell dysfunction contributes to a high PVL and/or HAM pathogenesis. Given the importance of virus-specific CD4$^+$ T cell responses in other viral infections, such as HIV and HCV, I wanted to gain insight into the differences in HTLV-1-specific CD4$^+$ T cell response between AC lPVL and AC hPVL and to identify CD4$^+$ T cell phenotypes associated with effective HTLV-1 control. Furthermore, given that CD4$^+$ T cells predominate in early HAM lesions and carry 95% of the HTLV-1 PVL [193], I aimed to further elucidate how HTLV-1-specific CD4$^+$ T cells in patients with HAM differ from AC hPVL, and gain insights into the mechanisms by which they can contribute to CNS pathology.

In this chapter, I identified HTLV-1-specific CD4$^+$ T cells by stimulating total PBMCs with heat-inactivated HTLV-1 and identified HTLV-1-specific CD4$^+$ T cells using the CD154 activation induced marker [69, 324]. I observed that the frequency and number of HTLV-1-specific CD4$^+$ T cells increased with PVL, and that patients with HAM and AC hPVL have the same number and frequency of HTLV-1-specific CD4$^+$ T cells. In agreement with previous studies, I show that HTLV-1-specific CD4$^+$ T cells are infected at higher rates relative to bulk CD4$^+$ T cells and this preferential infection is more pronounced in high PVL groups. Using functional and phenotype characterization, I show that HTLV-1-specific CD4$^+$ T cells from patients with HAM express higher levels of CD49d, indicating an enhanced capacity to migrate to the CNS. To gain insight into how HTLV-1-specific CD4$^+$ T cells may interact with glial cells and contribute to neuroinflammation, I co-cultured HTLV-1-specific CD4$^+$ T cells from UCs, AC lPVL, AC hPVL, and patients with HAM with astrocyte or microglial cell lines. HTLV-1-specific CD4$^+$ T cells from patients with HAM reduced the viability of both astrocytes and microglia in co-culture, induced the upregulation of the antigen presentation machinery, and increased astrocyte expression of proinflammatory cytokines and chemokines including IFN-γ and CXCL10, when compared to glial cells co-cultured with HTLV-1-specific CD4$^+$ T cells from AC hPVL matched in PVL. To gain insight into the mechanism of how HTLV-1-specific CD4$^+$ T cells induced these changes, I performed RNA-seq analysis on HTLV-

1-specific CD4$^+$ T cells from UCs, AC lPVL, AC hPVL, and patients with HAM. The transcriptional profile of HTLV-1-specific CD4$^+$ T cells was distinct in the 4 groups studied, and I identified 628 differentially expressed genes (DEGs) in patients with HAM when compared to AC hPVL, including the upregulation of genes for Eomesodermin (*EOMES*), semaphorin-4A (*SEMA4A*), IL-17 receptor C (*IL17RC*), *IL17RA*, and genes associated with an enhanced Th1 phenotype. Pathway enrichment analysis showed that HTLV-1-specific CD4$^+$ T cells in patients with HAM upregulate G alpha (12/13) signaling events, have increased novel melanoma antigen gene protein (NRAGE) death signaling through c-Jun N-terminal kinases (JNK), and increased signaling by p75 neurotrophin receptor (p75NTR) relative to AC hPVL. These pathways, in addition to Th1 cytokines, have the potential to modulate CNS resident cells. The data in this chapter provide a deeper understanding of the direct contribution of CD4$^+$ T cells to HAM pathogenesis and identifies novel potential targets, including CD49d and G (12/13) alpha signaling, for HAM treatment.

3.2 Results

3.2.1 Identification and initial characterization of HTLV-1-specific CD4$^+$ T cells

Throughout this chapter, HTLV-1-infected individuals were grouped into ACs with a PVL under 3% (low PVL, AC lPVL), ACs with a PVL above 3% (high PVL, AC hPVL), and untreated patients with HAM. The PVLs of the AC hPVL and HAM groups were matched to control for differences due to HTLV-1 infection (Table 2.1). Throughout this chapter, unless otherwise stated, I focused my statistical comparisons to identify relevant differences between UC and AC lPVL to identify changes that occur due to HTLV-1 infection, between AC lPVL and AC hPVL to identify differences associated with PVL, and between AC hPVL and HAM to identify differences associated with disease status. These comparisons aimed to gain insight into the mechanisms by which some ACs can effectively control HTLV-1 infection and maintain a low PVL, and identify differences between ACs and patients with HAM to gain insight into HAM pathogenesis while controlling for differences caused by PVL.

To identify HTLV-1-specific CD4$^+$ T cells, total PBMCs were stimulated with heat-inactivated HTLV-1 for 12 h. CD4$^+$ T cells from UCs, AC lPVL, AC hPVL, and patients with HAM were identified by flow cytometry (Figure 3.1), and HTLV-1-specific CD4$^+$ T cells were identified based on the expression of CD154 (Figure 3.2a) [69, 324].

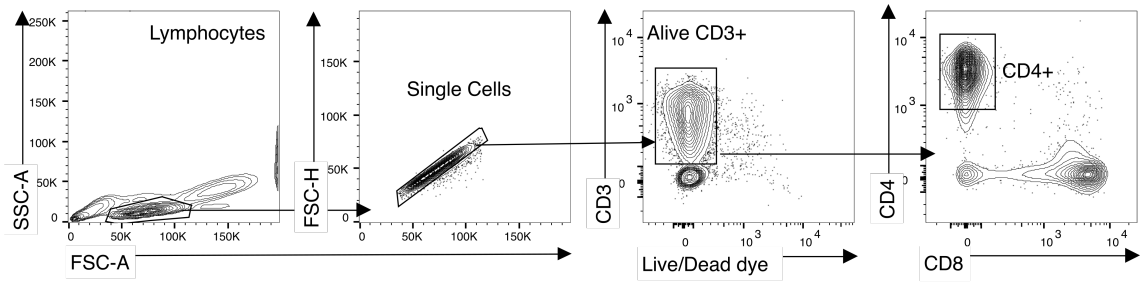


Figure 3.1: Gating strategy to identify CD4$^+$ T cells. Total PBMCs were stimulated with heat-inactivated HTLV-1 and the CD4$^+$ T cells identified by flow cytometry.

The frequency and number (in 10 million PBMCs) of HTLV-1-specific CD4$^+$ T cells were characterized in UCs and the different HTLV-1-infected groups (Figure 3.2b). Unsurprisingly, UCs that had never been exposed to the virus had very few CD154$^+$ CD4$^+$ T cells, and the cells that were CD154$^+$ were likely cross-reactive from previous infections or naï've cells. In HTLV-1-infected individuals, the number and frequency of HTLV-1-specific CD4$^+$ T cells significantly increased with PVL. There were no differences between AC hPVL and patients with HAM.

Intrigued by the observation that patients with higher PVLs also had more HTLV-1-specific CD4$^+$ T cells, I characterized the HTLV-1-infection rate of the HTLV-1 specific CD4$^+$ T cells by staining for the HTLV-1 protein Tax (Figure 3.2a). Tax is dynamically expressed, and all Tax$^+$ cells are likely to be infected, but not all infected cells are Tax$^+$ [209]. In agreement with previous studies, I observed that HTLV-1-specific CD4$^+$ T cells were infected at higher rates relative to the non-HTLV-1 specific CD4$^+$ T cells (Figure 3.2c) [301]. However, this preferential infection was more significant in high PVL groups, with only a mean of 13.2% of HTLV-1-specific CD4$^+$ T cells in AC lPVL expressing Tax, and 46.8% and 39.8% of HTLV-1-specific CD4$^+$ T cells expressing Tax in AC hPVL and HAM respectively. Given the dynamic nature of Tax expression, I confirmed that Tax expression at the 12 h timepoint in CD4$^+$ T cells correlates with the PVL measured by ddPCR, confirming that using Tax expression measured by flow cytometry at the 12 h timepoint is a reliable readout for infection (Figure 3.2d). These data suggest that

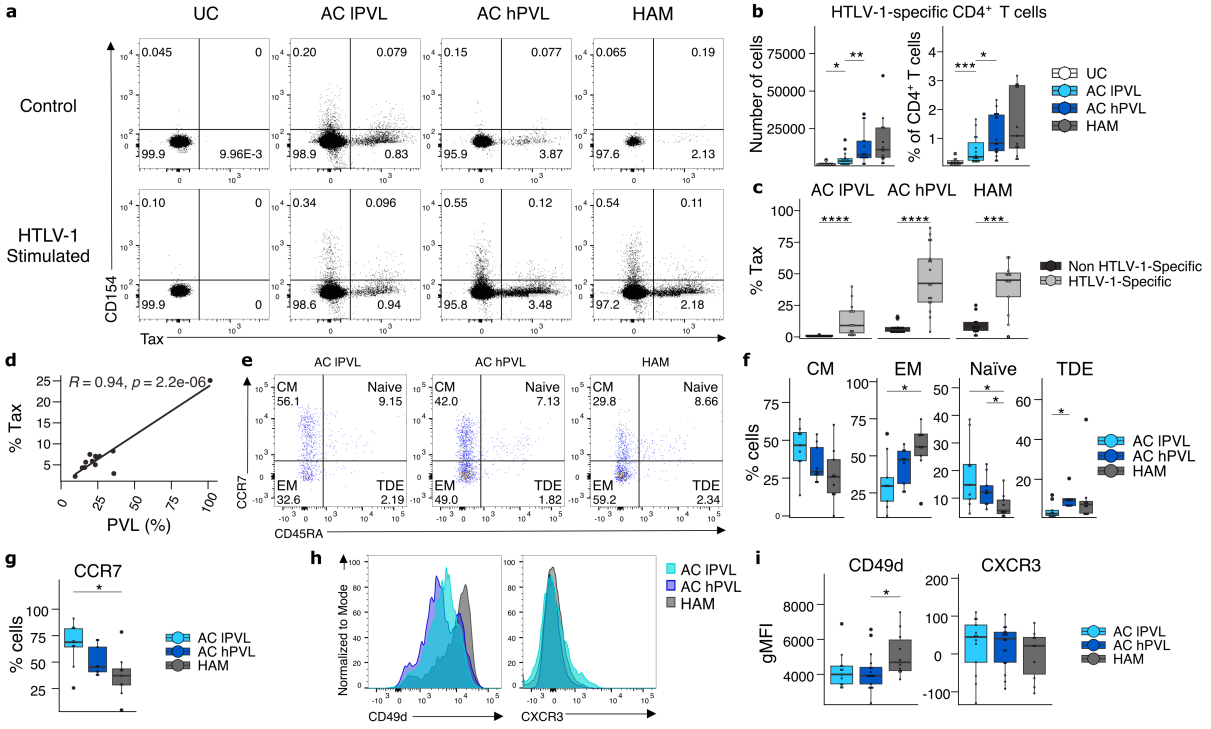


Figure 3.2: HTLV-1-specific CD4$^+$ T cell *ex vivo* identification and characterization. a. Representative flow plots showing CD154$^+$ and HTLV-1 Tax expression after a 12 h stimulation with heat-inactivated HTLV-1 or a control. **b.** Box and whisker plots showing the number and frequency of HTLV-1-specific CD4$^+$ T cells identified from 10 million PBMCs (n=15 UC, n=15 AC lPVL, n=17 AC hPVL, n=13 HAM). **c.** Box and whisker plots showing HTLV-1 Tax expression in HTLV-1-specific and non-specific CD4$^+$ T cells (n=15 AC lPVL, n=17 AC hPVL, n=13 HAM). **d.** Scatter plot of Tax expression in CD4$^+$ T cells after 12 h in culture vs. the PVL measured by ddPCR (n=7 AC hPVL, n=6 HAM). Representative flow plots (**e**) and box and whisker plots (**f**) showing the frequency of central memory (CM), effector memory (EM), naïve, and terminally differentiated effector (TDE) HTLV-1-specific CD4$^+$ T cells (n=9 AC lPVL, n=9 AC hPVL, n=9 HAM). **g**. Box and whisker plot showing CCR7 expression in HTLV-1-specific CD4$^+$ T cells (n=9 AC lPVL, n=9 AC hPVL, n=9 HAM). Representative histograms (**h**) and box and whisker plots (**i**) showing the gMFI of CD49d and CXCR3 expression in HTLV-1-specific CD4$^+$ T cells (n=13 AC lPVL, n=17 AC hPVL, n=10 HAM). **b)** Wilcoxon signed-rank unpaired test for comparisons between UC and AC lPVL, AC lPVL and AC hPVL, and AC hPVL and HAM; **c)** Wilcoxon signed-rank paired test for comparisons between HTLV-1-specific and non-HTLV-1-specific CD4$^+$ T cells; **d)** Pearson correlation coefficient (R) and p-value; **f)** Wilcoxon signed-rank paired test with Holm correction; **g)** T-test with Holm correction; **i)** T test for comparisons between AC lPVL and AC hPVL, AC hPVL and HAM; *p≤0.05, **p≤0.01, ***p≤0.001, ****p≤0.0001.

neither an increased frequency of HTLV-1-specific $CD4^+$ T cells nor a preferential HTLV-1 infection of these cells is associated with HAM pathogenesis, as there were no differences in hPVL between asymptomatic carriers and patients with HAM.

To gain further insight into the memory phenotype of HTLV-1-specific $CD4^+$ T cells in different HTLV-1-infected groups, the markers CCR7 and CD45RA were used to classify HTLV-1-specific $CD4^+$ T cells into central memory (CM, $CCR7^+CD45RA^-$), naïve ($CCR7^+CD45RA^+$), terminally differentiated effector (TDE, $CCR7^-CD45RA^+$), and effector memory (EM, $CCR7^-CD45RA^-$) cells (Figure 3.2e) [18, 82, 83]. Patients with HAM had significantly higher frequencies of EM cells relative to AC lPVL, with a similar but not significant trend relative to AC hPVL (Figure 3.2f). Patients with HAM had lower frequencies of naïve cells, with a similar but not significant trend in CM cells. The frequency of TDE cells increased significantly with PVL. HTLV-1-specific $CD4^+$ T cells in patients with HAM expressed significantly lower levels of the lymphocyte homing marker CCR7 (Figure 3.2g).

While HTLV-1-specific $CD4^+$ T cells from patients with HAM expressed lower levels of the lymph node homing marker CCR7, they expressed higher levels of the integrin and tissue homing marker CD49d (α chain of very late antigen-4 (VLA-4)) than AC hPVL but similar levels of CXCR3 relative to ACs (3.2h and 3.2i). The increased CD49d expression suggests an increased migratory capacity to tissues and the CNS. Overall these data show that the number of HTLV-1-specific $CD4^+$ T cells increases with PVL and is not affected by disease status, HTLV-1-specific $CD4^+$ T cells are infected by HTLV-1 at higher rates than non-HTLV-1-specific $CD4^+$ T cells, and patients with HAM have increased frequencies of EM cells with a potentially enhanced capacity to migrate to the CNS.

3.2.2 HTLV-1-specific CD4$^+$ T cells from patients with HAM induce proinflammatory astrocytes

Given the pathology of HAM, the increased potential for HTLV-1-specific CD4$^+$ T cell to migrate to the CNS as a result of high CD49d expression and the enhanced effector memory phenotype, I wanted to determine the effect of HTLV-1-specific CD4$^+$ T cells on CNS resident cells such as astrocytes and microglia. Astrocytes are the most abundant cell type in the CNS and play a crucial role in maintaining homeostasis, supporting neuronal function, and protecting the brain by controlling endothelial cells in the BBB and regulating neurotransmitter levels [342].

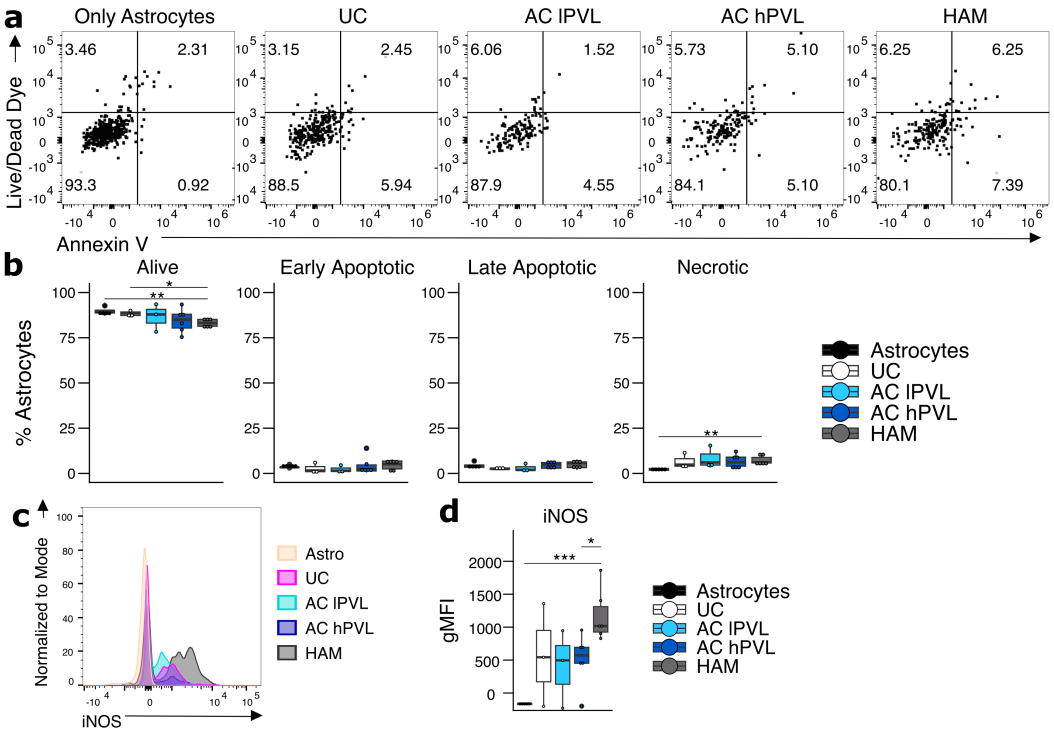


Figure 3.3: The effect of HTLV-1-specific CD4$^+$ T cells on the viability and iNOS expression of astrocytes. Representative flow plots (**a**) and box and whisker plots (**b**) showing the frequency of alive, early apoptotic, late apoptotic, and necrotic astrocytes after 48 h alone in culture or co-cultured with HTLV-1-specific CD4$^+$ T cells from different patient groups (n=5 only astrocytes, n=3 UC, n=3 AC lPVL, n=6 AC hPVL, n=6 HAM). Representative histogram (**c**) and box and whisker plot (**d**) showing the gMFI of iNOS of astrocytes after 48 h alone in culture or co-culture with HTLV-1-specific CD4$^+$ T cells from different groups (n=5 only astrocytes, n=3 UC, n=3 AC lPVL, n=6 AC hPVL, n=6 HAM). **b, d)** T-test with Holm correction; *p≤0.05, **p≤0.01, ***p≤0.001, ****p≤0.0001.

I sorted HTLV-1-specific CD4$^+$ T cells from UCs, AC lPVL, AC hPVL, and patients with HAM, expanded them *in vitro* for 17 days, and then placed them in co-culture with an astrocyte cell line (CCF-STTG1, an astrocytoma cell line) for 48 h with anti-CD3 and

anti-CD28 (to activate the $CD4^+$ T cells). Using a fixable viability dye and staining for Annexin V, I was able to identify alive (Annexin V^- and Live/Dead Dye^-), early apoptotic (Annexin V^+ and Live/Dead Dye^-), late apoptotic (Annexin V^+ and Live/Dead Dye^+), and necrotic (Annexin V^- and Live/Dead Dye^+) astrocytes after 48 h in culture alone or with HTLV-1-specific $CD4^+$ T cells from UCs, AC lPVL, AC hPVL, and patients with HAM (Figure 3.3a). There was a moderate but significant decrease in the viability of astrocytes co-cultured with HAM HTLV-1-specific $CD4^+$ T cells relative to astrocytes by themselves or astrocytes co-cultured with HTLV-1-specific $CD4^+$ T cells from UCs with 83.2%, 89.7%, and 89.7% viability respectively. The difference in viability is mainly due to an increased frequency of necrotic cells when in co-culture with HAM HTLV-1-specific $CD4^+$ T cells (Figure 3.3b). Overall the viability remained high and similar levels of viability were seen with cells from UCs, AC lPVL, and AC hPVL.

Despite only a moderate reduction in the viability of astrocytes by HTLV-1-specific $CD4^+$ T cells from patients with HAM, HTLV-1-specific $CD4^+$ T cells from patients with HAM induced increased astrocyte activation relative to AC hPVL as shown by the significantly higher geometric mean fluorescence intensity (gMFI) of iNOS (Figure 3.3c and 3.3d).

Astrocytes were also stained for activation markers and cytokines. Representative stainings can seen in Figure 3.4. For flow plots where there was no clear positive and negative population, fluorescence minus one controls (FMOs) were used to place the quadrants.

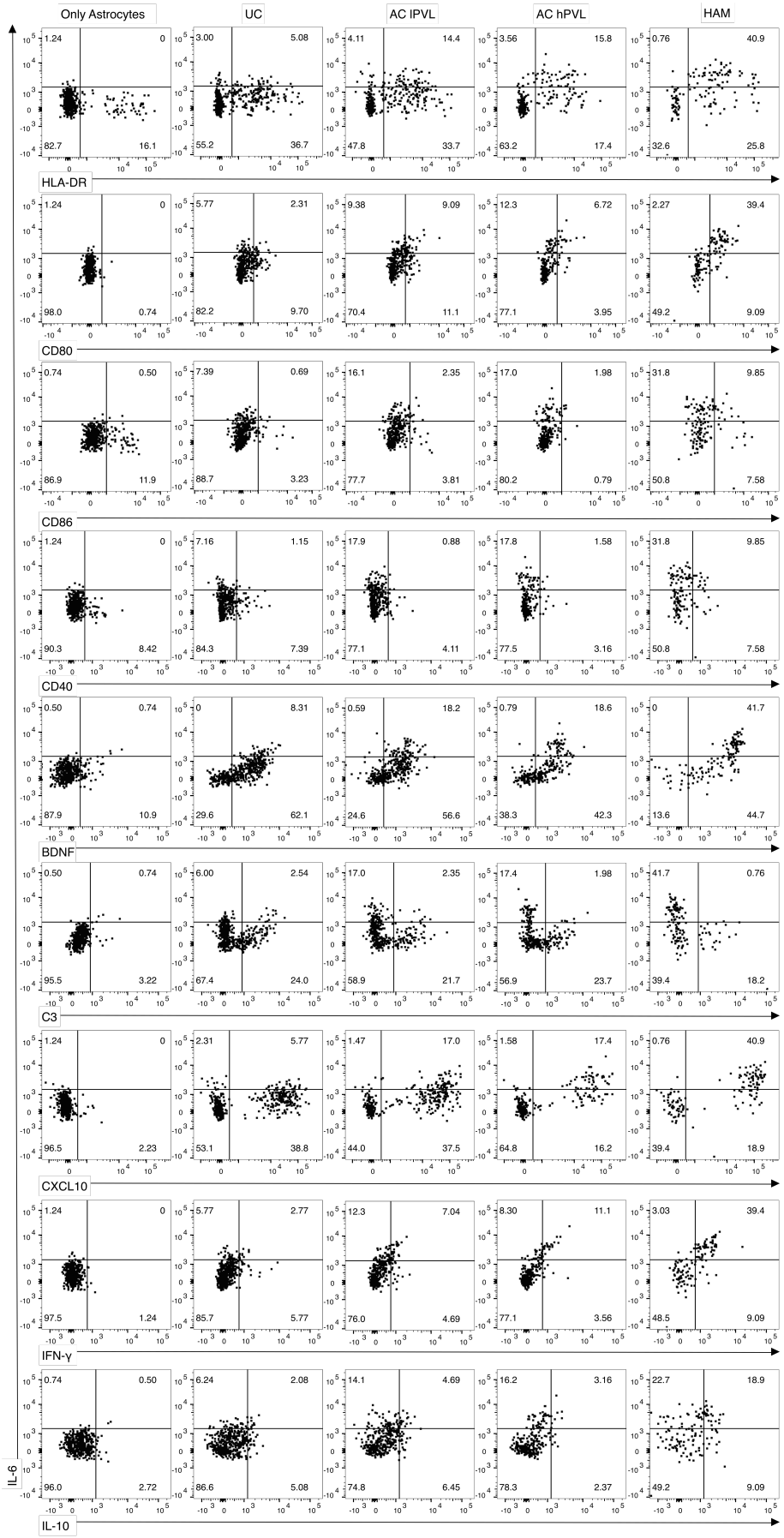


Figure 3.4: Representative flow staining of astrocytes after 48 h alone in culture or after co-culture with HTLV-1-specific CD4$^+$ T cells from different patient groups.

Astrocytes in co-culture with HTLV-1-specific CD4$^+$ T cells from all groups upregulated HLA-DR and CD80, and this trend was even more pronounced in astrocytes co-cultured with HTLV-1-specific CD4$^+$ T cells from patients with HAM (Figure 3.5). There was no change in CD86 expression between astrocytes alone in culture or in co-culture with CD4$^+$ T cells. Astrocytes co-cultured with HAM HTLV-1-specific CD4$^+$ T cells significantly upregulated CD40 relative to AC hPVL, and I also observed significantly higher levels of CXCL10 expression (Figure 3.5). Increased trends of IFN-γ and IL-6 expression were seen in astrocytes co-cultured with HAM HTLV-1-specific CD4$^+$ T cells relative to AC hPVL, but the difference was not statistically significant. Inflammatory astrocytes upregulate complement component 3 (C3) expression [276], but I observed no difference in C3 expression between high PVL HTLV-1-infected groups. Interestingly, in addition to the upregulation of proinflammatory cytokines and chemokines, HTLV-1-specific CD4$^+$ T cells from patients with HAM also induced higher levels of IL-10 and brain-derived neurotrophic factor (BDNF) expression, which are both considered anti-inflammatory cytokines. Overall, HTLV-1-specific CD4$^+$ cells from patients with HAM reduced astrocyte viability and induced upregulation of the antigen presentation machinery, CD40, and proinflammatory cytokines and chemokines.

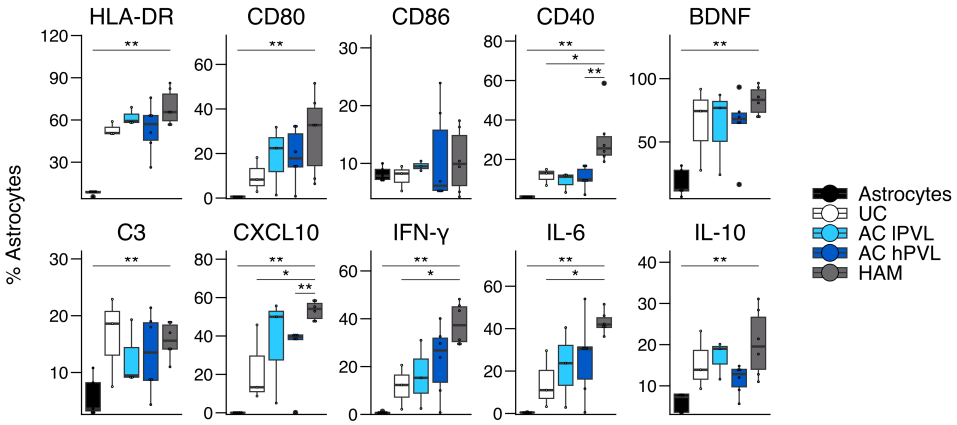


Figure 3.5: The effect of HTLV-1-specific CD4$^+$ T cells on astrocyte activation. Box and whisker plots showing the expression of markers and cytokines by astrocytes after 48 h alone in culture or co-culture with HTLV-1-specific CD4$^+$ T cells from different patient groups (n=5 only astrocytes, n=3 UC, n=3 AC lPVL, n=6 AC hPVL,n=6 HAM). Wilcoxon signed-rank unpaired test for comparisons between only astrocytes and HAM, UC and HAM, AC lPVL and AC hPVL, and AC hPVL and HAM; *p≤0.05, **p≤0.01, ***p≤0.001, ****p≤0.0001.

3.2.3 HTLV-1-specific CD4$^+$ T cells from all HTLV-1-infected groups activate microglia

Given that HTLV-1-specific CD4$^+$ T cells from patients with HAM-induced proinflammatory astrocytes, I wanted to determine whether HTLV-1-specific CD4$^+$ T cells had the potential to be reactivated once in the CNS. While my data suggest that activated astrocytes may be able to act as antigen-presenting cells, I wanted to study the effect of T cells on microglia, as microglia are the macrophages of the CNS and the main APC [343]. Following the same experimental strategy as in the experiments with astrocytes, I sorted HTLV-1-specific CD4$^+$ T cells from UCs and HTLV-1-infected patients, expanded them *in vitro* for 17 days, and then placed them in co-culture with a microglial cell line (HMC3-CRL-3304, an immortalized microglial cell line) for 48 h with anti-CD3 and anti-CD28.

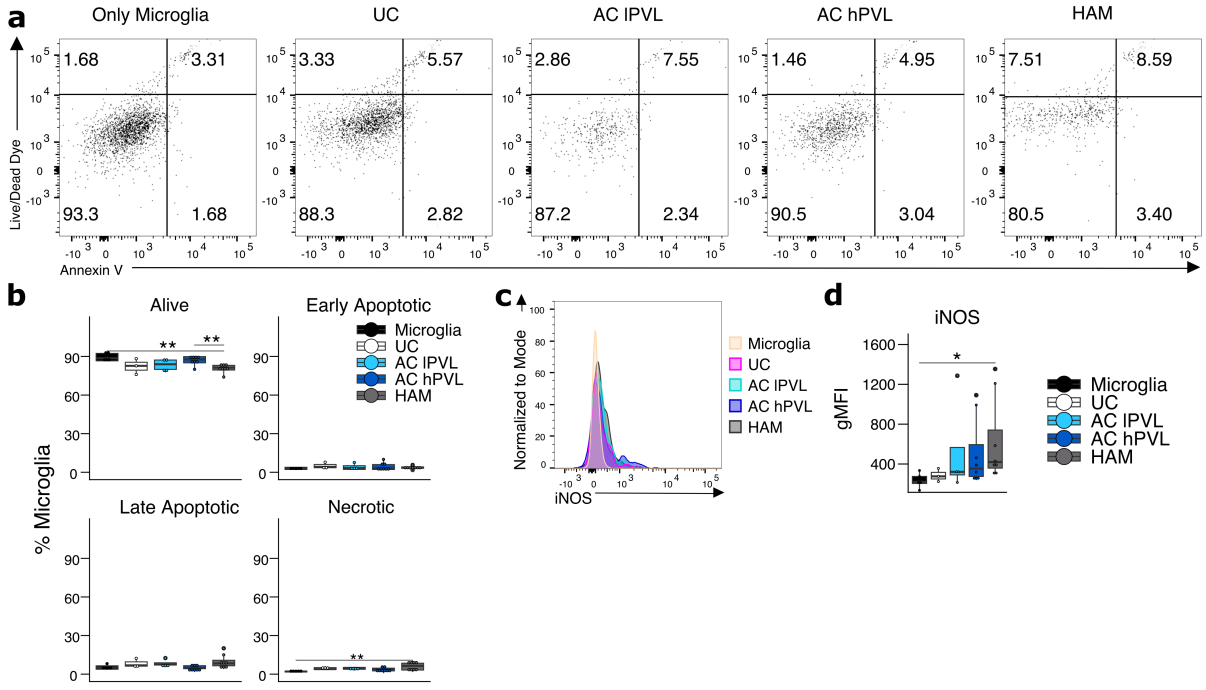


Figure 3.6: The effect of HTLV-1-specific CD4$^+$ T cells on microglia viability and iNOS expression. Representative flow plots (**a**) and box and whisker plots (**b**) showing the frequency of alive, early apoptotic, late apoptotic, and necrotic microglia after 48 h alone in culture or co-culture with HTLV-1-specific CD4$^+$ T cells from different groups (n=5 only microglia, n=3 UC, n=4 AC lPVL, n=8 AC hPVL, n=8 HAM). Representative histogram (**c**) and box and whisker plot (**d**) showing the gMFI of iNOS of microglia after 48 h alone in culture or co-culture with HTLV-1-specific CD4$^+$ T cells (n=5 only microglia, n=3 UC, n=4 AC lPVL, n=8 AC hPVL, n=8 HAM). **b, d)** T test with Holm correction; *p≤0.05, **p≤0.01, ***p≤0.001, ****p≤0.0001.

There was a small but significant decrease in the viability of microglia co-cultured with

HTLV-1-specific $CD4^+$ T cells from patients with HAM relative to both microglia cultured alone or with cells from AC hPVL (Figure 3.6a and 3.6b). This decreased viability was driven by significantly increased necrosis (Figure 3.6b). HTLV-1-specific $CD4^+$ T cells from all HTLV-1-infected groups induced the upregulation of iNOS indicating increased microglial activation (3.6c and 3.6d).

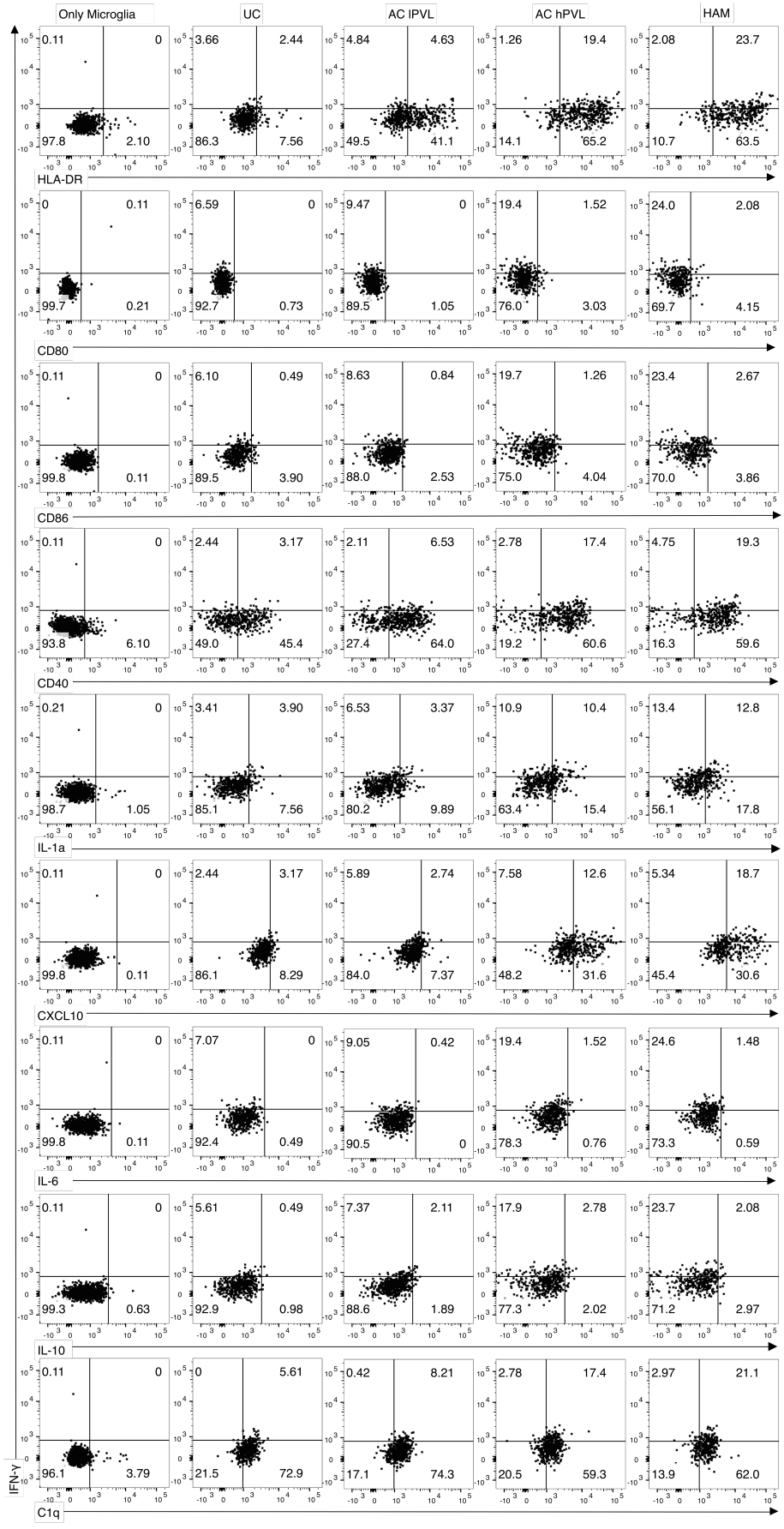


Figure 3.7: Representative flow staining of microglia alone or in co-culture with HTLV-1-specific CD4$^+$ T cells from different groups for 48 h.

Microglia were also stained for activation markers and cytokines. Representative stainings can be seen in Figure 3.7 and FMOs were used to place the quadrants. HTLV-1-specific CD4$^+$ T cells from all study groups induced the upregulation of CD80, CD40, and HLA-DR (Figure 3.8). Microglia co-cultured with HTLV-1-specific CD4$^+$ T cells from patients with HAM significantly upregulated CD80 relative to AC hPVL indicating increased upregulation of the antigen presentation machinery. HTLV-1-specific CD4$^+$ T cells from all groups induced the upregulation of IL-1a, CXCL10, IFN-γ, IL-10, and C1q. There were no significant differences in IL-6 expression between microglia co-cultured with HTLV-1-specific CD4$^+$ T cells and microglial alone in culture. Overall these data show that HTLV-1-specific CD4$^+$ T cells from UCs and all HTLV-1-infected groups induce microglia to express proinflammatory cytokines. HTLV-1-specific CD4$^+$ T cells from patients with HAM reduce the viability of microglia and induce increased upregulation of the class II antigen presentation machinery relative to AC hPVL.

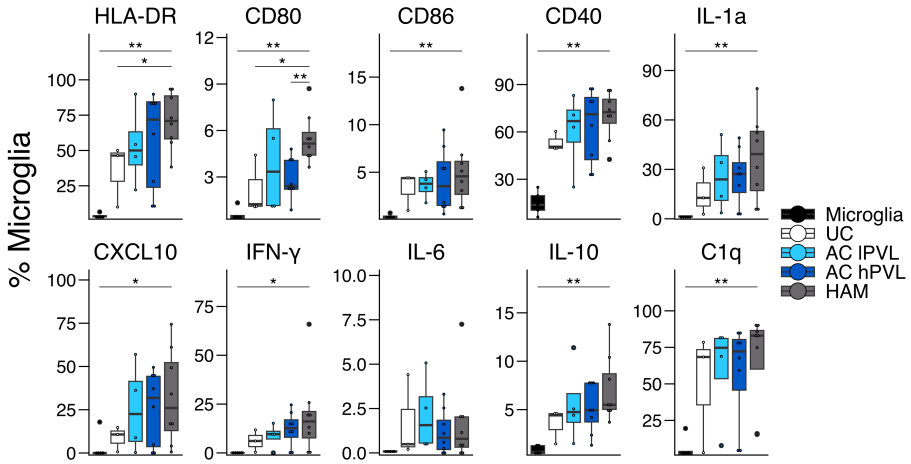


Figure 3.8: The effect of HTLV-1-specific CD4$^+$ T cells on microglia activation. Box and whisker plots showing the expression of markers and cytokines by microglia after 48 h alone in culture or co-culture with HTLV-1-specific CD4$^+$ T cells from different patient groups (n=3 UC, n=4 AC lPVL, n=8 AC hPVL,n=8 HAM). Wilcoxon signed-rank unpaired test for comparisons between just microglia and HAM, UC and HAM, AC lPVL and AC hPVL, and AC hPVL and HAM; *p$\leq$0.05, **p$\leq$0.01, ***p$\leq$0.001, ****p$\leq$0.0001.

3.2.4 Non-HTLV-1-specific CD4$^+$ T cells from patients with HAM induce moderate astrocytes and microglia activation

To determine whether the trends I observed in both astrocytes and microglia were unique to HTLV-1-specific T cells, I conducted the same experiments in parallel with non-HTLV-1 specific CD4$^+$ T cells from the same patients. After stimulating total PBMCs with heat-inactivated HTLV-1 for 12 h, in addition to sorting the HTLV-1-specific CD4$^+$ T cells, I also sorted the CD154$^-$ CD4$^+$ T cells and the cells were grown for 17 days *in vitro*, and then placed into co-culture with either astrocytes or microglia for 48 h with anti-CD3 and anti-CD28 stimulation.

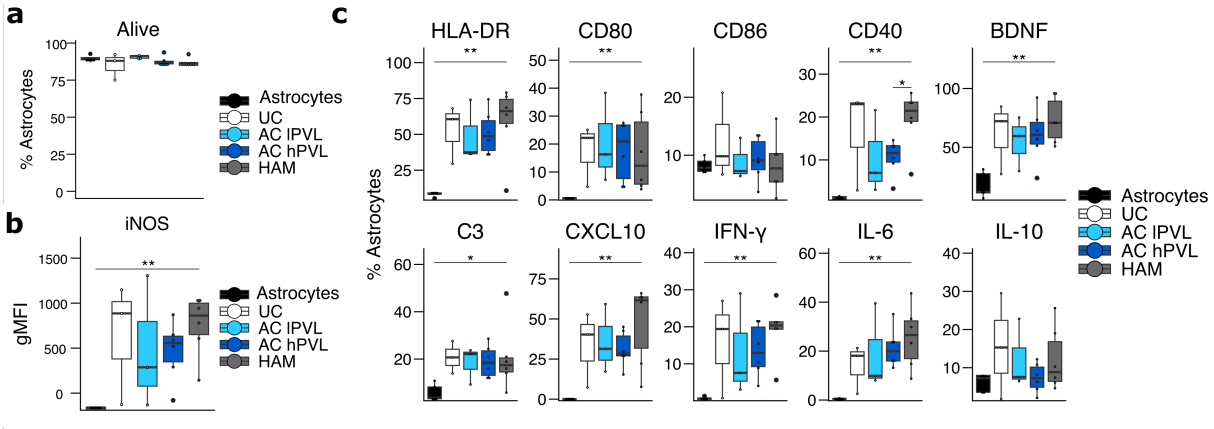


Figure 3.9: The effect of non-HTLV-1-specific CD4$^+$ T cells on astrocytes. **a.** Box and whisker plot showing the frequency of viable astrocytes after 48 h alone in culture or co-culture with non-HTLV-1-specific CD4$^+$ T cells from different groups (n=5 only astrocytes, n=3 UC, n=3 AC lPVL, n=6 AC hPVL, n=6 HAM). **b.** Box and whisker plot showing the gMFI of iNOS of astrocytes after 48 h alone in culture or co-culture with non-HTLV-1-specific CD4$^+$ T cells from different groups (n=5 only astrocytes, n=3 UC, n=3 AC lPVL, n=6 AC hPVL, n=6 HAM). **c.** Box and whisker plots showing the expression of markers and cytokines by astrocytes after 48 h alone in culture or co-culture with non-HTLV-1-specific CD4$^+$ T cells from different patient groups (n=5 only astrocytes, n=3 UC, n=3 AC lPVL, n=6 AC hPVL,n=6 HAM). **a, b)** T-test with Holm correction; **c)** Wilcoxon signed-rank unpaired test for comparisons between only astrocytes and HAM, UC and HAM, AC lPVL and AC hPVL, and AC hPVL and HAM; *p≤0.05, **p≤0.01, ***p≤0.001, ****p≤0.0001.

There were no significant differences in the viability of astrocytes cultured alone or with non-HTLV-1-specific CD4$^+$ T cells from different patient groups (Figure 3.9a). All non-HTLV-1-specific CD4$^+$ T cells increased iNOS expression (Figure 3.9b). Non-HTLV-1-specific CD4$^+$ T cells from all groups induced the upregulation of CD80 and HLA-DR and there was no change in CD86 expression (Figure 3.9c). There were trends in increased HLA-DR expression in astrocytes co-cultured with HAM cells relative to AC

hPVL, similar to the trends seen with HTLV-1-specific $CD4^+$ T cells (Figure 3.9c). As with the HTLV-1-specific $CD4^+$ T cells, CD40 expression was upregulated in all HTLV-1-infected groups and patients with HAM induced significantly higher levels of CD40 expression relative to AC hPVL, but the levels induced by HTLV-1-specific $CD4^+$ T cells were higher than those induced by non-HTLV-1-specific $CD4^+$ T cells (Figure 3.5 and 3.9c). There were no differences between HTLV-1-infected groups in IL-10, BDNF, C3, CXCL10, IFN-γ, or IL-6 expression (Figure 3.9c).

When placed in co-culture with microglia, non-HTLV-1-specific CD4$^+$ T cells from all groups reduced the viability of microglia (Figure 3.10a). This decreased viability was due to increased necrosis (Figure 3.10a). All groups induced increased iNOS expression in microglia relative to microglia in culture alone (Figure 3.10b). The antigen presentation machinery and CD40 were upregulated in all non-HTLV-1-specific CD4$^+$ T cell co-cultures (Figure 3.10c). While the differences were not significant, non-HTLV-1-specific CD4$^+$ T cells from patients with HAM seemed to induce higher CD86 expression relative to AC hPVL (Figure 3.10c). There were no significant differences between patients with HAM and AC hPVL in C1q, IL-10, IL-6, IL-1a, CXCL10, and IFN-γ expression.

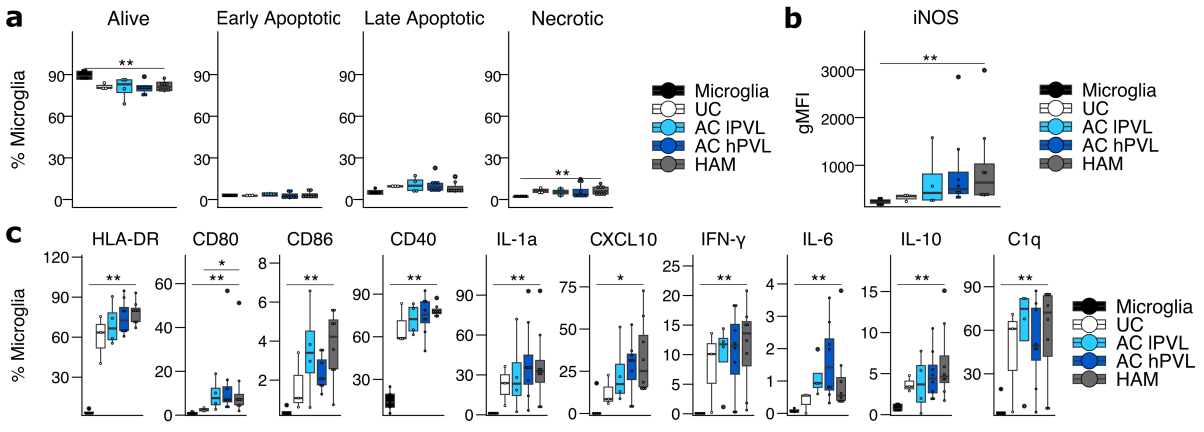


Figure 3.10: The effect of non-HTLV-1-specific CD4$^+$ T cell co-culture on microglia. a. Box and whisker plots showing the frequency of alive, early apoptotic, late apoptotic, and necrotic microglia after 48 h alone in culture or co-culture with non-HTLV-1-specific CD4$^+$ T cells from different groups (n=5 only microglia, n=3 UC, n=4 AC lPVL, n=8 AC hPVL, n=8 HAM). **b.** Box and whisker plot showing the gMFI of iNOS of microglia after 48h alone in culture or co-culture with non-HTLV-1-specific CD4$^+$ T cells from different groups (n=5 only microglia, n=3 UC, n=4 AC lPVL, n=8 AC hPVL, n=8 HAM). **c.** Box and whisker plots showing the expression of cell surface markers and cytokines of microglia after 48h alone in culture or co-culture with non-HTLV-1-specific CD4$^+$ T cells (n=5 only microglia, n=3 UC, n=4 AC lPVL, n=8 AC hPVL, n=8 HAM). **a, b)** T-test with Holm correction; **c)** Wilcoxon signed-rank unpaired test for comparisons between only astrocytes and HAM, UC and HAM, AC lPVL and AC hPVL, and AC hPVL and HAM; *p≤0.05, **p≤0.01, ***p≤0.001, ****p≤0.0001..

Overall, there were no significant differences in upregulation of the antigen presentation machinery or inflammatory cytokine expression between AC hPVL and HAM microglia c-cultures. Furthermore, given that only the HTLV-1-specific CD4$^+$ T cell population is being chronically activated by HTLV-1 antigen *in vivo*, it is likely that HTLV-1-specific CD4$^+$ T cells likely are more key to driving CNS inflammation and HAM pathogenesis. The upregulation of the class II antigen presentation machinery in astrocytes and microglia, and the high level of HTLV-1-infection of HTLV-1-specific CD4$^+$ T cells may allow HTLV-1-specific CD4$^+$ T cells to become reactivated once in the CNS. However

much remains to be uncovered about the mechanisms by which both HTLV-1-specific and non-HTLV-1-specific $CD4^+$ T cells from patients with HAM induce inflammatory glial cells.

3.2.5 Sorting and RNA sequencing of HTLV-1-specific CD4$^+$ T cells from different HTLV-1-infected groups

To gain insight into the potential mechanisms by which HTLV-1-specific CD4$^+$ T cells induce proinflammatory responses in astrocytes and microglia in patients with HAM, and how these cells may drive disease pathology *in vivo*, I sorted HTLV-1-specific CD4$^+$ T cells from UCs (n=9), AC lPVL (n=10), AC hPVL (n=7), and patients with HAM (n=9). These cells were then subjected to RNA sequencing to elucidate the transcriptional differences between these groups.

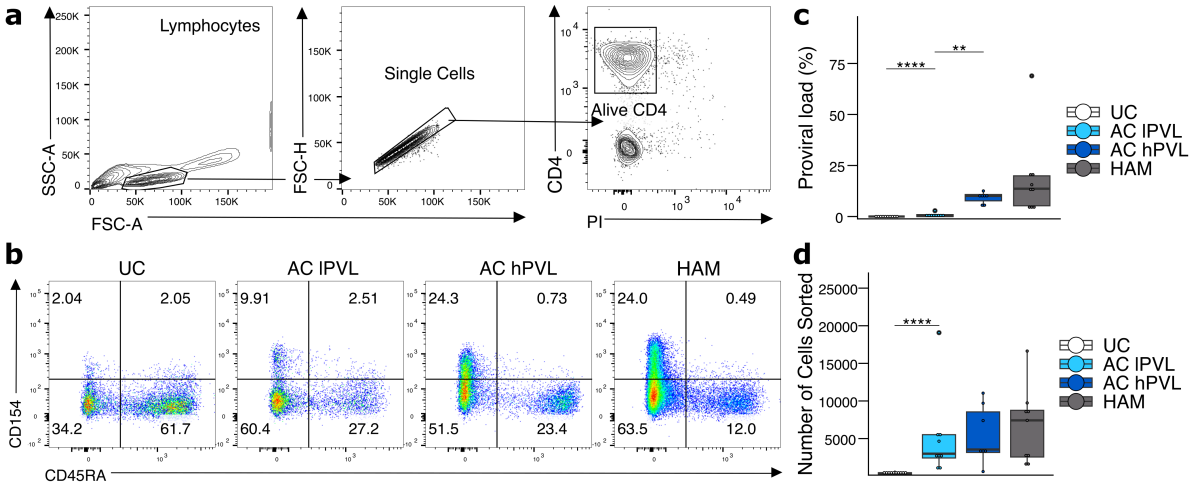


Figure 3.11: Gating strategy and sorting of HTLV-1-specific CD4$^+$ T cells for RNA-seq analysis. The gating strategy for the identification CD4$^+$ T cells (**a**) and HTLV-1-specific CD4$^+$ T cells using CD154 expression (**b**) after the simulation of 10 million PBMCs with heat-inactivated HTLV-1 for 12 h and the magnetic enrichment of CD154$^+$ cells. **c.** Box and whisker plot showing the PVL of PBMCs from which HTLV-1-specific CD4$^+$ T cells were isolated for RNA sequencing (n=9 UC, n=10 AC lPVL, n=7 AC hPVL, and n=9 HAM). **d.** Box and whisker plot showing the number of HTLV-1-specific CD4$^+$ T cells sorted per patient from 10 million PBMCs (n=9 UC, n=10 AC lPVL, n=7 AC hPVL, and n=9 HAM). **c, d)** Wilcoxon signed-rank unpaired test for comparisons between UC and AC lPVL, AC lPVL and AC hPVL, and AC hPVL and HAM; *p≤0.05, **p≤0.01, ***p≤0.001, ****p≤0.0001.

Fresh PBMCs were stimulated with heat-inactivated HTLV-1 for 12 h, the CD154$^+$ cells were magnetically enriched, I gated on viable CD4$^+$ T cells (Figure 3.11a) and sorted the CD154$^+$ HTLV-1-specific CD4$^+$ T cells (3.11b). As previously mentioned, I matched the PVLs of the AC hPVL and HAM groups to control for any transcriptional differences or changes caused by the level of HTLV-1 infection (Figure 3.11c). The number of HTLV-1-specific CD4$^+$ T cells sorted was lower in UCs and comparable between HTLV-1-infected groups with an average of 348, 4982, 5515, and 6634 HTLV-1-specific CD4$^+$ T cells sorted from 10 million PBMCs in UCs, AC lPVL, AC hPVL, and patients with

HAM, respectively (Figure 3.11d).

RNA sequencing was performed by the Oxford Genomics Centre using the ultra-low library preparation. The median number of reads per sample was 29,637,356, which indicates very good read depth despite the low number of input cells. The quality of the RNA was comparable between the different groups, with the total number of reads correlating well with the number of uniquely mapped reads (Figure 3.12a). There were no major duplications or other quality concerns with the RNA, and the percentage of the reads that uniquely mapped onto the genome was similar for all samples (Figure 3.12b). Given the lower number of input cells in UCs, it was not surprising that the number of genes detected in this group was significantly lower than for the HTLV-1-infected groups (Figure 3.12c). There were no significant differences in the number of genes detected between the HTLV-1-infected groups. Due to the higher number of genes detected in HTLV-1 patients relative to UCs, I conducted two separate differential gene expression analyses: one comparing all the HTLV-1-infected groups to the UCs, and a separate analysis comparing just the HTLV-1-infected groups to each other.

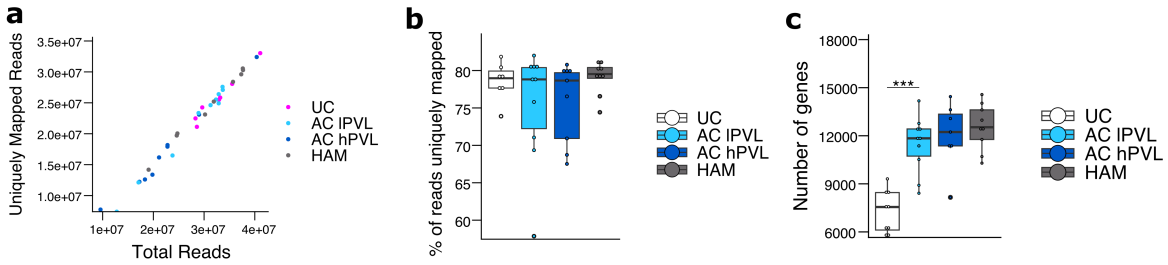


Figure 3.12: RNA sequencing of HTLV-1-specific CD4$^+$ T cells. a. Scatter plot showing the number of total reads vs. the number of uniquely mapped reads for the RNA-seq data. **b.** Box and whisker plot showing the percentage of reads that mapped uniquely to the genome (n=9 UC, n=10 AC lPVL, n=7 AC hPVL, and n=9 HAM). **c.** Box and whisker plot showing the number of genes that passed the threshold count in the RNA-seq analysis. **b, c)** Wilcoxon signed-rank unpaired test for comparisons between UC and AC lPVL, AC lPVL and AC hPVL, and AC hPVL and HAM; *p≤0.05, **p≤0.01, ***p≤0.001, ****p≤0.0001.

3.2.6 Transcriptional analysis of HTLV-1-specific CD4$^+$ T cells in HTLV-1-infected groups relative to UCs

Differential gene expression analysis was conducted by comparing each of the HTLV-1-infected groups to the UC group. In patients with HAM, 3187 upregulated and 280 downregulated DEGs were identified relative to UCs ($\geq$ 1.5-fold change and FDR $\leq$ 0.05, Figure 3.13a). In the AC hPVL vs. UC analysis, 3530 and 477 DEGs were found to be upregulated and downregulated, respectively. Similarly, in the AC lPVL vs. UC analysis, 2577 and 157 DEGs were identified as upregulated and downregulated, respectively. Notably, 1961 and 49 DEGs were upregulated and downregulated, respectively, across all three HTLV-1-infected groups relative to UCs (Figure 3.13a).

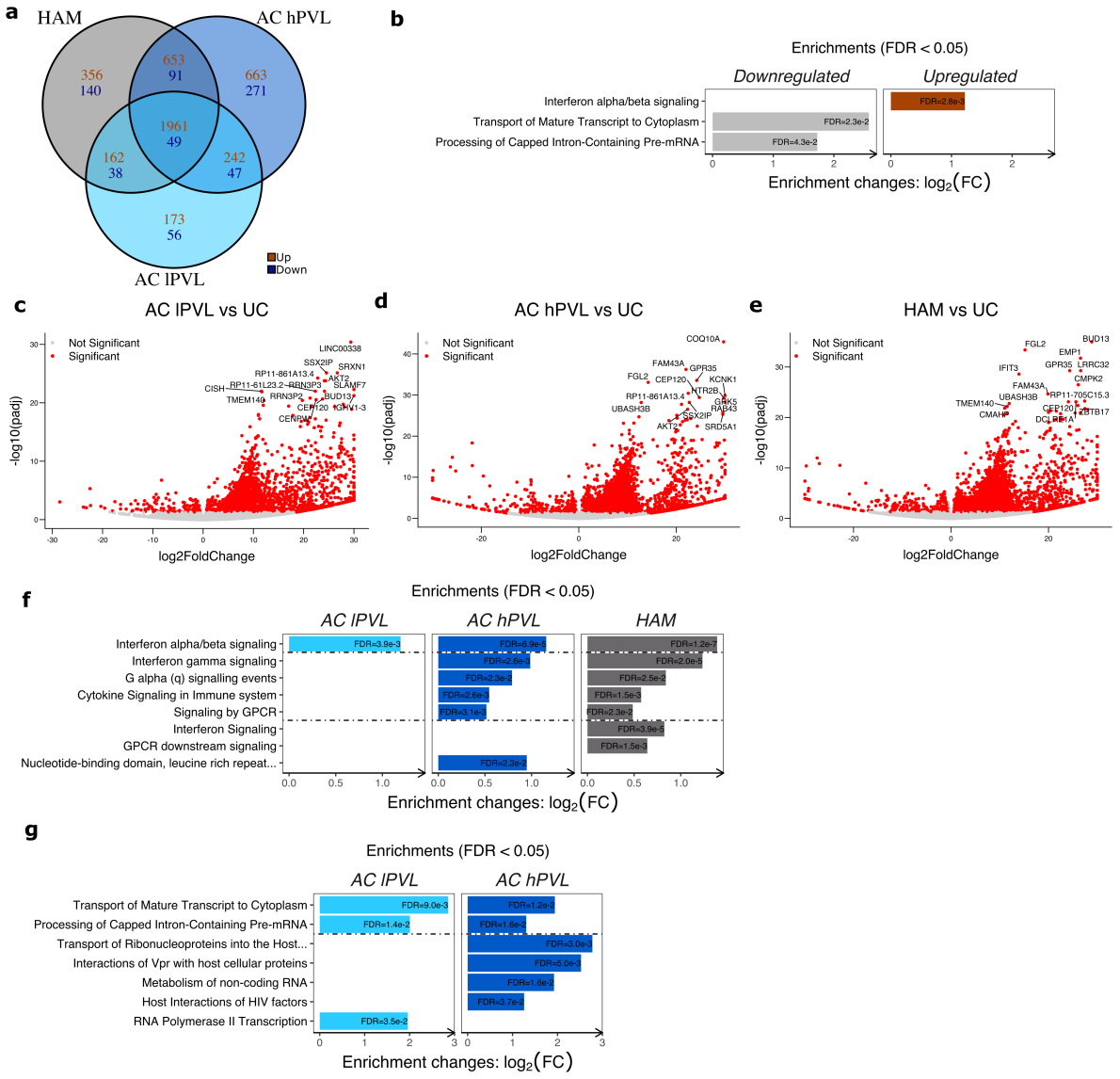


Figure 3.13: Transcriptional analysis of HTLV-1-specific CD4$^+$ T cells from AC lPVL, AC hPVL, and patients with HAM relative to UCs. a. Venn diagram showing the number of significantly upregulated (brown) and downregulated (blue) genes in AC lPVL, AC hPVL, and patients with HAM relative to UC ($\geq$ 1.5-fold change and FDR$\leq$ 0.05). **b.** Bar plots depicting significantly enriched (FDR$\leq$0.05) pathways from Reactome for genes up and downregulated by all HTLV-1 infected groups relative to UC ($\geq$1.5 fold increase for upregulated genes and $\geq$1.5 fold decrease for downregulated genes, FDR$\leq$0.05). Fold enrichment is plotted as log2 (fold-change, FC). **c-e.** Volcano plots of DEGs for HTLV-1-specific CD4$^+$ T cells in AC lPVL (**c**), AC hPVL (**d**), or patients with HAM vs. UCs (**e**). Genes with a fold change $\geq$1.5 and FDR$\leq$0.05 are shown in red. **f.** Bar plots depict significantly enriched (FDR$\leq$0.05) pathways from Reactome for HTLV-1-specific CD4$^+$ T cells from AC lPVL, AC hPVL, and HAM vs. UC using upregulated genes ($\geq$1.5 fold increase, FDR$\leq$0.05). **g.** Bar plots depicting significantly enriched (FDR$\leq$0.05) pathways from Reactome for HTLV-1-specific CD4$^+$ T cells from AC lPVL, AC hPVL, and HAM relative to UC using downregulated genes ($\geq$1.5 fold decrease, FDR$\leq$0.05). **b, f, g**) Bars are labeled with the adjusted p-value.

To gain insight into the function of the up and downregulated DEGs across all HTLV-1-infected groups relative to UC, I used the 1961 upregulated and the 49 downregulated DEGs common to all HTLV-1-infected groups relative to UC (Figure 3.13a), and performed pathway enrichment analysis with XGR [336] and pathway annotations from Reactome. All HTLV-1-infected groups had upregulated genes involved in the innate immune response including "interferon alpha/beta signaling" (Figure 3.13b). In terms of downregulated DEGs, all HTLV-1-infected groups had downregulated genes in the "transport of mature transcript to cytoplasm" and "processing of capped intron-containing pre-mRNA". A full list of the upregulated and downregulated genes in each of the pathways can be seen in Table 3.1 for the upregulated genes and Table 3.2 for the downregulated genes.

Despite a large overlap in the DEGs between HTLV-1-infected groups, the transcriptional profiles of HTLV-1-specific $CD4^+$ T cells in the different HTLV-1-infected groups were distinct, with many DEGs detected uniquely in each HTLV-1-infected group. The top 15 DEGs are displayed on volcano plots showing DEGs in AC lPVL (Figure 3.13c), AC hPVL (Figure 3.13d), and HAM (Figure 3.13e) relative to UCs. The top DEGs have a huge range of different functions highlighting the diversity of the transcriptional changes in HTLV-1-specific $CD4^+$ T cells in response to chronic infection. For example, the oncogene *AKT2* is upregulated in both AC lPVL and AC hPVL and is a serine theroine kinase involved in IL-9 signaling and insulin metabolism [344]. *CISH*, is also upregulated in AC lPVL, and is a negative regulator of cytokine signaling (Figure 3.13c) [345]. *UBASH3B*, which is upregulated in AC hPVL, inhibits epidermal growth factor receptor (EGFR) and platelet-derived growth factor receptor endocytosis and promotes T cell activation through the phosphorylation of zeta-chain-associated protein kinase 70 (Zap70) [346]. *LRRC32*, upregulated in HAM, is essential for the expression of TGF-β in activated Tregs [347] and *rp11-705c15.3* is an oncogene which drives cellular proliferation [348]. There is a huge diversity in the function of the DEGs detected.

To identify the up and downregulated pathways, I separated up and downregulated DEGs and performed pathway enrichment analysis with XGR [336] and pathway annotations from Reactome to gain insight into the pathways differentially expressed in HTLV-1-specific $CD4^+$ T cells from AC lPVL, AC hPVL, and patients with HAM relative to UCs. I first looked at significantly upregulated pathways (3.13f). "Interferon alpha/beta

signaling" was upregulated in all HTLV-1-infected groups relative to UCs (3.13f). Both AC hPVL and patients with HAM also upregulated "interferon gamma signaling", "G alpha (q) signaling events", "cytokine and immune system", and "signaling by G protein-coupled receptors (GPCR)". "Interferon signaling" and "GPCR downstream signaling" were only upregulated in patients with HAM relative to UCs. The upregulated "interferon-alpha/beta signaling" and the "interferon gamma signaling" pathways in patients with HAM included 49 and 50 upregulated genes, respectively, while the upregulated "interferon signaling" pathway included 130 upregulated genes demonstrating that not all the genes upregulated in these pathways overlapped (Table 3.5). Furthermore, the "GPCR downstream signaling" pathway included 162 upregulated genes, many of which overlapped with the 214 genes upregulated by the "signaling by GPCR" pathway in patients with HAM, but there remained many genes that were unique to each pathway (Table 3.5). In contrast to AC lPVL and HAM, AC hPVL upregulated "nucleotide-binding domain, leucine-rich repeat-containing receptor signaling pathways" relative to UC. Overall HTLV-1-specific $CD4^+$ T cells from high PVL groups were far more activated, with increased innate and adaptive immune responses relative to AC lPVL. Patients with HAM appeared to have increased interferon and downstream GPCR signaling relative to AC hPVL. A full list of the upregulated DEGs in each of the pathways can be seen in Table 3.3 for the AC lPVL vs. UC analysis, Table 3.4 for the AC hPVL vs. UC analysis, and Table 3.5 for that HAM vs. UC analysis.

There were no downregulated pathways in patients with HAM relative to UCs (Figure 3.13g). Both AC lPVL and AC hPVL downregulated the "transport of mature transcripts to the cytoplasm" and the "processing of capped intron-containing pre-mRNA", likely as a result of innate immune activation. In addition, AC hPVL also downregulated the "transport of ribonucleoproteins into the host nucleus", "metabolism of non-coding RNAs", and "interactions between HIV proteins and host-proteins". These downregulated pathways indicate reduced transcription and mRNA processing in ACs relative to patients with HAM. A full list of the downregulated DEGs in each of the pathways can be seen in Table 3.6 for the AC lPVL vs. UC analysis and Table 3.7 for the AC hPVL vs. UC analysis.

3.2.7 Transcriptional analysis of HTLV-1-specific CD4$^+$ T cells in HTLV-1-infected groups

Following the RNA-seq DEG analysis comparing each HTLV-1-infected group to UCs, I conducted the same analysis comparing each HTLV-1-infected group to each other. By only comparing the HTLV-1-infected groups, I was able to take advantage of the higher number of genes detected in these samples. I detected 406 upregulated genes and 222 downregulated genes in the HTLV-1-specific CD4$^+$ T cells of patients with HAM relative to AC hPVL ($\geq$ 1.5-fold change and FDR$\leq$ 0.05) (Figure 3.14a). For AC hPVL or HAM vs. AC lPVL, I detected 162 and 260 upregulated genes, respectively, and 439 and 295 downregulated genes, respectively (Figure 3.14a). Interestingly, there were no overlapping DEGS in the AC hPVL vs. AC lPVL analysis and the HAM vs. AC hPVL analysis.

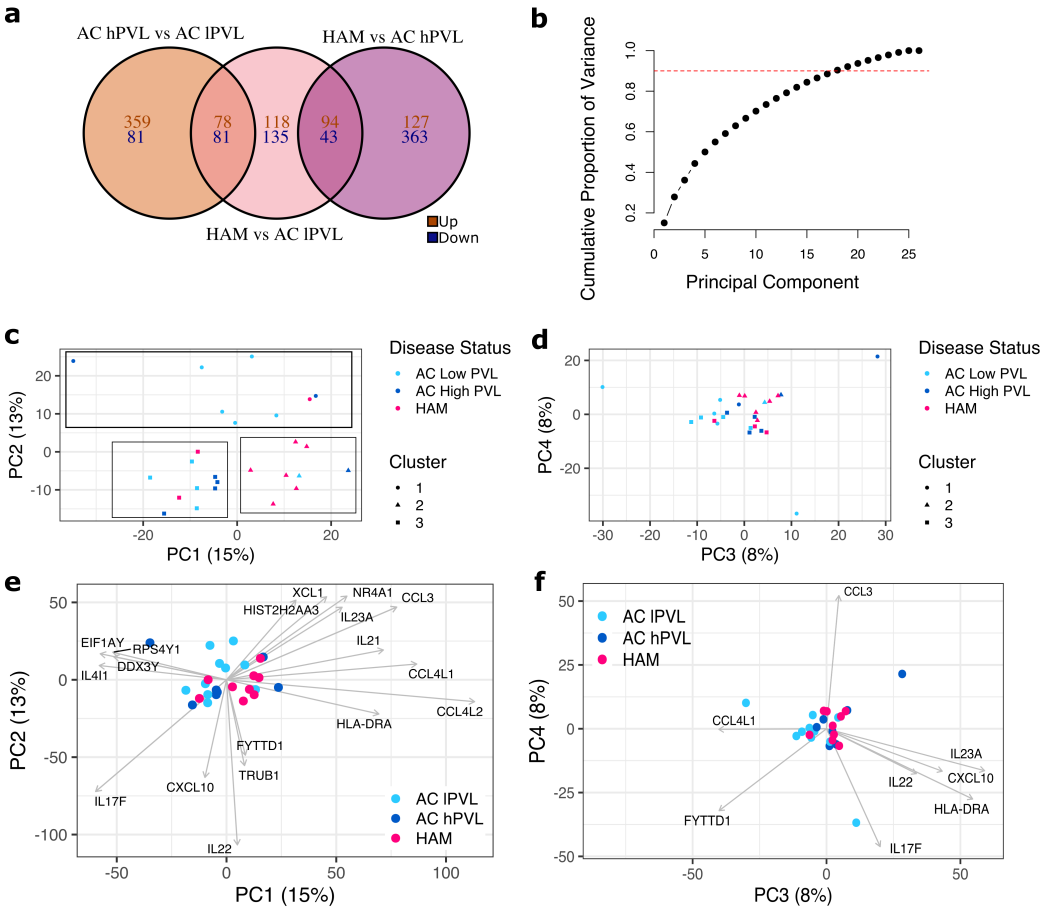


Figure 3.14: Venn diagram of differentially expressed genes and principal component analysis of HTLV-1-specific CD4$^+$ T cells. a. Venn diagram showing the upregulated (brown) and downregulated (blue) genes in HTLV-1-specific CD4$^+$ T cells (fold change $\geq$1.5 and FDR$\leq$0.05). **b.** Elbow plot showing the cumulative proportion of variance explained by each principal component. The red dashed line marks the 90% mark of cumulative variance. PCA plots, PC1 vs. PC2 (**c**) and PC3 vs. PC4 (**d**), computed from all genes detected in the HTLV-1-specific CD4$^+$ T cells from AC lPVL (light blue dots), AC hPVL (dark blue dots), and HAM (pink dots). The variance explained by each component is stated in brackets. K-mean clustering was used to identify 3 clusters in PC1 vs. PC2. **e-f.** PCA plots computed from all genes detected in the HTLV-1-specific CD4$^+$ T cells from AC lPVL (light blue dots), AC hPVL (dark blue dots), and HAM (pink dots) showing the genes driving separation along the different PC axes.

PCA was applied to examine the global distribution of gene expression profiles from HTLV-1-specific CD4$^+$ T cells from different HTLV-1-infected groups (AC lPVL n=10, AC hPVL n=7, HAM n=9). An elbow plot was used to explore the contribution of each principal component (PC) to the cumulative proportion of the variance in the dataset (Figure 3.14b). In this plot, 5 PCs are responsible for 50% of the cumulative variance, 14 PCs for 80%, and 19 PCs for 90%. The gradual increase in cumulative variance, with no sharp "elbow" point, implies that no single or few components dominate, and instead, multiple components are needed to capture the diversity in the data. The variance in each PC decreased as the PC number increased (Figure 3.14b). When PC1 was plotted against PC2, accounting for 28% of the variance, there was some separation between ACs and patients with HAM along PC1 but less along PC2 (Figure 3.14c). In the PC3 vs. PC4 plot, which accounted for a further 16% of the variance, there was some degree of separation between patients with HAM and ACs, indicating differences in their global gene expression (Figure 3.14d). However, the separation between patient groups in both plots (Figure 3.14c and 3.14d) is not completely distinct, and the patient groups do not form clearly defined clusters, suggesting some overlapping characteristics. I used a k-means clustering algorithm to identify 3 clusters (due to having 3 different patient groups) using the first 19 PCs (which are responsible for 90% of the cumulative variance (Figure 3.14c and 3.14d). These clusters, based on the first 19 PCs, are distinct on the PC1 vs PC2 plot (Figure 3.14c). Cluster 1 is primarily made up of lPVL ACs, in addition to 2 hPVL ACs and 1 patient with HAM. Cluster 2 is primarily made up of patients with HAM, and includes 6 of the 9 patients with HAM, in addition to 1 lPVL AC and 1 hPVL AC. Finally, cluster 3 is the most diverse but includes the largest group of AC hPVL patients with 4 AC hPVL, 4 AC lPVL, and 2 patients with HAM. The genes driving the partial separation along PC1 and PC2 are shown in Figure 3.14e, and PC3 and PC4 are shown in Figure 3.14f. Some of the genes driving this partial separation between HTLV-1-infected groups included *IL-23A, IL-21, IL-17F, IL-22, CCL4L1, CCL4L2*, and *CXCL10* which are associated with different T helper phenotypes or chemokines involved in T cell recruitment. IL-23A stabilizes Th17 cells [125], and IL-17F and IL-22 are Th17 cytokines[349], with IL-22 also being expressed by Th22 cells [133]. The chemokines CCL4L1 and CCL4L2, induce the chemotaxis of CCR5 and CCR1 expressing cells, typically Th1 cells and monocytes [350]. Furthermore, CXCL10 is a chemoattractant for CXCR3 expressing cells, which is

preferentially expressed in Th1 cells and $CD8^+$ T cells [351]. Other genes include the $CD4^+$ T cell activation-associated marker *HLA-DRA*, which is associated with patients with HAM on the PCA plot, and *XCL1* which codes for a cytokine expressed by activated T cells and NK cells, that facilitates cross-presentation in dendritic cells, allowing dendritic cells to activate naïve $CD8^+$ T cells, increase antigen uptake, and induces both innate and adaptive cytotoxic immunity [352]. The PCA analysis suggests that the HTLV-1-specific $CD4^+$ T cell responses tend to favor different helper phenotypes across the various HTLV-1-infected groups within this diverse cohort, however, there remains some overlap between the groups.

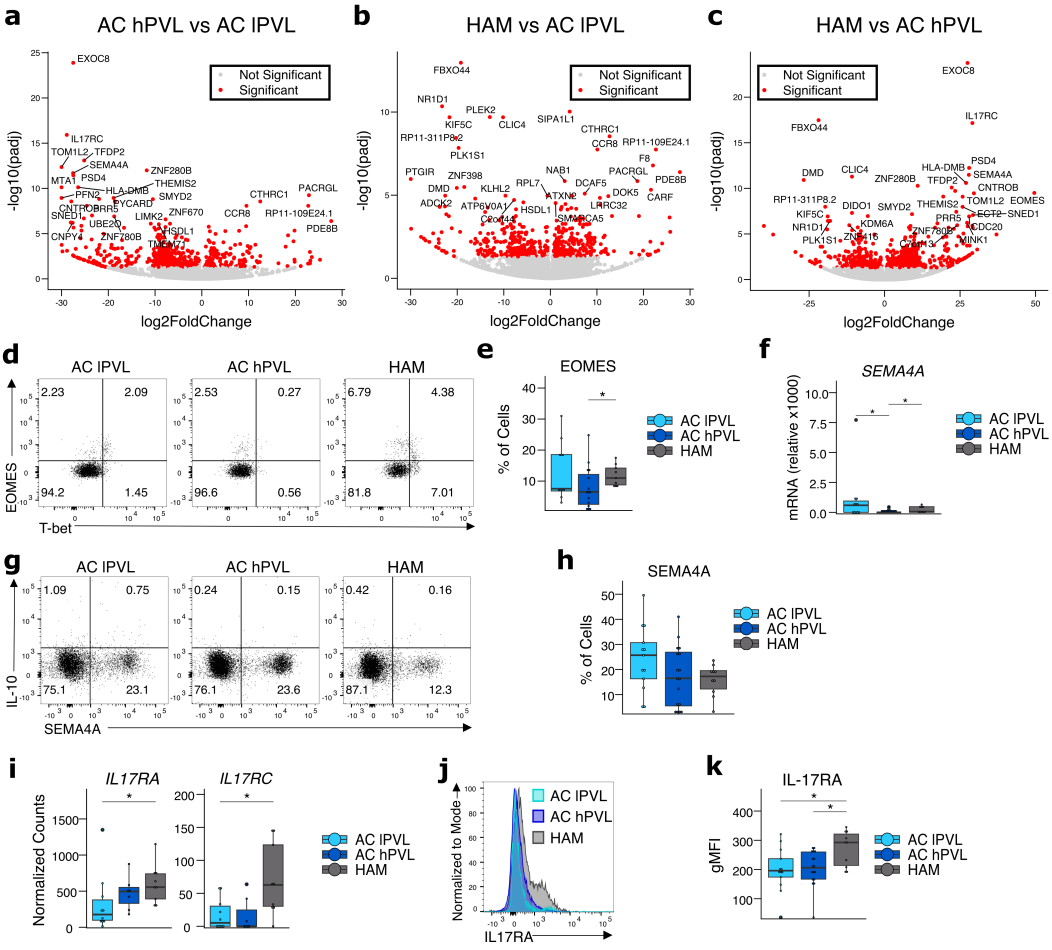


Figure 3.15: Transcriptional analysis of HTLV-1-specific CD4$^+$ T cells in HTLV-1- infected groups. a. a-c. Volcano plots of differentially expressed genes. Genes with fold change ≥1.5 and FDR≤0.05 are shown in red. Representative flow plot showing T-bet and EOMES staining (**d**) and box and whisker plot showing EOMES expression (**e**) in HTLTV-1-specific CD4$^+$ T cells (n=11 AC lPVL, n=15 AC hPVL, n=9 HAM). **f.** Box and whisker plot showing gene expression of *SEMA4A* relative to *B2M* measured by RT-PCR in sorted HTLV-1-specific CD4$^+$ T cells (n=10 AC lPVL, n=11 AC hPVL, n=9 HAM). Representative flow staining of SEMA4A and IL-10 (**g**) and box and whisker plot (**h**) showing SEMA4A expression in HTLV-1-specific CD4$^+$ T cells (n=13 AC lPVL, n=17 AC hPVL, n=10 HAM). **i.** Normalized gene counts for *IL17RA* and *IL17RC* (n=10 AC lPVL, n=7 AC hPVL, n=9 HAM). Representative histogram (**j**) and box and whisker plot (**k**) showing IL-17RA expression in HTLV-1-specific CD4$^+$ T cells (n=13 AC lPVL, n=17 AC hPVL, n=10 HAM). **e, j, h)** Wilcoxon signed-rank unpaired test for comparisons between AC lPVL and AC hPVL, AC hPVL and HAM; **i, k)** Wilcoxon signed-rank unpaired test with Holm correction for comparisons between AC lPVL and HAM, and AC hPVL and HAM; *p≤0.05, **p≤0.01, ***p≤0.001, ****p≤0.0001.

The top 30 DEGs between AC hPVL vs. AC lPVL, HAM vs. AC lPVL, and HAM vs. AC hPVL again include some genes associated with different T helper phenotypes (Figure 3.15a-c). The gene with the highest fold-difference expression between HAM and AC hPVL was *EOMES*, a T-box brain protein 1 (a subfamily of T-box genes) and transcription factor involved in the differentiation of $CD8^+$ T cells and regulation of the expression of lytic effector genes (Figure 3.15c) [353]. The upregulation of *EOMES* was validated at a protein level by flow cytometry in HTLV-1-specific $CD4^+$ T cells (Figure 3.15d and 3.15e).

Another interesting gene upregulated in patients with HAM relative to AC hPVL was *SEMA4A* which encodes for a soluble transmembrane protein that causes demyelination and oligodendrocyte death in EAE [354]. This increased *SEMA4A* expression was validated by RT-PCR in an expanded patient cohort that showed increased *SEMA4A* expression in AC lPVL and HAM relative to AC hPVL (Figure 3.15f). The expanded patient cohort comprised of both patients from the RNA-sequencing experiment and additional patients. To validate the increased *SEMA4A* expression at a protein level, SEMA4A protein expression was analyzed in HTLV-1-specific $CD4^+$ T cells after a 12 h stimulation with heat-inactivated HTLV-1 by flow cytometry (Figure 3.15g). Surprisingly, there was no significant difference in the frequency of $SEMA4A^+$ cells between the HTLV-1-infected groups (Figure 3.15h). Given that SEMA4A is also a secreted protein, the majority of the SEMA4A protein produced in HTLV-1-specific $CD4^+$ T cells from patients with HAM may be secreted. This needs to be further investigated by measuring the concentration of SEMA4A in the supernatant of HTLV-1-specific $CD4^+$ T cells.

IL17RC, which codes for one of 5 IL-17 receptor family proteins including IL-17RA, IL-17RB, IL-17RC, IL-17RD, and IL-17RE, is downregulated in AC hPVL vs. AC lPVL and upregulated in HAM vs. AC hPVL, as shown in the volcano plots (Figure 3.15a and 3.15c). The normalized gene counts for *IL17RA* and *IL17RC* are significantly upregulated in patients with HAM relative to AC lPVL, with similar non-significant trends relative to AC hPVL (Figure 3.15i). Increased IL-17RA expression in patients with HAM relative to ACs was validated by flow cytometry (Figure 3.15j and 3.15k). This increased IL-17 receptor expression may increase sensitivity to IL-17 signaling. Overall it is apparent that HTLV-1-specific $CD4^+$ T cells are transcriptionally distinct in lPVL relative to hPVL and are transcriptionally distinct in ACs relative to HAM.

3.2.8 HTLV-1-specific CD4$^+$ T cells in patients with HAM have an unfocused Th1 response

Given that many of the genes driving separation in the PCA plot between AC lPVL, AC hPVL, and patients with HAM are associated with different T helper phenotypes, I further investigated the expression of T-bet, ROR-γt, GATA3, and Foxp3 in HTLV-1-specific CD4$^+$ T cells at a protein level by flow cytometry (Figure 3.15d and 3.16a). HTLV-1-specific CD4$^+$ T cells from patients with HAM expressed significantly higher levels of the Th1 transcription factor T-bet relative to AC hPVL (Figure 3.16b). AC lPVL HTLV-1-specific CD4$^+$ T cells expressed significantly higher levels of ROR-γt relative to both AC hPVL and HAM, indicating a Th17 polarized response (Figure 3.16b). There were no significant differences in Foxp3 or GATA3 expression between HTLV-1-infected groups.

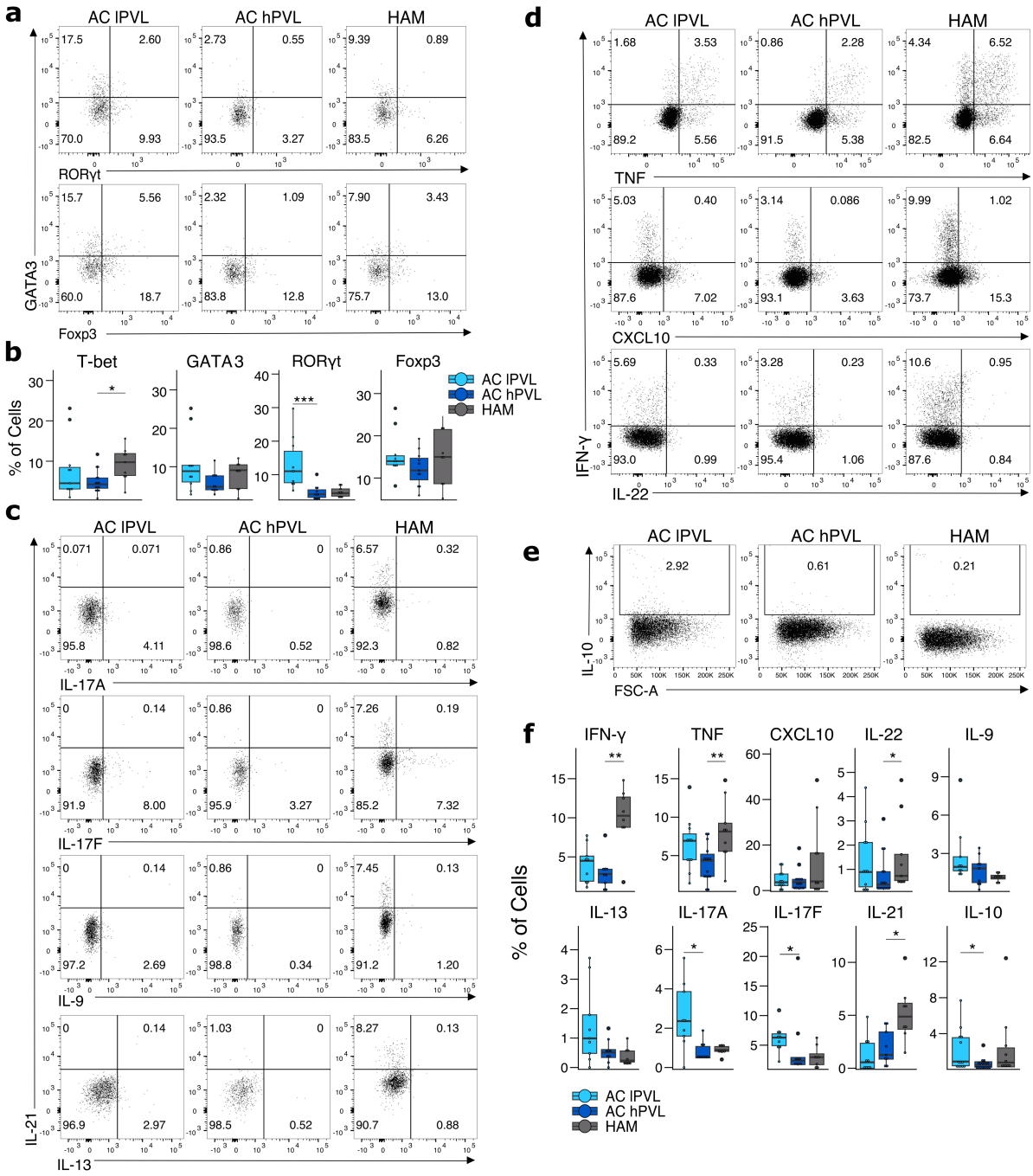


Figure 3.16: T helper phenotype of HTLV-1-specific CD4$^+$ T cells in AC lPVL, AC hPVL, and patients with HAM. Representative flow plot (**a**) and box and whisker plot (**b**) showing the expression of GATA3, RORγt, and Foxp3 (n=10 AC lPVL, n=11 AC hPVL, n=9 HAM) in HTLV-1-specific CD4$^+$ T cells. Representative flow plots (**c, d, e**) and box and whisker plots (**f**) showing the expression of TNF, CXCL10, IL-22 (n=11 AC lPVL, n=15 AC hPVL, n=9 HAM), IFN-γ, IL-17A, IL-17F, IL-9, IL-13, and IL-21 (n=9 AC lPVL, n=9 AC hPVL, n=8 HAM), and IL-10 (n=13 AC lPVL, n=17 AC hPVL, n=10 HAM) in HTLV-1-specific CD4$^+$ T cells after a 12 h stimulation with heat-inactivated HTLV-1. **b, f)** Wilcoxon signed-rank unpaired test for comparisons between AC lPVL and AC hPVL, and AC hPVL ands HAM; *p≤0.05, **p≤0.01, ***p≤0.001, ****p≤0.0001.

The cytokine expression patterns associated with different T helper phenotypes were further characterized in HTLV-1-specific $CD4^+$ T cells after a 12 h stimulation with heat-inactivated HTLV-1 (Figure 3.16c-e). In agreement with the transcription factor data, I observed significantly higher levels Th1 cytokines in patients with HAM relative to AC hPVL including increased IFN-γ, TNF, and increased trends in CXCL10 (Figure 3.16f). While TNF- is predominantly associated with Th1 cells, it is also produced by Th17, Th0, Th22, and occasionally by other T-helper subsets, reflecting its broad role in various immune responses and inflammatory processes [355]. Interestingly patients with HAM also expressed significantly higher levels of the Th17/Th22 cytokine IL-22 than AC hPVL, despite expressing comparable levels of ROR-γt (Figure 3.16b and Figure 3.16f). Patients with HAM also expressed significantly higher levels of the Tfh cytokine IL-21 relative to AC hPVL (Figure 3.16f).

In both the TF data and the cytokine data, there were non-significant trends that showed increased expression of Th1 cytokines IFN-γ and TNF in AC lPVL relative to AC hPVL. AC lPVL also expressed significantly higher levels of IL-17A and IL-17F relative to AC hPVL and patients with HAM, in agreement with the ROR-γt expression, and higher levels of IL-10 relative to AC hPVL.

Overall, the HTLV-1-specific $CD4^+$ T cell response in patients with HAM skews towards Th1, but with increased IL-22 and IL-21, indicating an unfocused highly inflammatory response. Th17 responses, with high IL-10, were associated with HTLV-1 viral control.

3.2.9 Pathway enrichment analysis of HTLV-1-specific CD4$^+$ T cells in different HTLV-1-infected groups

Given the high number of DEGs detected between HTLV-1-infected groups, pathway enrichment analysis was performed with XGR and pathway annotations from Reactome [336]. Interestingly, pathways enrichment identified "NRAGE signals death through JNK", "G alpha (12/13) signaling events", and "p75NTR receptor-mediated signaling" to be upregulated in HAM relative to AC hPVL (Figure 3.17a). Upon closer inspection, except *GNA12*, these pathways contained many of the same upregulated genes, including *FDG3, ABR, RIPK2, PREX1, ADCY7, ECT2*, and *ARDGAP4*, which are all involved in G alpha (12/13) signaling (Table 3.8). This increased GPCR signaling in patients with HAM relative to AC hPVL is in agreement with the upregulated downstream GPCR signaling seen in the HAM vs. UC analysis.

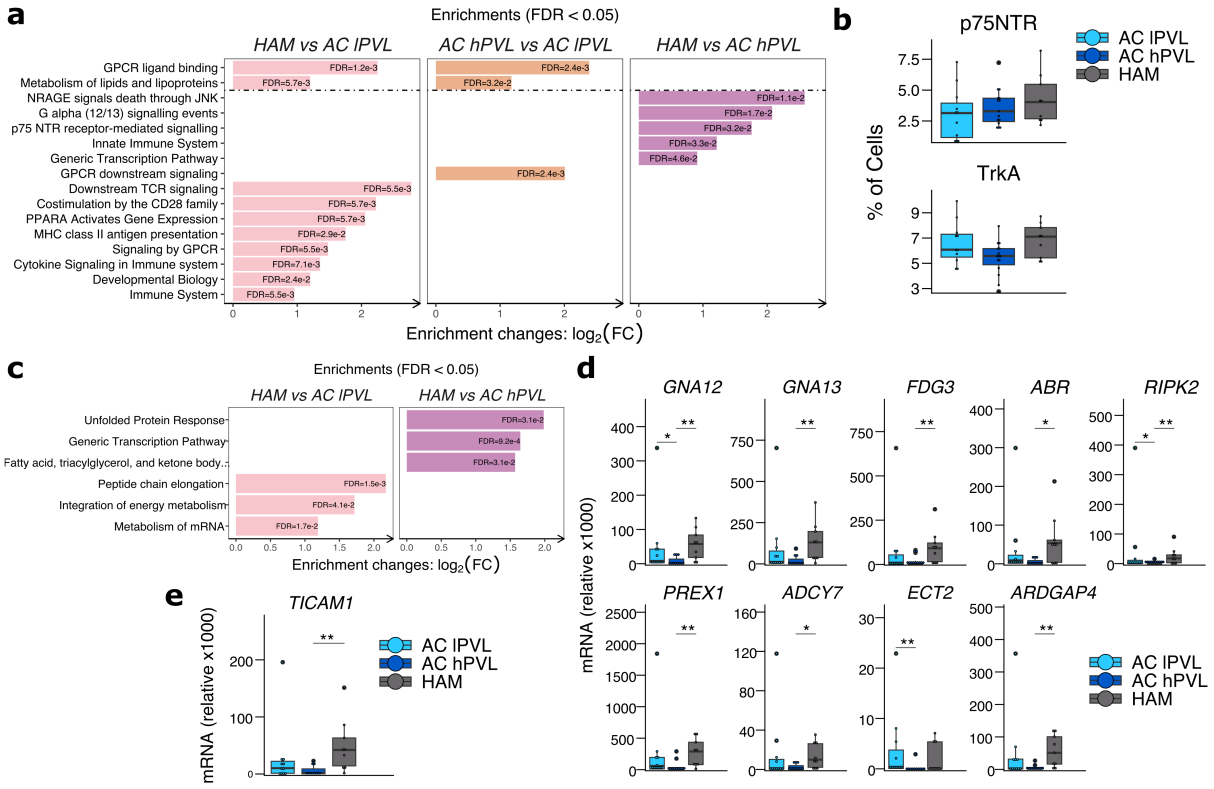


Figure 3.17: Pathway enrichment analysis in HTLV-1-specific CD4$^+$ T cells in different HTLV-1-infected groups. a. Bar plots depicting significantly enriched pathways from Reactome for HTLV-1-specific CD4$^+$ T cells from HAM vs. AC lPVL, AC hPVL vs. AC lPVL, and HAM vs. AC hPVL using upregulated genes ($\geq$1.5 fold increase, FDR$\leq$0.05). Fold enrichment is plotted as log2 (FC) and bars are labeled with the adjusted p-value. **b.** Box and whisker plot showing p75NTR and TrkA expression in HTLV-1-specific CD4$^+$ T cells (n=11 AC lPVL, n=15 AC hPVL, n=9 HAM). **c.** Bar plots depict significantly enriched (FDR$\leq$0.05) pathways from Reactome for HTLV-1-specific CD4$^+$ T cells from HAM vs. AC lPVL, AC hPVL vs. AC lPVL, and HAM vs. AC hPVL using downregulated genes ($\geq$1.5 fold decrease, FDR$\leq$0.05). Fold enrichment is plotted as log2 (FC) and bars are labeled with the adjusted p-value. **d.** Box and whisker plot showing relative gene expression of genes in the G alpha 12/13 signaling events pathway relative to *B2M* measured by RT-PCR in sorted HTLV-1-specific CD4$^+$ T cells (n=11 AC lPVL, n=11 AC hPVL, n=9 HAM). **e.** Box and whisker plot showing relative gene expression of *TICAM1* relative to *B2M* measured by RT-PCR in sorted HTLV-1-specific CD4$^+$ T cells (n=11 AC lPVL, n=11 AC hPVL, n=9 HAM). **b, d, e)** Wilcoxon signed-rank unpaired test for comparisons between AC lPVL and AC hPVL, and AC hPVL and HAM; *p$\leq$0.05, **p$\leq$0.01, ***p$\leq$0.001, ****p$\leq$0.0001.

p75NTR and tropomyosin receptor kinase A (TrkA) are upstream of NRAGE and JNK, and their ligands include nerve growth factor (NGF), BDNF, neurotrophin (NT) 3, and NT-4 [356]. p75NTR or TrkA were not differentially upregulated in HAM relative AC hPVL in the RNA-seq data, and this was confirmed at a protein level, indicating that the differences were downstream of the receptor (Figure 3.17b). Pathways that were upregulated in HAM vs. AC lPVL but not AC hPVL vs. AC lPVL, included downstream TCR signaling, co-stimulation by the CD28 family, and MHC class II antigen presentation indicating more activated HTLV-1-specific $CD4^+$ T cells with increased TCR signaling in patients with HAM relative to AC lPVL. A full list of the DEGs in the upregulated pathways can be seen in Table 3.8) for the HAM vs. AC hPVL analysis, Table 3.9 for the AC hPVL vs. AC lPVL analysis, and Table 3.10 for the HAM vs. AC lPVL analysis.

There were no downregulated pathways in AC hPVL relative to AC lPVL. The downregulated pathway with the largest fold-change in patients with HAM relative to AC hPVL was the unfolded protein response (UPR) (Figure 3.17c). The accumulation of unfolded or misfolded proteins in the endoplasmic reticulum activates the UPR [357]. Many acute and chronic viral infections activate the UPR [358]. The activation of the UPR results in the reduction of protein translation, the degradation of misfolded proteins, and the upregulation of molecular chaperone production, however in conditions of prolonged stress the UPR can also induce apoptosis [358]. The downregulation of the UPR in patients with HAM could lead to the survival of stressed and highly inflammatory cells. In addition to the UPR, patients with HAM downregulated "fatty acid, triacylglycerol, and ketone body metabolism" relative to AC hPVL and downregulated "integration of energy metabolism" relative to AC lPVL. The genes downregulated in the "fatty acid, triacylglycerol, and ketone body metabolism" pathway in patients with HAM relative to AC hPVL included *AGPAT1*, *GPD1L*, *GRHL1*, *MED15*, *MED8*, *NR1D1*, and *PPARG*. Highly activated T cells tend to rely more on glycolysis relative to fatty acid oxidation, therefore the downregulation of these pathways may indicate an increased reliance on glucose and an increased activation state of HTLV-1-specific $CD4^+$ T cells in patients with HAM [359]. A full list of the DEGs in the downregulated pathways can be seen in Table 3.11) for the HAM vs. AC hPVL analysis, and Table 3.12 for the HAM vs. AC lPVL analysis.

To validate the differential gene expression in these detected pathways, the relat-

ive gene expression of the genes in the G alpha (12/13) signaling events pathway was measured by RT-PCR in an expanded cohort of patients (Figure 3.17d). As expected, *GNA12, GNA13, FDG3, ABR, RIPK2, PREX1, ADCY7, ECT2*, and *ARDGAP4* were all expressed at higher levels in patients with HAM relative to AC hPVL. Interestingly, *GNA12, RIPK2, PREX1* and *ECT2* several of the genes were also upregulated in AC lPVL relative to AC hPVL, indicating that these genes may contribute to the maintenance of a low PVL in AC lPVL, but contribute to pathology in high PVLs.

To validate some of the differentially expressed genes in the innate immune system pathway which was upregulated in HAM relative to AC hPVL (Figure 3.17a), relative *TICAM1* expression was measured by RT-PCR in an expanded cohort of patients, and again confirmed the increased expression levels in patients with HAM relative to AC hPVL. Taken together, this data indicates that G alpha (12/13) signaling may be involved in HTLV-1-specific $CD4^+$ T cell dysfunction in patients with HAM and contribute to HAM pathogenesis. However, the mechanisms by which this pathway drives inflammation remain unclear.

3.2.10 Characterization of bulk CD4$^+$ T cells

Finally, to gain insight into whether the differences in T helper phenotypes of HTLV-1-specific CD4$^+$ T cells were also seen in the bulk CD4$^+$ T cells across different HTLV-1 infected groups, I characterized bulk CD4$^+$ T cells by flow cytometry. CD4$^+$ T cells were analyzed either *ex vivo* or after stimulation with PMA and ionomycin. The markers CCR7 and CD45RA were used to classify *ex vivo* CD4$^+$ T cells into central memory (CM), naïve, tTDE and EM cells (Figure 3.18a). Overall there were very minor differences in the antigen experience of bulk CD4$^+$ T cells in the different HTLV-1-infected groups, with no differences in the frequency of central memory or naïve cells (Figure 3.18b). High PVL groups had an increased frequency of effector memory cells relative to AC lPVL, and HTLV-1-infected individuals had a higher frequency of terminally differentiated effector cells relative to UCs.

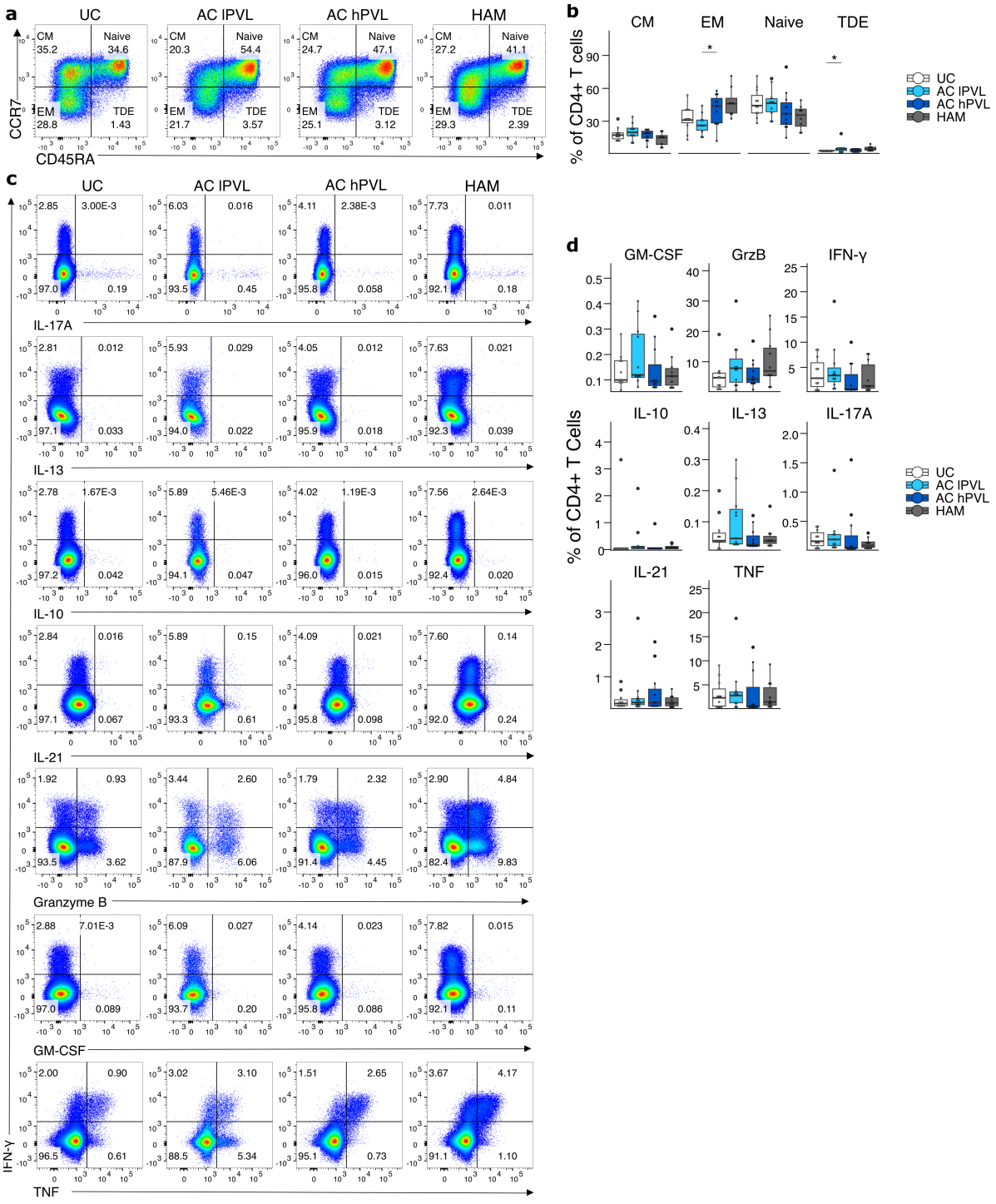


Figure 3.18: Characterization of bulk CD4$^+$ T cells in UCs, ACs, and patients with HAM. Representative flow plots (**a**) and box and whisker plots (**b**) showing the frequency of central memory (CM), naïve, effector memory (EM), and terminally differentiated effector (TDE) CD4$^+$ T cells in different study groups (n=11 UC, n=10 AC lPVL, n=11 AC hPVL, n=8 HAM). Representative flow plots (**c**) and box and whisker plots (**d**) showing granzyme B and cytokine expression in CD4$^+$ T cells in different groups after a 4-hour stimulation with PMA and ionomycin (n=11 UC, n=11 AC lPVL, n=11 AC hPVL, n=9 HAM). **b, d)** Wilcoxon signed-rank unpaired test for comparisons between UC and AC lPVL, AC lPVL and AC hPVL, and AC hPVL and HAM; *p≤0.05, **p≤0.01, ***p≤0.001, ****p≤0.0001.

To characterize the cytokine expression profile of bulk CD4$^+$ T cells in different HTLV-1-infected groups and UCs, I stimulated total PBMCs with PMA and ionomycin for 4 h and characterized the cytokine expression by flow cytometry (Figure 3.18c). Overall there were no statistically significant differences in cytokine or granzyme B expression between UCs and AC lPVL, AC lPVL and AC hPVL, or AC hPVL and patients with HAM (Figure 3.18d).

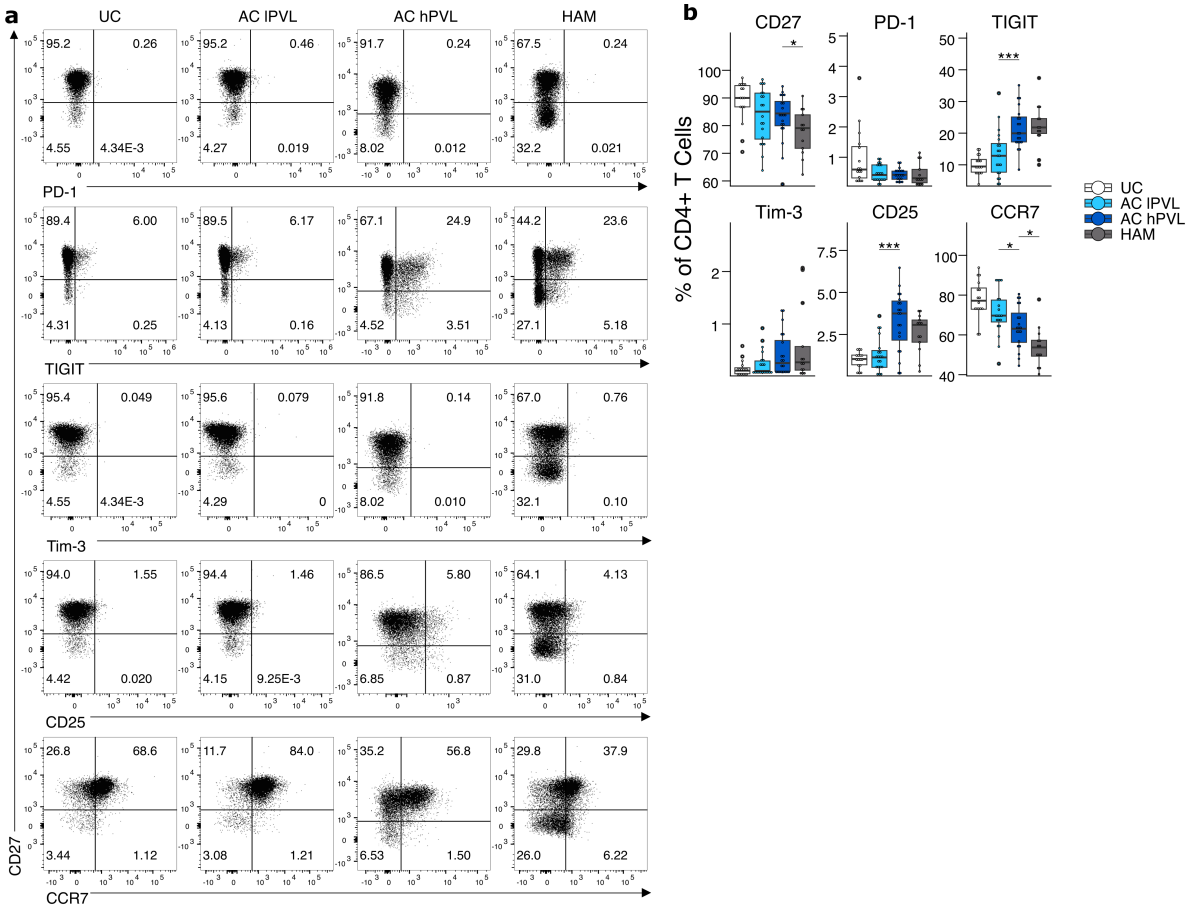


Figure 3.19: Characterization of surface markers on bulk CD4$^+$ T cells in UCs, ACs, and patients with HAM. Representative flow plots (**a**) and box and whisker plots (**b**) showing the expression of cell surface markers in *ex vivo* CD4$^+$ T cells (n=16 UC, n=20 AC lPVL, n=20 AC hPVL, n=13 HAM). **b)** Wilcoxon signed-rank unpaired test for comparisons between UC and AC lPVL, AC lPVL and AC hPVL, and AC hPVL and HAM; *p≤0.05, **p≤0.01, ***p≤0.001, ****p≤0.0001.

Finally, I characterized the expression of certain cell surface markers. I stained for CD27 to gain insight into T cell activation, PD-1, T cell immunoreceptor with immunoglobulin and ITIM domain (TIGIT), Tim-3, and CD25 to gain insight into inhibitory capacity, and CCR7 to assess lymph node homing capacity (Figure 3.19a and 3.19b). There were no significant differences in PD-1 and Tim-3 expression. CCR7 expression decreased significantly with PVL in ACs and decreased even further in patients with HAM. High PVL groups expressed higher levels of TIGIT and CD25, in agreement with previous studies [304]. Overall these data indicate only minor differences in the bulk $CD4^+$ T cell populations between HTLV-1-infected groups and UCs, with all groups producing similar levels of cytokines.

3.3 Discussion

The overall aim of this chapter was to characterize HTLV-1-specific $CD4^+$ T cells in different HTLV-1-infected groups to gain insight into HTLV-1-specific $CD4^+$ T cell responses associated with effective viral control, and signaling pathways and molecules associated with HAM pathogenesis. Throughout this chapter, I identified HTLV-1-specific $CD4^+$ T cells by stimulating total PBMCs with heat-inactivated HTLV-1, and using CD154 expression as a marker for HTLV-1-specificity. When controlling for PVL between patients with HAM and ACs, I observed that the frequency and number of HTLV-1-specific $CD4^+$ T cells increased with PVL, but did not change with disease status. In agreement with previous studies, I observed that HTLV-1-specific $CD4^+$ T cells are infected at higher rates than non-HTLV-1-specific $CD4^+$ T cells [301], and this preferential infection is even more pronounced in high PVL groups. HTLV-1-specific $CD4^+$ T cells from patients with HAM showed an increased effector memory phenotype and increased CD49d expression, indicating an enhanced effector phenotype and capacity to travel to the CNS. I showed that HTLV-1-specific $CD4^+$ T cells from patients with HAM reduced the viability of astrocytes and induced proinflammatory astrocytes which expressed significantly higher levels of CD40, iNOS, and CXCL10 relative to AC hPVL and IL-6 and and IFN-γ relative to UCs. While HTLV-1-specific $CD4^+$ T cells from all HTLV-1-infected groups induced the upregulation of the antigen presentation machinery in microglia, HTLV-1-specific $CD4^+$ T cells from patients with HAM induced significantly higher levels of CD80 expression and reduced microglial viability relative to AC hPVL. To gain insight into the mechanisms by which HTLV-1-specific $CD4^+$ T cells induced these changes, I performed RNA-seq analysis on HTLV-1-specific $CD4^+$ T cells from UCs, AC lPVL, AC hPVL, and patients with HAM. I identified 628 differentially expressed genes in patients with HAM when compared to AC hPVL, including the upregulation of *EOMES*, *SEMA4A*, *IL17RA*, *IL17RC*, and genes associated with an unfocused Th1 phenotype. I validated the RNA-seq findings at a protein level and showed that a Th17 response with some Th1 cytokine expression is associated with a low PVL, while HTLV-1-specific $CD4^+$ T cells in patients with HAM have an unfocused Th1 phenotype with high levels of Th1 cytokines, IL-22, and IL-21 expression. Pathway enrichment analysis showed that patients with HAM upregulate G alpha (12/13) signaling events, have increased NRAGE death signaling through JNK,

and increased signaling by p75NTR relative to AC hPVL. These pathways, molecules, and Th1 cytokines have the potential to modulate CNS resident cells and contribute to HAM pathogenesis. In this chapter, I have gained insights into $CD4^+$ T cells responses associated with a low PVL, and dysfunctional and inflammatory responses associated with HAM.

Previous studies identified HTLV-1-specific $CD4^+$ T cells by stimulating total PBMCs with a HTLV-1-peptide library for 6 h and using IFN-γ expression as a marker for HTLV-1-specificity [300, 301]. These studies showed that patients with HAM had a 25-fold greater frequency of IFN-γ^+ HTLV-1-specific $CD4^+$ T cells relative to ACs, and that these IFN-γ^+ HTLV-1-specific $CD4^+$ T cells were infected with HTLV-1 at higher rates relative to non-HTLV-1-specific $CD4^+$ T cells [300, 301]. However, the patients with HAM in these studies had significantly higher PVLs than the ACs, therefore it is likely, based on my data, that these observed differences in HTLV-1-specific $CD4^+$ T cell frequency between patients with HAM and ACs were due to differences in PVL rather than disease status.

In this chapter, I identified HTLV-1-specific $CD4^+$ T cells by stimulating total PBMCs with heat-inactivated HTLV-1 for 12 hours and defining $CD4^+$ T cells that expressed CD154 as HTLV-1-specific [323]. The use of CD154 to identify HTLV-1-specific $CD4^+$ T cells allows direct access to antigen-specific T cells from an unrestricted pool of epitopes, phenotypes, and TCR sequences [127, 316, 320, 323]. However, using CD154 as an activation-induced marker has limitations. CD154 is not exclusively expressed by virus-specific T cells; it can be upregulated in response to non-specific activation, which may lead to the inclusion of non-HTLV-1-specific cells. This non-specific activation could explain the presence of $CD154^+$ $CD4^+$ T cells in UCs after HTLV-1 stimulation, as well as the high proportion of naïve $CD154^+$ $CD4^+$ T cells in chronically infected patients. Additionally, using the whole heat-inactivated virus to stimulate PBMCs, rather than peptides, has its limitations. This approach depends on effective antigen processing and presentation, which can vary across different cell types, potentially leading to inconsistent T-cell activation. Moreover, whole virus stimulation may induce non-specific immune responses due to the presence of various viral components, whereas peptides provide more targeted and specific activation of virus-specific T cells. Despite these limitations, this technique remains a valuable tool that can offer significant insights into HTLV-1-specific

responses.

While many factors contribute to HAM pathogenesis, the best predictor of risk remains a high PVL. Therefore understanding the mechanisms by which some ACs can effectively control HTLV-1 infection is essential for reducing the risk of HTLV-1-associated diseases. The AC lPVL group had a lower frequency and number of HTLV-1-specific $CD4^+$ T cells, indicating that the HTLV-1-specific $CD4^+$ T cell response is more efficient, and requires fewer cells to control the infection than high PVL groups. While HTLV-1-specific $CD4^+$ T cells in all HTLV-1-infected groups were infected at higher rates than non-HTLV-1-specific $CD4^+$ T cells, this preferential infection was less severe in the AC lPVL group. While it is unclear if higher rates of preferential infection of HTLV-1-specific $CD4^+$ T cells in high PVL groups are a cause or consequence of high PVLs, high rates of infection of HTLV-1-specific $CD4^+$ T cells in high PVL groups may directly contribute to the inability to control HTLV-1-infection. When highly-infected HTLV-1-specific $CD4^+$ T cells become activated by chronic HTLV-1-antigen expression, they proliferate and directly contribute to higher PVLs. Furthermore, HTLV-1-specific $CD4^+$ T cells in AC lPVL expressed significantly higher levels of IL-10 than AC hPVL, which could reduce the proliferation of infected lymphocytes thereby reducing the mitotic proliferation of HTLV-1. In addition, HTLV-1-specific $CD4^+$ T cells in AC lPVL appear less activated than in high PVL groups, as shown by the pathway enrichment analysis relative to UCs (Figure 3.13f), despite being stimulated *ex vivo* with the same concentration of heat-inactivated HTLV-1. The HTLV-1-specific $CD4^+$ T cells in the AC lPVL group had significantly lower frequencies of effector memory and terminally differentiated effector cells relative to AC hPVL. Phenotypically, HTLV-1-specific $CD4^+$ T cells in AC lPVL had an increased Th17 phenotype, expressing high levels of ROR-γt, IL-17A, and IL-17F relative to AC hPVL. HTLV-1-specific $CD4^+$ T cells from AC lPVL also expressed non-significant trends in increased T-bet and Th1 cytokine expression including IFN-γ, TNF, and CXCL10 relative to AC hPVL. While strong Th1 responses are generally associated with strong antiviral functions [360], the role Th17 cells play in viral control is less understood [361]. Th17 responses have been associated with pathology in autoimmune and inflammatory conditions such as MS, RA, and IBD [362]. In chronic viral infections like HIV, HIV-specific $CD4^+$ T cells from elite controllers, people spontaneously controlling the virus, robustly expressed genes associated with Th1, Th17, and Th22 phenotypes, while HIV-

specific $CD4^+$ T cells in chronic HIV progressors showed a more Tfh phenotype [316]. While HTLV-1-specific $CD4^+$ T cells in AC hPVL did not seem to upregulate genes associated a Tfh phenotype, including *BCL6*, *CXCR5*, *PDCD1*, and did not express higher levels of IL-21, I did observe strong Th1 and Th17 cytokine responses in AC lPVL relative to AC hPVL. These data indicate that a small but efficient HTLV-1-specific $CD4^+$ T cell population, with strong Th1 and Th17 cytokine responses, and high IL-10 expression is associated with effective viral control in HTLV-1 infection.

While a high PVL is the biggest known risk factor for HAM, over 50% of HTLV-1-infected individuals have a PVL above 1%, and only a small minority go on to develop HAM [212]. Therefore, high PVL in isolation is not enough to drive HAM pathogenesis. HTLV-1-specific $CD4^+$ T cells from patients with HAM had an enhanced effector memory phenotype and expressed higher levels of CD49d than AC hPVL, indicating an enhanced capacity to migrate to the CNS. Anti-CD49d antibody natalizumab is an approved treatment for MS and has been shown to reduce lymphocyte infiltration in the CNS [363]. Given the similarity of HAM and MS symptoms and disease pathology, it may be of interest to further investigate the efficacy of natalizumab in reducing lymphocyte infiltration in the CNS in patients with HAM.

In addition to the increased capacity of HTLV-1-specific $CD4^+$ T cells from patients with HAM to migrate to the CNS, I showed that HTLV-1-specific $CD4^+$ T cells from patients with HAM can directly contribute to CNS inflammation and induce inflammatory glial cells. HTLV-1-specific $CD4^+$ T cells from patients with HAM reduced the viability of astrocytes and microglia, induced the upregulation of the antigen presentation machinery, and induced the production of proinflammatory cytokines in astrocytes relative to AC hPVL. The PVL of the AC hPVL and HAM groups were matched, and the HTLV-1-specific $CD4^+$ T cells were infected at comparable rates, therefore differences observed between AC hPVL and patients with HAM were not as a result of viral proteins or glial innate immune activation by HTLV-1, but rather functional and phenotypic differences between the HTLV-1-specific $CD4^+$ T cells. HTLV-1-specific $CD4^+$ T cells from patients with HAM showed enhanced Th1 responses relative to AC hPVL. IFN-γ and TNF have previously been shown to induce HLA-DR upregulation in astrocytes [364, 365], and astrocytes can act as antigen-presenting cells during Parkinson's disease [366]. Furthermore, microglia upregulated the antigen presentation machinery after co-culture with HTLV-1-

specific $CD4^+$ T cells from patients with HAM, and expressed significantly higher levels of CD80 relative to AC hPVL. My data shows that both astrocytes and microglia have the capacity to re-activate HTLV-1-specific $CD4^+$ T cells in the CNS in patients with HAM, and the high rate of HTLV-1-infection of HTLV-1-specific $CD4^+$ T cells in patients with HAM could serve as an HTLV-1 antigen reservoir.

In addition to the upregulation of the antigen presentation machinery in astrocytes, HTLV-1-specific $CD4^+$ T cells from patients with HAM, relative to AC hPVL, induced a large and significant increase in CD40 expression and increased expression of proinflammatory cytokines and chemokines including IFN-γ, IL-6, and CXCL10. HTLV-1-specific $CD4^+$ T cells express CD154, and CD40-CD154 interactions have been shown to induce the secretion of proinflammatory cytokines and chemokines in astrocytes, which trigger an autocrine activation of these cells that aggravate EAE [367]. It has been shown that stimulation of astrocytes with IFN-γ, TNF, or lipid polysaccharide (LPS), but not HIV proteins, or IL-6 results in the upregulation of CD40 [368]. Once activated by HAM HTLV-1-specific $CD4^+$ T cells, the astrocytes expressed high levels of CXCL10, which is elevated in the CSF of patients with HAM relative to both MS patients and UCs [351]. High levels of CXCL10 contribute to the recruitment of CXCR3 expressing cells, including Th1 cells and $CD8^+$ T cells, to the CNS. Interestingly, I did not see an increase in C3 expression in the astrocytes, as C3 is usually expressed in A1 astrocytes with an inflammatory phenotype [369].

Activated non-HTLV-1-specific $CD4^+$ T cells from patients with HAM were also able to induce more inflammatory glial cells relative to AC hPVL, indicating that both HTLV-1-specific and non-specific $CD4^+$ T cells in patients with HAM have the capacity to contribute to neuroinflammation when activated. However, unlike HTLV-1-specific $CD4^+$ T cells, non-HTLV-1-specific $CD4^+$ T cells are unlikely to be chronically activated *in vivo*. These findings build on earlier studies that observed phenotypic and morphological differences in astrocyte cell lines co-cultured with HTLV-1-infected lymphocyte lines from a patient with HAM or a control [288]. It has also previously been reported that contact with HTLV-1-infected cells can alter astrocyte metabolism, homeostasis, and cytokine secretion [278], however, the differences that I observed between AC hPVL and HAM are not due to HTLV-1 infection as the HAM and AC hPVL group were matched by PVL. When stimulated with PMA and ionomycin, non-HTLV-1 specific $CD4^+$ T cells in

patients with HAM produced similar levels of Th1 cytokines relative AC hPVL, however there may be differences in cytokine expression over the 48 h stimulation with anti-CD3 and anti-CD28 during the glial co-culture between HAM and AC hPVL $CD4^+$ T cells driving these changes in glial cells. Overall, while I have demonstrated that $CD4^+$ T cells in patients with HAM are dysfunctional and can induce proinflammatory astrocytes and microglia, much remains to be elucidated about underlying the mechanisms.

While the glial-$CD4^+$ T cell co-cultures provide valuable insights into the capacity of $CD4^+$ T cells from patients with HAM to contribute to neuroinflammation and HAM pathogenesis, several limitations must be acknowledged. First, the experiment lacks concurrent phenotypic analysis of T cells and glial cells at the same time point, which limits the ability to fully correlate functional outcomes with specific cellular states. Additionally, the use of cell lines (HMC3 microglia and CCF-STTG1 astrocytes) rather than primary cells may not fully recapitulate the *in vivo* environment, potentially affecting the physiological relevance of the findings. Moreover, $CD4^+$ T cells were stimulated with HTLV-1, then sorted, and subsequently cultured for 15 days with anti-CD3 and anti-CD28 stimulation in the presence of IL-2. This culture period expands the HTLV-1-specific $CD4^+$ T cell populations from a few hundred cells to over a million cells, potentially leading to the preferential expansion of certain clones, infection statuses, and phenotypes in the *in vitro* culture. Finally, these $CD4^+$ T cells were derived from peripheral blood, which may not accurately reflect the activity of $CD4^+$ T cells in the CNS/CSF. While valuable observations have been made, further mechanistic insights are warranted to better understand the specific roles and interactions of these cells in HAM pathogenesis.

This chapter shows that *ex vivo* HTLV-1-specific $CD4^+$ T cells in patients with HAM have an unfocused Th1 response and expressed higher levels of IFN-γ, TNF, IL-21, and IL-22 than AC hPVL. Previous studies have shown that an IFN-induced signature was present in all circulating leukocytes in patients with HAM, and its intensity correlated with the clinical severity of HAM [266]. Given the overlap in Type I and Type II IFN inducible genes, the study was unable to determine the source of the signal, but the data in this chapter suggest that HTLV-1-specific $CD4^+$ T cells have the capacity to contribute to this signature [266]. In addition to a strong Th1 response, HTLV-1-specific $CD4^+$ T cells in patients with HAM also expressed high levels of IL-22 and IL-21. IL-22 is a Th17 and Th22-associated cytokine and its role in neuroinflammation is not fully

understood. Previous studies have shown that MS patients have elevated levels of IL-22 in their serum and CSF especially during the acute phase of an MS flare [370]. IL-22 has been shown to disrupt the tight junctions of the BBB and increase permeability, which enables increased infiltration of lymphocytes to the CNS [349]. In contrast, however, IL-22 has been shown to bind astrocytes and decrease the apoptosis of TNF-treated astrocytes thereby showing a potential protective role [370]. IL-22 binding protein (IL22BP) is a secreted monomeric protein acting as an IL-22 antagonist with inhibitory effects on IL-22 activity, and polymorphisms in IL22BP are associated with MS [371]. However, when IL22BP was knocked down in mice, and researchers tried to induce EAE, the IL22BP knock-out mice showed a decreased neuroinflammatory profile with an overall less severe disease, strongly suggesting that IL-22 attenuates disease severity [369]. The role of IL-22 in patients with HAM is unclear, but the higher levels of IL-22 expression in HTLV-1-specific $CD4^+$ T cells may allow increased infiltration of HTLV-1-specific $CD4^+$ T cells into the CNS, and once in the CNS, IL-22 may reduce the apoptosis of inflammatory astrocytes and induce the expression of anti-inflammatory proteins such as BDNF and IL-10. In addition to the high levels of IL-22, HTLV-1-specific $CD4^+$ T cells from patients with HAM secreted high levels of IL-21, which drives strong B cell proliferation. However, the contribution of IL-21, B cells, and antibody responses to neuroinflammation in HAM have not been well characterized. Overall the Th1 response in patients with HAM has the capacity to drive neuroinflammation, but the roles of IL-22 and IL-21 in contributing to HAM pathogenesis remain unclear.

The transcriptional analysis of HTLV-1-specific $CD4^+$ T cells identified increased *EOMES*, *SEMA4A*, *IL17RA*, and *IL17RC* expression in patients with HAM relative to AC hPVL. While the exact function of EOMES in $CD4^+$ T cells remains unclear, $EOMES^+$ $CD4^+$ T cells are increased in the CSF and periphery of progressive MS patients, and EOMES expression is essential for the development of chronic neuroinflammation in EAE [372, 373]. Recently it was shown that EOMES deletion in mice, was sufficient to protect against CNS inflammation and EAE, and that EOMES is required for long-term maintenance of CNS-infiltrating $CD4^+$ T cells [374]. EOMES expression was shown to enhance $CD4^+$ T cell survival by increasing resistance to stress-induced cell death and increasing mitochondrial respiratory capacity [374]. I also observed increased *IL17RA* and *IL17RC* expression in HTLV-1-specific $CD4^+$ T cells from patients with HAM. Increased IL-17

signaling has been shown to increase effector CD4$^+$ T cell resistance to immune suppression [375], and therefore increased IL-17 receptor expression in HTLV-1-specific CD4$^+$ T cells in patients with HAM may result in increased activation and contribute to aberrant inflammation.

Lastly, the pathway enrichment analysis identified several interesting up and downregulated pathways in HTLV-1-specific CD4$^+$ T cells in patients with HAM relative to AC hPVL. G alpha 12/13 signaling events have a wide range of downstream effects. Some upstream GPCRs for G alpha 12/13 signaling include sphingosine-1-phosphate (S1P) receptor and lysophosphatidic acid (LPA) receptor [376]. S1P signaling enables CD4$^+$ T cells to egress from the lymph node into the periphery [377, 378]. The reduced expression of CCR7 in HTLV-1-specific CD4$^+$ T cells in patients with HAM indicates reduced trafficking of HTLV-1-specific CD4$^+$ T cells to lymph nodes. In MS, S1P signaling is blocked by fingolimod to reduce lymphocyte egress from the lymph node thereby decreasing lymphocyte infiltration in the CNS. Given similarities in MS and HAM pathology, blocking S1P signaling in HAM may be an interesting avenue for further investigation for treatment [377, 378]. Additionally, HTLV-1-specific CD4$^+$ T cells from patients with HAM downregulated the metabolism of fatty acids, triacylglycerol, and ketone bodies. Generally, activated CD4$^+$ T cells have a greater glycolytic dependency and a reduced fatty acid oxidation dependency [379]. Interestingly one of the genes downregulated in this pathway is *AGPAT1*, which encodes for an enzyme that converts LPA into phosphatidic acid (PA) [380]. The downregulation of this gene may result in an increased concentration of LPA, and therefore increased LPA signaling through G alpha 12/13 signaling pathways. The role these pathways play in contributing to HAM pathogenesis warrants further investigation and follow-up study to elucidate the mechanisms.

To summarize, I have shown in this chapter that a small population of highly efficient Th17 HTLV-1-specific CD4$^+$ T cells, some Th1 cytokine production, and high levels of IL-10 are associated with a low PVL, and I have identified numerous signaling pathways and molecules in HTLV-1-specific CD4$^+$ T cells that are associated with HAM. I hypothesize the following, HTLV-1-specific CD4$^+$ T cells have an enhanced capacity to migrate to the CNS due to an enhanced effector memory phenotype with high CD49d expression. High levels of Th1 cytokines and IL-22 released by HTLV-1-specific CD4$^+$ T cells in patients with HAM may contribute to disrupting the BBB and lymphocyte infiltration

into the CNS. Once in the CNS, HTLV-1-specific $CD4^+$ T cells induce proinflammatory microglia and astrocytes which upregulate the type II antigen presentation machinery, CD40, and proinflammatory cytokines. The high level of HTLV-1-infection of HTLV-1-specific $CD4^+$ T cells and the activation of APCs in the CNS, would allow for the re-activation of HTLV-1-specific $CD4^+$ T cells in the CNS. Proinflammatory cytokines and CD40-CD154 interactions between HTLV-1-specific $CD4^+$ T cells and astrocytes may induce further astrocyte activation and the secretion of proinflammatory cytokines and chemokines which further drive inflammation in an autocrine and paracrine manner. High levels of CXCL10 secreted by activated astrocytes recruit more Th1 and $CD8^+$ T cells to the CNS further driving CNS inflammation and HAM disease progression. An upregulation of IL-17 receptors decreases susceptibility to immune suppression. Finally, HTLV-1-specific $CD4^+$ T cells in patients with HAM upregulate G alpha 12/13 signaling events, and downregulate fatty acid, triacylglycerol, and ketone body metabolism, however how these pathways contribute to HAM pathogenesis is unclear and further mechanistic insight remains to be elucidated.

3.4 Appendix

3.4.1 Pathway enrichment in HTLV-1 infected groups relative to UC

Table 3.1: Enriched pathways from upregulated genes in all HTLV-1-infected groups relative to UCs

Pathway Name	*p* adj	Upregulated Genes
Interferon alpha/beta signaling	0.0028	ADAR, EGR1, GBP2, IFI35, IFI6, IFIT1, IFIT2, IFIT3, IFITM1, IFITM3, IP6K2, IRF1, IRF5, ISG20, MX1, MX2, OAS1, OAS2, OAS3, OASL, PTPN1, SOCS3, USP18, XAF1

Significantly enriched (FDR≤0.05) pathways from Reactome for upregulated genes (≥1.5 fold increase, FDR≤0.05) in all the HTLV-1-specific $CD4^+$ T cells from HTLV-1-infected groups relative to UCs.

Table 3.2: Enriched pathways from downregulated genes in all HTLV-1-infected groups relative to UCs

Pathway Name	*p* adj	Downregulated Genes
Transport of Mature Transcript to Cytoplasm	0.023	NUP188, NUP54, SRSF1, SRSF2, SRSF6
Processing of Capped Intron-Containing Pre-mRNA	0.046	NUP188, NUP54, PAPOLA, SF3A2, SRSF1, SRSF2, SRSF6

Significantly enriched (FDR≤0.05) pathways from Reactome for downregulated genes (≥1.5 fold decrease, FDR≤0.05) in all the HTLV-1-specific $CD4^+$ T cells from HTLV-1-infected groups relative to UCs.

Table 3.3: Upregulated pathways in AC lPVL relative to UC

Pathway Name	*p* adj	Upregulated Genes
Interferon alpha/beta signaling	0.0039	ADAR, EGR1, GBP2, IFI35, IFI6, IFIT1, IFIT2, IFIT3, IFITM1, IFITM3, IP6K2, IRF1, IRF5, ISG20, MX1, MX2, OAS1, OAS2, OAS3, OASL, PTPN1, SOCS3, USP18, XAF1

Significantly enriched (FDR≤0.05) pathways from Reactome for upregulated genes (≥1.5 fold increase, FDR≤0.05) in HTLV-1-specific $CD4^+$ T cells from AC lPVL relative to UCs.

Table 3.4: Upregulated pathways in AC hPVL relative to UC

Pathway Name	p adj	Upregulated Genes
Interferon alpha/beta signaling	0.000069	ADAR, EGR1, GBP2, IFI27, IFI35, IFI6, IFIT1, IFIT2, IFIT3, IFITM1, IP6K2, IRF1, IRF4, IRF5, IRF7, ISG15, ISG20, MX1, MX2, OAS1, OAS2, OAS3, OASL, PSMB8, PTPN1, RNASEL, SOCS1, SOCS3, STAT1, STAT2, USP18, XAF1
Interferon gamma signaling	0.0026	B2M, GBP1, GBP2, GBP4, GBP5, HLA-DPA1, HLA-DPB1, HLA-DQA1, HLA-DQA2, HLA-DRB1, HLA-DRB5, ICAM1, IFNG, IRF1, IRF4, IRF5, IRF7, JAK2, OAS1, OAS2, OAS3, OASL, PML, PRKCD, PTPN1, SOCS1, SOCS3, SP100, STAT1
Cytokine Signaling in Immune system	0.0026	ADAR, ARIH1, B2M, BTRC, CASP1, CHUK, CISH, CRKL, CSF2, DDX58, EGR1, EIF2AK2, EIF4E, EIF4E3, GBP1, GBP2, GBP4, GBP5, HLA-DPA1, HLA-DPB1, HLA-DQA1, HLA-DQA2, HLA-DRB1, HLA-DRB5, ICAM1, IFI27, IFI35, IFI6, IFIT1, IFIT2, IFIT3, IFITM1, IFNG, IKBKB, IL1RN, IL2, IL2RA, IL2RB, IL3, IL5, IL6, IL7, IP6K2, IRAK1, IRAK2, IRAK4, IRF1, IRF4, IRF5, IRF7, ISG15, ISG20, JAK2, KPNA2, KPNA3, MAP2K1, MAP3K3, MAP3K8, MX1, MX2, NEDD4, NOD2, NUP210, NUPL2, OAS1, OAS2, OAS3, OASL, PELI1, PIK3CA, PML, PRKACB, PRKCD, PSMB8, PTPN1, RNASEL, SOCS1, SOCS2, SOCS3, SP100, STAT1, STAT2, TAB3, TRAF6, UBA7, UBE2E1, USP18, VAV1, XAF1, YES1, YWHAZ
Signaling by GPCR	0.0031	ABR, ADCY3, ADORA2A, ADORA2B, AKAP13, AKT1, AKT2, ANXA1, ARHGEF1, ARHGEF12, ARHGEF18, ARHGEF3, CCL2, CCL22, CCL28, CCL3, CCL3L1, CCL3L3, CCL4, CCL7, CCR2, CCR5, CCR8, CD55, CDK5, CGA, CXCL10, DAGLB, DGKA, DGKD, DGKH, F2RL1, F2RL2, FFAR3, FZD6, GNA12, GNA15, GNAO1, GNAQ, GNB1, GNG10, GNG2, GNG4, GNGT2, GPR132, GPR18, GPR65, GRK5, HBEGF, HRH1, HRH2, HRH4, HTR2B, ITPR2, ITSN1, MAP2K1, NMB, NPW, P2RY14, PDE2A, PDE4B, PDE7A, PDE8A, PDE8B, PDPK1, PIK3CA, PIK3CG, PIK3R5, POMC, PPP2CB, PPP3CB, PRKACB, PRKAR2A, PRKCD, PTGER2, PTHLH, RASGRP1, RASGRP2, RGS1, RGS2, RHOB, RPS6KA1, RPS6KA2, RPS6KA3, SOS2, TIAM2, VAV1, WNT1, XCL1, XCL2
Nucleotide-binding domain, leucine rich repeat containing receptor (NLR) signaling pathways	0.023	AIM2, BIRC2, BIRC3, CASP1, CASP9, CHUK, CYLD, IKBKB, IRAK1, IRAK2, MAPK14, NLRP1, NLRP3, NOD2, P2RX7, PANX1, PSTPIP1, PYCARD, TAB3, TRAF6, TXN
G alpha (q) signalling events	0.023	ANXA1, DAGLB, DGKA, DGKD, DGKH, F2RL1, F2RL2, FFAR3, GNA15, GNAQ, GNB1, GNG10, GNG2, GNG4, GNGT2, GPR132, GPR65, GRK5, HRH1, HTR2B, ITPR2, NMB, PIK3CA, PRKCD, RASGRP1, RASGRP2, RGS2, XCL1, XCL2

Significantly enriched (FDR$\leq$0.05) pathways from Reactome for upregulated genes ($\geq$1.5 fold increase, FDR$\leq$0.05) in HTLV-1-specific CD4$^+$ T cells from AC hPVL relative to UCs.

Table 3.5: Upregulated pathways in HAM pelative to UC

Pathway Name	*p* adj	Upregulated Genes
Interferon alpha/beta signaling	$1.2x10^{-7}$	ADAR, EGR1, GBP2, HLA-A, IFI27, IFI35, IFI6, IFIT1, IFIT2, IFIT3, IFITM1, IP6K2, IRF1, IRF3, IRF4, IRF5, IRF7, ISG15, ISG20, MX1, MX2, OAS1, OAS2, OAS3, OASL, PSMB8, PTPN1, RNASEL, SOCS1, SOCS3, STAT1, STAT2, USP18, XAF1
Interferon gamma signaling	0.00002	B2M, GBP1, GBP2, GBP4, GBP5, HLA-A, HLA-DPA1, HLA-DPB1, HLA-DQA1, HLA-DQA2, HLA-DRB1, HLA-DRB5, ICAM1, IFNG, IRF1, IRF3, IRF4, IRF5, IRF7, JAK2, OAS1, OAS2, OAS3, OASL, PML, PRKCD, PTPN1, SOCS1, SOCS3, SP100, STAT1
Interferon Signaling	0.000039	ADAR, B2M, DDX58, EGR1, EIF2AK2, EIF4E, FLNB, GBP1, GBP2, GBP4, GBP5, HLA-A, HLA-DPA1, HLA-DPB1, HLA-DQA1, HLA-DQA2, HLA-DRB1, HLA-DRB5, ICAM1, IFI27, IFI35, IFI6, IFIT1, IFIT2, IFIT3, IFITM1, IFNG, IP6K2, IRF1, IRF3, IRF4, IRF5, IRF7, ISG15, ISG20, JAK2, KPNA2, KPNA3, MX1, MX2, NEDD4, NUP210, NUP214, OAS1, OAS2, OAS3, OASL, PML, PRKCD, PSMB8, PTPN1, RNASEL, SOCS1, SOCS3, SP100, STAT1, STAT2, UBA7, UBE2E1, USP18, XAF1
Cytokine Signaling in Immune system	0.0015	ADAM17, ADAR, B2M, CASP1, CHUK, CISH, CSF2, DDX58, EGR1, EIF2AK2, EIF4E, FLNB, GBP1, GBP2, GBP4, GBP5, HLA-A, HLA-DPA1, HLA-DPB1, HLA-DQA1, HLA-DQA2, HLA-DRB1, HLA-DRB5, ICAM1, IFI27, IFI35, IFI6, IFIT1, IFIT2, IFIT3, IFITM1, IFNG, IKBKB, IL2, IL2RA, IL2RB, IP6K2, IRAK2, IRAK4, IRF1, IRF3, IRF4, IRF5, IRF7, ISG15, ISG20, JAK2, KPNA2, KPNA3, MAP2K4, MAP3K8, MX1, MX2, NEDD4, NOD2, NUP210, NUP214, OAS1, OAS2, OAS3, OASL, PELI1, PIK3R1, PML, PRKACB, PRKCD, PSMB8, PTPN1, RNASEL, SOCS1, SOCS2, SOCS3, SP100, STAT1, STAT2, STAT3, TAB3, TRAF6, UBA7, UBE2E1, USP18, XAF1, YES1, YWHAZ
GPCR downstream signaling	0.0015	ABR, ADCY7, ADORA2A, ADORA2B, AKAP13, AKT1, AKT2, ANXA1, ARHGAP4, ARHGEF1, ARHGEF18, ARHGEF3, ARHGEF6, CCL28, CCR10, CCR2, CCR5, CCR8, CGA, CXCL10, DAGLB, DGKA, DGKD, DGKE, DGKH, F2RL1, F2RL2, FFAR3, FGD3, GNA12, GNA15, GNAQ, GNG2, GNG4, GNGT2, GPR132, GPR65, GRK5, HRH1, HRH2, HTR2B, ITPR2, ITSN1, NET1, NPW, P2RY14, PDE7A, PDE8A, PDE8B, PDPK1, PIK3R1, PIK3R5, POMC, PREX1, PRKCD, PTGER2, PTGER3, PTHLH, RAMP1, RASGRP1, RASGRP2, RGS1, RGS2, RHOB, TIAM2, XCL1, XCL2
Signaling by GPCR	0.023	ABR, ADCY7, ADORA2A, ADORA2B, AKAP13, AKT1, AKT2, ANXA1, ARHGAP4, ARHGEF1, ARHGEF18, ARHGEF3, ARHGEF6, CCL2, CCL22, CCL28, CCL3, CCL4, CCL7, CCR10, CCR2, CCR5, CCR8, CD55, CDK5, CGA, CXCL10, DAGLB, DGKA, DGKD, DGKE, DGKH, F2RL1, F2RL2, FFAR3, FGD3, FZD6, GNA12, GNA15, GNAQ, GNG2, GNG4, GNGT2, GPR132, GPR65, GRK5, HBEGF, HRH1, HRH2, HTR2B, ITPR2, ITSN1, NET1, NPW, P2RY14, PDE7A, PDE8A, PDE8B, PDPK1, PIK3R1, PIK3R5, POMC, PREX1, PRKACB, PRKCD, PTGER2, PTGER3, PTHLH, RAMP1, RASGRP1, RASGRP2, RGS1, RGS2, RHOB, RPS6KA1, TIAM2, WNT1, XCL1, XCL2
G alpha (q) signalling events	0.025	ANXA1, DAGLB, DGKA, DGKD, DGKE, DGKH, F2RL1, F2RL2, FFAR3, GNA15, GNAQ, GNG2, GNG4, GNGT2, GPR132, GPR65, GRK5, HRH1, HTR2B, ITPR2, PIK3R1, PRKCD, RASGRP1, RASGRP2, RGS2, XCL1, XCL2

Significantly enriched (FDR$\leq$0.05) pathways from Reactome for upregulated genes ($\geq$1.5 fold increase, FDR$\leq$0.05) in HTLV-1-specific $CD4^+$ T cells from HAM relative to UCs.

Table 3.6: Downregulated pathways in AC lPVL Relative to UC

Pathway Name	*p* adj	Downregulated Genes
Transport of Mature Transcript to Cytoplasm	0.0009	NUP188, NUP54, SRSF1, SRSF2, SRSF6
Processing of Capped Intron-Containing Pre-mRNA	0.014	NUP188, NUP54, PAPOLA, SF3A2, SRSF1, SRSF2, SRSF6
RNA Polymerase II Transcription	0.035	PAPOLA, SRSF1, SRSF2, SRSF6, TCEA1

Significantly enriched (FDR≤0.05) pathways from Reactome for downregulated genes (≥1.5 fold decrease, FDR≤0.05) in HTLV-1-specific $CD4^+$ T cells from AC lPVL relative to UCs.

Table 3.7: Downregulated pathways in AC hPVL relative to UC

Pathway Name	*p* adj	Downregulated Genes
Transport of Ribonucleoproteins into the Host Nucleus	0.003	KPNB1, NUP188, NUP43, NUP50, NUP54, NUP62, NUP93
Interactions of Vpr with host cellular proteins	0.005	HMGA1, NUP188, NUP43, NUP50, NUP54, NUP62, NUP93
Transport of Mature Transcript to Cytoplasm	0.012	NUP188, NUP43, NUP50, NUP54, NUP62, NUP93, SRSF1, SRSF2
Metabolism of non-coding RNA	0.016	NUP188, NUP43, NUP50, NUP54, NUP62, NUP93, PRMT5
Processing of Capped Intron-Containing Pre-mRNA	0.016	HNRNPM, LSM2, NUP188, NUP43, NUP50, NUP54, NUP62, NUP93, SF3B4, SNRNP40, SRSF1, SRSF2, YBX1
Host Interactions of HIV factors	0.037	AP1S1, HMGA1, KPNB1, NUP188, NUP43, NUP50, NUP54, NUP62, NUP93, PSMD1, PSMD5

Significantly enriched (FDR≤0.05) pathways from Reactome for downregulated genes (≥1.5 fold decrease, FDR≤0.05) in HTLV-1-specific $CD4^+$ T cells from AC hPVL relative to UCs.

3.4.2 Pathway enrichment in HTLV-1 infected groups

Table 3.8: Upregulated pathways in HAM relative to AC hPVL

Pathway Name	*p* adj	Upregulated Genes
NRAGE signals death through JNK	0.011	ABR, ARHGAP4, ECT2, FGD1, FGD3, PREX1
G alpha (12/13) signalling events	0.017	ABR, ARHGAP4, ECT2, FGD1, FGD3, GNA12, PREX1
p75 NTR receptor-mediated signalling	0.032	ABR, ARHGAP4, ECT2, FGD1, FGD3, PREX1, RIPK
Innate Immune System	0.033	CASP10, CFH, CREBBP, CTSS, IRAK2, LGMN, NLRX1, PIK3R4, PYCARD, RIPK2, TICAM1, UBA7
Generic Transcription Pathway	0.046	CREBBP, MED12, NR3C2, ZKSCAN5, ZNF138, ZNF155, ZNF227, ZNF263, ZNF28, ZNF43, ZNF431, ZNF519, ZNF530, ZNF544, ZNF558, ZNF597, ZNF611

Significantly enriched (FDR≤0.05) pathways from Reactome for upregulated genes (≥1.5 fold increase, FDR≤0.05) in HTLV-1-specific $CD4^+$ T cells from HAM relative to AC hPVL.

Table 3.9: Upregulated pathways in AC hPVL relative to AC lPVL

Pathway Name	*p* adj	Upregulated Genes
GPCR ligand binding	0.0024	CCR8, CGA, F2R, FZD6, HTR2B, PTHLH, XCL2
GPCR downstream signaling	0.0024	CCR8, CGA, F2R, GRK5, HTR2B, PDE8B, PTHLH, TIAM2, XCL2
Metabolism of lipids and lipoproteins	0.032	CGA, CYP7B1, GK, HMGCS1, NCOA2, PNPLA2, RXRA, SGPP2, SLC27A2, TIAM2

Significantly enriched (FDR≤0.05) pathways from Reactome for upregulated genes (≥1.5 fold increase, FDR≤0.05) in HTLV-1-specific $CD4^+$ T cells from AC hPVL relative to AC lPVL.

Table 3.10: Upregulated pathways in HAM relative to AC lPVL

Pathway Name	*p* adj	Upregulated Genes
GPCR ligand binding	0.0012	ADORA2B, CCL22, CCR8, CD55, CGA, F2R, FZD6, GPR132, PTGER4, WNT1
Downstream TCR signaling	0.0055	HLA-DQA1, HLA-DQA2, HLA-DRB1, HLA-DRB5, IKBKB
Signaling by GPCR	0.0055	ADORA2B, CCL22, CCR8, CD55, CGA, F2R, FZD6, GPR132, PDE8B, PRKCA, PTGER4, TIAM2, WNT1
Immune System	0.0055	ADAM17, ANAPC4, CBLB, CD200R1, CD55, CDH1, CYLD, EGR1, GAN, HLA-DQA1, HLA-DQA2, HLA-DRB1, HLA-DRB5, HUWE1, IKBKB, IL1RAP, IL2RA, IRAK2, ITGB1, MAP3K8, MTOR, NEDD4, PIK3R4, REL, SEC24D, TICAM1, TNFAIP3, UBE3
Costimulation by the CD28 family	0.0057	HLA-DQA1, HLA-DQA2, HLA-DRB1, HLA-DRB5, MAP3K8, MTOR
PPARA Activates Gene Expression	0.0057	GLIPR1, HMGCS1, MED22, NCOA2, RXRA, TIAM2, TXNRD1
Metabolism of lipids and lipoproteins	0.0057	ACSL4, CGA, CYP7B1, GK, GLIPR1, HMGCS1, MED22, NCOA2, PI4K2A, PIK3R4, RXRA, SGPP2, SMPD4, STARD4, TIAM2, TXNRD1
Cytokine Signaling in Immune system	0.0071	ADAM17, EGR1, HLA-DQA1, HLA-DQA2, HLA-DRB1, HLA-DRB5, IKBKB, IL1RAP, IL2RA, IRAK2, MAP3K8, NEDD4
Developmental Biology	0.024	EZR, FURIN, ITGB1, MED22, NCOA2, RGMB, RXRA, SEMA4D, ST8SIA4, WNT1
MHC class II antigen presentation	0.029	HLA-DQA1, HLA-DQA2, HLA-DRB1, HLA-DRB5, SEC24D

Significantly enriched (FDR$\leq$0.05) pathways from Reactome for upregulated genes ($\geq$1.5 fold increase, FDR$\leq$0.05) in HTLV-1-specific $CD4^+$ T cells from HAM relative to AC lPVL.

Table 3.11: Downregulated pathways in HAM relative to AC hPVL

Pathway Name	*p* adj	Downregulated Genes
Generic Transcription Pathway	0.00092	MAMLD1, MED15, MED8, NR1D1, NR4A3, PPARG, ZIK1, ZKSCAN8, ZNF222, ZNF398, ZNF416, ZNF45, ZNF552, ZNF582, ZNF773
Unfolded Protein Response	0.031	ERN1, EXOSC6, KHSRP, KLHDC3, MBTPS2
Fatty acid, triacylglycerol, and ketone body metabolism	0.031	AGPAT1, GPD1L, GRHL1, MED15, MED8, NR1D1, PPARG

Significantly enriched (FDR≤0.05) pathways from Reactome for downregulated genes (≥1.5 fold decrease, FDR≤0.05) in HTLV-1-specific $CD4^+$ T cells from HAM relative to AC hPVL.

Table 3.12: Downregulated pathways in HAM relative to AC lPVL

Pathway Name	*p* adj	Downregulated Genes
Peptide chain elongation	0.0015	RPL10, RPL11, RPL12, RPL3, RPL31, RPL7, RPLP0, RPS18, RPS3A, RPS6
Metabolism of mRNA	0.017	HSPB1, PSMD2, RPL10, RPL11, RPL12, RPL3, RPL31, RPL7, RPLP0, RPS18, RPS3A, RPS6
Integration of energy metabolism	0.041	ADCY3, AGPAT1, GNAQ, PRKAR2A, SLC25A5

Significantly enriched (FDR≤0.05) pathways from Reactome for downregulated genes (≥1.5 fold decrease, FDR≤0.05) in HTLV-1-specific $CD4^+$ T cells from HAM relative to AC lPVL.

4

CD8$^+$ T cells in HTLV-1 infection

4.1 Introduction

CD8$^+$ T cells play a crucial role in antiviral immunity. However, despite their essential role in antiviral responses, the HTLV-1-specific CD8$^+$ T cell response remains relatively uncharacterized. Demonstrating the importance of the HTLV-1-specific CD8$^+$ T cell response in HTLV-1 viral control, certain HLA-I alleles have been shown to be protective against HAM by being associated with a low PVL [193]. The HLA-A*02 allele was found to be protective as it binds several Tax epitopes unusually strongly, allowing for the induction of a more rapid CD8$^+$ T cell response [243]. While the majority of HTLV-1-specific CD8$^+$ T cell immunodominant antigens were found within the Tax protein [308], a robust HBZ-specific CD8$^+$ T cell response was required for efficient viral control in ACs [307, 309, 310, 311]. HLA-I alleles that present a high frequency and diversity of HBZ epitopes were found to be protective against the development of high PVLs [309]. Furthermore, previous studies found that the frequency of HTLV–1-specific CD8$^+$ T cells was significantly higher in patients with HAM relative to ACs, and that this frequency correlated positively with PVL and with the severity of disease [299, 313].

Very little is known about the role of CD8$^+$ T cells in HAM pathogenesis. While

$CD4^+$ T cells predominate in the early HAM lesions, the CD4:CD8 T cell ratio shifts as the CNS lesions become more chronic, and $CD8^+$ T cells predominate in older HAM lesions [158, 259]. While certain HLA-I genes have been associated with either low or high PVLs, no HLA-I genes have been directly implicated in HAM pathogenesis [193]. Tax HTLV-1-specific $CD8^+$ T cells in patients with HAM have been shown to downregulate Tim-3 expression relative to ACs, indicating less exhaustion in patients with HAM [381]. Given that $CD8^+$ T cells predominate in older HAM lesions [259], $CD4^+$ T cells are likely the instigators of HAM pathogenesis, and $CD8^+$ T cells contribute to the chronicity of inflammation and CNS damage. However, how $CD8^+$ T cells are recruited to the CNS or the mechanism by which they contribute to pathology remains unclear.

In this chapter, I identified HTLV-1-specific $CD8^+$ T cells by stimulating total PBMCs with heat-inactivated HTLV-1 for 12-20 h and identifying HTLV-1-specific $CD8^+$ T cells using the activation-induced markers CD137 and CD69 [75, 329]. High PVL groups had an increased frequency and number of HTLV-1-specific $CD8^+$ T cells, and HTLV-1-specific $CD8^+$ T cells were infected at higher rates with HTLV-1 relative to non-HTLV-1-specific $CD8^+$ T cells. HTLV-1-specific $CD8^+$ T cells from patients with HAM expressed significantly higher levels of IL-17A and increased trends in IFN-γ relative to AC hPVL. Furthermore, HTLV-1-specific $CD8^+$ T cells from patients with HAM induced the upregulation of the antigen presentation machinery and increased astrocyte expression of proinflammatory cytokines, demonstrating the potential of HTLV-1-specific $CD8^+$ T cells to contribute to HAM pathogenesis. Finally, I characterized bulk $CD8^+$ T cells in HTLV-1-infected individuals and showed that HTLV-1-infected individuals have more terminally differentiated effector $CD8^+$ T cells relative to UCs, but there were no major differences in the cytokine secretion profiles of $CD8^+$ T cells in UCs, AC lPVL, AC hPVL, and patients with HAM. $CD8^+$ T cells from patients with HAM expressed higher levels of CD49d relative to AC hPVL, indicating an enhanced capacity to migrate to the CNS and contribute to CNS inflammation. The data in this chapter provides a deeper understanding of both bulk and HTLV-1-specific $CD8^+$ T cells in HTLV-1 infection and their potential to contribute to HAM pathogenesis.

4.2 Results

4.2.1 Identification and characterization of HTLV-1-specific CD8$^+$ T cells

As in the previous chapter, HTLV-1-infected individuals were grouped into ACs with a PVL under 3% (AC lPVL), ACs with a PVL above 3% (AC hPVL), and patients with HAM. Again, the PVLs of the AC hPVL and HAM groups were matched to control for differences due to HTLV-1-infection. Throughout this chapter, unless otherwise stated, I focused my statistical comparisons between UC and AC lPVL to identify changes that occur due to HTLV-1 infection, between AC lPVL and AC hPVL to identify differences as a result of PVL, and between AC hPVL and HAM to identify difference due to disease status. CD8$^+$ T cells were identified by flow cytometry using the gating strategy shown in Figure 4.1.

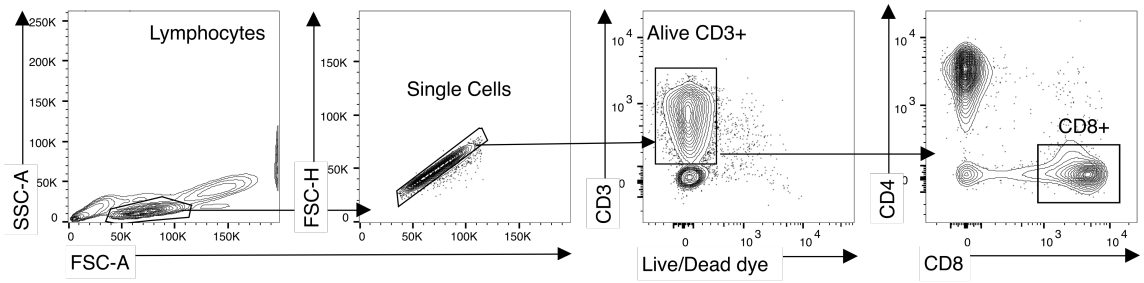


Figure 4.1: Gating strategy for the identification of CD8$^+$ T cells from total PBMCs.

To identify HTLV-1-specific CD8$^+$ T cells, total PBMCs were stimulated with heat-inactivated HTLV-1, and HTLV-1-specific CD8$^+$ T cells were identified based on the co-expression CD69 and CD137 on pre-gated CD8$^+$ T cells (Figure 4.2a) [75, 329]. The frequency and number (in 10 million PBMCs) of HTLV-1-specific CD8$^+$ T cells were characterized in UCs and the different HTLV-1-infected groups (Figure 4.2b). Unsurprisingly, UCs that had never been exposed to HTLV-1 had very few CD69$^+$CD137$^+$ CD8$^+$ T cells. In agreement with previous studies, the number and frequency of HTLV-1-specific CD8$^+$ T cells significantly increased with PVL (Figure 4.2b) [313]. There were no differences in the number or frequency of HTLV-1-specific CD8$^+$ T cells between AC hPVL and patients with HAM.

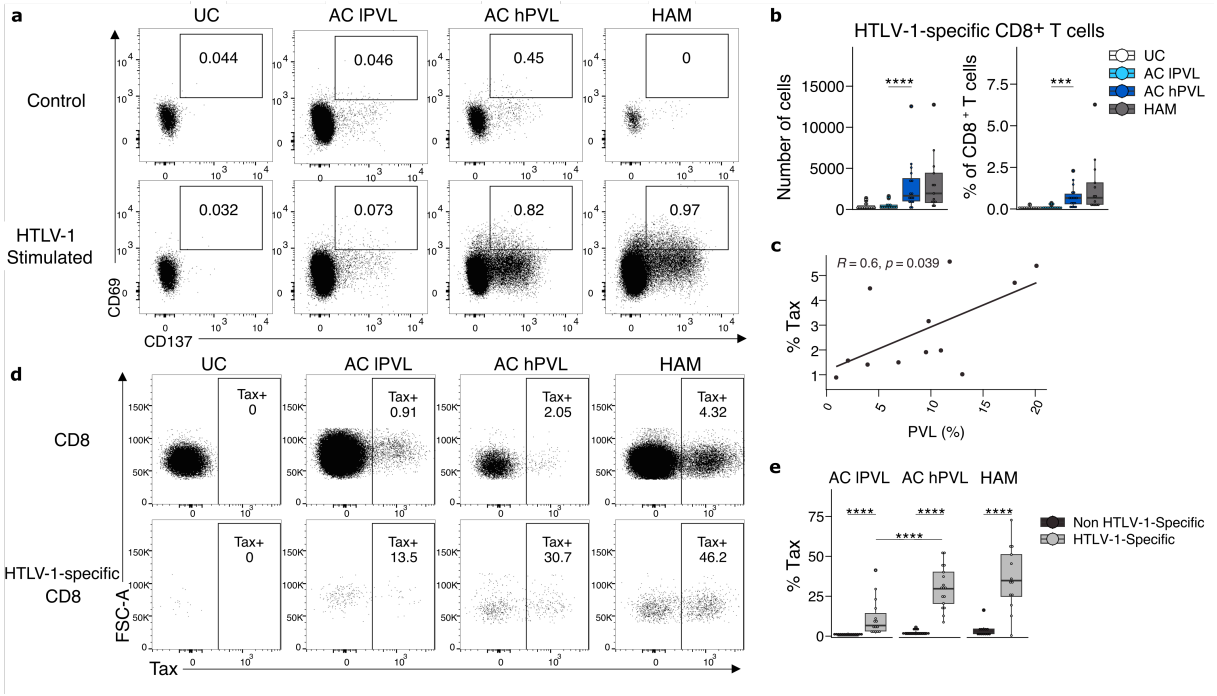


Figure 4.2: *Ex vivo* HTLV-1-specific CD8$^+$ T cell identification and characterization. a. Representative flow plots showing CD69 and CD137 expression after a 12 h stimulation with heat-inactivated HTLV-1 or a control. **b.** Box and whisker plots showing the number and frequency of HTLV-1-specific CD8$^+$ T cells identified from 10 million PBMCs (n=15 UC, n=15 AC lPVL, n=17 AC hPVL, n=13 HAM). **c.** Scatter plot of Tax expression after 12 h in culture vs. the PVL measured by ddPCR (n=7 AC hPVL, n=5 HAM). Representative flow plots (**d**) of Tax expression and box and whisker plots (**e**) of Tax$^+$ HTLV-1-specific CD8$^+$ T cells in different HTLV-1-infected groups (n=15 AC lPVL, n=17 AC hPVL, n=13 HAM); **b)** Wilcoxon signed-rank unpaired test for comparisons between UC and AC lPVL, AC lPVL and AC hPVL, and AC hPVL and HAM; **c)** Pearson correlation coefficient (R) and p-value; **e)** Wilcoxon signed-rank paired test with Holm correction; *p≤0.05, **p≤0.01, ***p≤0.001, ****p≤0.0001.

As with the HTLV-1-specific CD4$^+$ T cells, Tax expression in CD8$^+$ T cells correlated with the PVL measured by ddPCR allowing Tax expression to be used as a reliable readout

for HTLV-1 infection in $CD8^+$ T cells after 12 h in culture (Figure 4.2c). I characterized the HTLV-1-infection rate of the HTLV-1 specific $CD8^+$ T cells by staining for the HTLV-1 protein Tax (Figure 4.2d). Again, I observed that HTLV-1-specific $CD8^+$ T cells were infected at higher rates relative to the non-HTLV-1 specific $CD8^+$ T cells (Figure 4.2e). This preferential infection was more significant in high proviral load groups, with on average, only 11.3% of HTLV-1-specific $CD8^+$ T cells in AC lPVL expressing Tax, and 30.6% and 36.0% of HTLV-1-specific $CD8^+$ T cells expressing Tax in AC hPVL and HAM, respectively. The trends in HTLV-1-specific $CD8^+$ T cell frequency and numbers mirror the trends seen with HTLV-1-specific $CD4^+$ T cells, with increased rates of infection of HTLV-1-specific $CD8^+$ T cells and increased frequency of HTLV-1-specific $CD8^+$ T cells as PVL increases. There were no differences in the number, frequency, and HTLV-1 infection rate of HTLV-1-specific $CD8^+$ T cells between AC hPVL and patients with HAM, again indicating that HTLV-1-specific $CD8^+$ T cell frequency and HTLV-1-infection of HTLV-1-specific $CD8^+$ T cells are not driving factors of HAM pathogenesis.

4.2.2 Phenotypic characterization of HTLV-1-specific CD8$^+$ T cells

To assess differences in the phenotype of HTLV-1-specific CD8$^+$ T cells between different HTLV-1-infected groups, total PBMCs were stimulated with heat-inactivated HTLV-1 for 20 h and the cytokine expression patterns of HTLV-1-specific CD8$^+$ T cells were assessed by flow cytometry (Figure 4.3a). HTLV-1-specific CD8$^+$ T cells from patients with HAM expressed significantly higher levels of IL-17A relative to both AC lPVL and AC hPVL, and IFN-γ relative to AC lPVL, indicating a proinflammatory Tc17 and Tc1 phenotypes in patients with HAM (Figure 4.3b). There were no significant differences in granzyme B or IL-2 expression between different HTLV-1-infected groups. HTLV-1-specific CD8$^+$ T cells from AC hPVL expressed significantly higher levels of IFN-γ and increased trends in TNF relative to AC lPVL.

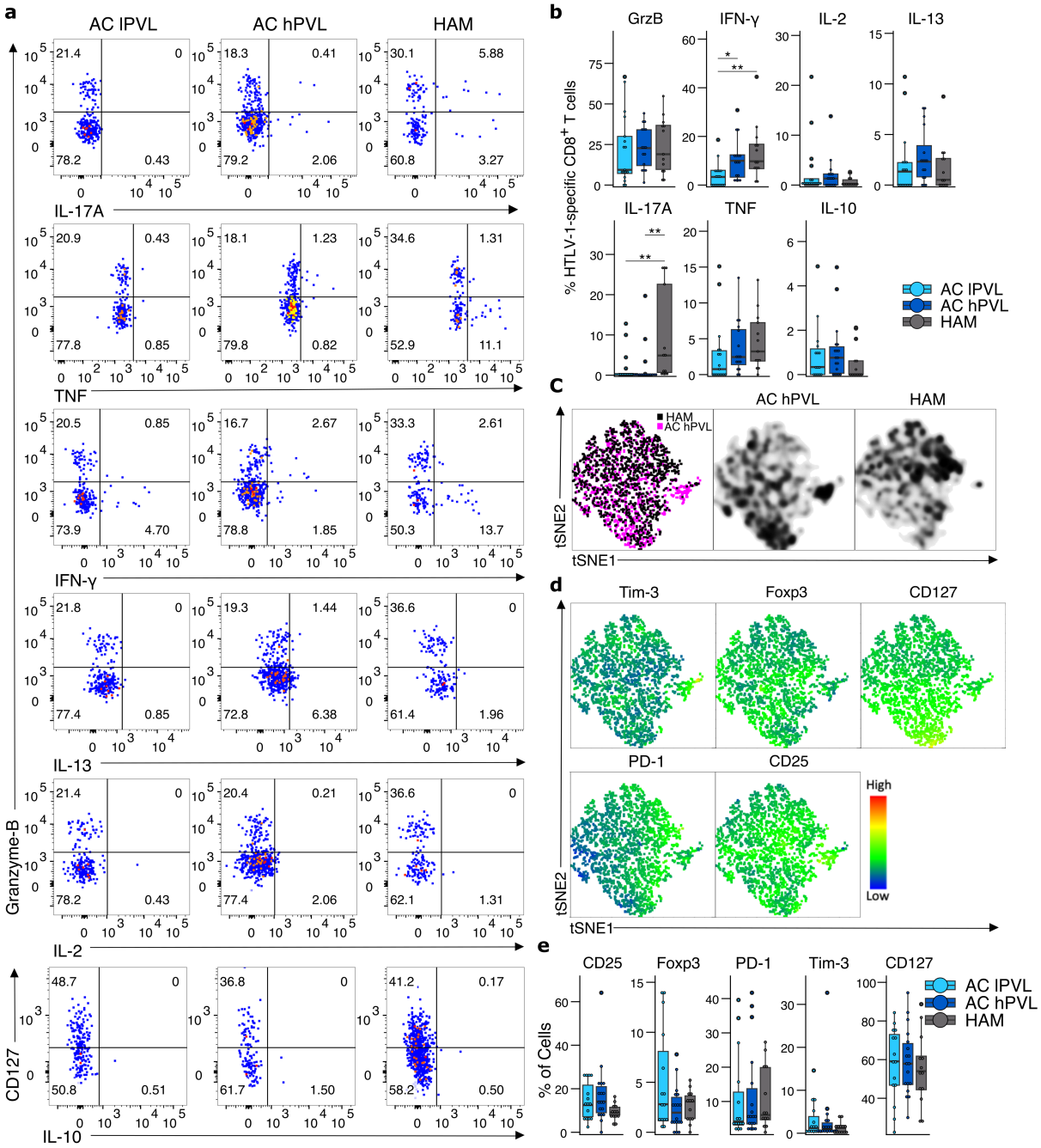


Figure 4.3: Characterization of HTLV-1-specific CD8$^+$ T cells. Representative flow plots (**a**) and box and whisker plots (**b**) showing cytokine expression in HTLV-1-specific CD8$^+$ T cells after a 20 h stimulation with heat-inactivated HTLV-1 in different HTLV-1-infected groups (n=17 AC lPVL, n=16 AC hPVL, n=13 HAM). **c.** tSNE plot obtained from a concatenated sample of HTLV-1-specific CD8$^+$ T cells (n=10 AC hPVL, n=10 HAM) showing the density of HTLV-1-specific CD8$^+$ from AC hPVL and patients with HAM. **d.** tSNE plots displaying the levels of expression of different markers on HTLV-1-specific CD8$^+$ T cells from AC hPVL and patient with HAM. **e.** Box and whisker plots showing the expression of internal and cell surface markers in HTLV-1-specific CD8$^+$ T cells in different HTLV-1-infected groups; **b, e)** Wilcoxon signed-rank unpaired test with Holm correction; *p≤0.05, **p≤0.01, ***p≤0.001, ****p≤0.0001.

HTLV-1-specific CD8$^+$ T cells from AC hPVL and patients with HAM exhibit partially distinct clustering patterns on a t-SNE plot using the markers Tim-3, Foxp3, CD127, PD-

1, and CD25 (Figure 4.3c). Foxp3, CD127, and CD25 are markers often used to identify Tregs [377], while the inhibitory markers PD-1 and Tim-3 after often used to identify exhausted cells [186, 381]. CD127 and Tim-3 were the main markers driving separation between AC hPVL and patients with HAM (Figure 4.3d). There were no differences in CD25, Foxp3, PD1, Tim-3, and CD127 expression between HTLV-1-infected groups (Figure 4.3e). Overall these data show that HTLV-1-specific $CD8^+$ T cells from patients with HAM have an enhanced Tc17 phenotype relative to AC hPVL.

4.2.3 HTLV-1-specific $CD8^+$ T cells from patients with HAM induce inflammatory astrocytes

Given that $CD8^+$ T cells predominate in older HAM CNS lesions [158, 259] and the enhanced expression of IL-17A by HTLV-1-specific $CD8^+$ T cells from patients with HAM, I wanted to observe the effect of HTLV-1-specific $CD8^+$ T cells on CNS resident cells.

HTLV-1-specific CD8$^+$ T cells from UCs, AC lPVL, AC hPVL, and patients with HAM were sorted and grown *in vitro* for 17 days, and then placed in co-culture with an astrocyte cell line (CCF-STTG1) for 48 h with anti-CD3 and anti-CD28 stimulation. Using a fixable viability dye and staining for Annexin V, I was able to identify alive (Annexin V$^-$ and Live/Dead Dye$^-$), early apoptotic (Annexin V$^+$ and Live/Dead Dye$^-$), late apoptotic (Annexin V$^+$ and Live/Dead Dye$^+$), and necrotic (Annexin V$^-$ and Live/Dead Dye$^+$) astrocytes after a 48 h culture alone or with HTLV-1-specific CD8$^+$ T cells from different patient groups (Figure 4.4a). There was a moderate but significant decrease in the viability of astrocytes co-cultured with HAM HTLV-1-specific CD8$^+$ T cells relative to astrocytes co-cultured with UC HTLV-1-specific CD8$^+$ T cells (Figure 4.4b). Overall the viability remained very high with little difference between AC lPVL, and AC hPVL, and patients with HAM.

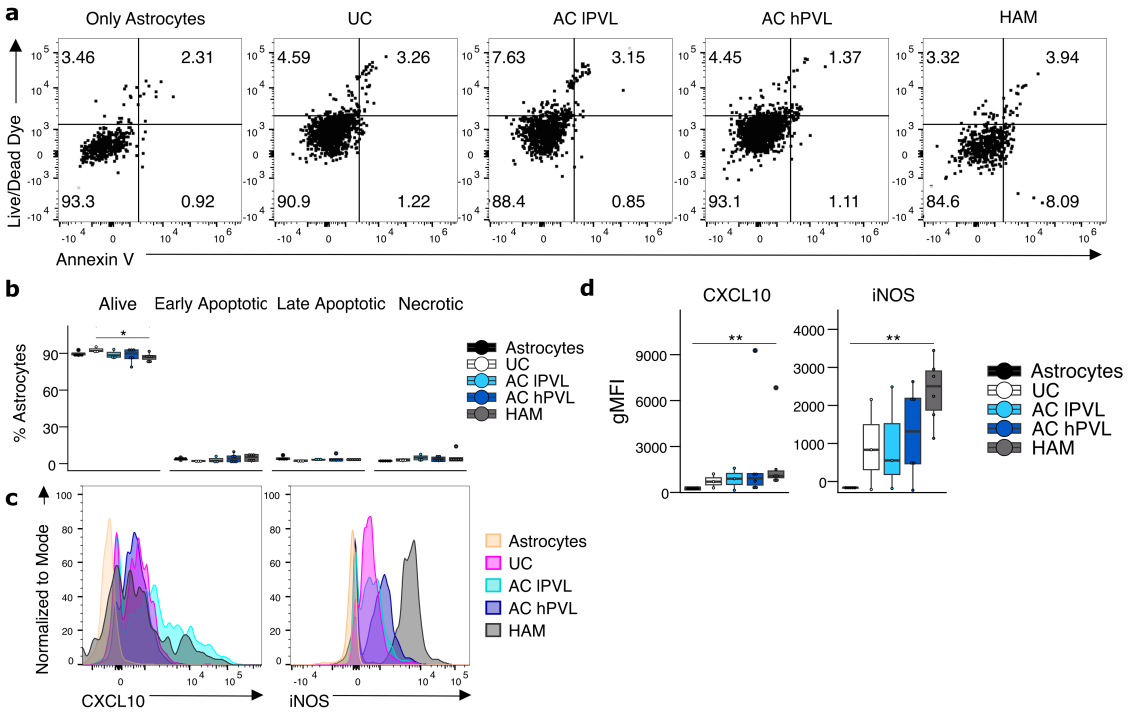


Figure 4.4: The effect of HTLV-1-specific CD8$^+$ T cells on astrocytes viability, and CXCL10 and iNOS expression. Representative flow plots (**a**) and box and whisker plots (**b**) showing the frequency of alive, early apoptotic, late apoptotic, and necrotic astrocytes after 48 h alone in culture or co-cultured with HTLV-1-specific CD8$^+$ T cells from different patient groups (n=5 only astrocytes, n=3 UC, n=3 AC lPVL, n=6 AC hPVL, n=6 HAM). Representative histograms (**c**) and box and whisker plots (**d**) showing the gMFI of CXCL10 and iNOS expression in astrocytes after 48 h alone in culture or co-culture with HTLV-1-specific CD8$^+$ T cells (n=5 only astrocytes, n=3 UC, n=3 AC lPVL, n=6 AC hPVL, n=6 HAM). **b, d)** T test with Holm correction; *p≤0.05, **p≤0.01, ***p≤0.001, ****p≤0.0001.

In addition to a moderate reduction in the viability of astrocytes by HTLV-1-specific $CD8^+$ T cells from patients with HAM, there was a trend in increased iNOS expression in astrocytes co-cultured with HTLV-1-specific $CD8^+$ T cells from patients with HAM relative to AC hPVL, but the difference was not statistically significant (Figure 4.4c and 4.4d). HTLV-1-specific $CD8^+$ T cells from all groups induced a moderate increase in CXCL10 and iNOS expression relative to astrocytes alone in culture (Figure 4.4d).

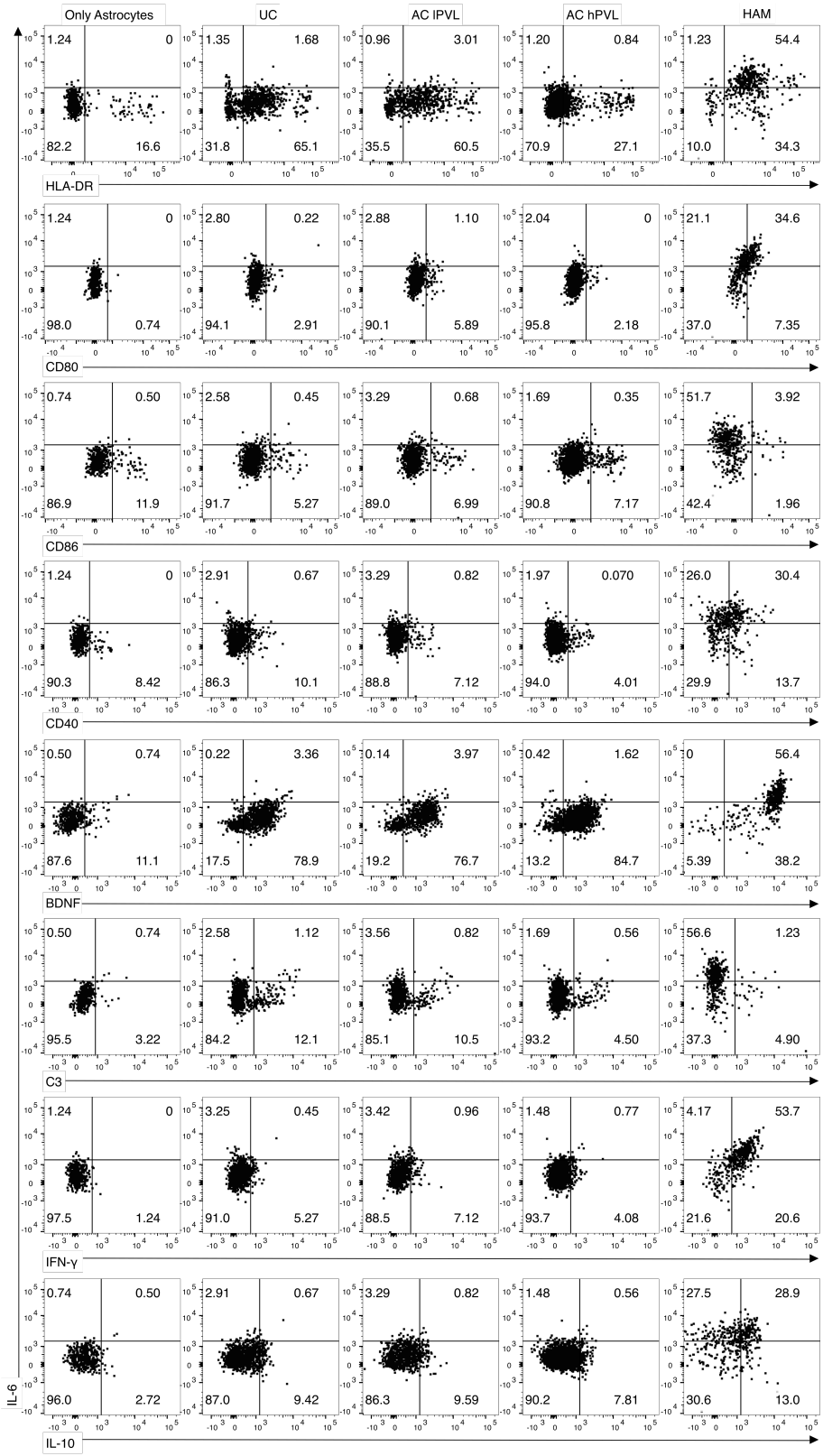


Figure 4.5: Representative flow staining of astrocytes after 48 h alone in culture or after co-culture with HTLV-1-specific CD8$^+$ T cells from different groups.

Furthermore, astrocytes in co-culture with HTLV-1-specific CD8$^+$ T cells from all

groups significantly upregulated the antigen presentation machinery (Figure 4.5 and Figure 4.6). Astrocytes in co-culture with HTLV-1-specific CD8$^+$ T cells from patients with HAM induced significantly more upregulation of HLA-DR, and there were trends in increased CD80 expression relative to AC hPVL (Figure 4.6). Furthermore, astrocytes co-cultured with HAM HTLV-1-specific CD8$^+$ T cells significantly upregulated CD40 relative to AC hPVL. I observed trends in higher levels of IL-6 and IFN-γ expression in astrocytes co-cultured with HAM HTLV-1-specific CD8$^+$ T cells relative to AC hPVL, but the differences were not statistically significant. HTLV-1-specific CD8$^+$ T cells did not induce the upregulation of CD86, and there were no significant differences between UCs and HTLV-1-infected groups in the induction of C3 in astrocytes. HTLV-1-specific CD8$^+$ T cells from patients with HAM induced increased BDNF expression in astrocytes relative to AC hPVL, and there were similar trends seen in IL-10. Overall, HTLV-1-specific CD8$^+$ T cells from patients with HAM induced the upregulation of HLA-DR, CD40, and BDNF with increased trends in the expression of CD80, IFN-γ, IL-6, IL-10, and iNOS relative to AC hPVL.

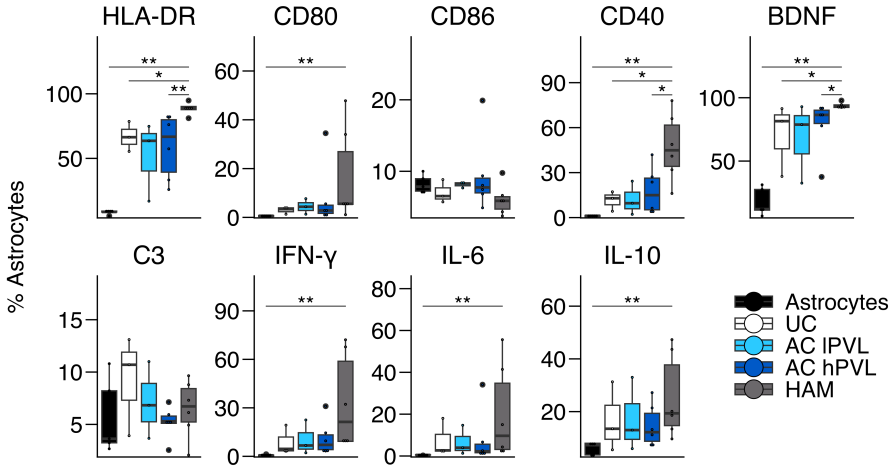


Figure 4.6: The effect of HTLV-1-specific CD8$^+$ T cells on astrocytes. Box and whisker plots showing the expression of cell surface markers and cytokines by astrocytes after 48 h alone in culture or co-culture with HTLV-1-specific CD8$^+$ T cells from different groups (n=5 only astrocytes, n=3 UC, n=3 AC lPVL, n=6 AC hPVL, n=6 HAM). Wilcoxon signed-rank unpaired test for comparisons between only astrocytes and HAM, UC and HAM, AC lPVL and AC hPVL, and AC hPVL and HAM; *p≤0.05, **p≤0.01, ***p≤0.001, ****p≤0.0001.

4.2.4 HTLV-1-specific CD8$^+$ T cells from all HTLV-1-infected groups activate microglia

Given that HTLV-1-specific CD8$^+$ T cells from patients with HAM-induced inflammatory astrocytes, I wanted to observe the impact of HTLV-1-specific CD8$^+$ T cells on microglia. I sorted HTLV-1-specific CD8$^+$ T cells from UCs and HTLV-1-infected groups, grew them *in vitro* for 17 days, and then placed them in co-culture with a microglial cell line (HMC3-CRL-3304) for 48 h with anti-CD3 and anti-CD28 stimulation.

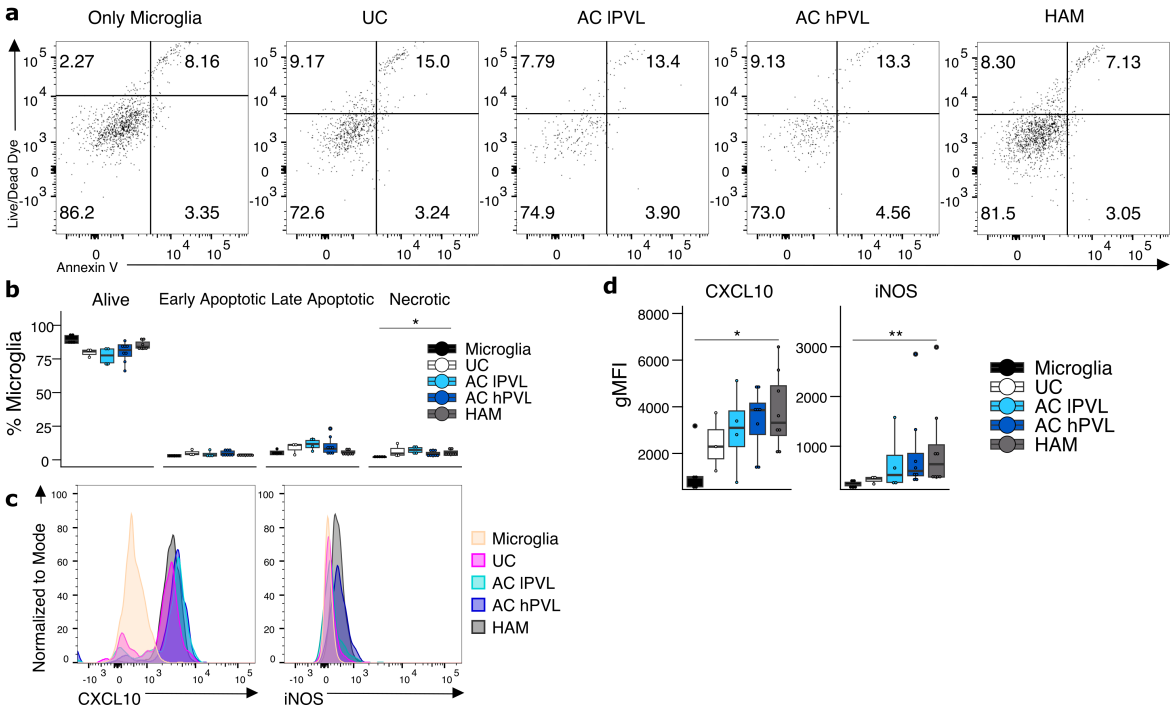


Figure 4.7: The effect of HTLV-1-specific CD8$^+$ T cells on the microglia viability, and iNOS and CXCL10 expression. Representative flow plots (**a**) and box and whisker plots (**b**) showing the frequency of alive, early apoptotic, late apoptotic, and necrotic microglia after 48 h alone in culture or co-culture with HTLV-1-specific CD8$^+$ T cells (n=5 only microglia, n=3 UC, n=4 AC lPVL, n=8 AC hPVL, n=8 HAM). Representative histograms (**c**) and box and whisker plots (**d**) showing the gMFI of CXCL10 and iNOS of microglia after 48 h alone in culture or co-culture with HTLV-1-specific CD8$^+$ T cells (n=5 only microglia, n=3 UC, n=4 AC lPVL, n=8 AC hPVL, n=8 HAM). **b, d)** T test with Holm correction; *p≤0.05, **p≤0.01, ***p≤0.001, ****p≤0.0001.

There were no significant differences in the frequency of alive microglia co-cultured with HTLV-1-specific CD8$^+$ T cells from patients with HAM relative to both microglia cultured alone or UCs and ACs, but HAM cells did induce increased necrosis (Figure 4.7a and 4.7b). All HTLV-1-specific CD8$^+$ T cells induced the upregulation of iNOS, and iNOS expression appeared higher after co-culture with cells from HTLV-1-infected groups indicating increased microglial activation (Figure 4.7c and 4.7d). All groups induced the

upregulation of CXCL10 expression and there were no significant differences between UCs and patients with HAM.

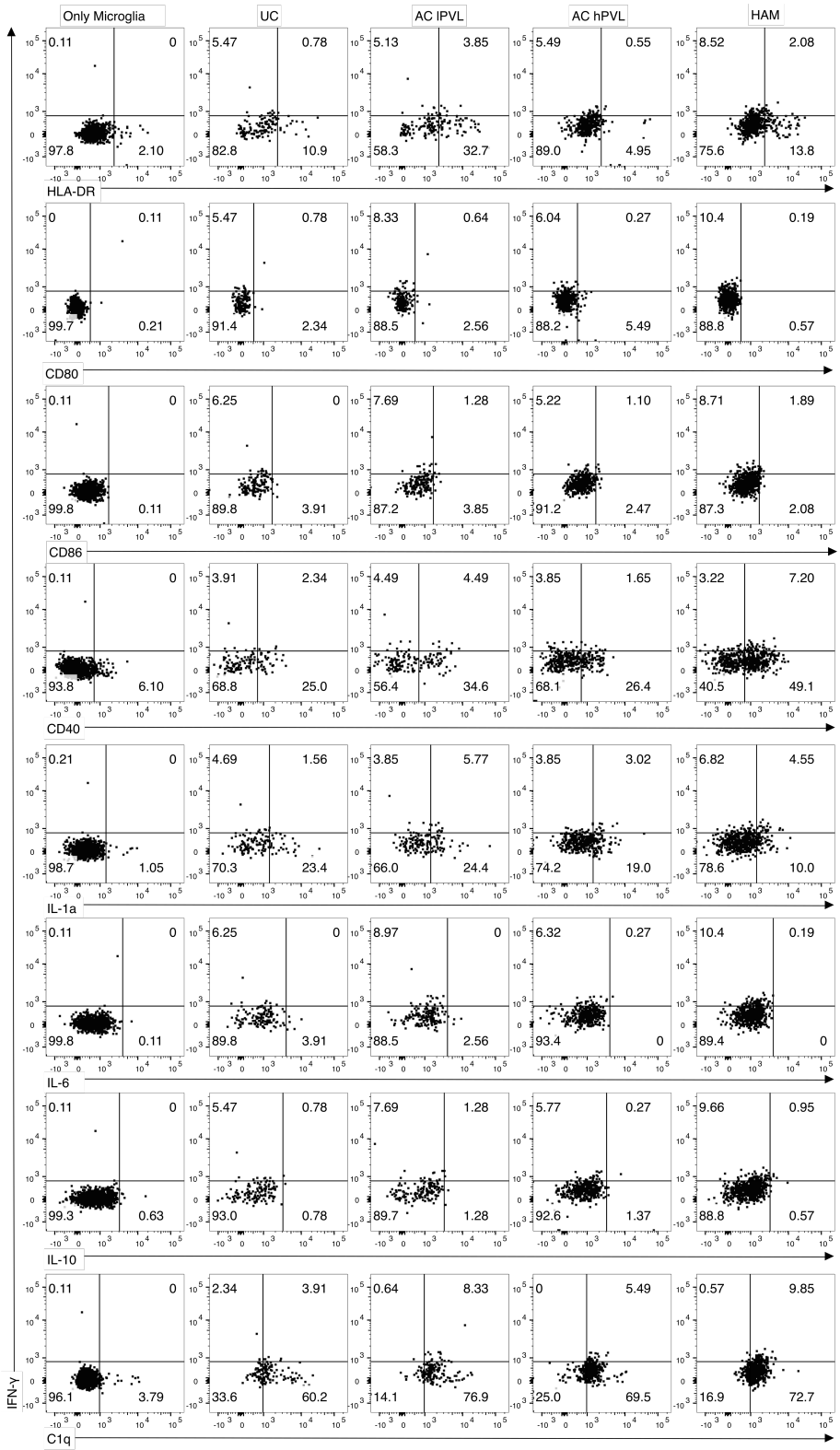


Figure 4.8: Representative flow staining of microglia alone in co-culture or after co-culture with HTLV-1-specific CD8$^+$ T cells from different groups for 48 h.

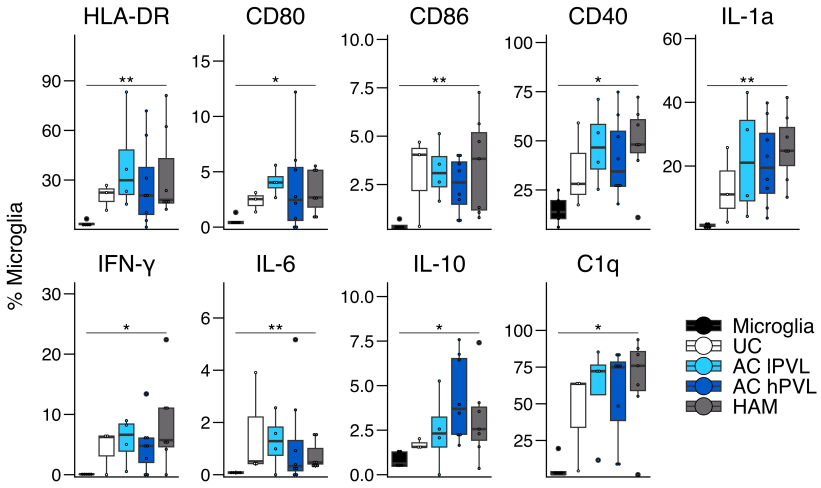


Figure 4.9: The effect of HTLV-1-specific CD8$^+$ T cells on microglia. Box and whisker plots showing the expression of cell surface markers and cytokines by microglia after 48h alone in culture or co-culture with HTLV-1-specific CD8$^+$ T cells (n=3 UC, n=4 AC lPVL, n=8 AC hPVL, n=8 HAM). Wilcoxon signed-rank unpaired test for comparisons between just microglia and HAM, UC and HAM, AC hPVL and HAM; *p≤0.05, **p≤0.01, ***p≤0.001, ****p≤0.0001.

Microglia co-cultured with HTLV-1-specific CD8$^+$ T cells from all groups induced the upregulation of the antigen presentation machinery and T cell co-stimulation molecules including HLA-DR, CD80, CD86, and CD40 (Figure 4.8 and Figure 4.9). There were no significant differences between UCs and HTLV-1-infected groups. All HTLV-1-specific CD8$^+$ T cells induced the upregulation of IL-1a, IFN-γ, IL-6, and C1q relative to microglia alone in culture. Overall these data show that HTLV-1-specific CD8$^+$ T cells from all HTLV-1-infected groups induce microglia to express proinflammatory cytokines and induce the upregulation of the antigen presentation machinery. There were no significant differences induced by HTLV-1-specific CD8$^+$ T cells from patients with HAM relative to AC hPVL.

4.2.5 Non-HTLV-1-specific CD8$^+$ T cells from patients with HAM induce astrocyte and microglia activation

To determine whether the trends I observed in both astrocytes and microglia were unique to HTLV-1-specific CD8$^+$ cells, I repeated the experiments with non-HTLV-1-specific CD8$^+$ T cells. Total PBMCs were stimulated heat-inactivated HTLV-1 for 12 h and the CD69$^-$CD137$^-$ CD8$^+$ T cells were sorted and grown for 17 days *in vitro*, and then placed into co-culture with either astrocytes or microglia for 48 hours with anti-CD3 and anti-CD28 stimulation.

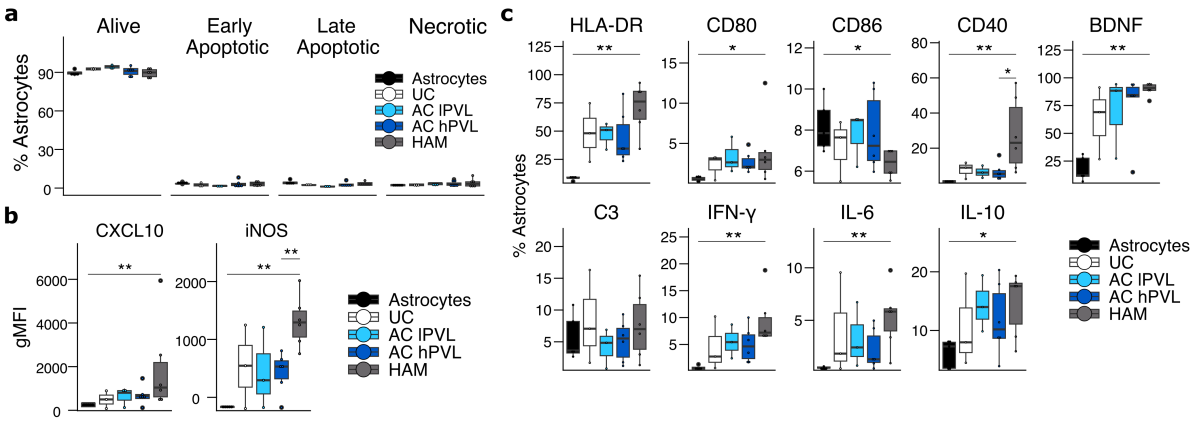


Figure 4.10: The effect of non-HTLV-1-specific CD8$^+$ T cells on astrocytes. **a.** Box and whisker plots showing the frequency of viable astrocytes after 48 h alone in culture or co-culture with non-HTLV-1-specific CD8$^+$ T cells (n=5 only astrocytes, n=3 UC, n=3 AC lPVL, n=6 AC hPVL, n=6 HAM). **b.** Box and whisker plots showing the gMFI of CXCL10 and iNOS of astrocytes after 48 h alone in culture or co-culture with non-HTLV-1-specific CD8$^+$ T cells (n=5 only astrocytes, n=3 UC, n=3 AC lPVL, n=6 AC hPVL, n=6 HAM). **c.** Box and whisker plots showing the expression of cell surface markers and cytokines of astrocytes after 48 h alone in culture or co-culture with non-HTLV-1-specific CD8$^+$ T cells (n=5 only astrocytes, n=3 UC, n=3 AC lPVL, n=6 AC hPVL, n=6 HAM). **a, b)** T-test with Holm correction; **c)** Wilcoxon signed-rank unpaired test for comparisons between only astrocytes and HAM, UC and HAM, AC lPVL and AC hPVL, and AC hPVL and HAM; *p≤0.05, **p≤0.01, ***p≤0.001, ****p≤0.0001.

There were no significant differences in the viability of astrocytes cultured alone or with non-HTLV-1-specific CD8$^+$ T cells from different patient groups (Figure 4.10a). All non-HTLV-1-specific CD8$^+$ T cells increased CXCL10 expression (Figure 4.10b). Non-HTLV-1-specific CD8$^+$ T cells from patients with HAM induced significantly higher iNOS expression in astrocytes relative to AC hPVL.

Non-HTLV-1-specific CD8$^+$ T cells from all groups induced the upregulation of CD80 and HLA-DR, with trends of increased HLA-DR expression in astrocytes co-cultured with HAM non-HTLV-1-specific CD8$^+$ T cells relative to AC hPVL (Figure 4.10c). As with

the HTLV-1-specific CD8$^+$ T cells, CD40 expression was upregulated in all groups and patients with HAM induced significantly higher levels of CD40 expression relative to AC hPVL, but the levels induced by HTLV-1-specific CD8$^+$ T cells were higher than those induced by non-HTLV-1-specific CD4$^+$ T cells (Figure 4.6 and 4.10c). There were no significant differences between groups in IL-6, IFN-γ, IL-10, BDNF, or C3 expression.

When placed in co-culture with microglia, non-HTLV-1-specific CD8$^+$ T cells from all groups reduced the viability of microglia, mainly through increased necrosis (Figure 4.11a). There were no significant changes in CXCL10 and iNOS expression in microglia (Figure 4.11b). The antigen presentation machinery, HLA-DR, CD80, and CD86, in addition to CD40 were upregulated in all non-HTLV-1-specific CD8$^+$ T cell co-cultures, but there were no significant differences between HTLV-1-infected groups (Figure 4.11c). There were no significant differences between HTLV-1-infected groups in C1q, IL-10, IL-6, IL-1a, and IFN-γ expression. Overall, non-HTLV-1-specific CD8$^+$ T cells from patients with HAM were also able to induce more pro-inflammatory astrocytes relative to AC hPVL, but there were no significant differences observed in microglia co-cultured with non-HTLV-1-specific CD8$^+$ T cells from different HTLV-1-infected groups.

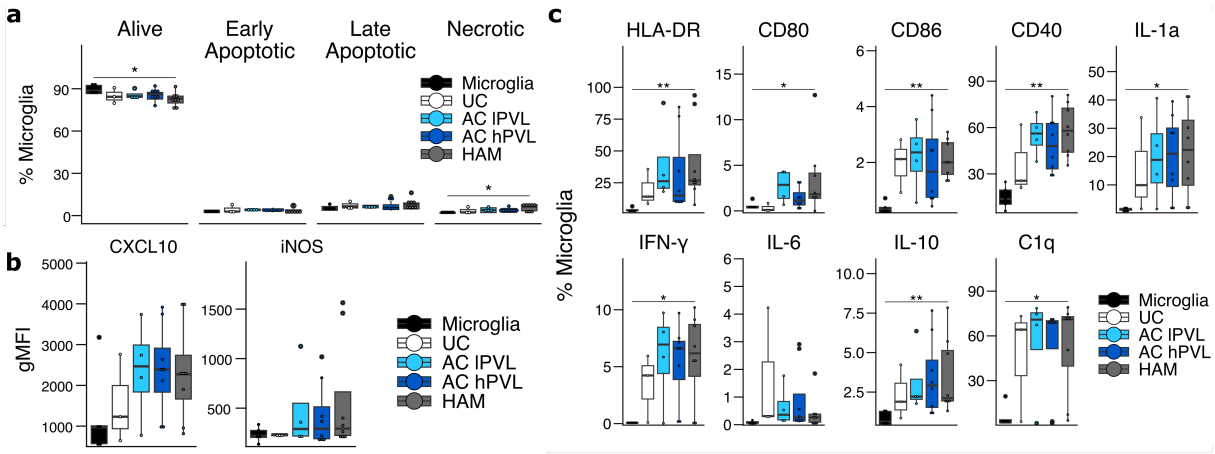


Figure 4.11: The effect of non-HTLV-1-specific CD8$^+$ T cells on microglia. **a.** Box and whisker plots showing the frequency of alive, early apoptotic, late apoptotic, and necrotic microglia after 48 h alone in culture or co-culture with non-HTLV-1-specific CD8$^+$ T cells (n=5 only microglia, n=3 UC, n=4 AC lPVL, n=8 AC hPVL, n=8 HAM). **b.** Box and whisker plots showing the gMFI of CXCL10 and iNOS of microglia after 48 h alone in culture or co-culture with non-HTLV-1-specific CD8$^+$ T cells (n=5 only microglia, n=3 UC, n=4 AC lPVL, n=8 AC hPVL, n=8 HAM). **c.** Box and whisker plots showing the expression of cell surface markers and cytokines of microglia after 48h alone in culture or co-culture with non-HTLV-1-specific CD8$^+$ T cells (n=5 only microglia, n=3 UC, n=4 AC lPVL, n=8 AC hPVL, n=8 HAM). **a, b)** T-test with Holm correction; **c)** Wilcoxon signed-rank unpaired test for comparisons between only astrocytes and HAM, UC and HAM, AC lPVL and AC hPVL, and AC hPVL and HAM; *p≤0.05, **p≤0.01, ***p≤0.001, ****p≤0.0001..

4.2.6 Characterization of bulk CD8$^+$ T cells

Finally, determine whether the differences I observed in phenotype and cytokine expression in HTLV-1-specific CD8$^+$ T cells between HTLV-1-infected groups also occurred in the bulk CD8$^+$ T cell population, I deeply characterized the phenotype of bulk CD8$^+$ T cells by multidimensional flow cytometry.

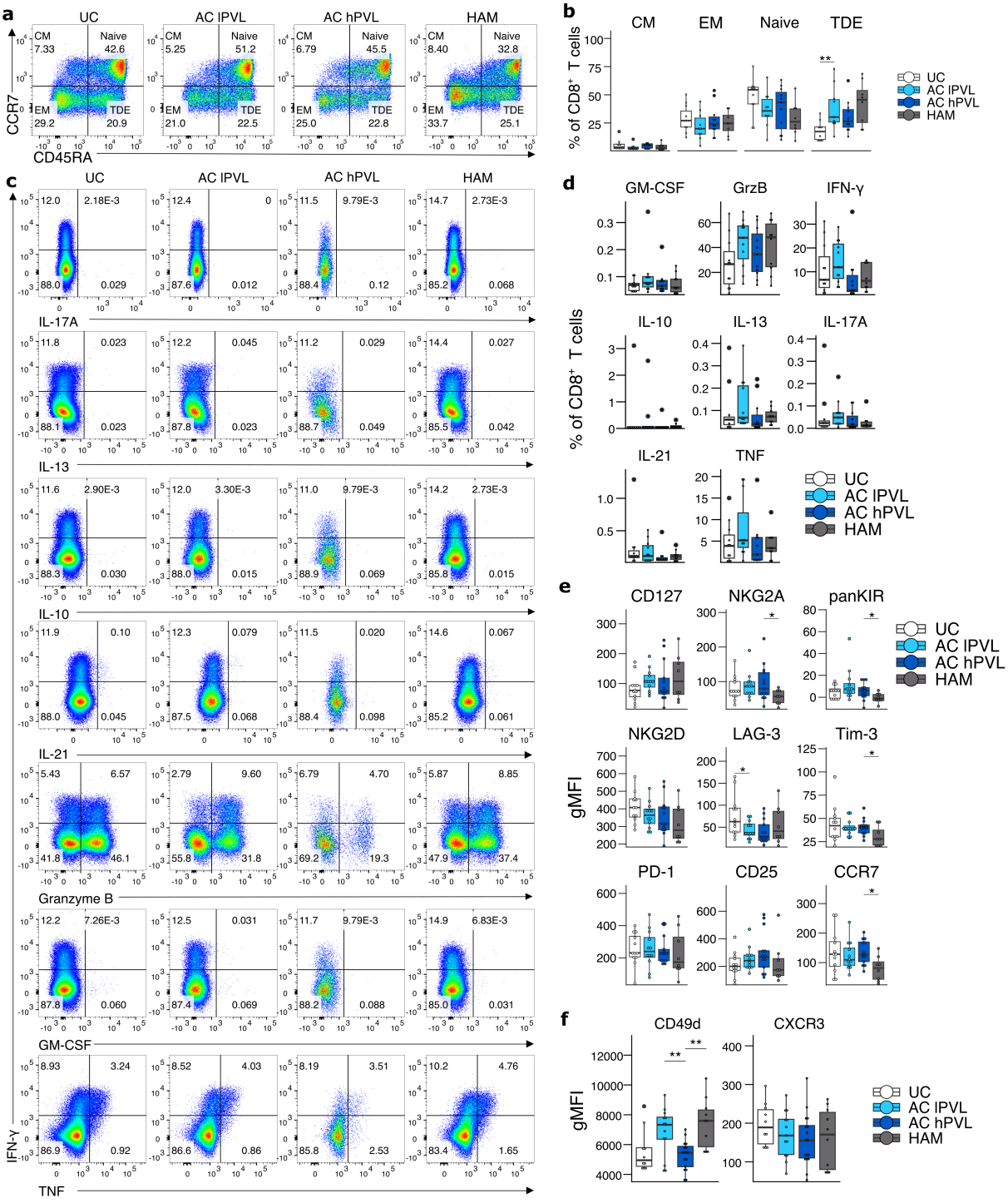


Figure 4.12: Characterization of bulk CD8$^+$ T cells in UCs, ACs, and patients with HAM. Representative flow plots (**a**) and box and whisker plots (**b**) showing the frequency of central memory (CM), naïve, effector memory (EM), and terminally differentiated effector (TDE) CD8$^+$ T cell populations in different groups (n=11 UC, n=10 AC lPVL, n=11 AC hPVL, n=8 HAM). Representative flow plots (**c**) and box and whisker plots (**d**) showing granzyme B and cytokine expression in CD8$^+$ T cells in different groups after a 4 h stimulation with PMA and ionomycin (n=11 UC, n=11 AC lPVL, n=11 AC hPVL, n=9 HAM). **e.** Box and whisker plots showing the gMFI of cell surface markers in *ex vivo* CD8$^+$ T cells (n=12 UC, n=12 AC lPVL, n=13 AC hPVL, n=8 HAM). *f.* Box and whisker plots showing the gMFI of CD49d and CXCR3 in CD8$^+$ T cells (n=10 UC, n=13 AC lPVL, n=17 AC hPVL, n=10 HAM). **b, d, f)** Wilcoxon signed-rank unpaired test for comparisons between UC and AC lPVL, AC lPVL and AC hPVL, and AC hPVL and HAM; **e)** T test for comparisons between UC and AC lPVL, AC lPVL and AC hPVL, and AC hPVL and HAM; *p≤0.05, **p≤0.01, ***p≤0.001, ****p≤0.0001.

As in the previous chapter, CCR7 and CD45RA were used to classify *ex vivo* $CD8^+$ T cells into central memory, naïve, terminally differentiated effector, and effector memory cells (Figure 4.12a) [18, 82, 83]. While there were no differences in the antigen experience of the bulk $CD8^+$ T cell population between HTLV-1-infected groups, HTLV-1-infected groups had higher frequencies of terminally differentiated effector cells relative to UCs (Figure 4.12b).

To characterize the cytokine expression profile of the bulk $CD8^+$ T cell population in different HTLV-1-infected groups and UCs, total PBMCs were stimulated with PMA and ionomycin for 4 h, and cytokine expression was characterized by flow cytometry (Figure 4.12c). Overall there were no statistically significant differences in cytokine or granzyme B expression when comparing UCs and AC lPVL, AC lPVL and AC hPVL, or AC hPVL and patients with HAM (Figure 4.12d).

Finally the *ex vivo* expression of certain cell surface markers including CD127, NK group 2 member (NKG2) A, NKG2D, panKIR, lymphocyte activation gene-3 (LAG-3), Tim-3, PD-1, and CD25 were characterized (Figure 4.12e). In agreement with previous studies, $CD8^+$ T cells from patients with HAM showed decreased Tim-3 expression relative to AC hPVL [381]. Patients with HAM also expressed decreased levels of the inhibitory NKG2A receptor, CCR7, and KIRs relative to AC hPVL. There were no significant differences in CD127, NKG2D, LAG-3, PD-1, or CD25 expression between HTLV-1-infected groups. Given the decreased expression of the lymph node homing marker CCR7, I measured the expressed of CD49d and CXCR3, and observed increased expression of CD49d in $CD8^+$ T cells in patients with HAM relative to AC hPVL indicating an enhanced capacity to migrate to the CNS (Figure 4.12f). AC hPVL also expressed significantly lower levels of CD49d relative to AC lPVL, indicating AC hPVL may downregulate CD49d expression as PVL increases, with possible protective effects. There were no differences in CXCR3 expression between HTLV-1-infected groups or UCs. Overall these data indicate only minor differences in the bulk $CD8^+$ T cell populations between HTLV-1-infected groups, with all groups producing similar levels of cytokines and comparable levels of antigen experience. $CD8^+$ T cells from patients with HAM appear to have an enhanced capacity to migrate to the CNS due to increased CD49d expression.

4.3 Discussion

In this chapter, I showed that high PVL groups had an increased frequency and number of HTLV-1-specific $CD8^+$ T cells, and HTLV-1-specific $CD8^+$ T cells were infected at higher rates with HTLV-1 relative to non-HTLV-1-specific $CD8^+$ T cells in all HTLV-1-infected groups. HTLV-1-specific $CD8^+$ T cells from patients with HAM expressed significantly higher levels of IL-17A relative to AC hPVL, and appear to have an enhanced capacity to migrate to the CNS due to increased CD49d expression. When in co-culture with cells from the CNS, both HTLV-1-specific and non-specific $CD8^+$ T cells from patients with HAM induced the upregulation of the antigen presentation machinery and increased astrocyte expression of proinflammatory cytokines, demonstrating the potential of both HTLV-1-specific and non-specific $CD8^+$ T cells to contribute to HAM pathogenesis. Finally, I showed that despite an increased frequency of terminally differentiated effector $CD8^+$ T cells in HTLV-1-infected individuals relative to UCs, $CD8^+$ T cells had similar cytokine secretion profiles regardless of HTLV-1-infection or disease status. The data in this chapter provides a deeper understanding of $CD8^+$ T cells in controlling HTLV-1-infection and their potential contribution to CNS inflammation during HAM pathogenesis.

Previous studies characterizing HTLV-1-specific $CD8^+$ T cells used either tetramers or IFN-γ secretion after stimulation with a HTLV-1 peptide library as a read-out for HTLV-1-specificity [299, 313]. In agreement with these studies, I observed an increased frequency of HTLV-1-specific $CD8^+$ T cells in high PVL groups. These studies also reported an increased frequency of HTLV-1-specific $CD8^+$ T cells in patients with HAM, and the frequency was correlated with disease severity, leading to the suggestion that HTLV-1–specific $CD8^+$ T cells are the main subset of pathogenic lymphocytes HAM [299, 313]. However, the authors did not match the PVL of the AC and HAM groups, and the mean PVL in patients with HAM and ACs was 39.4% and 1.5%, respectively [313]. When controlling for PVL, I observed no differences in the frequency of HTLV-1-specific $CD8^+$ T cells in patients with HAM relative to AC hPVL. Additionally, I observed that HTLV-1-specific $CD8^+$ T cells were preferentially infected with HTLV-1, and this preferential infection was more extreme in high PVLs. This could be both a driver or a consequence of a high PVL.

In HIV infection, there does not appear to be a correlation between HIV viral loads and HIV-specific $CD8^+$ T cell frequencies [199]. HIV-specific $CD8^+$ T cells in elite controllers, HIV-infected individuals who appear to spontaneously control HIV infection without antiretroviral treatment, are more polyfunctional than in chronic progressors [199]. However, again it is difficult to assess whether this is a cause or consequence of HIV viral loads, as HIV-specific $CD8^+$ T cells in individuals with lower HIV viral loads are likely to be less exhausted. In HTLV-1-specific $CD8^+$ T cells, I observed increased IFN-γ expression in AC hPVL relative to AC lPVL, which may be a consequence of HTLV-1-infection rather than HTLV-1-specific $CD8^+$ T cells responses as HTLV-1-infected T cells have been shown to spontaneously express IFN-γ [382]. The lack of differences in cytokine or granzyme B expression between AC lPVL and AC hPVL indicates that the phenotype of HTLV-1-specific $CD8^+$ T cells does not play a large role in HTLV-1 viral control. The diversity of Tax and HBZ epitopes presented to $CD8^+$ T cells, controlled by HLA genotypes, identified in previous studies appear to have a larger impact on HTLV-1 viral control [243, 307, 309, 310, 311].

This work demonstrates that both HTLV-1-specific and non-specific $CD8^+$ T cells have the capacity to contribute to CNS inflammation. $CD8^+$ T cells predominate in both older HAM and MS CNS lesions and the ratio between $CD4^+$ and $CD8^+$ T cells can be as extreme as 1:10 [158, 161, 251, 259]. In addition to HAM $CD8^+$ T cells having an enhanced capacity to migrate to the CNS due to high CD49d expression, HTLV-1-specific $CD8^+$ T cells from patients with HAM expressed significantly higher levels of IL-17A relative to AC hPVL. IL-17 has been heavily implicated in MS pathogenesis, and interestingly a large percentage of $CD8^+$ T cells in MS lesions express high levels of IL-17A [383]. IL-17A is associated with the breakdown of the BBB in relapsing-remitting MS [384]. Furthermore, when placed in co-culture with astrocytes, HTLV-1-specific $CD8^+$ T cells from patients with HAM induced significant upregulation of HLA-DR and CD40, with increased trends in iNOS, CD80, IFN-γ, and IL-6 relative to cells from AC hPVL. The expression of pathogenic cytokines like IL-17A and IFN-γ by HTLV-1-specific $CD8^+$ T cells, and the ability of both HTLV-1-specific and non-specific $CD8^+$ T cells to induce inflammatory astrocytes demonstrate their capacity to contribute and drive the chronicity of inflammation in the CNS. As with the glial-$CD4^+$ T cell co-cultures, the glial-$CD8^+$ T cell co-culture experiments provide valuable insights into the capacity of $CD8^+$ T cells

from patients with HAM to contribute to neuroinflammation and HAM pathogenesis. However, the same limitations previously discussed apply. Without concurrent phenotypic analysis of T cells and glial cells at the same time point, the ability to gain insight into the mechanisms driving these changes in glial cells in the *in vitro* culture remains limited. The mechanisms by which $CD8^+$ T cells induce these changes in astrocytes remain to be elucidated, underscoring the need for further mechanistic studies to fully understand these interactions.

Given that $CD8^+$ T cell dysfunction or exhaustion is common in chronic viral infection, I also characterized the bulk $CD8^+$ T cell population. Exhausted $CD8^+$ T cells are characterized by progressive loss of effector functions, such as cytokine production and killing function, and the expression of multiple inhibitory receptors such as PD-1, LAG-3, and Tim-3 [385]. In agreement with previous studies, I observed lower Tim-3 expression in $CD8^+$ T cells from patients with HAM relative to AC hPVL [381], but no differences in PD-1 or LAG-3. Bulk $CD8^+$ T cells in HTLV-1-infected groups also produced similar levels of cytokines, indicating no major differences between HTLV-1-infected groups in $CD8^+$ T cell exhaustion. The decreased Tim-3 expression in $CD8^+$ T cells in patients with HAM has been proposed to lead to a persistent and deleterious effector $CD8^+$ T cells leading to more inflammation. I observed no differences in Tim-3, Foxp3, or PD-1 expression in HTLV-1-specific $CD8^+$ T cells and similar cytokine secretion profiles between AC lPVL and AC hPVL indicating that there are no major differences in HTLV-1-specific $CD8^+$ T cells associated with increased PVL.

Several interesting questions arise from this work, including questions about the mechanisms by which $CD8^+$ T cells induce proinflammatory astrocytes and the role Tc17 cells play in driving neuroinflammation. These questions warrant further follow-up. Overall, the data in this chapter shows that patients with HAM have enhanced Tc17 HTLV-1-specific $CD8^+$ T cell responses, and $CD8^+$ T cells have the capacity to contribute to neuroinflammation in HAM.

5

$CD4^+CD8^+$ T cells in HTLV-1 infection

This chapter has been adapted from my published article: Maher, A.K., Aristodemou A., Giang N., Tanaka, Y., Taylor G.P., Bangham R.M C., Dominguez-Villar M. HTLV-1 induces an inflammatory $CD4^+$ $CD8^+$ T cell population in HTLV-1-Associated Myelopathy. *JCI Insight*. 2024;9(1):e173738. https://doi.org/10.1172/jci.insight.173738. JCI insight allows for the reuse of materials without permission as long as the original source is cited. I collected all the data in this paper, and all the written text is my work, guided and corrected by my supervisor Dr. Margarita Dominguez-Villar. Figures and text have been adapted for this thesis.

5.1 Introduction

Mature $CD4^+CD8^+$ double positive (DP) T cells account for approximately 1-3% of peripheral T cells in UCs [61, 162, 163]. DP T cells exhibit phenotypic heterogeneity and increased frequencies in various diseases, including autoimmune conditions like MS, SS, and RA, viral infections such as HIV, HCV, and EBV, and certain cancers. DP T cells appear cytotoxic in viral infections, suppressive in autoimmune diseases like SS and IBD, and display variable functionalities in cancers [61, 162]. Given the different behavior of

DP T cells in the context of chronic viral infection, autoimmunity, and cancer, studies on DP T cells in HTLV-1-infected individuals may be particularly insightful into the diverse functions of DP T cells as HTLV-1 is a chronic viral infection that can result in either ATL or inflammatory conditions. DP T cells in HTLV-1-infected individuals remain uncharacterized. There have been several reported cases of $CD4^+CD8^+$ ATL which described a more aggressive form of the disease with a worse prognosis, but $CD4^+CD8^+$ ATL remains very rare [386, 387]. A previous study showed that HTLV-1 infection of $CD8^+$ single positive (SP) T cells, but not $CD4^+$ SP T cells, resulted in the emergence of a $CD4^+CD8^+$ population after 2 weeks in culture (n=3), however, there were no controls for the effects of long-term *in vitro* tissue culture or co-culture with the HTLV-1-infected lymphocyte cell line MT2. There have been no previous studies on *ex vivo* DP T cells in HTLV-1 carriers or studies that explored the role of DP T cells in HAM.

The overall aim of this chapter was to gain a greater understanding of DP T cells during HTLV-1-infection by characterizing the frequency of DP T cells in different HTLV-1-infected groups, by characterizing the phenotype and contribution of DP T cells to anti-HTLV-1-immunity and inflammation, and by investigating the origin of mature peripheral DP T cells in HTLV-1 infection. In this chapter, I show that patients with HAM have a higher frequency of peripheral DP T cells than ACs with a similar PVL. Moreover, DP T cells are infected with HTLV-1 at a higher rate than $CD4^+$ or $CD8^+$ SP T cells and account for approximately 8% of the total HTLV-1 PVL. In HTLV-1-infected individuals, DP T cells are proinflammatory and express high levels of IFN-γ, TNF, IL-17A, IL-21 and granzyme B, suggesting both cytotoxic and helper phenotypes, and contain increased frequencies of HTLV-1-specific cells as compared to their $CD4^+$ and $CD8^+$ SP counterparts. Mechanistically, I demonstrate that HTLV-1 infection of SP T cells triggers the emergence of DP T cell populations from both $CD4^+$ and $CD8^+$ SP T cells *in vitro* by modulating the expression of the transcription factors ThPOK and RunX3. I show that chemokine and integrin receptors involved in lymphocyte migration to the CNS, including CD49d and CXCR3 are more highly expressed by DP T cells than by $CD4^+$ and $CD8^+$ SP cells, suggesting that DP T cells possess an enhanced ability to migrate to the CNS. Finally, DP T cells induce proinflammatory astrocytes *in vitro* which express high levels of CXCL10, IFN-γ, and IL-6 indicating that DP T cells have the capacity to directly contribute to CNS pathology.

5.2 Results

5.2.1 Patients with HAM have an increased frequency of DP T cells

As in the previous chapters, HTLV-1-infected individuals were grouped into ACs with a PVL under 3% (low PVL, AC lPVL), ACs with a PVL above 3% (high PVL, AC hPVL), and patients with HAM. The PVLs of the AC hPVL and HAM groups were matched to control for differences due to HTLV-1 infection (Figure 5.1a).

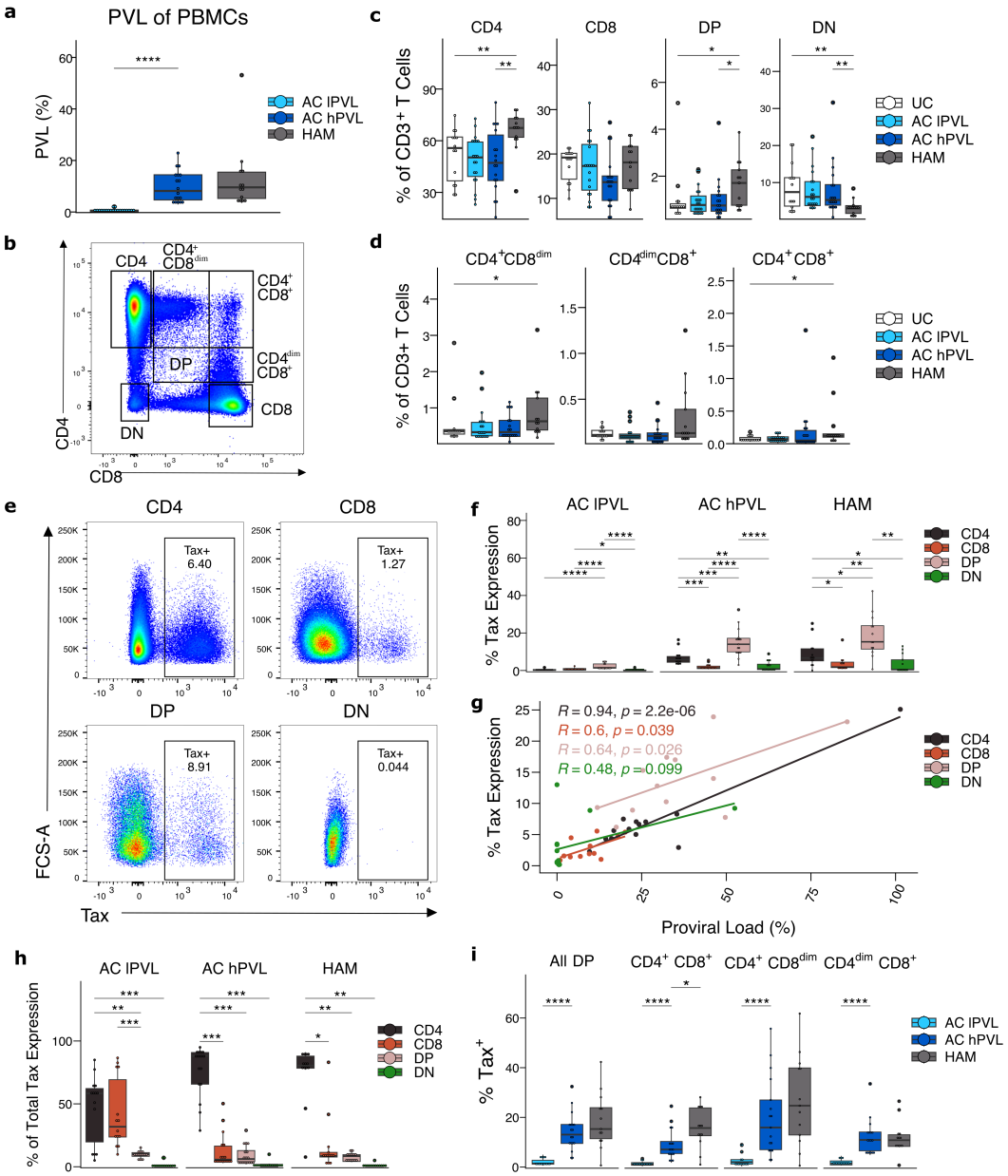


Figure 5.1: Frequency and HTLV-1 infection of DP T cells. a. Box and whisker plot showing the HTLV-1 PVL in total PBMCs (n=19 AC lPVL, n=18 AC hPVL, n=13 HAM). Representative flow plot **(b)** and box and whisker plots **(c-d)** showing the frequency of T cells and DP T cell sub-populations in different groups (n= 14 UC, n=19 AC lPVL, n=18 AC hPVL, n=13 HAM). **e.** Representative flow plots showing Tax expression in a patient with HAM in different T cell populations after 12 h in culture. **f.** Box and whisker plots of Tax expression in different T cell populations after 12 h in culture (n=15 AC lPVL, n=17 AC hPVL, n=*13* HAM). **g.** Scatter plot of Tax expression after 12 h in culture vs. the PVL measured by ddPCR (CD4 and DN: n=7 AC hPVL, n=6 HAM; CD8 and DP: n=7 AC hPVL, n=5 HAM). **h.** Box and whisker plots displaying the contribution of $CD4^+$ SP, $CD8^+$ SP, DP, and DN T cells to total Tax expression in $CD3^+$ T cells (n=15 AC lPVL, n=16 AC hPVL, n=13 HAM). **i.** Box and whisker plots of Tax expression in DP T cell sub-populations (n=15 AC lPVL, n=16 AC hPVL, n=13 HAM). **c, d)** Wilcoxon signed-rank unpaired test for comparisons between UC and AC lPVL, UC and HAM, AC lPVL and AC hPVL, and AC hPVL and HAM; **f, h)** Wilcoxon signed-rank paired test with Holm correction for multiple comparisons; **g)** Pearson correlation coefficient (R) and p-value; **i)** Wilcoxon signed-rank unpaired test for comparisons between AC lPVL and AC hPVL, and AC hPVL and HAM; *p≤0.05, **p≤0.01, ***p≤0.001, ****p≤0.0001. (Figure adapted from Maher A.K *et al.*, 2024 [1]).

I initially examined the *ex vivo* frequencies of peripheral $CD4^+$ SP, $CD8^+$ SP, DP, and double negative (DN) T cells in HTLV-1-infected individuals and UCs (Figure 5.1b). DP cells displayed varying levels of $CD4^+$ and $CD8^+$ expression. Thus, 3 sub-populations could be identified, i.e. $CD4^+$ $CD8^{dim}$ $CD8^+CD4^{dim}$, and $CD4^+$ $CD8^+$ ($CD4^{bright}CD8^{bright}$) (Figure 5.1b). Patients with HAM displayed a higher frequency of DP T cells compared to ACs and UCs with a mean DP T cell frequency of 1.03%, 0.95%, 1.02%, and 1.64% in UCs, AC lPVL, AC hPVL, and patients with HAM respectively (Figure 5.1c). $CD3^+$ T cells from patients with HAM also contained higher frequencies of $CD4^+$ SP T cells and a lower frequency of DN T cells than both ACs and UCs. $CD4^+CD8^{dim}$ T cells had the highest frequency in all HTLV-1-infected groups (Figure 5.1d). The higher frequency of DP T cells in patients with HAM was mainly driven by increased frequencies of $CD4^+CD8^{dim}$ and $CD4^{dim}CD8^+$ T cells (Figure 5.1d).

To determine whether DP T cells were infected by HTLV-1, I examined the expression of the HTLV-1 protein Tax in different T cell populations after 12 h in culture (Figure 5.1e). The frequency of Tax expressing cells was higher in DP T cells as compared to $CD4^+$ SP T cells, which are considered to be the main HTLV-1 reservoir [196], $CD8^+$ SP T cells, and DN T cells in all HTLV-1-infected groups (Figure 5.1f). In AC hPVL and patients with HAM, there was a 2-fold higher frequency of Tax expression in DP cells as compared to $CD4^+$ SP T cells (6.65% and 8.84% Tax^+ cells in $CD4^+$ SP T cells in AC hPVL and HAM, respectively, compared to 14.1% and 18.3% Tax^+ cells in DP T cells, respectively). Although Tax is expressed dynamically by infected cells [209, 212], in my experimental setting Tax expression by T cells after 12 h in culture strongly correlated with the PVL of sorted $CD4^+$ SP, $CD8^+$ SP, DP and DN T cells measured by ddPCR (Figure 5.1g) [388], which allowed me to use Tax expression at 12 h as a reliable readout for PVL and infection rate. The high levels of Tax expression in DP T cells were not due to different Tax expression dynamics in the different T cell populations (Figure 5.1g). Overall, the mean DP T cell contribution in all HTLV-1-infected groups to the PVL burden was 8.2%, despite DP T cells accounting for less than 2% of the total $CD3^+$ T cell population (Figure 5.1h). In AC hPVL and patients with HAM, $CD8^+$ SP T cells and DP T cells contributed equally to the total HTLV-1 PVL burden, while the majority of the HTLV-1 PVL in hPVL groups was carried in $CD4^+$ SP T cells, in agreement with previous studies [196]. However, the PVL burden in AC lPVL was distributed more evenly between $CD4^+$ and $CD8^+$ SP

T cells with 47% and 42% of the total Tax expression, respectively. Patients with HAM and AC hPVL did not differ in their PVL distribution and $CD4^+$ and $CD8^+$ SP T cells expressed on average 78% and 13% of the total Tax, respectively. Moreover, high rates of Tax expression were seen in all DP T cell sub-populations (Figure 5.1i). Patients with HAM displayed significantly higher rates of HTLV-1 infection in $CD4^+CD8^+$ T cells than AC hPVLs and there was a similar trend in $CD4^+CD8^{dim}$ T cells, which harbored the highest rate of infection of all DP T cell sub-populations. Overall, DP T cells are more abundant in patients with HAM compared to ACs and are infected at higher rates with HTLV-1 than all other T cell populations.

5.2.2 DP T cells are a distinct T cell population in ACs

Given the high rate of HTLV-1 infection of DP T cells, I characterized the phenotype of DP T cells from UCs and HTLV-1-infected groups *ex vivo* by high dimensional flow cytometry and compared them to $CD4^+$ and $CD8^+$ SP T cells. I examined the expression of Tim-3, PD-1, TIGIT, CD25, Foxp3, CCR7, CD45RA, and CD27 as markers of exhaustion, activation, and antigen experience (representative flow stainings shown in Figure 5.2 and 5.4a).

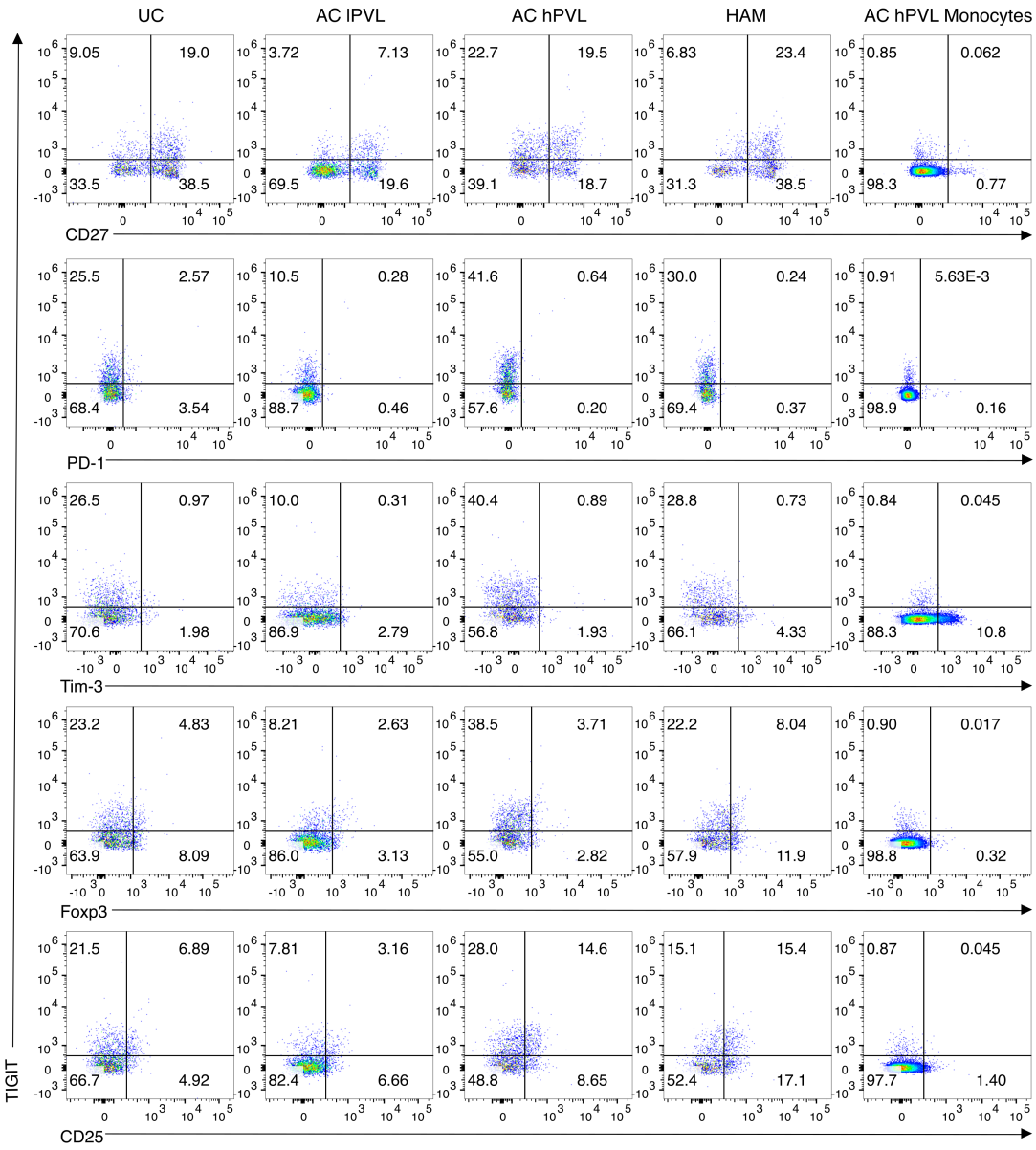


Figure 5.2: DP T cells *ex vivo* phenotyping flow staining. Representative flow plots of DP T cells from UCs and HTLV-1-infected groups expressing various *ex vivo* markers. (Figure adapted from Maher A.K *et al.*, 2024 [1]).

I focused my analysis on characterizing the phenotype of DP T cells in ACs (n=12 AC lPVL and n=12 AC hPVL) to gain insight into the phenotype of the DP T cell population in asymptomatic HTLV-1 infection. Dimensionality reduction demonstrated that the phenotype of DP T cells in ACs was different from those of $CD4^+$ and $CD8^+$ SP T cells on a tSNE plot (Figure 5.3a and 5.3b). In addition, the DP T cell sub-populations are also partially clustered separately from each other (Figure 5.3c). The main markers driving the clustering were CD27, Foxp3, PD-1, TIGIT, and CCR7 (Figure 5.3d). Relative to both SP T cell populations, DP T cells expressed less CD27, and more PD-1, Tim-3, and CD127 (Figure 5.3e). DP T cells expressed more TIGIT and CD25 than $CD4^+$ SP T cells but the level of these markers was lower (TIGIT) or equal to (CD25) than on $CD8^+$ SP T cells. In addition, DP T cells expressed similar levels of Foxp3 as $CD4^+$ SP T cells and higher than $CD8^+$ SP T cells, but lower levers of the lymph node homing marker CCR7 than $CD4^+$ SP T cells.

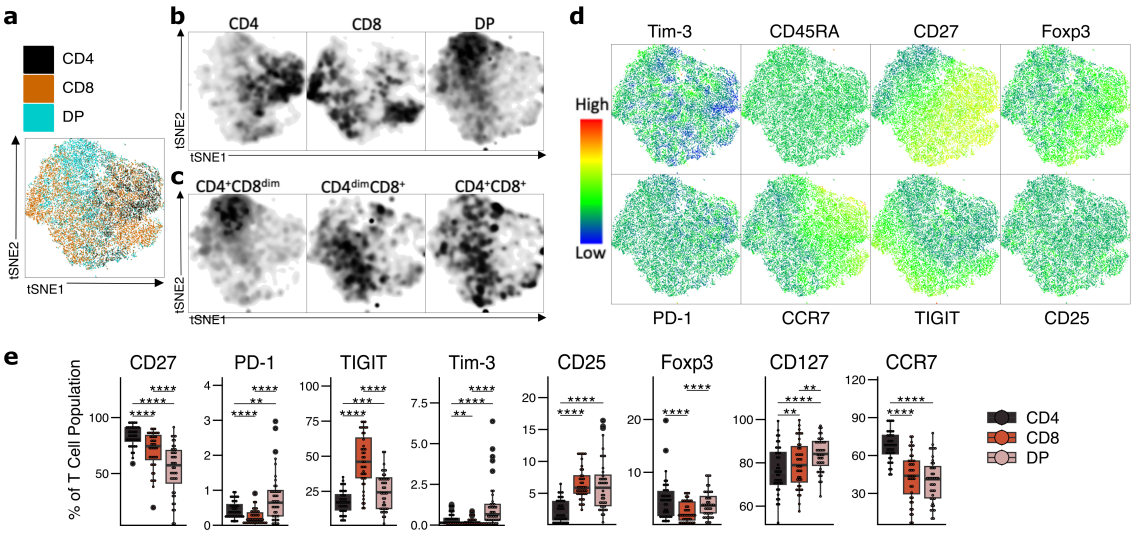


Figure 5.3: Characterization of DP T cells in HTLV-1 ACs. a. tSNE plot obtained from a concatenated sample of *ex vivo* $CD3^+$ T cells (n=14 AC lPVL, n=14 AC hPVL). **b and c.** tSNE plots showing the density of $CD4^+$ SP, $CD8^+$ SP, and DP or $CD4^+$ $CD8^{dim}$, $CD4^{dim}CD8^+$, and $CD4^+$ $CD8^+$ T cells. **d.** tSNE plots displaying the levels of expression of different markers. **e.** Box and whisker plots showing the percentage expression of markers in *ex vivo* in $CD4^+$ SP, $CD8^+$ SP, and DP T cells from ACs (n=20 AC lPVL, n=20 AC hPVL). **e)** Wilcoxon signed-rank paired test with Holm correction for multiple comparisons; *p≤0.05, **p≤0.01, ***p≤0.001, ****p≤0.0001. (Figure adapted from Maher A.K *et al.*, 2024 [1]).

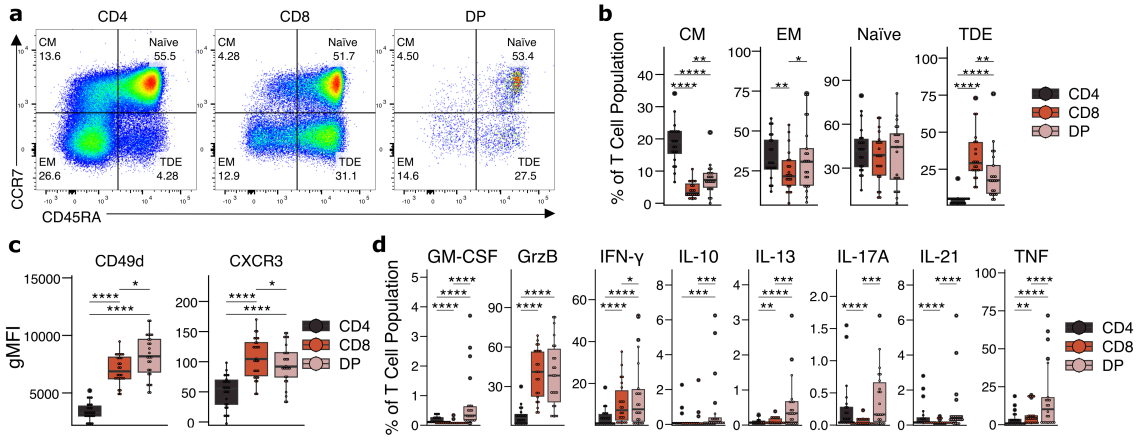


Figure 5.4: Characterization of DP T cells antigen experience and cytokine expression in HTLV-1 ACs. Representative flow plots showing (**a**) and box and whisker plots (**b**) showing the frequency of central memory (CM), naïve, terminally differentiated effector (TDE), and effector memory (EM) in DP T cells (n=10 AC lPVL, n=11 AC hPVL). **c.** Box and whisker plot showing the gMFI of CD49d and CXCR3 (n=12 AC lPVL, n=14 AC hPVL). **d.** Box and whisker plot of the expression of cytokines and granzyme B after a 4 h stimulation with PMA and ionomycin (n=11 AC lPVL, n=11 AC hPVL). **b, d)** Wilcoxon signed-rank paired test with Holm correction for multiple comparisons; **c)** T test with Holm correction for multiple comparisons; *p≤0.05, **p≤0.01, ***p≤0.001, ****p≤0.0001. (Figure adapted from Maher A.K *et al.,* 2024 [1]).

CCR7 and CD45RA were used to classify cells into central memory (CM), naïve, terminally differentiated effector (TDE), and effector memory (EM) cells (Figure 5.4a) [18, 82, 83]. Interestingly, approximately 50% of the DP T cells had a naïve phenotype, similar to their respective $CD4^+$ and $CD8^+$ SP T cells populations (Figure 5.4b). In contrast, DP cells displayed a distinct distribution of memory phenotypes compared to SP $CD4^+$ and $CD8^+$ T cells, and while DP cells contained a higher frequency of CM and EM than $CD8^+$ SP T cells, this frequency was lower than in $CD4^+$ SP T cells. A larger proportion of DP T cells had a TDE phenotype compared to $CD4^+$ SP T cells, but that proportion was smaller than in $CD8^+$ SP T cells.

While DP T cells expressed lower levels of the lymph node homing marker CCR7 than $CD4^+$ SP T cells (Figure 5.3e), they expressed higher levels of the tissue homing marker CD49d than both SP T cells populations and higher levels of CXCR3 than CD4 SP T cells (Figure 5.4c), suggesting increased migratory capacity to tissues. To explore the functionality of DP T cells in ACs, I determined the cytokine expression profile *ex vivo* after a 4 h stimulation with PMA and ionomycin (Figure 5.4d, representative flow stainings shown in Figure 5.5). DP T cells displayed a proinflammatory phenotype clearly different from their SP $CD4^+$ and $CD8^+$ T cell counterparts. DP T cells expressed high levels of TNF, comparable levels of IFN-γ and granzyme B to those of $CD8^+$ SP

T cells, and levels of IL-17A and IL-21 similar to $CD4^+$ SP T cells. DP T cells also expressed higher levels of GM-CSF, IL-10, and IL-13 than either SP T cell population, but the overall expression was low. These data suggest the DP T cells are polyfunctional, proinflammatory, and display both helper and cytotoxic phenotypes in HTLV-1 ACs.

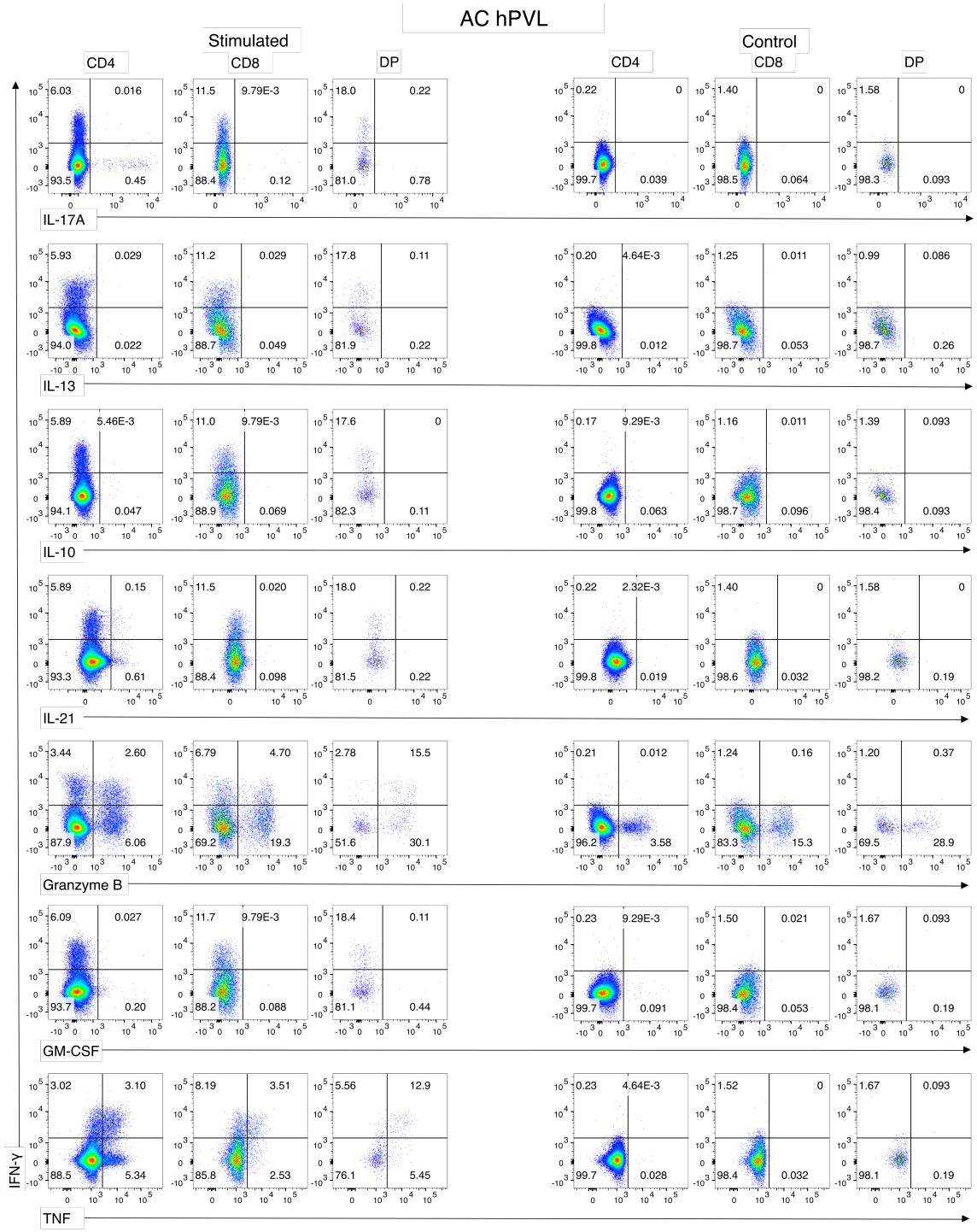


Figure 5.5: DP Cytokine phenotyping in AC hPVL. Representative flow plots showing cytokine expression by DP T cells from an AC hPVL after stimulation with PMA and ionomycin for 4 h. (Figure adapted from Maher A.K *et al.,* 2024 [1]).

5.2.3 Contribution of DP T cells to anti-HTLV-1 immune response

Given the high proinflammatory cytokine potential of DP T cells, I investigated the contribution of DP T cells to anti-HTLV-1 immunity and inflammation. PBMCs from ACs were stimulated with heat-inactivated HTLV-1 and HTLV-1-specific $CD4^+$ and $CD8^+$ SP T cells were identified based on the expression of CD154 or the co-expression of CD69 and CD137 respectively (Figure 5.6a and 5.6b) [324, 329]. Intriguingly, there was no significant difference in the expression of CD154 or CD137 and CD69 by DP T cells stimulated with HTLV-1 or a vehicle-stimulated control in HTLV-1-infected carriers (5.6c and 5.6d), suggesting the DP T cells may have been recently activated by their cognate antigen *in vivo*. Additionally, despite expressing high levels of CD154, DP T cells only accounted for approximately 6.5% of HTLV-1-specific $CD4^+$ expressing T cells in HTLV-1-infected people.

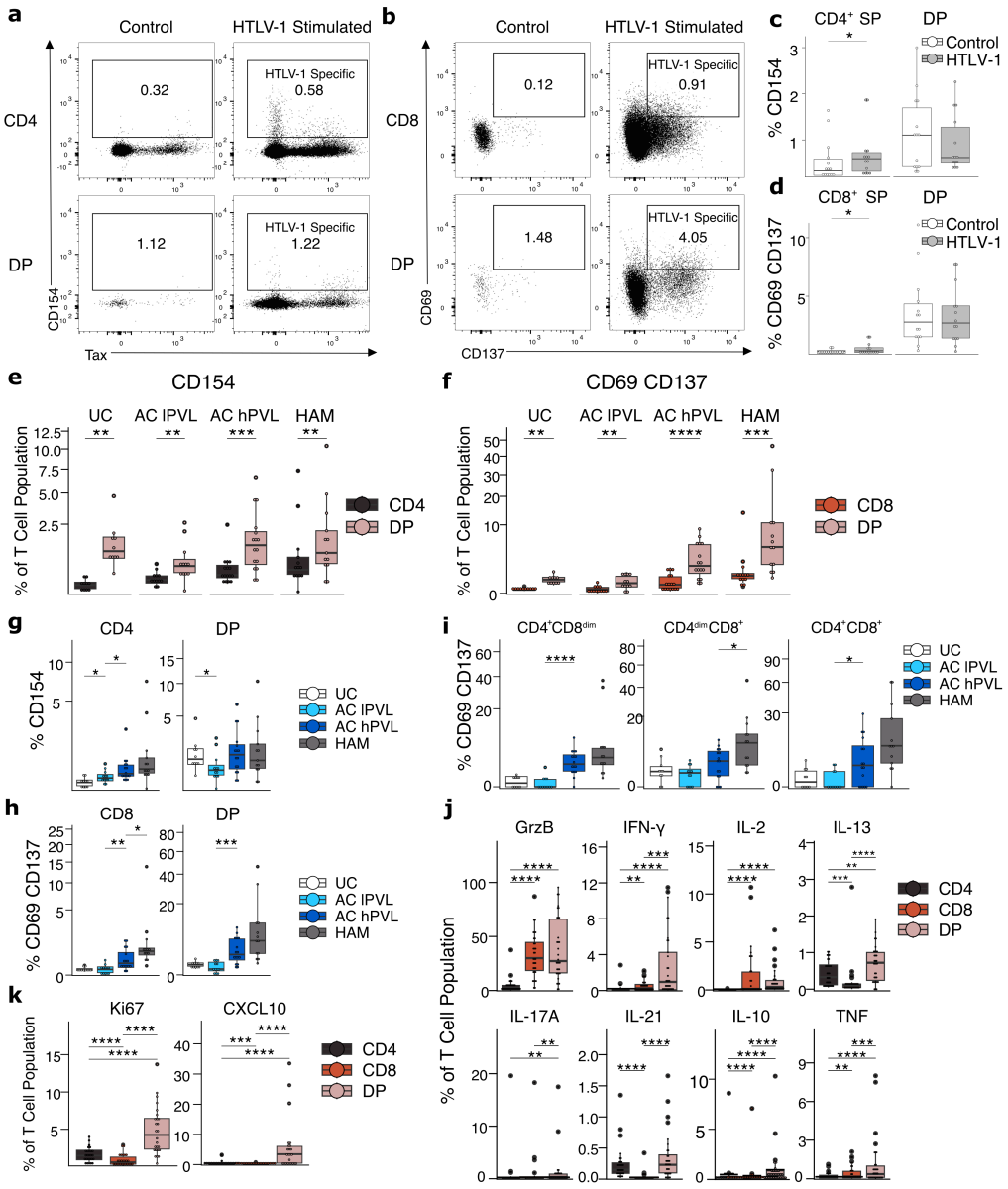


Figure 5.6: Contribution of DP T cells to HTLV-1-specific immunity. Representative flow plots showing the expression of CD154 and Tax by $CD4^+$ SP and DP T cells (**a**) or the expression of CD69 and CD137 by $CD8^+$ SP T and DP T cells (**b**) in an AC hPVL after a 12 h stimulation with HTLV-1. **c, d.** Box and whisker plots showing CD154 expression by $CD4^+$ SP and DP T cells or CD69 and CD137 co-expression by $CD8^+$ SP and DP T cells in ACs and patients with HAM after stimulation with HTLV-1 or a control (n= 14) **e, f.** Box and whisker plots showing the frequency of $CD4^+$ SP and DP T cells expressing CD154, or $CD8^+$ SP and DP T cells co-expressing CD69 and CD137 (n= 10 UC, n= 12 AC lPVL, n=16 AC hPVL, n=13 HAM). **g, h.** Box and whisker plots comparing the frequency of $CD154^+$ $CD4^+$ SP and DP T cells, or $CD69^+CD137^+$ $CD8^+$ SP and DP T cells (n= 10 UC, n= 12 AC lPVL, n=16 AC hPVL, n=13 HAM). **i.** Box and whisker plots comparing the frequency of $CD69^+CD137^+$ T cells in DP T cell sub populations (n= 10 UC, n= 12 AC lPVL, n=16 AC hPVL, n=13 HAM). **j.** Box and whisker plots showing the expression of cytokines and granzyme B in $CD4^+$ SP, $CD8^+$ SP, and DP T cells from ACs after stimulation with HTLV-1 for 20 h (n= 17 AC lPVL, n=16 AC hPVL). **k.** Box and whisker plots showing Ki67 and CXCL10 expression in $CD4^+$ SP, $CD8^+$ SP, and DP T cells from ACs after stimulation with HTLV-1 for 12 h (n= 12 AC lPVL, n=14 AC hPVL). **c-f, j, k)** Wilcoxon signed-rank paired test with Holm correction for multiple comparisons; **g-i)** Wilcoxon signed-rank unpaired test for comparisons between UC and AC lPVL, AC lPVL and AC hPVL, and AC hPVL and HAM; *p≤0.05, **p≤0.01, ***p≤0.001, ****p≤0.0001. (Figure adapted from Maher A.K *et al.,* 2024 [1]).

The frequency of $CD154^+$ and $CD69^+CD137^+$ cells were higher in DP T cells than $CD4^+$ or $CD8^+$ SP T cells (Figure 5.6e and 5.6f). This trend was consistent across UCs, ACs, and patients with HAM. There were no significant differences in the frequency of $CD154^+$ HTLV-1-specific DP T cells among the different HTLV-1-infected groups (Figure 5.6g). DP T cells, similarly to $CD8^+$ SP T cells in the previous chapter, contained a higher frequency of $CD69^+CD137^+$ cells in high proviral load groups, and $CD4^{dim}CD8^+$ DP T cells from patients with HAM expressed significantly higher levels of $CD69^+CD137^+$ than AC hPVL (Figure 5.6h and 5.6i).

In agreement with the results obtained by polyclonal stimulation (Figure 5.4d), DP T cells produced higher levels of inflammatory cytokines than SP T cells following stimulation with HTLV-1 and expressed high levels of IFN-γ, TNF, and IL-17A (Figure 5.6j). However, it is unclear whether these responses are truly HTLV-1-specific as both HTLV-1-stimulated and unstimulated DP T cells expressed high levels of AIMs (Figure 5.6c and 5.6d) possibly indicating recent activation by their cognate antigen in the periphery before *in vitro* stimulation with HTLV-1. Again, DP T cells expressed levels of granzyme B similar to $CD8^+$ SP T cells and levels of IL-21 similar to $CD4^+$ SP T cells. In addition to producing high levels of proinflammatory cytokines, DP T cells also displayed increased proliferation measured by marker of proliferation Kiel 67 (Ki67) and expressed higher levels of CXCL10 relative to SP T cells (Figure 5.6k). Overall, these data suggest that DP T cells contain an increased frequency of activated cells compared to both $CD4^+$ and $CD8^+$ SP T cells and display a polyfunctional, proinflammatory phenotype.

5.2.4 HTLV-1-specific DP T cells are phenotypically distinct in ACs and patients with HAM

To determine whether HTLV-1-specific DP T cells were different in UCs, ACs, and patients with HAM, I characterized DP T cells in these different groups (n=11 in each group) after stimulation with heat-inactivated HTLV-1.

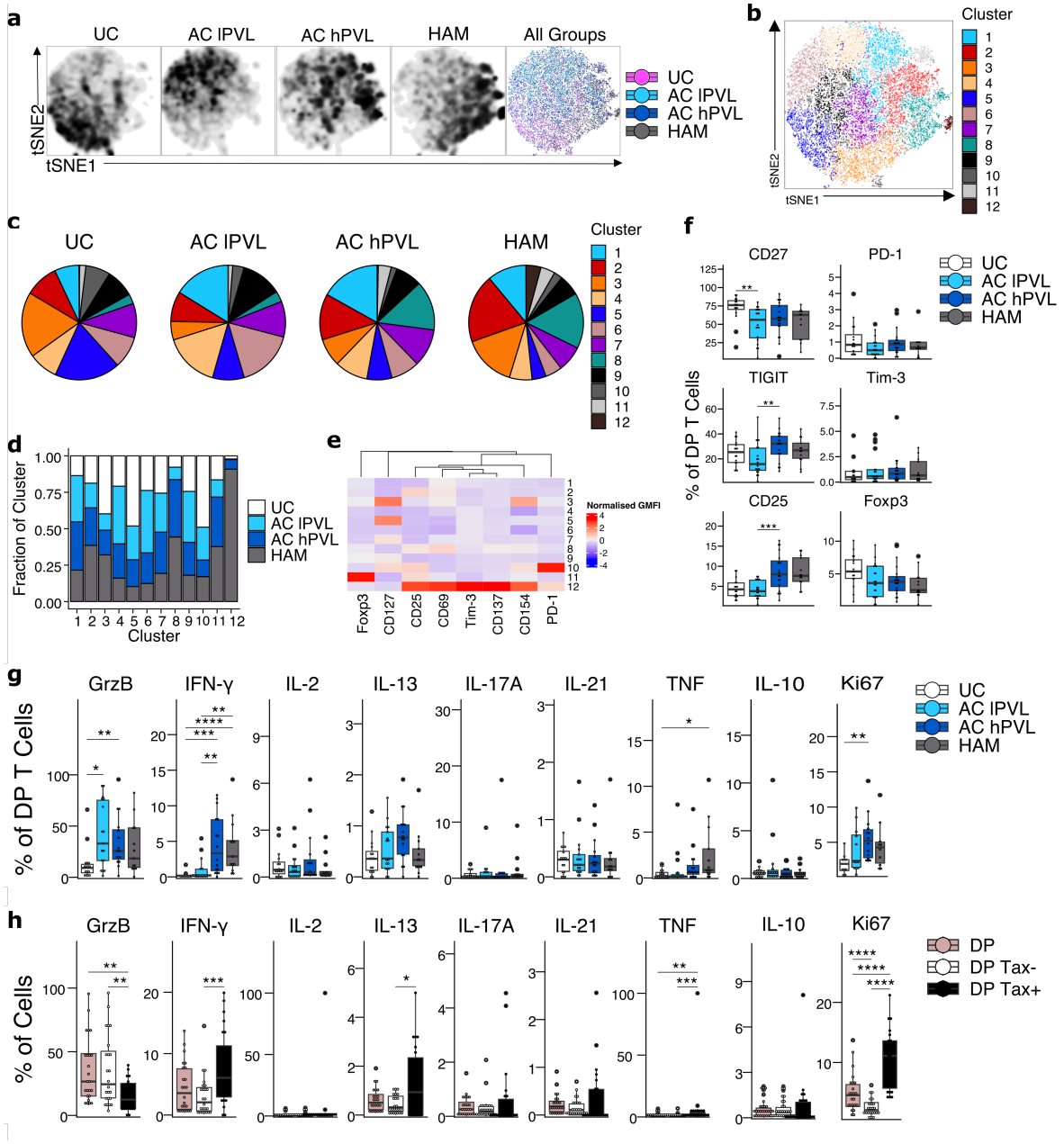


Figure 5.7: Phenotype of DP T cells in UCs, ACs, and patients with HAM. a. tSNE plots from a concatenated sample of DP T cells (n=11 each group). **b.** tSNE plot depicting the cell clusters identified by Phenograph. **c.** Pie charts showing the fraction of cells within each cell cluster in UCs or HTLV-1-infected groups. **d.** Bar graph showing the distribution (fraction) of cells from each patient group in each identified cluster. **e.** Heatmap of the expression of markers by each cluster displayed as modified z-scores using median values. **f.** Box and whisker plots showing the expression of cell surface markers in *ex vivo* DP T cells (n= 16 UC, n= 20 AC lPVL, n=20 AC hPVL, n=13 HAM). **g.** Box and whisker plots showing cytokine, Ki67, and granzyme B expression by DP T cells after stimulation with heat-inactivated HTLV-1 for 20 h (n= 16 UC, n= 17 AC lPVL, n=16 AC hPVL, n=13 HAM). **h.** Box and whisker plots showing cytokine, Ki67, and granzyme B expression by Tax$^-$ DP T cells and HTLV-1-infected Tax$^+$ DP T cells after stimulation with heat-inactivated HTLV-1 for 20 h (n=13 AC hPVL, n=11 HAM). **f, g)** Wilcoxon signed-rank unpaired test for comparisons between UC and AC lPVL, AC lPVL and AC hPVL, and AC hPVL and HAM; **h)** Wilcoxon signed-rank paired test with Holm correction for multiple comparisons; *p≤0.05, **p≤0.01, ***p≤0.001, ****p≤0.0001. (Figure adapted from Maher A.K *et al.,* 2024 [1]).

Dimensionality reduction tools demonstrated that while there was some overlap in the global phenotype of the four groups, HTLV-1-specific DP T cells from these four groups were distinct from each other on a tSNE plot (Figure 5.7a). To further describe the phenotypic differences, I applied a clustering algorithm using markers of T cell activation (CD154, CD69, CD137), Treg-associated markers (CD25, CD127, Foxp3), and other inhibitory markers (PD-1, Tim-3). 12 sub-populations of DP T cells were identified based on the expression of these markers (Figure 5.7b). The size and proportion of cells in these sub-populations varied between HTLV-1-infected groups and UCs (Figure 5.7c and 5.7d). Clusters 3 and 5 were predominant in UCs; clusters 1, 4, and 6 were predominant in AC lPVL; clusters 1, 2, and 8 made up large proportions of the DP T cells in AC hPVL, and a large proportion of HAM DP T cells fell into clusters 2, 3, and 8 (Figure 5.7c). Moreover, HAM DP T cells were over-represented in clusters 2, 3, 8, 11, and 12 and were under-represented in clusters 1, 4, 5, and 6 (Figure 5.7d). Cluster 12 was almost entirely composed of HAM DP T cells and was characterized by the expression of high levels of T cell activation markers (CD154, CD137, CD69, and CD25), high levels of Tim-3 and moderate to low expression of Foxp3, and CD127 (Figure 5.7e). Cluster 5, which consisted mainly of DP T cells from UCs and AC lPVL, was characterized by the expression of high levels of CD127, and low levels of CD69 (Figure 5.7e). *Ex vivo* DP T cells from HTLV-1 carriers expressed lower levels of CD27 than UCs, TIGIT was expressed at higher levels on DP T cells from AC hPVL relative to both AC lPVL and HAM, and there was a trend towards increased CD25 expression with increased PVL (Figure 5.7f).

The cytokine expression profiles of DP T cells after stimulation with heat-inactivated HTLV-1 were also compared between groups. DP T cells from ACs expressed higher levels of granzyme B than UCs (Figure 5.7g). High PVL groups expressed higher levels of IFN-γ and TNF than AC lPVL. HAM DP T cells produced more TNF than ACs and UCs, but the difference was only statistically significant with UCs. There were no significant differences in the levels of IL-2, IL-13, IL-17A, IL-21, and IL-10 expression between HTLV-1-infected groups and UCs. DP T cells from HTLV-1 carriers had increased proliferation compared to UCs as measured by Ki67 expression. These data suggest that HTLV-1-specific DP T cells are phenotypically different among HTLV-1-infected groups but display similar capacity to secrete proinflammatory cytokines and cytotoxic molecules.

Given the heterogeneity of the DP T cell population, I wanted to elucidate whether this

proinflammatory cytotoxic helper phenotype was due to HTLV-1-infected or uninfected DP T cells or both. I used Tax expression in high PVL groups to identify HTLV-1-infected DP T cells and characterized the cytokine expression profile of Tax^+ and Tax^- DP T cells after a 20 h stimulation with heat-inactivated HTLV-1 (Figure 5.7h). There was no difference in the expression of IL-2, IL-17A, IL-21, and IL-10 between Tax^+ and Tax^- DP T cells. Tax^+ DP cells expressed less granzyme B than DP Tax^- cells, and more IFN-γ, IL-13, TNF, and Ki67. The mean granzyme B expression in $CD4^+$ SP, $CD8^+$ SP, Tax^- DP, and Tax^+ DP T cells was 4.7%, 36.6%, 35.2%, and 15.3% respectively. Despite Tax^+ DP T cells expressing less granzyme B than Tax^- DP T cells, they were still significantly more cytotoxic than $CD4^+$ SP T cells. Overall, both Tax^+ and Tax^- DP T cells are highly proinflammatory when stimulated with HTLV-1 and express high levels of IL-21 and other helper cytokines, but Tax^+ DP T cells appear to be more proinflammatory and less cytotoxic than Tax^- DP T cells.

5.2.5 DP T cells induce proinflammatory astrocytes

Given the increased migratory capacity of DP T cells due to high CD49d and CXCR3 expression, their proinflammatory cytotoxic helper phenotype, and their increased frequency in patients with HAM, I wanted to explore the role DP T cells may play in HAM pathogenesis in the CNS.

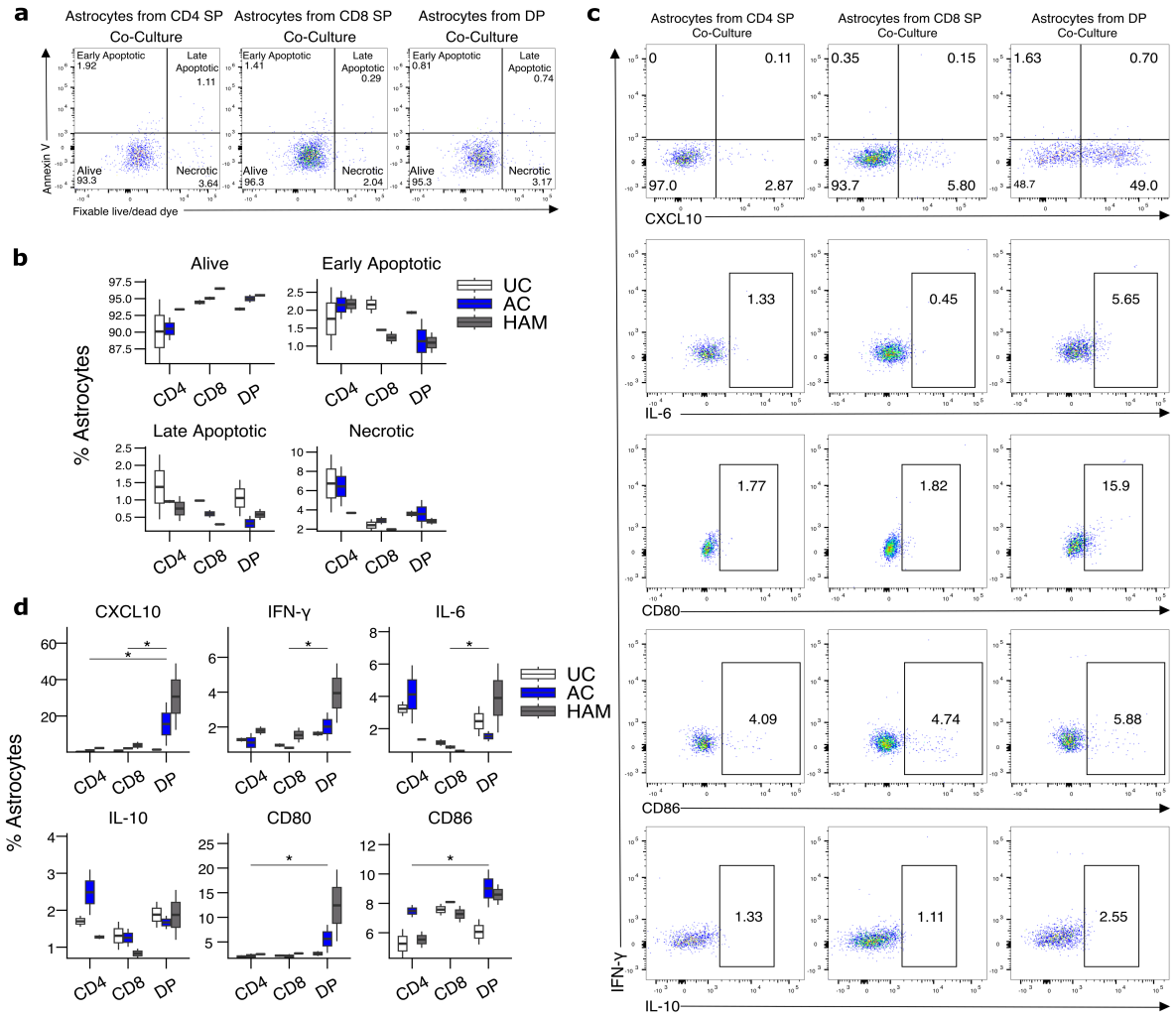


Figure 5.8: Astrocyte co-cultured with HTLV-1-stimulated DP cells. a. Representative plots showing the viability and Annexin V staining of astrocytes after 36 h of co-culture with pre-HTLV-1 stimulated $CD4^+$ SP, $CD8^+$ SP, or DP T cells from a patient with HAM. Dying astrocytes can be separated into alive, early apoptotic, late apoptotic, and necrotic. **b.** Box and whisker plots showing the percentage of alive and dying astrocytes (n=2 UC, n=2 AC, n=2 HAM). Representative flow plots **(c)** and summary box and whisker plots **(d)** showing the expression of cell surface markers, cytokines, and chemokines in astrocytes co-cultured with HTLV-1-stimulated $CD4^+$ SP, $CD8^+$ SP, or DP T cells (n=2 UC, n=2 AC, n=2 HAM). **b, d)** Wilcoxon signed-rank paired test for comparisons between $CD4^+$ SP and DP or $CD8^+$ SP and DP; *p≤0.05, **p≤0.01, ***p≤0.001, ****p≤0.0001. (Figure adapted from Maher A.K *et al.,* 2024 [1]).

I stimulated total PBMCs with heat-inactivated HTLV-1 for 12 h and then flow-sorted $CD4^+$ SP, $CD8^+$ SP, and DP T cells from UCs, ACs, and patients with HAM, and placed these HTLV-1-stimulated sorted cells in co-culture with an astrocyte cell line (CCF-STTG1) for 36 h. There was no significant difference in the viability of the astrocytes in the different co-culture conditions (Figure 5.8a-b). Intriguingly, viability seemed to be higher in astrocytes co-cultured with DP T cells relative to astrocytes co-cultured with $CD4^+$ SP T cells, but the trend was not significant (Figure 5.8b). To determine whether DP T cells could change the phenotype of the astrocytes relative to $CD4^+$ and $CD8^+$ SP T cells, a combination of different cell surface markers, cytokines and chemokines were measured by flow cytometry (Figure 5.8c). DP T cells induced a large statistically significant increase in CXCL10, IFN-γ, CD80, and CD86 expression, especially in the astrocytes co-cultured with DP T cells from patients with HAM (Figure 5.8d). Astrocytes co-cultured with DP T cells expressed significantly more IL-6 than those co-cultured with CD8 SP T cells but not CD4 SP T cells. No difference in IL-10 expression was seen. These data clearly show that DP T cells, and particularly DP T cells from patients with HAM, induce proinflammatory astrocytes which have the potential to contribute to CNS pathology.

5.2.6 HTLV-1 infection of SP T cells gives rise to a DP T cells population

Given that the increased frequency of DP T cells in patients with HAM compared to ACs did not seem to be due to increased proliferation, I questioned how this expanded highly HTLV1-infected DP T cell population arose. I infected flow-sorted SP $CD4^+$ and $CD8^+$ T cells from uninfected individuals with HTLV-1 by co-culturing them with irradiated MT-2 cells, a leukemic HTLV-1-infected cell line [389]. $CD4^+$ and $CD8^+$ SP T cells were also co-cultured with irradiated MT-2 cells in the presence of raltegravir [390], and with the non-HTLV-1-infected leukemic cell line Jurkat (JKT) as controls. SP T cells co-cultured with MT-2 cells and raltegravir (MT-2+R) were therefore exposed to HTLV-1 virions/proteins and other materials secreted by MT-2 cells but were not stably infected by HTLV-1 [391, 392], and JKT cells were used to control for long term *in vitro* culture and exposure to foreign non-HTLV-1 proteins and other secreted materials [393]. If a

DP T cell population were to emerge from the sorted SP T cells co-cultured with MT-2 cells, these controls would allow me to determine whether it was due to stable HTLV-1 infection, the activity or exposure to HTLV-1 virions and proteins, or T cell activation due to exposure to other foreign materials such as exosomes and cytokines.

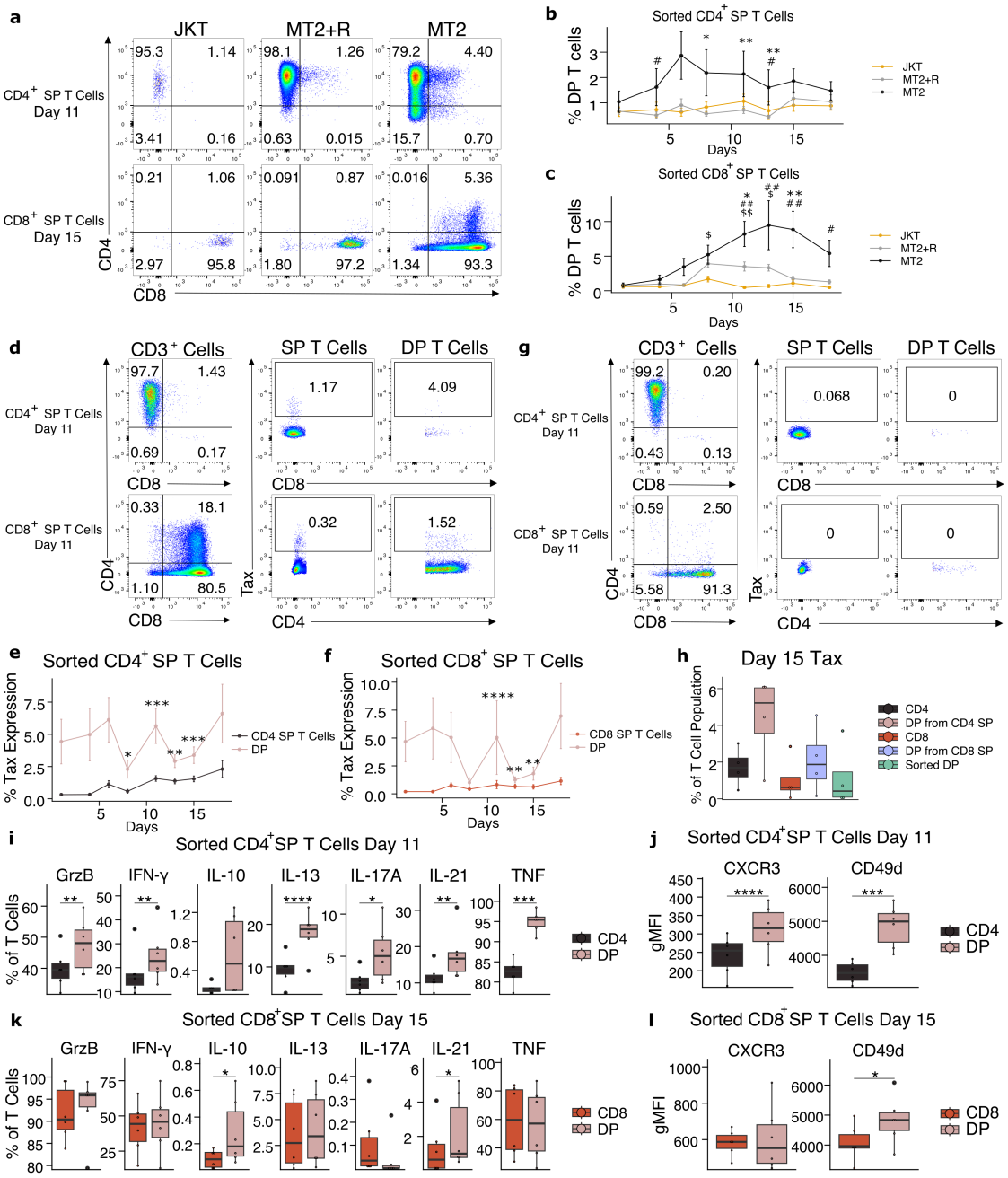


Figure 5.9: Origin of DP T cells in HTLV-1 infection. a. Representative flow plots (**a**) and line graphs (**b, c**) showing the frequency of emerged DP T cells during co-culture of SP T cells with JKT, MT-2+R, or MT-2 cells. Representative flow plots showing CD4 and CD8 expression, and Tax expression in SP T cells and DP T cells during co-culture with MT-2 cells **(d)** or MT-2+R **(g)**. **e, f.** Line graphs showing Tax expression by SP T cells and the emerged DP T cells during co-culture with MT-2 cells. **h.** Box and whisker plot showing Tax expression in CD4$^+$ SP T cells, emerged DP T cells from CD4$^+$ SP T cells, CD8$^+$ SP T cells, emerged DP T cells from CD8$^+$ SP T cells, and naturally occurring DP T cells on day 15 of co-culture with MT-2 cells (n= 4). **i-l.** Box and whisker plots showing cytokine and granzyme B expression, and the gMFI of cell surface markers in SP T cells and the newly emerged DP T cells, after stimulation with PMA and ionomycin (n=6). **b, c, e, f)** mean ± standard error of the mean (SEM) error (n=15). **b, c)** Wilcoxon signed-rank unpaired test, *p≤0.05, **p≤0.01, ***p≤0.001 for comparisons between MT-2 and MT-2+R; #p≤0.05, ##p≤0.01, ###p≤0.001 for comparisons between MT-2 and JKT; $P≤0.05, $$P≤0.01, $$$P≤0.001 for comparisons between MT-2+R and JKT; **e, f)** Wilcoxon signed-rank paired test for comparisons between SP T cells and DP T cells at each time point; **i-k)** Wilcoxon signed-rank paired test and l) Paired T-test; *p≤0.05, **p≤0.01, ***p≤0.001, ****p≤0.0001 for comparisons between SP T cells and DP T cells. (Figure adapted from Maher A.K *et al.,* 2024 [1]).

By measuring CD4 and CD8 expression every 2-3 days in the sorted SP T cell populations, I observed the emergence of DP T cell populations from both the sorted $CD4^+$ and $CD8^+$ SP T cells co-cultured with MT-2 cells, but not from the JKT controls (Figure 5.9a-c). A small DP T cell population appeared to emerge from $CD8^+$ SP T cells co-cultured with MT-2+ raltegravir, but the DP T cell population is significantly smaller than that induced by the MT-2 cell co-culture and shorter-lived (Figure 5.9c). Most of the DP T cells that emerged from $CD4^+$ and $CD8^+$ SP T cells were $CD4^+$ $CD8^{dim}$ and $CD4^{dim}CD8^+$ respectively (Figure 5.9a). DP T cell frequency peaked between days 6-11 in the sorted $CD4^+$ SP T cells and between days 11-15 in the sorted $CD8^+$ SP T cells. The DP T cell population that emerged from $CD8^+$ SP T cells was larger than that derived from $CD4^+$ SP T cells (Figure 5.9b and 5.9c).

I measured Tax expression in the cultured cells to track HTLV-1 infection (Figure 5.9d). DP T cells derived from both $CD4^+$ and $CD8^+$ SP T cells expressed higher levels of Tax than their parent SP T cell population, indicating higher rates of infection in the newly generated DP T cell populations (Figure 5.9e and 5.9f) and consistent with the increased infection of *ex vivo* DP T cells (Figure 5.1f). There was no/very little Tax expression in cells that were co-cultured in the presence of raltegravir, confirming that HTLV-1 was not able to productively infect these cells (Figure 5.9g). I also sorted naturally occurring peripheral DP T cells from UCs and co-cultured them with MT-2 cells. Sorted naturally occurring DP T cells expressed levels of Tax similar to the SP T cells co-cultured with MT-2 cells and less Tax than the DP T cells that emerged from the SP T cells (Figure 5.9h), suggesting that naturally occurring DP T cells from UCs are not preferentially infected with HTLV-1 *in vitro*, and supporting the notion that the high level of DP T cell infection is due to HTLV-1-infected SP T cells differentiating into DP T cells.

To assess whether the DP T cells I generated *in vitro* reflected the phenotype of *ex vivo* DP T cells in HTLV-1 carriers, I characterized the cytokine expression profiles and cell surface markers in the emerged DP T cell population. I stimulated the cells with PMA and ionomycin for 4 h on day 11 or 15 of the sorted $CD4^+$ or $CD8^+$ SP T cell-MT-2 co-cultures, respectively, and compared the phenotype of the emerged DP T cells to the remaining parent SP T cell population. The DP T cells that emerged from the $CD4^+$ SP T cells upregulated granzyme B and became more proinflammatory, expressing significantly

higher levels of IFN-γ, IL-13, IL-17A, IL-21, and TNF (Figure 5.9i). I also observed an increase in CXCR3 and CD49d expression in the DP T cells when compared to $CD4^+$ SP T cells (Figure 5.9j). The DP T cells that emerged from $CD8^+$ SP T cells expressed higher levels of IL-21 than their parent population which would result in an increased helper phenotype (Figure 5.9k). These DP T cells also upregulated the expression of IL-10 and CD49d, but there was no significant change in the expression of granzyme B, IFN-γ, IL-13, IL-17A, TNF, and CXCR3 (Figure 5.9k and 5.9l). These data are consistent with my observations *ex vivo* where DP T cells expressed comparable levels of granzyme B and IFN-γ to $CD8^+$ SP T cells and higher than $CD4^+$ SP T cells, lower levels of CXCR3 than $CD8^+$ SP T cells and higher than $CD4^+$ SP T cells, and higher levels of IL-13, IL-17A, IL-21, TNF and CD49d than either SP T population (Figure 5.4c and 5.4d).

5.2.7 Involvement of ThPOK and RunX3 in DP T cell generation and stability

Little is known about how peripheral DP T cells emerge in UCs or during chronic viral infections. The transcription factors RunX3 and ThPoK have been shown to regulate thymic $CD8^+$ and $CD4^+$ T cell lineage commitment respectively and are thought to be mutually exclusively expressed in naïve T cells [394, 395, 396].

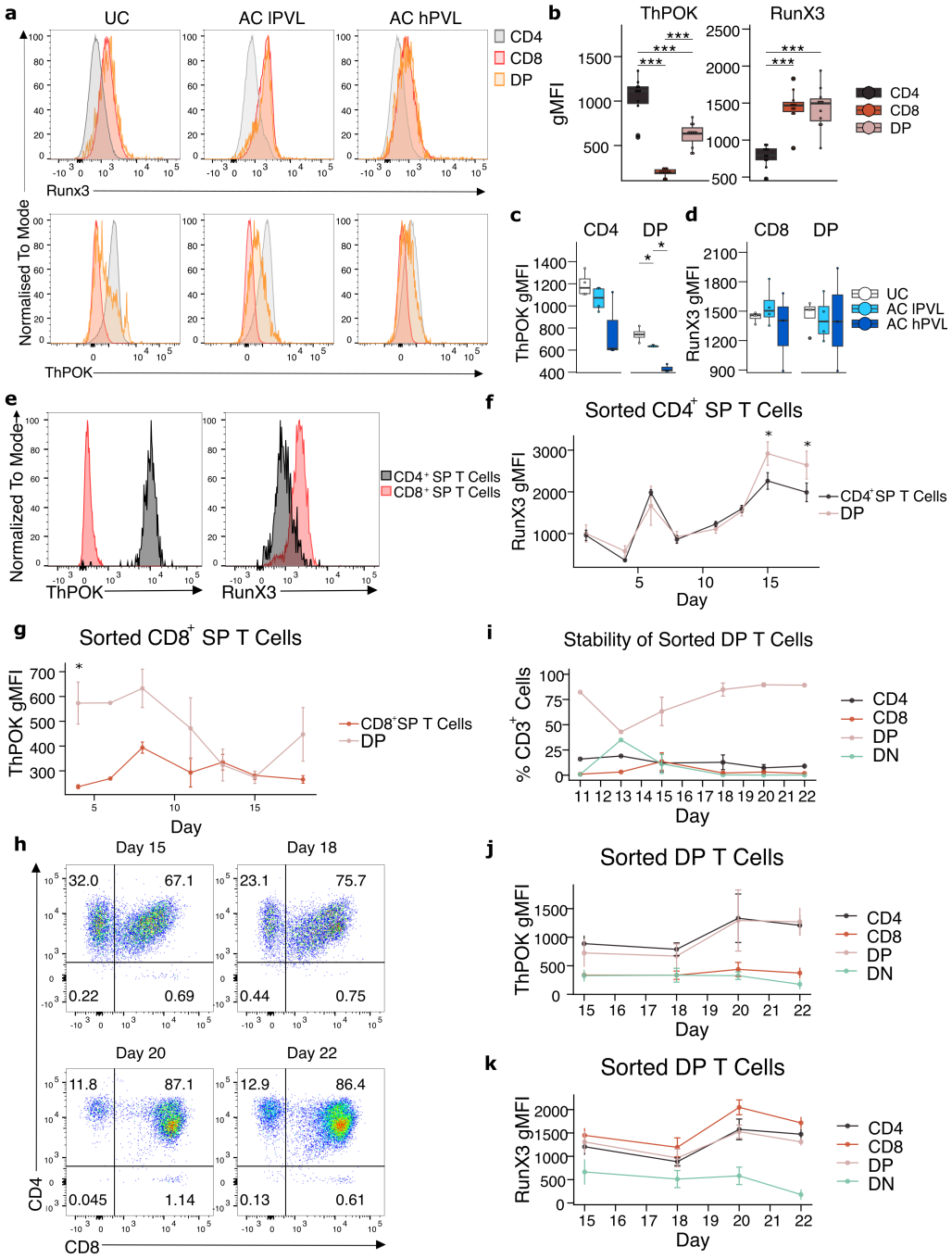


Figure 5.10: Mechanism of CD4 and CD8 co-expression. a. Representative examples **(a)** and summary gMFI **(b)** of *ex vivo* Runx3 and ThPOK expression in CD4$^+$ SP, CD8$^+$ SP, and DP T cells (n= 11). **c, d.** Box and whisker plots showing the *ex vivo* gMFI of ThPOK and RunX3 (n=4 UC, n=4 AC lPVL, n=3 AC hPVL). **e.** Histograms showing the expression of RunX3 and ThPOK in sorted CD4$^+$ and CD8$^+$ SP T cells on Day 1 of co-culture with MT-2 cells. **f, g.** Line graphs showing the gMFI of RunX3 or ThPOK in emerged DP T cells and CD4$^+$ SP or CD8$^+$ T cells during co-culture with MT-2 cells; mean ± SEM error (n= 5). Representative flow plots **(h)** and line graph **(i)** showing the percentage of CD4$^+$ SP, CD8$^+$ SP, DP, and DN T cells that emerge from sorted naturally occurring DP T cells co-cultured with MT-2 cells; mean ± SEM error (n= 3). **j, k.** Line graphs showing the gMFI of ThPOK or RunX3 in CD4$^+$ SP, CD8$^+$ SP, DP, and DN T cell populations that emerged from sorted naturally occurring DP T cells co-cultured with MT-2 cells; mean ± SEM error (n=3). **b)** Wilcoxon signed-rank paired test with Holm correction; **c, d)** Wilcoxon signed-rank unpaired test for comparisons between UC and AC lPVL, and AC lPVL and AC hPVL. f, g) Paired T-test for comparisons between SP and DP T cells at each time point; *p≤0.05, **p≤0.01, ***p≤0.001, ****p≤0.0001. (Figure adapted from Maher A.K *et al.,* 2024 [1]).

Ex vivo DP T cells from UCs and ACs expressed an intermediate level of ThPOK relative to $CD8^+$ and $CD4^+$ SP T cells, and comparable Runx3 levels to $CD8^+$ SP T cells (Figure 5.10a and 5.10b). Interestingly, both $CD4^+$ SP and DP T cells from AC hPVL expressed lower levels of ThPOK as compared to AC lPVL who in turn expressed lower levels than UCs (Figure 5.10c). There was no difference in RunX3 expression between patient groups (Figure 5.10d).

While expression of ThPOK and RunX3 is thought to be mutually exclusive in naïve T cells, I decided to examine the expression of both transcription factors in SP T cells as they were co-cultured with MT-2 cells to induce DP T cells. Sorted $CD4^+$ and $CD8^+$ SP T cells expressed high levels of ThPOK and RunX3 respectively after 24 h in co-culture with MT-2 cells (Figure 5.10e), but both RunX3 and ThPOK levels varied during the 18-day co-culture with MT-2 cells (Figure 5.10f and 5.10g). Significantly increased expression of RunX3 in the emerging DP T cell population compared to the parent $CD4^+$ T cell population was observed at later time points (Figure 5.10f). In the sorted $CD8^+$ SP T cells, the emerged DP T cell population expressed significantly higher ThPOK levels compared to $CD8^+$ SP T cells, which gradually became more similar to that of the bulk $CD8^+$ SP T cell population over time (Figure 5.10g).

The expression of CD4 and CD8 in the sorted, naturally occurring, DP T cells from UCs was not stable over time when co-cultured *in vitro* with MT-2 cells (Figure 5.10h and 5.10i). While the majority of sorted DP T cells remained DP, $CD4^+$ SP, $CD8^+$ SP, and DN T cell populations emerged (Figure 5.10h and 5.10i). The emerged $CD8^+$ SP and DN T cells downregulated ThPOK, but not the $CD4^+$ SP T cell population (Figure 5.10j). RunX3 was upregulated by the $CD8^+$ SP T cell population that emerged and downregulated by the DN population (Figure 5.10k). These results suggest that ThPOK is associated with $CD4^+$ expression in SP T cells and RunX3 is associated with $CD8^+$ SP T cells. However, ThPOK and RunX3 expression appears to be dynamic and was not always correlated with $CD4^+$ or $CD8^+$ expression. It is likely that other transcription factors and/or HTLV-1 proteins are involved in DP T cell differentiation in infected cells.

5.3 Discussion

The overall aims of this chapter were to explore the phenotype, frequency, and antigen-specificity of DP T cells in HTLV-1 infection. In this chapter, I showed that DP T cells in HTLV-1 carriers were highly HTLV-1-infected, were more abundant in patients with HAM, and were highly proinflammatory with a helper/cytotoxic phenotype. These DP T cells expressed high levels of CD49d and CXCR3 suggesting an enhanced capacity to migrate to the CNS, and DP T cells were able to induce proinflammatory astrocytes demonstrating their potential to contribute to HAM pathogenesis. Mechanistically I showed that HTLV-1-infected DP T cell populations were generated by infection of SP $CD4^+$ and $CD8^+$ T cells. The increased migratory capacity and proinflammatory phenotype of DP T cells, and their ability to induce proinflammatory astrocytes suggest that they could contribute to CNS pathology. A summary of the findings in this chapter is shown in Figure 5.11.

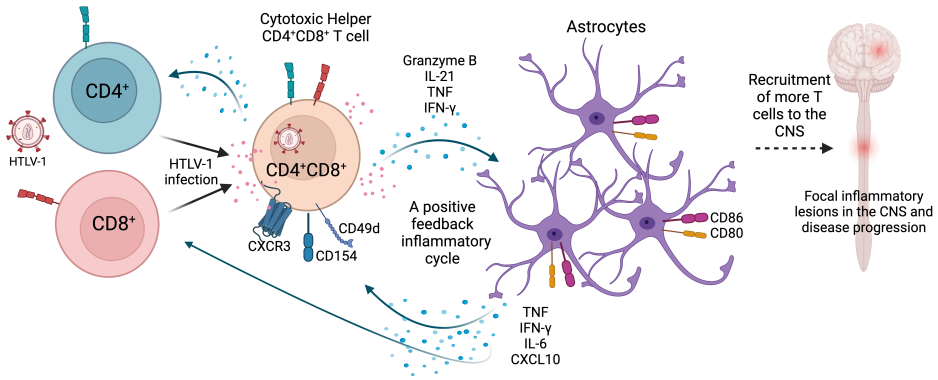


Figure 5.11: Hypothesized contribution of DP T cells neuroinflammation in HAM. HTLV-1 infects SP T cells and a small subset of HTLV-1-infected SP T cells differentiate into highly proinflammatory DP T cells with a helper and cytotoxic phenotype. High CXCR3 and CD49d expression facilitates the migration of DP T cells to the CNS, where DP T cells induce proinflammatory astrocytes which secrete high levels of CXCL10. CXCL10 recruits more CXCR3-expressing cells to the CNS, establishing a positive inflammatory feedback loop contributing to HAM disease progression. Figure created using BioRender (Figure adapted from Maher A.K *et al.*, 2024 [1]).

DP T cells in HTLV-1-infected individuals are heterogeneous, but they all display a highly inflammatory phenotype with high levels of activation-induced markers and proinflammatory cytokines. The co-expression of helper cytokines, granzyme B, and CD154 suggests that DP T cells can act as both helper cells, providing help to both B and

$CD8^+$ T cells [397], but that they can also perform cytotoxic functions that are potentially detrimental in patients with HAM. Approximately half of DP T cells in ACs are antigen-experienced, as shown by the downregulation of CD27, which is associated with T cell differentiation, and higher levels of CD127 than SP T cells. While HTLV-1 infection has been shown to increase $Foxp3^+$ expression, higher Foxp3 expression in DP T cells relative to $CD8^+$ SP T cells could be indicative of an activated non-regulatory phenotype [304, 398, 399]. Despite this proinflammatory effector phenotype, DP T cells also expressed high levels of inhibitory receptors PD-1, Tim-3, and TIGIT. High levels of inhibitory receptor expression in chronic viral infections are often associated with T cell exhaustion [400]. However, DP T cells in persons infected with HTLV-1 are still able to proliferate at a higher rate than SP T cell populations when stimulated with HTLV-1 and have a higher cytokine secretion potential. This observation, in addition to the high levels of activation-induced marker expression observed, suggests that DP T cells are an active effector T cell population in HTLV-1 infection.

The increased frequency of highly inflammatory DP T cells in patients with HAM may contribute to tissue damage in the CNS. $CD4^+CD8^+$ T cells in patients with HAM were infected at higher rates and $CD4^{dim}CD8^+$ T cells expressed significantly more CD69 and CD137 than AC hPVL. Expanded DP T cell populations have been associated with other inflammatory diseases including MS and RA as well as in viral infections such as HIV, HCV, and EBV [167, 166, 168, 169, 170, 401], but it is unclear if these expanded DP T cell populations cause inflammation or are a consequence of inflammation, both may likely be true. I showed that DP T cells induced proinflammatory astrocytes causing them to secrete high levels of CXCL10, IFN-γ, and IL-6, and upregulate CD80 and CD86. My results support the hypothesis that inflammatory DP T cells in HTLV-1- infection can contribute to HAM pathogenesis. Indeed, DP T cells in HTLV-1 carriers express high levels of molecules involved in T cell migration to tissues, including CXCR3 and CD49d. CD49d is a major integrin that allows activated T cells to cross the BBB, and antibodies blocking VLA-4 are a current MS treatment [184, 402, 403]. In agreement with this, DP T cells have been shown to be enriched in the CSF relative to the periphery of patients with MS and patients with non-inflammatory neurological diseases [184]. In addition to producing CXCL10 themselves, DP T cells are able to induce proinflammatory astrocytes which produce high levels of CXCL10 which chemoattracts CXCR3 expressing

cells including Th1 cells, $CD8^+$ T cells, and DP T cells [283, 284, 404, 405]. CXCR3 has been shown to activate peripheral immune cells, microglia, and CNS resident macrophages during brain injury to direct them to the lesion site [281, 282, 283, 284, 285, 286]. CXCL9 and CXCL10 are found at higher concentrations in the CSF of patients with HAM than in MS patients, who in turn have significantly higher levels than healthy controls, and the main source of CXCL10 in the CSF of patients with HAM is thought to be astrocytes [287]. Despite DP T cells being enriched in the CSF of MS patients, DP T cells did not appear to be present in active MS lesions from autopsy material from MS patients [287]. This is consistent with my *in vitro* data where I did not see a decrease in astrocyte viability during the co-culture with DP T cells, but I did observe changes to the astrocyte phenotype that would recruit more T cells to the CNS and drive inflammation. DP T cells in HTLV-1 carriers also expressed high levels of activation-induced markers CD154, CD137, and CD69 in response to HTLV 1 stimulation, and $CD49d^+CD154^+$ lymphocytes have been shown to reprogram oligodendrocytes into immune reactive cells in MS [406], further supporting the potential for DP cells in HTLV-1 infection to contribute to CNS pathology. DP T cells caused the upregulation of the co-stimulatory molecules CD80 and CD86 in astrocytes, which could help re-activate T cells once in the CNS. In addition, the high HTLV-1 infection rate of DP T cells also provides a potential source of antigen for local reactivation once in the CNS. These results warrant further studies on the role DP T cells play in recruiting other T cells to the CNS, their contribution to inflammation in the CNS, and their role in CNS pathology.

My data suggest that the majority of infected DP T cells arise from SP T cells. These data are in agreement with works demonstrating that $CD4^+CD8^+$ T cells in an HIV infected person share their TCR sequence with $CD4^+$ SP T cells [163, 407], excess IL-4 has been shown to induce CD8 expression on $CD4^+$ SP T cells but not $CD8^+$ SP T cells [408], and $CD4^{dim}CD8^+$ T cells have previously been described as an activated $CD8^+$ T cell phenotype [409, 410]. Moreover, mature antigen-stimulated $CD4^+$ T cells have been shown to terminate the expression of ThPOK and activate the expression of genes of the $CD8^+$ T cell lineage, resulting in cytotoxic $CD4^+CD8^+$ T cells which were MHC-II-restricted [411]. My results demonstrate that HTLV-1 infection drives the emergence of a DP T cell population from both SP T cell populations which are highly HTLV-1-infected. High proliferation rates of infected DP T cells likely contribute to expanding the HTLV-

1-infected DP T cell population in addition to the *de novo* HTLV-1 infection. The DP T cell population that emerged during MT-2 co-culture of SP T cells from UCs appeared to be partially stable and whether this is the case for *in vivo* generated DP T cells in HTLV-1-infected people remains to be determined. My data suggest that *de novo* HTLV-1 infection of SP T cells results in the co-expression of CD4 and CD8 in a subset of infected cells and correlates with ThPOK and RunX3 expression, but other transcription are likely involved in the re-acquisition of CD4 or CD8 expression. The underlying mechanisms of how HTLV-1 induces this population warrant further investigations: possibilities include the specific location of the HTLV-1 integration site in the host cell genome, the cytokine milieu, or the activity of HTLV-1 proteins.

Several interesting questions emerge from this work, including elucidation of whether these DP T cells are MHC-I or MHC-II restricted, molecular mechanisms by which HTLV-1 infection and viral proteins induce the DP T cell population, and identification of integration sites of HTLV-1-infected DP and SP infected T cells to determine if the integration site loci drive the co-expression of CD4 and CD8. Follow-up studies on the role and generation of DP T cells in HTLV-1 infection are warranted to answer these questions.

6

Discussion and Conclusion

The overall aim of this PhD was to explore mechanisms of T cell dysfunction during HTLV-1 infection. T cell dysfunction in the context of this thesis included T cell exhaustion, T cell dysfunction in cytokine production, HTLV-1-specific T cells polarized towards a particular phenotype, the inability to maintain a low PVL, and the direct contribution of T cells to CNS inflammation. I aimed to gain insight into the T cell responses in ACs with a low PVL effectively controlling the virus relative to ACs with a high PVL, to gain insights into mechanisms of effective viral control. I also wanted to gain insight into the mechanisms by which T cells in patients with HAM contribute to CNS inflammation and HAM pathogenesis. I have addressed the four main aims of this PhD and gained significant insight into both bulk and HTLV-1-specific T cell responses in UCs, AC lPVL, AC hPVL, and patients with HAM. My work builds on several studies that started to characterize HTLV-1-specific T cell responses in HTLV-1-infected groups [298, 300, 301, 308, 412]. However, to the best of my knowledge, this is the first work that uses AIMs to identify HTLV-1-specific T cells rather than cytokine secretion or tetramers, allowing access to a larger and less biased antigen-specific T cell population. Furthermore, very few previous studies have matched the PVL of AC hPVL and patients with HAM to be able to make comparisons based on disease status while controlling for differences due

to HTLV-1 infection [244, 298]. Controlling for the PVL between AC hPVL and patients with HAM, allows me to make conclusions based on disease status, and gives insight into the transition from AC hPVL to HAM.

In this thesis, I identified HTLV-1-specific $CD4^+$ and $CD8^+$ T cells by stimulating total PBMCs with heat-inactivated HTLV-1 for 12-20 h. $CD4^+$ T cells expressing CD154 were defined as HTLV-1-specific, while HTLV-1-specific $CD8^+$ T cells were identified based on CD69 and CD137 expression. Using AIMs allowed access to a diverse antigen-specific T cell pool, not restricted by TCR sequences or cytokine expression [127, 316, 320, 323, 329]. While previous studies on HTLV-1-specific $CD4^+$ T cells used IFN-γ secretion after stimulation with HTLV-1-peptides to identify HTLV-1-specific $CD4^+$ T cells, this will have biased the population identified to a particular phenotype [300, 301]. Furthermore, it would have been impossible to sort and culture HTLV-1-specific T cells identified by intracellular cytokine expression. In addition, using cytokine expression to identify HTLV-1-specific T cells is particularly challenging given that HTLV-1-infected T cells spontaneously produce IFN-γ and TNF after more than 6 hours in culture [209]. Given that I was using whole heat-inactivated HTLV-1, stimulation experiments were at least 12 h long to allow the ACPs to process and present the antigen to the T cells. This longer stimulation time would make it difficult to differentiate between activated T cells and HTLV-1-infected T cells. For the reasons outlined above, throughout this thesis AIMs were used to identify HTLV-1-specific T cells, however, there are also limitations when using AIMs. As previously discussed AIMs are not always uniquely expressed by virus-specific T cells and can be elevated due to non-specific activation, which may result in the inclusion of non-HTLV-1-specific cells in the analysis. As discussed in the $CD4^+$ T cell chapter, this non-specific activation could explain the presence of HTLV-1-specific T cells in UCs after HTLV-1 stimulation, in addition to the high proportion of naïve T cells in chronically infected patients. Furthermore, cytokine expression in HTLV-1-specific T cell populations was low, despite these cells not appearing exhausted based on inhibitory receptor expression and their proliferative capacity *in vitro*. Additionally, using the whole heat-inactivated virus to stimulate PBMCs, rather than peptides, presents both strengths and limitations. Using the entire viral proteome means that T cells will encounter an unrestricted pool of epitopes processed and presented in a physiologically relevant manner by APCs. However, this approach relies on effective antigen processing

and presentation, which can vary across different APC types and may vary between patient groups, potentially leading to inconsistent T-cell activation. This issue may be more pronounced for $CD8^+$ T cells, as it generally takes more time for APCs to process and present antigens to $CD8^+$ T cells compared to $CD4^+$ T cells. Ultimately, while the methods employed in this thesis to identify HTLV-1-specific T cells offer valuable insights, they also present certain challenges and limitations that should be carefully considered.

In the $CD4^+$ and $CD8^+$ T cell chapters, I show that despite an increased terminally differentiated effector phenotype in HTLV-1-infected groups, bulk $CD4^+$ and $CD8^+$ T cells and from UCs, AC lPVL, AC hPVL, and patients with HAM are phenotypically very similar, with no significant differences in their cytokine expression profiles. When focusing my analysis on HTLV-1-specific T cells, I showed that both the frequency and number of HTLV-1-specific $CD4^+$ and $CD8^+$ T cells increase with PVL. Furthermore, both HTLV-1-specific $CD4^+$ and $CD8^+$ T cells are infected at higher rates than non-HTLV-1-specific $CD4^+$ T cells, and this preferential infection is more pronounced and severe in high PVL groups. It is unclear whether this increased infection of the HTLV-1-specific T cell populations in high PVL groups relative to low PVL groups is a cause or consequence of high PVLs. I showed that a Th17-type HTLV-1-specific $CD4^+$ T cell response, with Th1 cytokine expression, and high IL-10 expression is associated with a low PVL. There were no major differences in the phenotypes of HTLV-1-specific $CD8^+$ T cells between AC lPVL and AC hPVL. Overall, robust Th17-responses are associated with HTLV-1 viral control.

In this work, I show that several different T cell populations in patients with HAM are able to induce pro-inflammatory astrocytes and microglia, suggesting that they have the capacity to contribute to CNS inflammation *in vivo*. Both HTLV-1-specific $CD4^+$ and $CD8^+$ T cells in patients with HAM induce significantly higher upregulation of the antigen presentation machinery, CD40, and pro-inflammatory cytokines in astrocytes relative to AC hPVL. Similar trends were seen with bulk $CD4^+$ T cells and $CD8^+$ T cells stimulated with anti-CD3 and anti-CD28, and DP T cells stimulated with HTLV-1. Acute infections may activate antigen-specific T cell populations which could instigate or contribute to CNS inflammation. However, only HTLV-1-specific T cells, and possibly auto-reactive T cells, would be persistently chronically activated *in vivo*, and therefore the HTLV-1-specific T cells are still likely to be the main instigators and drivers of CNS inflammation.

To confirm this hypothesis, the antigen specificity of T cells in the CNS lesions and CSF of patients with HAM would need to be characterized. There currently is no evidence of auto-reactive or cross-reactive T cells in the literature in relation to HTLV-1 infection.

To gain insights into the mechanisms by which HTLV-1-specific $CD4^+$ and $CD8^+$ T cells from patients with HAM-induced proinflammatory glial cells, I deeply characterized both populations by flow cytometry and subjected HTLV-1-specific $CD4^+$ T cells to RNA-seq analysis. I identified 628 differentially expressed genes in patients with HAM when compared to AC hPVL, including the upregulation of *EOMES*, *IL17RA*, *IL17RC*, and genes associated with an unfocused Th1 phenotype. Th1 cytokines, such as IFN-γ, and TNF are neurotoxic at high concentrations and can cause bystander damage [156, 157, 158, 264, 265]. Furthermore, IFN-γ regulates the passage of leukocytes into the CNS [266, 267]. In addition, IL-17 has been also shown to play a key role in driving chronic CNS inflammation in many neurological diseases [126]. Interestingly, HTLV-1-specific $CD8^+$ T cells from patients with HAM showed a strong Tc17 phenotype relative to AC hPVL and expressed high levels of IL-17A. DP T cells stimulated with HTLV-1 also expressed high levels of IL-17A, and IL-17A from both these populations have the capacity to contribute to neuroinflammation. Furthermore, HTLV-1-specific $CD4^+$ T cells from patients with HAM expressed significantly higher levels of *IL17RA* and *IL17RC* compared to AC hPVL. This increased expression enhances IL-17 signaling, known to boost the resistance of effector $CD4^+$ T cells to immune suppression [375].

RNA-seq pathway enrichment analysis showed that patients with HAM upregulate G alpha (12/13) signaling events, have increased NRAGE death signaling through JNK, and increased signaling by p75NTR relative to AC hPVL. Increased signaling through GPCRs is upregulated in patients with HAM, but the ligands driving this signaling remain unidentified and the impact of the GPCR signaling on the $CD4^+$ T cell phenotype or functionality is unclear. It would be interesting to understand more about the mechanism by which these pathways contribute to HAM pathogenesis, such as whether they are involved in T cell activation, migration, cytokine secretion, or another process entirely.

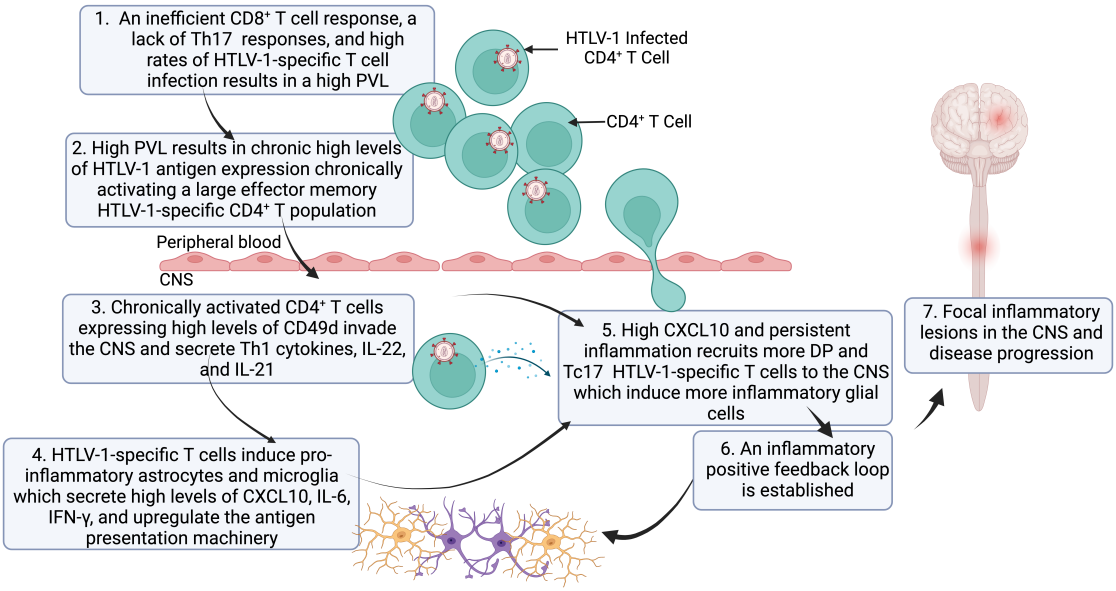


Figure 6.1: Summary of new insights into the hypothesized mechanism of HAM pathogenesis. Figure created using BioRender.

Taken together these data contribute to a greater understanding of the mechanisms of HAM pathogenesis and can inform the current hypothesis surrounding HAM pathogenesis, summarized in Figure 6.1. Overall my data and data from previous studies indicate that poor control of HTLV-1 infection due to a lack of Th17 responses, a high infection rate of the HTLV-1-specific T cell populations, and certain HLA-genotypes results in a high PVL [193]. Chronic high level of HTLV-1 antigen expression persistently activates a large, inefficient, and highly HTLV-1-infected HTLV-1-specific $CD4^+$ T cell populations. High CD49d expression facilitates migration to the CNS, and high levels of IFN-γ, TNF, and IL-22 expression disrupt BBB tight junctions allowing easier passage of lymphocytes into the CNS. Once in the CNS, HTLV-1-specific $CD4^+$ T cells activate and induce proinflammatory astrocytes and microglia, which can act as APCs and re-activate HTLV-1-specific T in the CNS. Inflammatory astrocytes and microglia secrete high levels of pro-inflammatory cytokines and chemokines such as IFN-γ, IL-6, and CXCL10. High levels of CXCL10 recruit more CXCR3 expressing cells such as Th1 cells, $CD8^+$ T cells, and DP T cells to the CNS. Both Tc17 HTLV-1-specific $CD8^+$ T cells and highly proinflammatory DP T cells further contribute to CNS inflammation, establishing a positive feedback inflammatory cycle, eventually resulting in persistent chronic inflammation in the CNS and disease progression.

This work has identified CD49d as an interesting target for HAM treatment. CD49d

is expressed at higher levels on HTLV-1-specific $CD4^+$ T cells, $CD8^+$ T cells, and DP T cells in patients with HAM relative to AC hPVL. Anti-CD49d antibody natalizumab is an approved treatment for MS and has been shown to reduce lymphocyte infiltration in the CNS [363]. Given that both HTLV-1-specific and non-specific $CD4^+$ T cells, $CD8^+$ T cells, and DP T cells were able to induce pro-inflammatory glial cells, reducing any lymphocyte entry into the CNS is likely to reduce CNS inflammation. Furthermore, targeting S1P signaling may also be of interest in HAM treatment, as S1P is upstream of G12/G13 alpha signaling [413], which was upregulated in HTLV-1-specific $CD4^+$ T cells in patients with HAM relative to AC hPVL. However, the mechanism by which this pathway contributes to HAM needs to be further elucidated and the ligands driving this signaling first need to be identified. Overall this thesis has characterized T cell responses that are associated with a low PVL and efficient viral control, in addition to gaining insight into T cell phenotypes, signaling pathways, and molecules that are associated with the transition from AC to HAM.

7

Final Words and Future Directions

This thesis has made several significant observations that increase our understanding of the mechanisms of effective HTLV-1 control and HAM pathogenesis. However, this thesis is limited to the study of peripheral T cells and extrapolating observations to the CNS. While studying peripheral T cells can give insights into systemic trends and phenotypes, they are unlikely to completely capture the T cell dysfunction that is happening within inflamed tissues. Studying mechanisms of HAM pathogenesis has historically been incredibly difficult as there is no suitable mouse model and collecting CSF from patients with HAM is difficult. Lumbar punctures for patients with HAM are extremely infrequent in the UK and tend to occur when treatments are failing, and ACs do not receive lumbar punctures at the National Centre for Human Retrovirology. Peripheral blood is much less difficult to acquire. Furthermore, T cells are first activated in the periphery before traveling to inflamed tissues, and therefore insights can still be gained from peripheral T cells which can then be validated in cells from the CSF of patients with HAM.

My observations in peripheral T cells in ACs and patients with HAM raise several interesting questions and open up many future avenues for exploration. Firstly, it would be interesting to characterize the antigen-specificity of T cells in the CSF of patients with HAM and determine their transcriptional profile. Secondly, it would be valuable to

determine whether HTLV-1-specific T cells in the CSF of patients with HAM are cross-reactive with other auto-antigens or pathogens. When sorting HTLV-1-specific $CD4^+$ T cells from UCs for RNA-seq analysis, only 50% of these cells expressed CD45RA (Figure 3.11b), indicating that the remaining 50% were antigen-experienced. Identifying the antigens that induce cross-reactive HTLV-1-specific $CD4^+$ T cells would provide important insights. Additionally, understanding whether pre-existing cross-reactive T cells offer protection against high PVLs during new HTLV-1 infections would be highly informative.

The RNA-seq data raises a lot of interesting questions about the of role G alpha (12/13) signaling events, increased NRAGE death signaling through JNK, and signaling by p75NTR in HAM pathogenesis. Follow-up experiments are needed to determine how these pathways affect $CD4^+$ T cell phenotypes, migration to the CNS, and interactions with glial cells. Some upstream GPCRs for G12/G13 signaling include the S1P and LPA receptor [376]. Future experiments could include observing changes in cytokine expression patterns in bulk memory $CD4^+$ T cells from UCs when stimulated with S1P or LPA. Furthermore, the glial-T cell co-culture experiments could repeated to gain further insight using the following modification: before HTLV-1-specific $CD4^+$ T cells from AC hPVL are placed in co-culture with glial cells, they could also be pre-stimulated with S1P or LPA and then placed in co-culture to determine whether the activation of these pathways induces more pro-inflammatory astrocytes or microglia than without the pre-stimulation with S1P and LPA. The RNA-seq data also identified the down-regulation of the metabolism of fatty acids, triacylglycerol, and ketone bodies in HTLV-1-specific $CD4^+$ T cells in patients with HAM relative to AC hPVL. A full characterization of the metabolic profile of HTLV-1-specific $CD4^+$ T cells in different HTLV-1-infected groups by SCENITH^{TM} or Seahorse could give insight into the energetic status of the cells and the impact on their effector phenotype [335]. In addition, the role of EOMES on the phenotype and effector functions of $CD4^+$ T cells in patients with HAM needs to be further explored.

Finally, the identification of a HAM-like phenotype in previous studies [244] in a subset of high PVL ACs allows us to assess the role of the differentially expressed pathways and molecules between AC hPVL and patients with HAM in early HAM pathogenesis. Follow-up studies characterizing T cell populations in this HAM-like cohort are warranted.

Overall I have made several interesting observations that contribute to our understand-

ing of effective HTLV-1-control and T cell contribution to HAM pathogenesis which need to be validated in T cells from the CSF of patients with HAM. Uncovering more about the mechanism by which HTLV-1-specific $CD4^+$ T cells induce pro-inflammatory astrocytes using the RNA-seq data to guide experimental design could identify novel targets for HAM treatment. This thesis offers a deep characterization of T cell responses in HTLV-1-infected individuals, insight into the mechanisms of virus-induced neuroinflammation, and identifies novel potential targets for HAM treatment.

List of Acronyms

ACs asymptomatic carriers

AC hPVL AC high PVL

AhR aryl hydrocarbon receptor

AIDS acquired immune deficiency syndrome

AIMs activation induced markers

ALCAM activated leukocyte cell adhesion molecule

AC lPVL AC low PVL

APCs antigen presenting cells

ARTE antigen-specific T cell enrichment

ATL adult T-cell leukemia/lymphoma

B2M beta-2 microglobulin

BBB blood-brain barrier

Bcl-6 B-cell lymphoma 6

BCR B cell receptor

BDNF brain-derived neurotrophic factor

C1q complement component 1q

C3 complement component 3

CBP CREB binding protein

CCL CC motif chemokine ligand

CCR C-C chemokine recptor

CD cluster of differentiation

cDNA complementary DNA

CM, CCR7^{+}CD45RA^{-} central memory

CNS central nervous system

CREB cyclic adenosine monophosphate cAMP response element binding protein

CSF cerebrospinal fluid

CSFE carboxyfluorescein succinimidyl ester

Ct cycle threshold

CTLA-4 cytotoxic T-lymphocyte associated protein 4

CXCR C-X-C motif receptor

CXCL10 chemokine IFN-γ inducible protein 10 kDa

DEGs differentially expressed genes

DENV dengue virus

ddPCR digital droplet PCR

DMSO dimethyl sulfoxide

DN double negative, CD4^{-}CD8^{-}

DNA deoxyribonucleic acid

DP double positive, CD4^{+}CD8^{+}

EAE experimental autoimmune encephalomyelitis

EBV Epstein-Barr virus

EGFR epidermal growth factor receptor

ELISA enzyme-linked immunosorbent assay

EM, CCR7^{-}CD45RA^{-} effector memory

EOMES Eomesodermin

FasL Fas ligand

FBS fetal calf serum

FC fold change

FcϵRI low-affinity IgE receptor

FcϵRII high-affinity IgE receptor

FcR Fc receptor

FDR false discover rate

FMOs fluorescence minus one controls

Foxp3 forkhead box P3

FSC forward scatter

GATA3 GATA-binding protein 3

GLAST glutamate aspartate transporter

GLT-1 glutamate transporter 1

GLUT-1 Glucose transporter 1

GM-CSF granulocyte-macrophage colony-stimulating factor

gMFI geometric mean fluorescence intensity

GPCR G protein-coupled receptors

h hours

HAM/TSP HTLV-1-associated myelopathy/tropic spastic paraparesis

HBZ HTLV-1 basic leucine zipper factor

HCMV human cytomegalovirus

HCV hepatitis C virus

HIV human immunodeficiency viruse

HLA-I Human leukocyte antigens class I

hnRNP-A1 anti-heterogeneous nuclear ribonuclear protein A1

HS human serum

hTERT human telomerase reverse transcriptase

HTLV-1 Human T Cell Leukemia Virus Type 1

HSC hematopoietic stem cells

HSPGs heparan sulfate proteoglycans

IBD inflammatory bowel disease

ICAM-1 intercellular adhesion molecule 1

ICOS inducible T-cell COStimulator

IFN interferon

IFNs-I/III type I and III interferons

Ig immunoglobulin

IL interleukin

IL17RC IL-17 receptor C

IL22BP IL-22 binding protein

iNOS inducible nitric oxide synthase

IRF3 interferon regulatory factor 3

IRF4 interferon regulatory factor 4

ISGs interferon-stimulated genes

iTreg induced Treg

JKT Jurkat cells

JNK c-Jun N-terminal kinases

Ki67 marker of proliferation Kiel 67

KIR killer immunoglobulin-like receptor

LAG-3 lymphocyte activation gene-3

LPA lysophosphatidic acid

LPS lipid polysaccharide

LTR long terminal repeat

MHC major histocompatibility complex

MHC-I major histocompatibility complex class I

MHC-II major histocompatibility complex class II

min minutes

MS multiple sclerosis

mRNA messenger ribonucleic acid

NF-κB nuclear factor kappa-light-chain-enhancer of activated B cells

NGF nerve growth factor

NK natural killer

NKG2 NK group 2 member

NRP-1 neuropilin-1

NRAGE novel melanoma antigen gene protein

NT neurotrophin

nTregs natural Tregs

p75NTR p75 neurotrophin receptor

PA phosphatidic acid

PAMPs Pathogen-associated molecular patterns

PBMC periphreal blood mononuclear cell

PBS phosphate buffered saline

PCA Principal component analysis

PC principal component

PCR polymerase chain reaction

PD-1 programmed cell death protein 1

PI propidium iodide

PMA phorbol 12-myristate 13-acetate

PRRs pattern recognition receptors

PVL provial load

RA rheumatoid arthritis

ROR-γt retinoic acid-related orphan receptor γt

RT reverse transcription

RT-PCR real-time reverse transcription–polymerase chain reaction

RNA ribonucleic acid

RNA-seq RNA sequencing

RunX3 runt-related transcription factor 3

S1P sphingosine-1-phosphate

SNPs single nucleotide polymorphisms

SP single positive, $CD4^{+}CD8^{-}$ or $CD4^{-}CD8^{+}$

SSC side scatter

SEM standard error of the mean

SEMA4A semaphorin-4A

SS systemic sclerosis

STAT1 signal and transducer of activation 1

T-bet T-box expressed in T cells

TBK1 TANK-binding kinase 1

Tc T cytotoxic

TCR T cell receptor

TDE, CCR7$^-$CD45RA$^+$ terminally differentiated effector

TGF-β Transforming growth factor-β

Th T helper

ThPOK T-helper-inducing POZ/Krüppel-like factor

TIGIT T cell immunoreceptor with immunoglobulin and ITIM domain

Tim-3 T-cell immunoglobulin and mucin-domain containing-3

TFs transcription factors

Tfh follicular helper T cell

TNF tumour necrosis factor

TNFR TNF receptor

Tr1 regulatory type 1 cells

Tregs regulatory T cells

TrkA tropomyosin receptor kinase A

TRM tissue resident memory

TSCM stem cell-like memory

tSNE t-distributed Stochastic Neighbor Embedding

UCs uninfected controls

UPR unfolded protein response

UTR untranslated region

VDJ variability, diversity, and joining

VLA-4 very late antigen-4

vs. versus

WHO World Health Organization

Zap70 zeta-chain-associated protein kinase 70

Bibliography

[1] Allison K. Maher, Aris Aristodemou, Nicolas Giang, Yuetsu Tanaka, Charles Rm Bangham, Graham P. Taylor, and Margarita Dominguez-Villar. HTLV-1 induces an inflammatory CD4+CD8+ T cell population in HTLV-1-associated myelopathy. *JCI insight*, 9(1), 2024.

[2] Jean S. Marshall, Richard Warrington, Wade Watson, and Harold L. Kim. An introduction to immunology and immunopathology. *Allergy, Asthma and Clinical Immunology*, 14(2):1–10, sep 2018.

[3] K Murphy and C Weaver. *Janeway's immunobiology*. Garland Science, New York, NY, 9th edition, 2016.

[4] R. Valiathan, M. Ashman, and D. Asthana. Effects of Ageing on the Immune System: Infants to Elderly. *Scandinavian Journal of Immunology*, 83(4):255–266, apr 2016.

[5] Shizuo Akira, Satoshi Uematsu, and Osamu Takeuchi. Pathogen Recognition and Innate Immunity. *Cell*, 124(4):783–801, feb 2006.

[6] Taro Kawai and Shizuo Akira. The role of pattern-recognition receptors in innate immunity: update on Toll-like receptors. *Nature Immunology 2010 11:5*, 11(5):373–384, apr 2010.

[7] Paola M Barral, Devanand Sarkar, Zao-zhong Su, Glen N Barber, Rob DeSalle, Vincent R Racaniello, and Paul B Fisher. Functions of the cytoplasmic RNA sensors RIG-I and MDA-5: key regulators of innate immunity. *Pharmacology therapeutics*, 124(2):219–234, nov 2009.

[8] Finlay McNab, Katrin Mayer-Barber, Alan Sher, Andreas Wack, and Anne O'Garra. Type I interferons in infectious disease. *Nature Reviews Immunology 2015 15:2*, 15(2):87–103, jan 2015.

[9] Joseph P. Mizgerd, Matt R. Spieker, and Claire M. Doerschuk. Early Response Cytokines and Innate Immunity: Essential Roles for TNF Receptor 1 and Type I IL-1 Receptor During Escherichia coli Pneumonia in Mice. *The Journal of Immunology*, 166(6):4042–4048, mar 2001.

[10] Lee W. Ott, Katheryn A. Resing, Alecia W. Sizemore, Joshua W. Heyen, Ross R. Cocklin, Nathan M. Pedrick, H. Cary Woods, Jake Y. Chen, Mark G. Goebl,

Frank A. Witzmann, and Maureen A. Harrington. Tumor Necrosis Factor-α - and Interleukin-1-Induced Cellular Responses: Coupling Proteomic and Genomic Information. *Journal of proteome research*, 6(6):2176, 2007.

[11] Sean Diehl and Mercedes Rincón. The two faces of IL-6 on Th1/Th2 differentiation. *Molecular Immunology*, 39(9):531–536, dec 2002.

[12] Jason G. Cyster and Christopher D.C. Allen. B Cell Responses: Cell Interaction Dynamics and Decisions, apr 2019.

[13] Donna L. Farber, Naomi A. Yudanin, and Nicholas P. Restifo. Human memory T cells: Generation, compartmentalization and homeostasis. *Nature Reviews Immunology*, 14(1):24–35, 2014.

[14] David H. Raulet and Russell E. Vance. Self-tolerance of natural killer cells. *Nature Reviews Immunology 2006 6:7*, 6(7):520–531, jul 2006.

[15] Alex M. Abel, Chao Yang, Monica S. Thakar, and Subramaniam Malarkannan. Natural killer cells: Development, maturation, and clinical utilization. *Frontiers in Immunology*, 9(AUG):1869, aug 2018.

[16] Takumi Kawasaki and Taro Kawai. Toll-like receptor signaling pathways. *Frontiers in Immunology*, 5(SEP):461, sep 2014.

[17] Mihai G. Netea, Leo A.B. Joosten, Eicke Latz, Kingston H.G. Mills, Gioacchino Natoli, Hendrik G. Stunnenberg, Luke A.J. O'Neill, and Ramnik J. Xavier. Trained immunity: A program of innate immune memory in health and disease. *Science*, 352(6284):427, apr 2016.

[18] A Lanzavecchia and F Sallusto. Dynamics of T lymphocyte responses: intermediates, effectors, and memory cells. *Science*, 290(5489):92–97, oct 2000.

[19] Munir Akkaya, Kihyuck Kwak, and Susan K. Pierce. B cell memory: building two walls of protection against pathogens, apr 2020.

[20] Francisco A. Bonilla and Hans C. Oettgen. Adaptive immunity. *Journal of Allergy and Clinical Immunology*, 125(2 SUPPL. 2):S33–S40, 2010.

[21] Hergen Spits. Development of $\alpha\beta$ T cells in the human thymus. *Nature Reviews Immunology 2002 2:10*, 2(10):760–772, oct 2002.

[22] Tucker W. Lebien and Thomas F. Tedder. B lymphocytes: how they develop and function. *Blood*, 112(5):1570–1580, sep 2008.

[23] Benjamin E. Willcox, George F. Gao, Jessica R. Wyer, John E. Ladbury, John I. Bell, Bent K. Jakobsen, and P. Anton Van der Merwe. TCR binding to peptide-MHC stabilizes a flexible recognition interface. *Immunity*, 10(3):357–365, mar 1999.

[24] Brahma V Kumar, Thomas J Connors, and Donna L Farber. Human T Cell Development, Localization, and Function throughout Life. *Immunity*, 48:202–213, 2018.

[25] Thomas Korn and Axel Kallies. T cell responses in the central nervous system. *Nature Reviews Immunology 2017 17:3*, 17(3):179–194, jan 2017.

[26] Vitaly V. Ganusov and Rob J. De Boer. Do most lymphocytes in humans really reside in the gut? *Trends in Immunology*, 28(12):514–518, dec 2007.

[27] Rachael A. Clark. Skin-Resident T Cells: The Ups and Downs of On Site Immunity. *Journal of Investigative Dermatology*, 130(2):362–370, feb 2010.

[28] Michio Tomura, Naoki Yoshida, Junko Tanaka, Satoshi Karasawa, Yoshihiro Miwa, Atsushi Miyawaki, and Osami Kanagawa. Monitoring cellular movement in vivo with photoconvertible fluorescence protein "Kaede" transgenic mice. *Proceedings of the National Academy of Sciences of the United States of America*, 105(31):10871–10876, aug 2008.

[29] Morgan C. Hunter, Alvaro Teijeira, and Cornelia Halin. T Cell Trafficking through Lymphatic Vessels. *Frontiers in Immunology*, 7(DEC):1, 2016.

[30] Stephen C. Jameson and David Masopust. Understanding Subset Diversity in T Cell Memory. *Immunity*, 48(2):214–226, 2018.

[31] Shimon Sakaguchi, Tomoyuki Yamaguchi, Takashi Nomura, and Masahiro Ono. Regulatory T Cells and Immune Tolerance. *Cell*, 133(5):775–787, 2008.

[32] A. P. Dalmasso, C. Martinez, K. Sjodin, and R. A. Good. Studiest on the role of the thymus in immunobiology; reconstitution of immunologic capacity in mice thymectomized at birth. *The Journal of experimental medicine*, 118(6):1089–1109, 1963.

[33] Stephen M Hedrick, David I Cohen, Ellen A Nielsen, and Mark M Davis. Isolation of cDNA clones encoding T cell-specific membrane-associated proteins. 1984. *Journal of immunology (Baltimore, Md. : 1950)*, 175(5):2771–2775, sep 2005.

[34] Marie Malissen, Karyl Minard, Shelley Mjolsness, Mitchell Kronenberg, Joan Goverman, Tim Hunkapiller, Michael B. Prystowsky, Yasunobu Yoshikai, Frank Fitch, Tak W. Mak, and Leroy Hood. Mouse T cell antigen receptor: Structure and organization of constant and joining gene segments encoding the β polypeptide. *Cell*, 37(3):1101–1110, jul 1984.

[35] I Schwartz, R H A Babbitt, B P Allen, P M Matsueda, G Haber, E Vnanue, E R Buus, S Sette, A Colon, S M Jenis, D M Grey, H M Buus, S M Miles, C Grey, and H M Allen. Predictable acquisition of a new MHC recognition specificity following expression of a transfected T-cell receptor β-chain gene. *Nature 1987 329:6136*, 329(6136):256–259, 1987.

[36] Michael S. Krangel. Mechanics of T cell receptor gene rearrangement. *Current Opinion in Immunology*, 21(2):133–139, apr 2009.

[37] Hiroyuki Takaba and Hiroshi Takayanagi. The Mechanisms of T Cell Selection in the Thymus. *Trends in Immunology*, 38:805–816, 2017.

[38] Yousuke Takahama, Kensuke Takada, Shigeo Murata, and Keiji Tanaka. β5t-containing thymoproteasome: specific expression in thymic cortical epithelial cells and role in positive selection of CD8+ T cells. *Current Opinion in Immunology*, 24(1):92–98, feb 2012.

[39] Graham Anderson and Yousuke Takahama. Thymic epithelial cells: working class heroes for T cell development and repertoire selection. *Trends in Immunology*, 33(6):256–263, jun 2012.

[40] Kensuke Takada and Yousuke Takahama. Positive-Selection-Inducing Self-Peptides Displayed by Cortical Thymic Epithelial Cells. *Advances in Immunology*, 125(1):87–110, jan 2015.

[41] Harald von Boehmer, Hung Sia Teh, and Pawel Kisielow. The thymus selects the useful, neglects the useless and destroys the harmful. *Immunology today*, 10(2):57–61, 1989.

[42] Ronald N. Germain. T-cell development and the CD4–CD8 lineage decision. *Nature Reviews Immunology 2002 2:5*, 2(5):309–322, 2002.

[43] Shinichiro Sawada, John D. Scarborough, Nigel Killeen, and Dan R. Littman. A lineage-specific transcriptional silencer regulates CD4 gene expression during T lymphocyte development. *Cell*, 77(6):917–929, jun 1994.

[44] Wilfried Ellmeier, Shinichiro Sawada, and Dan R. Littman. The regulation of CD4 and CD8 coreceptor gene expression during T cell development. *Annual review of immunology*, 17:523–554, 1999.

[45] Wilfried Ellmeier, Mary Jean Sunshine, Kasia Losos, Farah Hatam, and Dan R. Littman. An enhancer that directs lineage-specific expression of CD8 in positively selected thymocytes and mature T cells. *Immunity*, 7(4):537–547, 1997.

[46] Ed Palmer. Negative selection — clearing out the bad apples from the T-cell repertoire. *Nature Reviews Immunology 2003 3:5*, 3(5):383–391, may 2003.

[47] Hiroyuki Takaba and Hiroshi Takayanagi. The Mechanisms of T Cell Selection in the Thymus. *Trends in Immunology*, 38(11):805–816, 2017.

[48] Ted H. Hansen and Marlene Bouvier. MHC class i antigen presentation: Learning from viral evasion strategies. *Nature Reviews Immunology*, 9(7):503–513, 2009.

[49] Kiley R. Prilliman, Mark Lindsey, Kenneth W. Jackson, Jeffrey Cole, Ron Bonner, and William H. Hildebrand. Complexity among constituents of the HLA-B*1501 peptide motif. *Immunogenetics*, 48(2):89–97, 1998.

[50] Robert G. Urban, Roman M. Chicz, William S. Lane, Jack L. Strominger, Armin Rehm, Marcel J.H. Kenter, Fons G.C.M. Uytdehaag, Hidde Ploegh, Barbara Uchanska-Ziegler, and Andreas Ziegler. A subset of HLA-B27 molecules contains peptides much longer than nonamers. *Proceedings of the National Academy of Sciences of the United States of America*, 91(4):1534–1538, feb 1994.

[51] Andreas Blees, Dovile Januliene, Tommy Hofmann, Nicole Koller, Carla Schmidt, Simon Trowitzsch, Arne Moeller, and Robert Tampé. Structure of the human MHC-I peptide-loading complex. *Nature*, 551(7681):525–528, 2017.

[52] Jiaren Sun, Daniel J. Leahy, and Paula B. Kavathas. Interaction Between CD8 and Major Histocompatibility Complex (MHC) Class I Mediated by Multiple Contact Surfaces that Include the $\alpha 2$ and $\alpha 3$ Domains of MHC Class I. *Journal of Experimental Medicine*, 182(5):1275–1280, 1995.

[53] Nu Zhang and Michael J. Bevan. CD8+ T Cells: Foot Soldiers of the Immune System. *Immunity*, 35(2):161–168, 2011.

[54] Hans Raskov, Adile Orhan, Jan Pravsgaard Christensen, and Ismail Gögenur. Cytotoxic CD8+ T cells in cancer and cancer immunotherapy. *British Journal of Cancer 2020 124:2*, 124(2):359–367, sep 2020.

[55] Paul A. Roche and Kazuyuki Furuta. The ins and outs of MHC class II-mediated antigen processing and presentation. *Nature Reviews Immunology*, 15(4):203–216, mar 2015.

[56] Roman M. Chicz, Robert G. Urban, William S. Lane, Joan C. Gorga, Lawrence J. Stern, Dario A.A. Vignali, and Jack L. Strominger. Predominant naturally processed peptides bound to HLA-DR1 are derived from MHC-related molecules and are heterogeneous in size. *Nature 1992 358:6389*, 358(6389):764–768, 1992.

[57] M Srinivasan, S Z Domanico, P T Kaumaya, and S K Pierce. Peptides of 23 residues or greater are required to stimulate a high affinity class II-restricted T cell response. *European journal of immunology*, 23(5):1011–1016, may 1993.

[58] Rolf Konig, Li-yun Huang, and Ronald N Germain. MHC class II interaction with CD4 mediated by a region analogous to the MHC class I binding site for CD8. *Letters to Nature*, 356(April):796–798, 1992.

[59] Rishi Vishal Luckheeram, Rui Zhou, Asha Devi Verma, and Bing Xia. CD4 +T cells: Differentiation and Functions. *Clinical and Developmental Immunology*, 2012:12, 2012.

[60] X Tao, S Constant, P Jorritsma, and K Bottomly. Strength of TCR signal determines the costimulatory requirements for Th1 and Th2 CD4+ T cell differentiation. *Journal of immunology (Baltimore, Md. : 1950)*, 159(12):5956–5963, dec 1997.

[61] M L Blue, J F Daley, H Levine, and S F Schlossman. Coexpression of T4 and T8 on peripheral blood T cells demonstrated by two-color fluorescence flow cytometry. *Journal of immunology (Baltimore, Md. : 1950)*, 134(4):2281–2286, apr 1985.

[62] Luis J. Sigal and Kenneth L. Rock. Bone marrow-derived antigen-presenting cells are required for the generation of cytotoxic T lymphocyte responses to viruses and use transporter associated with antigen presentation (TAP)-dependent and -independent pathways of antigen presentation. *The Journal of experimental medicine*, 192(8):1143–1150, oct 2000.

[63] Luis J. Sigal, Shane Crotty, Raul Andino, and Kenneth L. Rock. Cytotoxic T-cell immunity to virus-infected non-haematopoietic cells requires presentation of exogenous antigen. *Nature 1999 402:6763*, 402(6763):25–29, dec 1999.

[64] Laurel L. Lenz, Eric A. Butz, and Michael J. Bevan. Requirements for bone marrow-derived antigen-presenting cells in priming cytotoxic T cell responses to intracellular pathogens. *The Journal of experimental medicine*, 192(8):1135–1142, oct 2000.

[65] Elodie Segura and Sebastian Amigorena. Cross-presentation by human dendritic cell subsets. *Immunology Letters*, 158(1-2):73–78, mar 2014.

[66] Olivier P. Joffre, Elodie Segura, Ariel Savina, and Sebastian Amigorena. Cross-presentation by dendritic cells. *Nature Reviews Immunology*, 12(8):557–569, aug 2012.

[67] Philippe Bousso. T-cell activation by dendritic cells in the lymph node: lessons from the movies. *Nature Reviews Immunology 2008 8:9*, 8(9):675–684, sep 2008.

[68] M K Jenkins, P S Taylor, S D Norton, and K B Urdahl. CD28 delivers a costimulatory signal involved in antigen-specific IL-2 production by human T cells. *Journal of Immunology*, 147(8), 1991.

[69] Seth Lederman, Michael J. Yellin, Alexander Krichevsky, John Belko, Julie J. Lee, and Leonard Chess. Identification of a novel surface protein on activated CD4 + T cells that induces contact-dependent B cell differentiation (Help). *Journal of Experimental Medicine*, 175(4):1091–1101, apr 1992.

[70] Denise Gay, Paul Maddon, Rafick Sekaly, Mary Anne Talle, Maurice Godfrey, Eric Long, Gideon Goldstein, Leonard Chess, Richard Axel, John Kappler, and Philippa Marrack. Functional interaction between human T-cell protein CD4 and the major histocompatibility complex HLA-DR antigen. *Nature*, 328(6131):626–629, 1988.

[71] Sheng Zhang, Hongjun Zhang, and Jiandong Zhao. The role of CD4 T cell help for CD8 CTL activation, jul 2009.

[72] Suzanne P.M. Welten, Cornelis J.M. Melief, and Ramon Arens. The distinct role of T cell costimulation in antiviral immunity. *Current opinion in virology*, 3(4):475–482, 2013.

[73] Priyanka A. Duttagupta, Alina C. Boesteanu, and Peter D. Katsikis. Costimulation signals for memory CD8+ T cells during viral infections. *Critical reviews in immunology*, 29(6):469–486, 2009.

[74] Heon Park, Zhaoxia Li, Xuexian O. Yang, Seon Hee Chang, Roza Nurieva, Yi Hong Wang, Ying Wang, Leroy Hood, Zhou Zhu, Qiang Tian, and Chen Dong. A distinct lineage of CD4 T cells regulates tissue inflammation by producing interleukin 17. *Nature Immunology*, 6(11):1133–1141, 2005.

[75] Matthias Wolfl, William Y Ho, Hieu Nguyen, Thomas J Manley, Marie Bleakley, Philip D Greenberg, and J Kuball. Activation-induced expression of CD137 permits detection, isolation, and expansion of the full repertoire of CD8+ T cells responding to antigen without requiring knowledge of epitope specificities. *Blood*, 110(0006-4971 (Print)):201–210, 2007.

[76] Michael P. Holt, George A. Punkosdy, Deborah D. Glass, and Ethan M. Shevach. TCR Signaling and CD28/CTLA-4 Signaling Cooperatively Modulate T Regulatory Cell Homeostasis. *The Journal of Immunology*, 198(4):1503–1511, 2017.

[77] Marine de Marcken, Khushwant Dhaliwal, Ann Caroline Danielsen, Anne Sophie Gautron, and Margarita Dominguez-Villar. TLR7 and TLR8 activate distinct pathways in monocytes during RNA virus infection. *Science Signaling*, 12(605):1347, oct 2019.

[78] Kiyoshi Hirahara and Toshinori Nakayama. CD4+ T-cell subsets in inflammatory diseases: Beyond the Th1/Th2 paradigm. *International Immunology*, 28(4):163–171, apr 2016.

[79] Andreas Hutloff, Anna M. Dittrich, Katja C. Beier, Barbara Eljaschewitsch, Regine Kraft, Ionnis Anagnostopoulos, and Richard A. Kroczek. ICOS is an inducible T-cell co-stimulator structurally and functionally related to CD28. *Nature*, 402(6763):21–24, dec 1999.

[80] Marion Pepper and Marc K. Jenkins. Origins of CD4+ effector and central memory T cells. *Nature Immunology*, 12(6):467–471, 2011.

[81] Nicholas P. Restifo and Luca Gattinoni. Lineage relationship of effector and memory T cells. *Current opinion in immunology*, 25(5):556–563, oct 2013.

[82] F Sallusto, D Lenig, R Förster, M Lipp, and A Lanzavecchia. Two subsets of memory T lymphocytes with distinct homing potentials and effector functions. *Nature*, 401(6754):708–712, oct 1999.

[83] F Sallusto, E Kremmer, B Palermo, A Hoy, P Ponath, S Qin, R Förster, M Lipp, and A Lanzavecchia. Switch in chemokine receptor expression upon TCR stimulation reveals novel homing potential for recently activated T cells. *European journal of immunology*, 29(6):2037–2045, jun 1999.

[84] Sasitorn Yenyuwadee, Jose Luis Sanchez-Trincado Lopez, Rushil Shah, Pamela C. Rosato, and Vassiliki A. Boussiotis. The evolving role of tissue-resident memory T cells in infections and cancer. *Science Advances*, 8(33):5871, aug 2022.

[85] Yutong Wang, Feng Qiu, Yifan Xu, Xiaorui Hou, Zhili Zhang, Lei Huang, Huijun Wang, Hui Xing, and Sha Wu. Stem cell-like memory T cells: The generation and application. *Journal of leukocyte biology*, 110(6):1209–1223, dec 2021.

[86] Susan L. Swain, K. Kai McKinstry, and Tara M. Strutt. Expanding roles for CD4+ T cells in immunity to viruses. *Nature Reviews Immunology 2012 12:2*, 12(2):136–148, jan 2012.

[87] Jean Paul Coutelier, Jos T.M. Van Der Logt, Frans W.A. Heessen, Guy Warnier, and Jacques Van Snick. IgG2a restriction of murine antibodies elicited by viral infections. *The Journal of experimental medicine*, 165(1):64–69, jan 1987.

[88] Jordy Saravia, Nicole M. Chapman, and Hongbo Chi. Helper T cell differentiation. *Cellular Molecular Immunology 2019 16:7*, 16(7):634–643, mar 2019.

[89] Yoshinori Shimamoto, Masaharu Miyahara, Hiroko Yamada, Keisuke Shibata, Miwako Matsuzaki, and Kazutoshi Ono. Adult T-cell leukaemia/lymphoma with multiple integrations of human T-cell lymphotropic virus type I proviral DNA: Differing clinical features are linked to varied proviral integration. *British Journal of Haematology*, 92(3):632–638, 1996.

[90] Jens Geginat, Moira Paroni, Stefano Maglie, Johanna Sophie Alfen, Ilko Kastirr, Paola Gruarin, Marco de Simone, Massimiliano Pagani, and Sergio Abrignani. Plasticity of human CD4 T cell subsets. *Frontiers in Immunology*, 5(DEC):630, dec 2014.

[91] Giorgio Trinchieri, Stefan Pflanz, and Robert A. Kastelein. The IL-12 family of heterodimeric cytokines: new players in the regulation of T cell responses. *Immunity*, 19(5):641–644, 2003.

[92] Geanncarlo Lugo-Villarino, Roberto Maldonado-López, Richard Possemato, Cristina Peñaranda, and Laurie H. Glimcher. T-bet is required for optimal production of IFN-gamma and antigen-specific T cell activation by dendritic cells. *Proceedings of the National Academy of Sciences of the United States of America*, 100(13):7749–7754, jun 2003.

[93] Maryam Afkarian, John R. Sedy, Jianfei Yang, Nils G. Jacobson, Nezih Cereb, Soo Y. Yang, Theresa L. Murphy, and Kenneth M. Murphy. T-bet is a STAT1-induced regulator of IL-12R expression in naïve CD4+ T cells. *Nature immunology*, 3(6):549–557, 2002.

[94] Vanja Lazarevic, Xi Chen, Jae Hyuck Shim, Eun Sook Hwang, Eunjung Jang, Alexandra N. Bolm, Mohamed Oukka, Vijay K. Kuchroo, and Laurie H. Glimcher. T-bet represses T(H)17 differentiation by preventing Runx1-mediated activation of the gene encoding RORγt. *Nature immunology*, 12(1):96–104, jan 2011.

[95] Eun Sook Hwang, Susanne J. Szabo, Pamela L. Schwartzberg, and Laurie H. Glimcher. T helper cell fate specified by kinase-mediated interaction of T-bet with GATA-3. *Science*, 307(5708):430–433, jan 2005.

[96] Ivana M. Djuretic, Ditsa Levanon, Varda Negreanu, Yoram Groner, Anjana Rao, and K. Mark Ansel. Transcription factors T-bet and Runx3 cooperate to activate Ifng and silence Il4 in T helper type 1 cells. *Nature immunology*, 8(2):145–153, feb 2007.

[97] G. Del Prete. Human Th1 and Th2 lymphocytes: their role in the pathophysiology of atopy. *Allergy*, 47(5):450–455, 1992.

[98] Flávia Castro, Ana Patrícia Cardoso, Raquel Madeira Gonçalves, Karine Serre, and Maria José Oliveira. Interferon-gamma at the crossroads of tumor immune surveillance or evasion. *Frontiers in Immunology*, 9(MAY):847, may 2018.

[99] Mallary C. Greenlee-Wacker and William M. Nauseef. IFN-γ targets macrophage-mediated immune responses toward Staphylococcus aureus . *Journal of Leukocyte Biology*, 101(3):751–758, mar 2017.

[100] R. B. Rock, S. Hu, A. Deshpande, S. Munir, B. J. May, C. A. Baker, P. K. Peterson, and V. Kapur. Transcriptional response of human microglial cells to interferon-γ. *Genes Immunity 2005 6:8*, 6(8):712–719, sep 2005.

[101] Kate Schroder, Paul J. Hertzog, Timothy Ravasi, and David A. Hume. Interferon-γ: an overview of signals, mechanisms and functions. *Journal of Leukocyte Biology*, 75(2):163–189, 2004.

[102] U. Boehm, T. Klamp, M. Groot, and J. C. Howard. Cellular responses to interferon-gamma. *Annual review of immunology*, 15:749–795, 1997.

[103] George D. Kalliolias and Lionel B. Ivashkiv. TNF biology, pathogenic mechanisms and emerging therapeutic strategies. *Nature reviews. Rheumatology*, 12(1):49, jan 2016.

[104] Javier Cote-Sierra, Gilles Foucras, Liying Guo, Lynda Chiodetti, Howard A. Young, Jane Hu-Li, Jinfang Zhu, and William E. Paul. Interleukin 2 plays a central role in Th2 differentiation. *Proceedings of the National Academy of Sciences of the United States of America*, 101(11):3880, mar 2004.

[105] Jinfang Zhu, Liying Guo, Cynthia J. Watson, Jane Hu-Li, and William E. Paul. Stat6 Is Necessary and Sufficient for IL-4's Role in Th2 Differentiation and Cell Expansion. *The Journal of Immunology*, 166(12):7276–7281, jun 2001.

[106] Jinfang Zhu, Hidehiro Yamane, Javier Cote-Sierra, Liying Guo, and William E. Paul. GATA-3 promotes Th2 responses through three different mechanisms: induction of Th2 cytokine production, selective growth of Th2 cells and inhibition of Th1 cell-specific factors. *Cell Research 2006 16:1*, 16(1):3–10, jan 2006.

[107] Jinfang Zhu. T helper 2 (Th2) cell differentiation, type 2 innate lymphoid cell (ILC2) development and regulation of interleukin-4 (IL-4) and IL-13 production. *Cytokine*, 75(1):14–24, sep 2015.

[108] Jinfang Zhu, Javier Cote-Sierra, Liying Guo, and William E. Paul. Stat5 Activation Plays a Critical Role in Th2 Differentiation. *Immunity*, 19(5):739–748, nov 2003.

[109] Valérie Staudt, Evita Bothur, Matthias Klein, Karen Lingnau, Sebastian Reuter, Nadine Grebe, Bastian Gerlitzki, Markus Hoffmann, Alexander Ulges, Christian Taube, Nina Dehzad, Marc Becker, Michael Stassen, Andrea Steinborn, Michael Lohoff, Hansjörg Schild, Edgar Schmitt, and Tobias Bopp. Interferon-regulatory factor 4 is essential for the developmental program of T helper 9 cells. *Immunity*, 33(2):192–202, aug 2010.

[110] Marc Veldhoen, Catherine Uyttenhove, Jacques van Snick, Helena Helmby, Astrid Westendorf, Jan Buer, Bruno Martin, Christoph Wilhelm, and Brigitta Stockinger. Transforming growth factor-beta 'reprograms' the differentiation of T helper 2 cells and promotes an interleukin 9-producing subset. *Nature immunology*, 9(12):1341–1346, 2008.

[111] Caroline L. Sokol, Ngoc Quynh Chu, Shuang Yu, Simone A. Nish, Terri M. Laufer, and Ruslan Medzhitov. Basophils function as antigen-presenting cells for

an allergen-induced T helper type 2 response. *Nature immunology*, 10(7):713–720, 2009.

[112] Choong Eun Lee, Suk Ran Yoon, and Kwang Ho Pyun. Interleukin-4 signals regulating CD23 gene expression in human B cells: protein kinase C-independent signaling pathways. *Cellular immunology*, 146(1):171–185, 1993.

[113] John W. Steinke and Lary Borish. Th2 cytokines and asthma. Interleukin-4: its role in the pathogenesis of asthma, and targeting it for asthma treatment with interleukin-4 receptor antagonists. *Respiratory research*, 2(2):66–70, 2001.

[114] Hano Toru, Chisei Ra, Shigeaki Nonoyama, Katsuhiro Suzuki, Jun Ichi Yata, and Tatsutoshi Nakahata. Induction of the high-affinity IgE receptor (Fc epsilon RI) on human mast cells by IL-4. *International immunology*, 8(9):1367–1373, 1996.

[115] Ramona Hurdayal and Frank Brombacher. The role of IL-4 and IL-13 in cutaneous Leishmaniasis. *Immunology letters*, 161(2):179–183, 2014.

[116] Fred D. Finkelman, Thomas A. Wynn, Debra D. Donaldson, and Joseph F. Urban. The role of IL-13 in helminth-induced inflammation and protective immunity against nematode infections. *Current opinion in immunology*, 11(4):420–426, 1999.

[117] Lei Jia and Changyou Wu. Differentiation, regulation and function of Th9 cells. *Advances in experimental medicine and biology*, 841:181–207, 2014.

[118] Paul R Mangan, Laurie E Harrington, Darrell B O'Quinn, Whitney S Helms, Daniel C Bullard, Charles O Elson, Robin D Hatton, Sharon M Wahl, Trenton R Schoeb, and Casey T Weaver. Transforming growth factor-beta induces development of the T(H)17 lineage. *Nature*, 441(7090):231–234, may 2006.

[119] Marc Veldhoen, Richard J Hocking, Christopher J Atkins, Richard M Locksley, and Brigitta Stockinger. TGFbeta in the context of an inflammatory cytokine milieu supports de novo differentiation of IL-17-producing T cells. *Immunity*, 24(2):179–189, feb 2006.

[120] Estelle Bettelli, Yijun Carrier, Wenda Gao, Thomas Korn, Terry B. Strom, Mohamed Oukka, Howard L. Weiner, and Vijay K. Kuchroo. Reciprocal developmental pathways for the generation of pathogenic effector TH17 and regulatory T cells. *Nature*, 441(7090):235–238, may 2006.

[121] Mandy J. McGeachy and Daniel J. Cua. Th17 Cell Differentiation: The Long and Winding Road. *Immunity*, 28(4):445–453, apr 2008.

[122] Priscilla W. Lee, Alan J. Smith, Yuhong Yang, Amanda J. Selhorst, Yue Liu, Michael K. Racke, and Amy E. Lovett-Racke. IL-23R–activated STAT3/STAT4 is essential for Th1/Th17-mediated CNS autoimmunity. *JCI Insight*, 2(17), sep 2017.

[123] Roza Nurieva, Xuexian O. Yang, Gustavo Martinez, Yongliang Zhang, Athanasia D. Panopoulos, Li Ma, Kimberly Schluns, Qiang Tian, Stephanie S. Watowich, Anton M. Jetten, and Chen Dong. Essential autocrine regulation by IL-21 in the generation of inflammatory T cells. *Nature*, 448(7152):480–483, jul 2007.

[124] Thomas Korn, Estelle Bettelli, Wenda Gao, Amit Awasthi, Anneli Jäger, Terry B. Strom, Mohamed Oukka, and Vijay K. Kuchroo. IL-21 initiates an alternative pathway to induce proinflammatory T(H)17 cells. *Nature*, 448(7152):484–487, jul 2007.

[125] Claire L. Langrish, Yi Chen, Wendy M. Blumenschein, Jeanine Mattson, Beth Basham, Jonathan D. Sedgwick, Terrill McClanahan, Robert A. Kastelein, and Daniel J. Cua. IL-23 drives a pathogenic T cell population that induces autoimmune inflammation. *The Journal of experimental medicine*, 201(2):233–240, jan 2005.

[126] Jelena Milovanovic, Aleksandar Arsenijevic, Bojana Stojanovic, Tatjana Kanjevac, Dragana Arsenijevic, Gordana Radosavljevic, Marija Milovanovic, and Nebojsa Arsenijevic. Interleukin-17 in Chronic Inflammatory Neurological Diseases. *Frontiers in Immunology*, 11:947, jun 2020.

[127] Petra Bacher, Thordis Hohnstein, Eva Beerbaum, Axel A Brakhage, Carsten Schwarz, and Alexander Scheffold. Human Anti-fungal Th17 Immunity and Pathology Rely on Cross-Reactivity against Candida albicans. *Cell*, 176:1340–1355.e15, 2019.

[128] Laura A. Tesmer, Steven K. Lundy, Sujata Sarkar, and David A. Fox. Th17 cells in human disease. *Immunological Reviews*, 223(1):87, jun 2008.

[129] Sarah L. Gaffen. Structure and signalling in the IL-17 receptor family. *Nature Reviews Immunology 2009 9:8*, 9(8):556–567, jul 2009.

[130] Warren J. Leonard and Rosanne Spolski. Interleukin-21: a modulator of lymphoid proliferation, apoptosis and differentiation. *Nature reviews. Immunology*, 5(9):688–698, sep 2005.

[131] Lauren A Zenewicz, George D Yancopoulos, David M Valenzuela, Andrew J Murphy, Margaret Karow, and Richard A Flavell. Interleukin-22 but not interleukin-17 provides protection to hepatocytes during acute liver inflammation. *Immunity*, 27(4):647–659, oct 2007.

[132] Shean J Aujla, Yvonne R Chan, Mingquan Zheng, Mingjian Fei, David J Askew, Derek A Pociask, Todd A Reinhart, Florencia McAllister, Jennifer Edeal, Kristi Gaus, Shahid Husain, James L Kreindler, Patricia J Dubin, Joseph M Pilewski, Mike M Myerburg, Carol A Mason, Yoichiro Iwakura, and Jay K Kolls. IL-22 mediates mucosal host defense against Gram-negative bacterial pneumonia. *Nature medicine*, 14(3):275–281, mar 2008.

[133] Qi Jiang, Guocan Yang, Fan Xiao, Jue Xie, Shengjun Wang, Liwei Lu, and Dawei Cui. Role of Th22 Cells in the Pathogenesis of Autoimmune Diseases. *Frontiers in Immunology*, 12(July):1–14, 2021.

[134] Shane Crotty. T follicular helper cell differentiation, function, and roles in disease. *Immunity*, 41(4):529, oct 2014.

[135] Amania A. Sheikh and Joanna R. Groom. Transcription tipping points for T follicular helper cell and T-helper 1 cell fate commitment. *Cellular Molecular Immunology 2020 18:3*, 18(3):528–538, sep 2020.

[136] Jinyong Choi, Huitian Diao, Caterina E Faliti, Jacquelyn Truong, Meghan Rossi, Simon Bélanger, Bingfei Yu, Ananda W Goldrath, Matthew E Pipkin, and Shane Crotty. Bcl-6 is the nexus transcription factor of T follicular helper cells via repressor-of-repressor circuits. *Nature Immunology*, 21(7):777–789, 2020.

[137] Raul Elgueta, Micah J. Benson, Victor C. De Vries, Anna Wasiuk, Yanxia Guo, and Randolph J. Noelle. Molecular mechanism and function of CD40/CD40L engagement in the immune system. *Immunological reviews*, 229(1):152–172, may 2009.

[138] Bernhard Moser. CXCR5, the Defining Marker for Follicular B Helper T (TFH) Cells. *Frontiers in Immunology*, 6(JUN), 2015.

[139] Roza I Nurieva and Yeonseok Chung. Understanding the development and function of T follicular helper cells. *Cellular Molecular Immunology*, 7(3):190–197, 2010.

[140] Maria Grazia Roncarolo, Silvia Gregori, Rosa Bacchetta, Manuela Battaglia, and Nicola Gagliani. The Biology of T Regulatory Type 1 Cells and Their Therapeutic Application in Immune-Mediated Diseases. *Immunity*, 49(6):1004–1019, 2018.

[141] Zhiyuan Li, Dan Li, Andy Tsun, and Bin Li. FOXP3+ regulatory T cells and their functional regulation. *Cellular and Molecular Immunology*, 12(5):558–565, 2015.

[142] Liang Zhou, Jared E. Lopes, Mark M.W. Chong, Ivaylo I. Ivanov, Roy Min, Gabriel D. Victora, Yuelei Shen, Jianguang Du, Yuri P. Rubtsov, Alexander Y. Rudensky, Steven F. Ziegler, and Dan R. Littman. TGF-β-induced Foxp3 inhibits Th17 cell differentiation by antagonizing RORγt function. *Nature*, 453(7192):236, may 2008.

[143] Ming O. Li, Yisong Y. Wan, and Richard A. Flavell. T cell-produced transforming growth factor-beta1 controls T cell tolerance and regulates Th1- and Th17-cell differentiation. *Immunity*, 26(5):579–591, may 2007.

[144] Wan Jun Chen, Wenwen Jin, Neil Hardegen, Ke Jian Lei, Li Li, Nancy Marinos, George McGrady, and Sharon M. Wahl. Conversion of peripheral CD4+CD25- naive T cells to CD4+CD25+ regulatory T cells by TGF-beta induction of transcription factor Foxp3. *The Journal of experimental medicine*, 198(12):1875–1886, dec 2003.

[145] Dario A.A. Vignali, Lauren W. Collison, and Creg J. Workman. How regulatory T cells work. *Nature Reviews Immunology 2008 8:7*, 8(7):523–532, jul 2008.

[146] Anne O'Garra, Pedro L. Vieira, Paulo Vieira, and Anne E. Goldfeld. IL-10–producing and naturally occurring CD4+ Tregs: limiting collateral damage. *Journal of Clinical Investigation*, 114(10):1372, nov 2004.

[147] Ashutosh Chaudhry, Robert M. Samstein, Piper Treuting, Yuqiong Liang, Marina C. Pils, Jan Michael Heinrich, Robert S. Jack, F. Thomas Wunderlich, Jens C. Brüning, Werner Müller, and Alexander Y. Rudensky. Interleukin-10 signaling in

regulatory T cells is required for suppression of Th17 cell-mediated inflammation. *Immunity*, 34(4):566, apr 2011.

[148] Angelika Schmidt, Nina Oberle, and Peter H. Krammer. Molecular mechanisms of Treg-mediatedt cell suppression. *Frontiers in Immunology*, 3(MAR):51, mar 2012.

[149] Luis J Sigal. Activation of CD8 T Lymphocytes during Viral Infections.

[150] David J. Zammit, Linda S. Cauley, Quynh Mai Pham, and Leo Lefrançois. Dendritic Cells Maximize the Memory CD8 T Cell Response to Infection. *Immunity*, 22(5):561, may 2005.

[151] Matthew F. Mackey, Richard J. Barth, and Randolph J. Noelle. The role of CD40/CD154 interactions in the priming, differentiation, and effector function of helper and cytotoxic T cells. *Journal of leukocyte biology*, 63(4):418–428, 1998.

[152] Daphne Y. Ma and Edward A. Clark. The role of CD40 and CD40L in Dendritic Cells. *Seminars in immunology*, 21(5):265, oct 2009.

[153] Pierre Golstein and Gillian M. Griffiths. An early history of T cell-mediated cytotoxicity. *Nature Reviews Immunology 2018 18:8*, 18(8):527–535, apr 2018.

[154] S. S. Metkar, M. Marchioretto, V. Antonini, L. Lunelli, B. Wang, R. Jc Gilbert, G. Anderluh, R. Roth, M. Pooga, J. Pardo, J. E. Heuser, M. D. Serra, and C. J. Froelich. Perforin oligomers form arcs in cellular membranes: A locus for intracellular delivery of granzymes. *Cell Death and Differentiation*, 22(1):74–85, 2015.

[155] Adam J. Caulfield and Wyndham W. Lathem. Disruption of Fas-Fas Ligand Signaling, Apoptosis, and Innate Immunity by Bacterial Pathogens. *PLOS Pathogens*, 10(8):e1004252, aug 2014.

[156] Moe Moe Aye, E. Matsuoka, T. Moritoyo, F. Umehara, M. Suehara, Y. Hokezu, H. Yamanaka, Y. Isashiki, M. Osame, and S. Izumo. Histopathological analysis of four autopsy cases of HTLV-I-associated myelopathy/tropical spastic paraparesis: inflammatory changes occur simultaneously in the entire central nervous system. *Acta Neuropathologica 2000 100:3*, 100(3):245–252, 2000.

[157] Shuji Izumo. Neuropathology of HTLV-1-associated myelopathy (HAM/TSP): The 50th Anniversary of Japanese Society of Neuropathology. *Neuropathology*, 30(5):480–485, oct 2010.

[158] Fujio Umehara, Shuji Izumo, Masanori Nakagawa, Alicia T. Ronquillo, Kouichi Takahashi, Kenji Matsumuro, Eiichi Sato, and Mitsuhiro Osame. Immunocytochemical analysis of the cellular infiltrate in the spinal cord lesions in HTLV-I-associated myelopathy. *Journal of Neuropathology and Experimental Neurology*, 52(4):424–430, 1993.

[159] Tim R. Mosmann, Li Li, and Subash Sad. Functions of CD8 T-cell subsets secreting different cytokine patterns. *Seminars in Immunology*, 9(2):87–92, 1997.

[160] Hans Willi Mittrücker, Alexander Visekruna, and Magdalena Huber. Heterogeneity in the Differentiation and Function of CD8+ T Cells. *Archivum Immunologiae et Therapiae Experimentalis*, 62(6):449–458, dec 2014.

[161] Eric S. Huseby, Priya G. Huseby, Shivanee Shah, Rebecca Smith, and Brian D. Stadinski. Pathogenic CD8T cells in multiple sclerosis and its experimental models. *Frontiers in Immunology*, 3(MAR):1–9, 2012.

[162] Nana H. Overgaard, Ji-Won Jung, Raymond J. Steptoe, and James W. Wells. CD4 + /CD8 + double-positive T cells: more than just a developmental stage? . *Journal of Leukocyte Biology*, 97(1):31–38, jan 2015.

[163] P. Sala, E. Tonutti, C. Feruglio, F. Florian, and A. Colombatti. Persistent Expansions of CD4+ CD8+ Peripheral Blood T Cells. *Blood*, 82(5):1546–1552, sep 1993.

[164] Ludger Klein, Bruno Kyewski, Paul M. Allen, and Kristin A. Hogquist. Positive and negative selection of the T cell repertoire: what thymocytes see (and don't see). *Nature Reviews Immunology 2014 14:6*, 14(6):377–391, may 2014.

[165] Yann Parel and Carlo Chizzolini. CD4+ CD8+ double positive (DP) T cells in health and disease, mar 2004.

[166] Frederick E Munschauer, Carleton Stewart, Lawrence Jacobs, Samer Kaba, Zahra Ghorishi, Steven J Greenberg, and Diane Cookfair. Circulating CD3 + CD4 + CD8 + T Lymphocytes in Multiple Sclerosis. *Journal of Clinical Immunology*, 13(2), 1993.

[167] S Berrih, C Gaud, M A Bach, H Le Brigand, J P Binet, and J F Bach. Evaluation of T cell subsets in myasthenia gravis using anti-T cell monoclonal antibodies. *Clinical and experimental immunology*, 45(1):1–8, jul 1981.

[168] C Ortolani, E Forti, E Radin, R Cibin, and A Cossarizza. Cytofluorimetric identification of two populations of double positive (CD4+,CD8+) T lymphocytes in human peripheral blood. *Biochemical and biophysical research communications*, 191(2):601–609, mar 1993.

[169] L Weiss, A Roux, S Garcia, C Demouchy, N Haeffner-Cavaillon, M D Kazatchkine, and M L Gougeon. Persistent expansion, in a human immunodeficiency virus-infected person, of V beta-restricted CD4+CD8+ T lymphocytes that express cytotoxicity-associated molecules and are committed to produce interferon-gamma and tumor necrosis factor-alpha. *The Journal of infectious diseases*, 178(4):1158–1162, oct 1998.

[170] Nascimbeni M, Pol S, and Saunier B. Distinct CD4+ CD8+ double-positive T cells in the blood and liver of patients during chronic hepatitis B and C. *PloS one*, 6(5), 2011.

[171] Quandt Dagmar, Rothe Kathrin, Scholz Roger, Baerwald Christoph W, and Wagner Ulf. Peripheral CD4CD8 Double Positive T Cells with a Distinct Helper Cytokine Profile are Increased in Rheumatoid Arthritis. *PloS one*, 9(3), mar 2014.

[172] Scott G. Kitchen, Nicole R. Jones, Stuart LaForge, Jason K. Whitmire, Bien Aimee Vu, Zoran Galic, David G. Brooks, Stephen J. Brown, Christina M.R. Kitchen, and Jerome A. Zack. CD4 on CD8+ T cells directly enhances effector function and is a target for HIV infection. *Proceedings of the National Academy of Sciences of the United States of America*, 101(23):8727–8732, jun 2004.

[173] Scott G Kitchen, Jason K Whitmire, Nicole R Jones, Zoran Galic, Christina M R Kitchen, Rafi Ahmed, and Jerome A Zack. The CD4 molecule on CD8+ T lymphocytes directly enhances the immune response to viral and cellular antigens. *Proceedings of the National Academy of Sciences of the United States of America*, 102(10):3794–3799, mar 2005.

[174] Guillaume Sarrabayrouse, Murielle Corvaisier, Laure-Hélène Ouisse, Céline Bossard, Bernard Le Mével, Lucien Potiron, Guillaume Meurette, Nadine Gervois, and Francine Jotereau. Tumor-reactive CD4+ CD8$\alpha\beta$+ CD103+ $\alpha\beta$T cells: a prevalent tumor-reactive T-cell subset in metastatic colorectal cancers. *International journal of cancer*, 128(12):2923–2932, jun 2011.

[175] Juliette Desfrançois, Agnès Moreau-Aubry, Virginie Vignard, Yann Godet, Amir Khammari, Brigitte Dréno, Francine Jotereau, and Nadine Gervois. Double positive CD4CD8 alphabeta T cells: a new tumor-reactive population in human melanomas. *PloS one*, 5(1):e8437, jan 2010.

[176] M Bagot, H Echchakir, F Mami-Chouaib, M H Delfau-Larue, D Charue, A Bernheim, S Chouaib, L Boumsell, and A Bensussan. Isolation of tumor-specific cytotoxic CD4+ and CD4+CD8dim+ T-cell clones infiltrating a cutaneous T-cell lymphoma. *Blood*, 91(11):4331–4341, jun 1998.

[177] Perrine Bohner, Mathieu F. Chevalier, Valérie Cesson, Sonia Christina Rodrigues-Dias, Florence Dartiguenave, Rodolfo Burruni, Thomas Tawadros, Massimo Valerio, Ilaria Lucca, Denise Nardelli-Haefliger, Patrice Jichlinski, and Laurent Derré. Double positive CD4+CD8+ T cells are enriched in urological cancers and favor T helper-2 polarization. *Frontiers in Immunology*, 10(MAR):622, mar 2019.

[178] Guillaume Sarrabayrouse, Céline Bossard, Joe Marc Chauvin, Anne Jarry, Guillaume Meurette, Elodie Quévrain, Chantal Bridonneau, Laurence Preisser, Karim Asehnoune, Nathalie Labarrière, Frédéric Altare, Harry Sokol, and Francine Jotereau. CD4CD8$\alpha\alpha$ Lymphocytes, A Novel Human Regulatory T Cell Subset Induced by Colonic Bacteria and Deficient in Patients with Inflammatory Bowel Disease. *PLoS Biology*, 12(4):e1001833, 2014.

[179] Marc A. Frahm, Ralph A. Picking, JoAnn D. Kuruc, Kara S. McGee, Cynthia L. Gay, Joseph J. Eron, Charles B. Hicks, Georgia D. Tomaras, and Guido Ferrari. CD4+CD8+ T-cells Represent a Significant Portion of the Anti-HIV T-cell Response to Acute HIV Infection. *Journal of immunology (Baltimore, Md. : 1950)*, 188(9):4289, may 2012.

[180] Maria A. Suni, Smita A. Ghanekar, David W. Houck, Holden T. Maecker, Susan B. Wormsley, Louis J. Picker, Ronald B. Moss, and Vernon C. Maino. CD4+CD8dim T lymphocytes exhibit enhanced cytokine expression, proliferation and cytotoxic

activity in response to HCMV and HIV-1 antigens. *European Journal of Immunology*, 31(8):2512–2520, 2001.

[181] Esther Dawen Yu, Hao Wang, Ricardo da Silva Antunes, Yuan Tian, Rashmi Tippalagama, Shakila U. Alahakoon, Gayani Premawansa, Ananda Wijewickrama, Sunil Premawansa, Aruna Dharshan De Silva, April Frazier, Alba Grifoni, Alessandro Sette, and Daniela Weiskopf. A Population of CD4+CD8+ Double-Positive T Cells Associated with Risk of Plasma Leakage in Dengue Viral Infection. *Viruses 2022, Vol. 14, Page 90*, 14(1):90, jan 2022.

[182] Gobardhan Das, Mathew M. Augustine, Jyoti Das, Kim Bottomly, Prabir Ray, and Anuradha Ray. An important regulatory role for CD4+CD8$\alpha\alpha$ T cells in the intestinal epithelial layer in the prevention of inflammatory bowel disease. *Proceedings of the National Academy of Sciences of the United States of America*, 100(9):5324–5329, apr 2003.

[183] Yann Parel, Michel Aurrand-Lions, Agneta Scheja, Jean Michel Dayer, Eddy Roosnek, and Carlo Chizzolini. Presence of CD4+CD8+ double-positive T cells with very high interleukin-4 production potential in lesional skin of patients with systemic sclerosis. *Arthritis and Rheumatism*, 56(10):3459–3467, oct 2007.

[184] Waschbisch A, Sammet L, Schröder S, Lee DH, Barrantes-Freer A, Stadelmann C, and Linker RA. Analysis of CD4+ CD8+ double-positive T cells in blood, cerebrospinal fluid and multiple sclerosis lesions. *Clinical and Experimental Immunology*, 177(2):404–411, 2014.

[185] Tom Cupedo, Maho Nagasawa, Kees Weijer, Bianca Blom, and Hergen Spits. Development and activation of regulatory Tcells in the human fetus. *European Journal of Immunology*, 35(2):383–390, feb 2005.

[186] Mohamed A. ElTanbouly and Randolph J. Noelle. Rethinking peripheral T cell tolerance: checkpoints across a T cell's journey. *Nature Reviews Immunology*, 21(4):257–267, 2021.

[187] Rong Fu Wang. CD8+ regulatory T cells, their suppressive mechanisms, and regulation in cancer. *Human Immunology*, 69(11):811–814, nov 2008.

[188] Maria K. Smatti, Farhan S. Cyprian, Gheyath K. Nasrallah, Asmaa A. Al Thani, Ruba O. Almishal, and Hadi M. Yassine. Viruses and Autoimmunity: A Review on the Potential Interaction and Molecular Mechanisms. *Viruses*, 11(8):1–18, 2019.

[189] Antoine Gessain and Olivier Cassar. Epidemiological aspects and world distribution of HTLV-1 infection. *Frontiers in Microbiology*, 3(NOV), 2012.

[190] Fernando A. Proietti, Anna Bárbara F. Carneiro-Proietti, Bernadette C. Catalan-Soares, and Edward L. Murphy. Global epidemiology of HTLV-I infection and associated diseases. *Oncogene*, 24(39):6058–6068, sep 2005.

[191] Carolina Alvarez, Eduardo Gotuzzo, Anne Mieke Vandamme, and Kristien Verdonck. Family aggregation of human T-lymphotropic virus 1-associated diseases: A systematic review. *Frontiers in Microbiology*, 7(OCT):1674, oct 2016.

[192] Masako Iwanaga, Toshiki Watanabe, Atae Utsunomiya, Akihiko Okayama, Kaoru Uchimaru, Ki Ryang Koh, Masao Ogata, Hiroshi Kikuchi, Yasuko Sagara, Kimiharu Uozumi, Manabu Mochizuki, Kunihiro Tsukasaki, Yoshio Saburi, Masaomi Yamamura, Junji Tanaka, Yukiyoshi Moriuchi, Shigeo Hino, Shimeru Kamihira, and Kazunari Yamaguchi. Human T-cell leukemia virus type I (HTLV-1) proviral load and disease progression in asymptomatic HTLV-1 carriers: a nationwide prospective study in Japan. *Blood*, 116(8):1211–1219, aug 2010.

[193] Charles R M Bangham. Human T Cell Leukemia Virus Type 1: Persistence and Pathogenesis. *Annual Review of Immunology*, (36:43–71), 2018.

[194] Mohamed Nejmeddine and Charles R M Bangham. The HTLV-1 Virological Synapse. *Viruses*, 2:1427–1447, 2010.

[195] Kathryn S. Jones, Cari Petrow-Sadowski, Ying K. Huang, Daniel C. Bertolette, and Francis W. Ruscetti. Cell-free HTLV-1 infects dendritic cells leading to transmission and transformation of CD4+ T cells. *Nature Medicine*, 14(4):429–436, 2008.

[196] Anat Melamed, Daniel J. Laydon, Hebah Al Khatib, Aileen G. Rowan, Graham P. Taylor, and Charles R.M. Bangham. HTLV-1 drives vigorous clonal expansion of infected CD8+ T cells in natural infection. *Retrovirology*, 12(1):1–10, nov 2015.

[197] Maria A Demontis, Silva Hilburn, and Graham P Taylor. Human T cell lymphotropic virus type 1 viral load variability and long-term trends in asymptomatic carriers and in patients with human T cell lymphotropic virus type 1-related diseases. *AIDS research and human retroviruses*, 29(2):359–364, feb 2013.

[198] Abelardo Araujo, Charles R M Bangham, Jorge Casseb, Eduardo Gotuzzo, Steve Jacobson, Fabiola Martin, Augusto Penalva De Oliveira, Marzia Puccioni-Sohler, Graham P Taylor, and Yoshihisa Yamano. Management of HAM/TSP Systematic Review and Consensus-based Recommendations 2019. 11(1):49–56, 2021.

[199] David R. Collins, Gaurav D. Gaiha, and Bruce D. Walker. CD8+ T cells in HIV control, cure and prevention. *Nature Reviews Immunology*, 20(8):471–482, 2020.

[200] Nicolas A Gillet, Nirav Malani, Anat Melamed, Niall Gormley, Richard Carter, David Bentley, Charles Berry, Frederic D Bushman, Graham P Taylor, and Charles R M Bangham. The host genomic environment of the provirus determines the abundance of HTLV-1-infected T-cell clones. 2011.

[201] Svetlana Kalinichenko, Dmitriy Komkov, and Dmitriy Mazurov. HIV-1 and HTLV-1 Transmission Modes: Mechanisms and Importance for Virus Spread. *Viruses*, 14(1), jan 2022.

[202] M Yoshida. Multiple viral strategies of HTLV-1 for dysregulation of cell growth control. *Annual review of immunology*, 19:475–496, 2001.

[203] Anders Vahlne. A historical reflection on the discovery of human retroviruses. *Retrovirology*, 6(1):1–9, may 2009.

[204] Masako Iwanaga, Toshiki Watanabe, Atae Utsunomiya, Akihiko Okayama, Kaoru Uchimaru, Ki Ryang Koh, Masao Ogata, Hiroshi Kikuchi, Yasuko Sagara, Kimiharu Uozumi, Manabu Mochizuki, Kunihiro Tsukasaki, Yoshio Saburi, Masaomi Yamamura, Junji Tanaka, Yukiyoshi Moriuchi, Shigeo Hino, Shimeru Kamihira, and Kazunari Yamaguchi. Human T-cell leukemia virus type I (HTLV-1) proviral load and disease progression in asymptomatic HTLV-1 carriers: a nationwide prospective study in Japan. *Blood*, 116(8):1211–1219, aug 2010.

[205] M. Fujii, K. Iwai, M. Oie, M. Fukushi, N. Yamamoto, M. Kannagi, and N. Mori. Activation of Oncogenic Transcription Factor AP-1 in T Cells Infected with Human T Cell Leukemia Virus Type 1. *AIDS Research and Human Retroviruses*, 16(16):1603–1606, jul 2004.

[206] Aris E.N. Aristodemou, David S. Rueda, Graham P. Taylor, and Charles R.M. Bangham. *The transcriptome of HTLV-1-infected primary cells following reactivation reveals changes to host gene expression central to the proviral life cycle*, volume 19. 2023.

[207] M. Matsuoka and K. T. Jeang. Human T-cell leukemia virus type 1 (HTLV-1) and leukemic transformation: Viral infectivity, Tax, HBZ and therapy. *Oncogene*, 30(12):1379–1389, 2011.

[208] Martin R. Billman, David Rueda, and Charles R.M. Bangham. Single-cell heterogeneity and cell-cycle-related viral gene bursts in the human leukaemia virus HTLV-1 [version 2; referees: 2 approved, 1 approved with reservations]. *Wellcome Open Research*, 2:1–29, 2017.

[209] Helen Kiik, Saumya Ramanayake, Michi Miura, Yuetsu Tanaka, Anat Melamed, and Charles R.M. Bangham. Time-course of host cell transcription during the HTLV-1 transcriptional burst. *PLoS Pathogens*, 18(5):1–27, 2022.

[210] Joshua Arnold, Brenda Yamamoto, Min Li, Andrew J. Phipps, Ihab Younis, Michael D. Lairmore, and Patrick L. Green. Enhancement of infectivity and persistence in vivo by HBZ, a natural antisense coded protein of HTLV-1. *Blood*, 107(10):3976–3982, 2006.

[211] Anne Sophie Kuhlmann, Julien Villaudy, Louis Gazzolo, Marc Castellazzi, Jean Michel Mesnard, and Madeleine Duc Dodon. HTLV-1 HBZ cooperates with JunD to enhance transcription of the human telomerase reverse transcriptase gene (hTERT). *Retrovirology*, 4(92), 2007.

[212] Charles R.M. Bangham, Abelardo Araujo, Yoshihisa Yamano, and Graham P. Taylor. HTLV-1-associated myelopathy/tropical spastic paraparesis. *Nature Reviews*, 1, jun 2015.

[213] Graham P. Taylor and Masao Matsuoka. Natural history of adult T-cell leukemia/lymphoma and approaches to therapy. *Oncogene 2005 24:39*, 24(39):6047–6057, sep 2005.

[214] Abelardo Q-C Araujo. Neurologic complications of HTLV-1: a review. *Revista Brasileira de Neurologia*, 55(2).

[215] Gill Schierhout, Skye McGregor, Antoine Gessain, Lloyd Einsiedel, Marianne Martinello, and John Kaldor. Association between HTLV-1 infection and adverse health outcomes: a systematic review and meta-analysis of epidemiological studies. *The Lancet Infectious Diseases*, 20(1):133–143, jan 2020.

[216] F Komurian, F Pelloquin, and G de Thé. In vivo genomic variability of human T-cell leukemia virus type I depends more upon geography than upon pathologies. *Journal of virology*, 65(7):3770–3778, jul 1991.

[217] Charles R.M. Bangham. Human T-cell leukaemia virus type I and neurological disease. *Current opinion in neurobiology*, 3(5):773–778, 1993.

[218] M. Shimoyama. Diagnostic criteria and classification of clinical subtypes of adult T-cell leukaemia-lymphoma. *British Journal of Haematology*, 79(3):428–437, nov 1991.

[219] Maria A Demontis, Silva Hilburn, and Graham P Taylor. Human T Cell Lymphotropic Virus Type 1 Viral Load Variability and Long-Term Trends in Asymptomatic Carriers and in Patients with Human T Cell Lymphotropic Virus Type 1-Related Diseases. *AIDS Research and Human Retroviruses*, 29(2):359–364, aug 2012.

[220] Lies Boelen, Bisrat Debebe, Marcos Silveira, Arafa Salam, Julia Makinde, Chrissy H. Roberts, Eddie C.Y. Wang, John Frater, Jill Gilmour, Katie Twigger, Kristin Ladell, Kelly L. Miners, Jyothi Jayaraman, James A. Traherne, David A. Price, Ying Qi, Maureen P. Martin, Derek C. Macallan, Chloe L. Thio, Jacquie Astemborski, Gregory Kirk, Sharyne M. Donfield, Susan Buchbinder, Salim I. Khakoo, James J. Goedert, John Trowsdale, Mary Carrington, Simon Kollnberger, and Becca Asquith. Inhibitory killer cell immunoglobulin-like receptors strengthen CD8+ T cell–mediated control of HIV-1, HCV, and HTLV-1. *Science Immunology*, 3(29):2892, nov 2018.

[221] Charles R.M. Bangham and Lee Ratner. How does HTLV-1 cause adult T-cell leukaemia/lymphoma (ATL)? *Current Opinion in Virology*, 14:93–100, 2015.

[222] Yu Mitagami, Jun ichirou Yasunaga, Haruka Kinosada, Koichi Ohshima, and Masao Matsuoka. Interferon-γ Promotes Inflammation and Development of T-Cell Lymphoma in HTLV-1 bZIP Factor Transgenic Mice. *PLOS Pathogens*, 11(8):e1005120, aug 2015.

[223] Jean Michel Mesnard, Benoit Barbeau, Raymond Césaire, and Jean Marie Péloponèse. Roles of HTLV-1 basic Zip Factor (HBZ) in Viral Chronicity and Leukemic Transformation. Potential New Therapeutic Approaches to Prevent and Treat HTLV-1-Related Diseases. *Viruses*, 7(12):6490, dec 2015.

[224] Céline Vernin, Morgan Thenoz, Christiane Pinatel, Antoine Gessain, Olivier Gout, Marie Hélène Delfau-Larue, Nicolas Nazaret, Catherine Legras-Lachuer, Eric Wattel, and Franck Mortreux. HTLV-1 bZIP factor HBZ promotes cell proliferation and genetic instability by activating oncomiRs. *Cancer Research*, 74(21):6082–6093, nov 2014.

[225] S Takemoto, M Matsuoka, K Yamaguchi, and K Takatsuki. A Novel Diagnostic Method of Adult T-Cell Leukemia: Monoclonal Integration of Human T-Cell Lymphotropic Virus Type I Provirus DNA Detected by Inverse Polymerase Chain Reaction. *Blood*, 84(9):3080–3085, nov 1994.

[226] World Health Organization. WHO diagnostic guidlines of HAM. *Weekly Epidemiological Rec*, 49:382–383, 1989.

[227] Abelardo Araujo, Charles R.M. Bangham, Jorge Casseb, Eduardo Gotuzzo, Steve Jacobson, Fabiola Martin, Augusto Penalva de Oliveira, Marzia Puccioni-Sohler, Graham P. Taylor, and Yoshihisa Yamano. Management of HAM/TSP. *Neurology: Clinical Practice*, 0:10.1212/CPJ.0000000000000832, 2020.

[228] Stéphane Olindo, Philippe Cabre, Agnes Lézin, Harold Merle, Martine Saint-Vil, Aissatou Signate, Mickael Bonnan, Aurelie Chalon, Lionel Magnani, Raymond Cesaire, and Didier Smadja. Natural history of human T-lymphotropic virus 1-associated myelopathy: a 14-year follow-up study. *Archives of neurology*, 63(11):1560–1566, nov 2006.

[229] Fabiola Martin, Alexandra Fedina, Silva Youshya, and Graham P Taylor. A 15-year prospective longitudinal study of disease progression in patients with HTLV-1 associated myelopathy in the UK. *Journal of neurology, neurosurgery, and psychiatry*, 81(12):1336–1340, dec 2010.

[230] Stéphane Olindo, Philippe Cabre, Agnes Lézin, Harold Merle, Martine Saint-Vil, Aissatou Signate, Mickael Bonnan, Aurelie Chalon, Lionel Magnani, Raymond Cesaire, and Didier Smadja. Natural History of Human T-Lymphotropic Virus 1–Associated Myelopathy: A 14-Year Follow-up Study. *Archives of Neurology*, 63(11):1560–1566, nov 2006.

[231] E M Maloney, F R Cleghorn, O S Morgan, P Rodgers-Johnson, B Cranston, N Jack, W A Blattner, C Bartholomew, and A Manns. Incidence of HTLV-I-associated myelopathy/tropical spastic paraparesis (HAM/TSP) in Jamaica and Trinidad. *Journal of acquired immune deficiency syndromes and human retrovirology : official publication of the International Retrovirology Association*, 17(2):167–170, feb 1998.

[232] M A S D Lima, R B S Bica, and A Q C Araújo. Gender influence on the progression of HTLV-I associated myelopathy/tropical spastic paraparesis., feb 2005.

[233] Carlos Toro, Berta Rodés, Eva Poveda, and Vincent Soriano. Rapid development of subacute myelopathy in three organ transplant recipients after transmission of human T-cell lymphotropic virus type I from a single donor. *Transplantation*, 75(1):102–104, jan 2003.

[234] M Osame, R Janssen, H Kubota, H Nishitani, A Igata, S Nagataki, M Mori, I Goto, H Shimabukuro, and R Khabbaz. Nationwide survey of HTLV-I-associated myelopathy in Japan: association with blood transfusion. *Annals of neurology*, 28(1):50–56, jul 1990.

[235] J E Kaplan, M Osame, H Kubota, A Igata, H Nishitani, Y Maeda, R F Khabbaz, and R S Janssen. The risk of development of HTLV-I-associated myelopathy/tropical spastic paraparesis among persons infected with HTLV-I. *Journal of acquired immune deficiency syndromes*, 3(11):1096–1101, 1990.

[236] Edward L. Murphy, J. Fridey, J. W. Smith, J. Engstrom, R. A. Sacher, K. Miller, J. Gibble, J. Stevens, R. Thomson, D. Hansma, J. Kaplan, R. Khabbaz, and G. Nemo. HTLV-associated myelopathy in a cohort of HTLV-I and HTLV-II blood donors. *Neurology*, 48(2):315–320, feb 1997.

[237] J R Orland, J Engstrom, J Fridey, R A Sacher, J W Smith, C Nass, G Garratty, B Newman, D Smith, B Wang, K Loughlin, and E L Murphy. Prevalence and clinical features of HTLV neurologic disease in the HTLV Outcomes Study. *Neurology*, 61(11):1588–1594, dec 2003.

[238] Stéphane Olindo, Agnès Lézin, Philippe Cabre, Harold Merle, Martine Saint-Vil, Mireille Edimonana Kaptue, Aïssatou Signate, Raymond Césaire, and Didier Smadja. HTLV-1 proviral load in peripheral blood mononuclear cells quantified in 100 HAM/TSP patients: a marker of disease progression. *Journal of the neurological sciences*, 237(1-2):53–59, oct 2005.

[239] M Nagai, K Usuku, W Matsumoto, D Kodama, N Takenouchi, T Moritoyo, S Hashiguchi, M Ichinose, C R Bangham, S Izumo, and M Osame. Analysis of HTLV-I proviral load in 202 HAM/TSP patients and 243 asymptomatic HTLV-I carriers: high proviral load strongly predisposes to HAM/TSP. *Journal of neurovirology*, 4(6):586–593, dec 1998.

[240] Alison M Vine, Aviva D Witkover, Alun L Lloyd, Katie J M Jeffery, Asna Siddiqui, Sara E F Marshall, Mike Bunce, Nobutaka Eiraku, Shuji Izumo, Koichiro Usuku, Mitsuhiro Osame, and Charles R M Bangham. Polygenic control of human T lymphotropic virus type I (HTLV-I) provirus load and the risk of HTLV-I-associated myelopathy/tropical spastic paraparesis. *The Journal of infectious diseases*, 186(7):932–939, oct 2002.

[241] Charles R M Bangham, Lucy B Cook, and Anat Melamed. HTLV-1 clonality in adult T-cell leukaemia and non-malignant HTLV-1 infection. *Seminars in cancer biology*, 26:89–98, jun 2014.

[242] Charles R.M. Bangham. CTL quality and the control of human retroviral infections. *European Journal of Immunology*, 39(7):1700–1712, 2009.

[243] Katie J.M. Jeffery, Koichiro Usuku, Sarah E. Hall, Wataru Matsumoto, Graham P. Taylor, Jeanette Procter, Mike Bunce, Graham S. Ogg, Kenneth I. Welsh, Jonathan N. Weber, Alun L. Lloyd, Martin A. Nowak, Masahiro Nagai, Daisuke Kodama, Shuji Izumo, Mitsuhiro Osame, and Charles R.M. Bangham. HLA alleles determine human T-lymphotropic virus-I (HTLV-I) proviral load and the risk of HTLV-I-associated myelopathy. *Proceedings of the National Academy of Sciences of the United States of America*, 96(7):3848–3853, 1999.

[244] Daniel Harding, Carolina Rosadas, Sandra Maria Tsoti, Amanda Heslegrave, Molly Stewart, Peter Kelleher, Henrik Zetterberg, Graham P. Taylor, and Divya Dhasmana. Refining the risk of HTLV-1-associated myelopathy in people living with HTLV-1: identification of a HAM-like phenotype in a proportion of asymptomatic carriers. *Journal of NeuroVirology*, 28(4-6):473–482, 2022.

[245] K J Jeffery, A A Siddiqui, M Bunce, A L Lloyd, A M Vine, A D Witkover, S Izumo, K Usuku, K I Welsh, M Osame, and C R Bangham. The influence of HLA class I alleles and heterozygosity on the outcome of human T cell lymphotropic virus type I infection. *Journal of immunology (Baltimore, Md. : 1950)*, 165(12):7278–7284, dec 2000.

[246] B C Catalan-Soares, Anna Bárbara F Carneiro-Proietti, F G Da Fonseca, R Correa-Oliveira, D Peralva-Lima, R Portela, J G Ribas, D U Gonçalves, and F A Proietti. HLA class I alleles in HTLV-1-associated myelopathy and asymptomatic carriers from the Brazilian cohort GIPH. *Medical microbiology and immunology*, 198(1):1–3, feb 2009.

[247] Michael Talledo, Giovanni López, Jeroen R Huyghe, Kristien Verdonck, Vanessa Adaui, Elsa González, Iván Best, Daniel Clark, Guido Vanham, Eduardo Gotuzzo, Guy Van Camp, and Lut Van Laer. Evaluation of host genetic and viral factors as surrogate markers for HTLV-1-associated myelopathy/tropical spastic paraparesis in Peruvian HTLV-1-infected patients. *Journal of medical virology*, 82(3):460–466, mar 2010.

[248] Romain Deschamps, Odile Béra, Gilda Belrose, Agnès Lezin, Rémi Bellance, Aissatou Signate, Philippe Cabre, Didier Smadja, Raymond Césaire, and Stephane Olindo. Absence of consistent association between human leukocyte antigen-I and -II alleles and human T-lymphotropic virus type 1 (HTLV-1)-associated myelopathy/tropical spastic paraparesis risk in an HTLV-1 French Afro-Caribbean population. *International journal of infectious diseases : IJID : official publication of the International Society for Infectious Diseases*, 14(11):e986–90, nov 2010.

[249] Ana Treviño, Jose L Vicario, Mariola Lopez, Patricia Parra, Rafael Benito, Raul Ortiz de Lejarazu, Jose M Ramos, Jorge Del Romero, Carmen de Mendoza, and Vincent Soriano. Association between HLA alleles and HAM/TSP in individuals infected with HTLV-1. *Journal of neurology*, 260(10):2551–2555, oct 2013.

[250] Sandra Rocha Gadelha, Luiz Carlos Junior Alcântara, Gisele Calazans Costa, Angelina Xavier Acosta, Domingos Rios, Simone Kashima, Dimas Tadeu Covas, and Bernardo Galvão-Castro. Correlation between polymorphisms at interleukin-6 but not at interleukin-10 promoter and the risk of human T lymphotropic virus type I-associated myelopathy/tropical spastic paraparesis in Brazilian individuals. *Journal of medical virology*, 80(12):2141–2146, dec 2008.

[251] Satoshi Nozuma, Eiji Matsuura, Toshio Matsuzaki, Osamu Watanabe, Ryuji Kubota, Shuji Izumo, and Hiroshi Takashima. Familial clusters of HTLV-1-associated myelopathy/tropical spastic paraparesis. *PloS one*, 9(5):e86144, 2014.

[252] Yuzo Iwasaki. Human T cell Leukemia Virus Type I Infection and Chronic Myelopathy, 1993.

[253] W F Hickey, B L Hsu, and H Kimura. T-lymphocyte entry into the central nervous system. *Journal of neuroscience research*, 28(2):254–260, feb 1991.

[254] Joan Goverman. Autoimmune T cell responses in the central nervous system. *Nature reviews. Immunology*, 9(6):393, jun 2009.

[255] Melanie Laschinger, Peter Vajkoczy, and Britta Engelhardt. Encephalitogenic T cells use LFA-1 for transendothelial migration but not during capture and initial adhesion strengthening in healthy spinal cord microvessels in vivo. 2002.

[256] P. Vajkoczy, M. Laschinger, and B. Engelhardt. α4-integrin-VCAM-1 binding mediates G protein–independent capture of encephalitogenic T cell blasts to CNS white matter microvessels. *Journal of Clinical Investigation*, 108(4):557, aug 2001.

[257] Shalina S. Ousman and Paul Kubes. Immune surveillance in the central nervous system. *Nature Neuroscience 2012 15:8*, 15(8):1096–1101, jul 2012.

[258] Richard M. Ransohoff, Pia Kivisäkk, and Grahame Kidd. Three or more routes for leukocyte migration into the central nervous system. *Nature reviews. Immunology*, 3(7):569–581, jul 2003.

[259] Y. Iwasaki, Y. Ohara, I. Kobayashi, and S. I. Akizuki. Infiltration of helper/inducer T lymphocytes heralds central nervous system damage in human T-cell leukemia virus infection. *American Journal of Pathology*, 140(5):1003–1008, 1992.

[260] S Izumo, T Ijichi, I Higuchi, A Tashiro, K Takahashi, and M Osame. Neuropathology of HTLV-I-associated myelopathy–a report of two autopsy cases. *Acta paediatrica Japonica : Overseas edition*, 34(3):358–364, jun 1992.

[261] Céline Curis, Florent Percher, Patricia Jeannin, Thomas Montange, Sébastien A. Chevalier, Danielle Seilhean, Luis Cartier, Pierre-Olivier Couraud, Olivier Gout, Antoine Gessain, Pierre-Emmanuel Ceccaldi, and Philippe V. Afonso. Human T-Lymphotropic Virus Type 1-Induced Overexpression of Activated Leukocyte Cell Adhesion Molecule (ALCAM) Facilitates Trafficking of Infected Lymphocytes through the Blood-Brain Barrier. *Journal of Virology*, 90(16):7303–7312, 2016.

[262] Jean Bernard Dietrich. The adhesion molecule ICAM-1 and its regulation in relation with the blood-brain barrier. *Journal of Neuroimmunology*, 128(1-2):58–68, 2002.

[263] Ana Laura Fazio, Wesley Kendle, Kimson Hoang, Erica Korleski, Isabelle Lemasson, and Nicholas Polakowski. Human T-Cell Leukemia Virus Type 1 (HTLV-1) bZIP Factor Upregulates the Expression of ICAM-1 To Facilitate HTLV-1 Infection. *Journal of Virology*, 93(19), oct 2019.

[264] Tetsuya Mizuno, Guiqin Zhang, Hideyuki Takeuchi, Jun Kawanokuchi, Jinyan Wang, Yoshifumi Sonobe, Shijie Jin, Naoki Takada, Yukio Komatsu, and Akio Suzumura. Interferon-gamma directly induces neurotoxicity through a neuron specific, calcium-permeable complex of IFN-gamma receptor and AMPA GluR1 receptor.

FASEB journal : official publication of the Federation of American Societies for Experimental Biology, 22(6):1797–1806, jun 2008.

[265] Emmanuel Hanon, Peter Goon, Graham P Taylor, Hitoshi Hasegawa, Yuetsu Tanaka, Jonathan N Weber, and Charles R M Bangham. High production of interferon γ but not interleukin-2 by human T-lymphotropic virus type I–infected peripheral blood mononuclear cells. *Blood*, 98(3):721–726, aug 2001.

[266] Sonja Tattermusch, Jason A. Skinner, Damien Chaussabel, Jacques Banchereau, Matthew P. Berry, Finlay W. McNab, Anne O'Garra, Graham P. Taylor, and Charles R.M. Bangham. Systems biology approaches reveal a specific interferon-inducible signature in HTLV-1 associated myelopathy. *PLoS Pathogens*, 8(1):1002480, jan 2012.

[267] Yukio Takeshita and Richard M. Ransohoff. Inflammatory cell trafficking across the blood-brain barrier: Chemokine regulation and in vitro models. *Immunological Reviews*, 248(1):228–239, jul 2012.

[268] Eiji Matsuura, Ryuji Kubota, Yuetsu Tanaka, Hiroshi Takashima, and Shuji Izumo. Visualization of HTLV-1-Specific Cytotoxic T Lymphocytes in the Spinal Cords of Patients With HTLV-1-Associated Myelopathy/Tropical Spastic Paraparesis. *Journal of Neuropathology Experimental Neurology*, 74:2–14, 2015.

[269] Yuzo Iwasaki. Human T cell Leukemia Virus Type I Infection and Chronic Myelopathy. *Brain Pathology*, 3(1):1–10, 1993.

[270] F Alcindor, R Valderrama, M Canavaggio, H Lee, A Katz, C Montesinos, R E Madrid, R R Merino, and P A Pipia. Imaging of human T-lymphotropic virus type I-associated chronic progressive myeloneuropathies. *Neuroradiology*, 35(1):69–74, 1992.

[271] Motohiro Yukitake, Eisaburo Sueoka, Naoko Sueoka-Aragane, Akemi Sato, Hiromi Ohashi, Yusuke Yakushiji, Mineki Saito, Mitsuhiro Osame, Shuji Izumo, and Yasuo Kuroda. Significantly increased antibody response to heterogeneous nuclear ribonucleoproteins in cerebrospinal fluid of multiple sclerosis patients but not in patients with human T-lymphotropic virus type I-associated myelopathy/tropical spastic paraparesis. *Journal of neurovirology*, 14(2):130–135, apr 2008.

[272] E. Matsuoka, N. Takenouchi, K. Hashimoto, N. Kashio, T. Moritoyo, I. Higuchi, Y. Isashiki, E. Sato, M. Osame, and S. Izumo. Perivascular T cells are infected with HTLV-I in the spinal cord lesions with HTLV-I-associated myelopathy/tropical spastic paraparesis: Double staining of immunohistochemistry and polymerase chain reaction in situ hybridization. *Acta Neuropathologica*, 96(4):340–346, oct 1998.

[273] Yifei Dong and V. Wee Yong. When encephalitogenic T cells collaborate with microglia in multiple sclerosis. *Nature Reviews Neurology*, 15(12):704–717, 2019.

[274] Chittappen K. Prajeeth, Kirsten Löhr, Stefan Floess, Julian Zimmermann, Reiner Ulrich, Viktoria Gudi, Andreas Beineke, Wolfgang Baumgärtner, Marcus Müller, Jochen Huehn, and Martin Stangel. Effector molecules released by Th1 but not

Th17 cells drive an M1 response in microglia. *Brain, Behavior, and Immunity*, 37:248–259, 2014.

[275] Áine C. Murphy, Stephen J. Lalor, Marina A. Lynch, and Kingston H.G. Mills. Infiltration of Th1 and Th17 cells and activation of microglia in the CNS during the course of experimental autoimmune encephalomyelitis. *Brain, Behavior, and Immunity*, 24(4):641–651, 2010.

[276] Shane A. Liddelow, Kevin A. Guttenplan, Laura E. Clarke, Frederick C. Bennett, Christopher J. Bohlen, Lucas Schirmer, Mariko L. Bennett, Alexandra E. Münch, Won Suk Chung, Todd C. Peterson, Daniel K. Wilton, Arnaud Frouin, Brooke A. Napier, Nikhil Panicker, Manoj Kumar, Marion S. Buckwalter, David H. Rowitch, Valina L. Dawson, Ted M. Dawson, Beth Stevens, and Ben A. Barres. Neurotoxic reactive astrocytes are induced by activated microglia. *Nature 2017 541:7638*, 541(7638):481–487, jan 2017.

[277] Martina Kunkl, Carola Amormino, Valentina Tedeschi, Maria Teresa Fiorillo, and Loretta Tuosto. Astrocytes and Inflammatory T Helper Cells: A Dangerous Liaison in Multiple Sclerosis. *Frontiers in Immunology*, 13:230, feb 2022.

[278] Raphaël Szymocha, Hideo Akaoka, Magali Dutuit, Christophe Malcus, Marianne Didier-Bazes, Marie-Françoise Belin, and Pascale Giraudon. Human T-Cell Lymphotropic Virus Type 1-Infected T Lymphocytes Impair Catabolism and Uptake of Glutamate by Astrocytes via Tax-1 and Tumor Necrosis Factor Alpha. *Journal of Virology*, 74(14):6433–6441, 2000.

[279] Michael A. Wheeler, Iain C. Clark, Emily C. Tjon, Zhaorong Li, Stephanie E.J. Zandee, Charles P. Couturier, Brianna R. Watson, Giulia Scalisi, Sarah Alkwai, Veit Rothhammer, Assaf Rotem, John A. Heyman, Shravan Thaploo, Liliana M. Sanmarco, Jiannis Ragoussis, David A. Weitz, Kevin Petrecca, Jeffrey R. Moffitt, Burkhard Becher, Jack P. Antel, Alexandre Prat, and Francisco J. Quintana. MAFG-driven astrocytes promote CNS inflammation. *Nature*, 578(7796):593–599, 2020.

[280] Hitoshi Ando, Tomoo Sato, Utano Tomaru, Mari Yoshida, Atae Utsunomiya, Junji Yamauchi, Natsumi Araya, Naoko Yagishita, Ariella Coler-Reilly, Yukiko Shimizu, Kazuo Yudoh, Yasuhiro Hasegawa, Kusuki Nishioka, Toshihiro Nakajima, Steven Jacobson, and Yoshihisa Yamano. Positive feedback loop via astrocytes causes chronic inflammation in virus-associated myelopathy. *Brain*, 136(9):2876–2887, sep 2013.

[281] B Lu, A Humbles, D Bota, C Gerard, B Moser, D Soler, A D Luster, and N P Gerard. Structure and function of the murine chemokine receptor CXCR3. *European journal of immunology*, 29(11):3804–3812, nov 1999.

[282] K E Cole, C A Strick, T J Paradis, K T Ogborne, M Loetscher, R P Gladue, W Lin, J G Boyd, B Moser, D E Wood, B G Sahagan, and K Neote. Interferon-inducible T cell alpha chemoattractant (I-TAC): a novel non-ELR CXC chemokine with potent activity on activated T cells through selective high affinity binding to CXCR3. *The Journal of experimental medicine*, 187(12):2009–2021, jun 1998.

[283] M Loetscher, P Loetscher, N Brass, E Meese, and B Moser. Lymphocyte-specific chemokine receptor CXCR3: regulation, chemokine binding and gene localization. *European journal of immunology*, 28(11):3696–3705, nov 1998.

[284] M Loetscher, B Gerber, P Loetscher, S A Jones, L Piali, I Clark-Lewis, M Baggiolini, and B Moser. Chemokine receptor specific for IP10 and mig: structure, function, and expression in activated T-lymphocytes. *The Journal of experimental medicine*, 184(3):963–969, sep 1996.

[285] Angelika Rappert, Ingo Bechmann, Tatyana Pivneva, Jacqueline Mahlo, Knut Biber, Christiane Nolte, Adam D Kovac, Craig Gerard, Hendrikus W G M Boddeke, Robert Nitsch, and Helmut Kettenmann. CXCR3-dependent microglial recruitment is essential for dendrite loss after brain lesion. *The Journal of neuroscience : the official journal of the Society for Neuroscience*, 24(39):8500–8509, sep 2004.

[286] Marius Krauthausen, Simon Saxe, Julian Zimmermann, Michael Emrich, Michael T Heneka, and Marcus Müller. CXCR3 modulates glial accumulation and activation in cuprizone-induced demyelination of the central nervous system. *Journal of neuroinflammation*, 11:109, jun 2014.

[287] Koichi Narikawa, Kazuo Fujihara, Tatsuro Misu, Juan Feng, Juichi Fujimori, Ichiro Nakashima, Isabelle Miyazawa, Hiroshi Saito, Shigeru Sato, and Yasuto Itoyama. CSF-chemokines in HTLV-I-associated myelopathy: CXCL10 up-regulation and therapeutic effect of interferon-α. *Journal of Neuroimmunology*, 159(1-2):177–182, feb 2005.

[288] Eduardo Samo Gudo, Suse Dayse Silva-Barbosa, Leandra Linhares-Lacerda, Marcelo Ribeiro-Alves, Suzana Corte Real, Dumith Chequer Bou-Habib, and Wilson Savino. HAM/TSP-derived HTLV-1-infected T cell lines promote morphological and functional changes in human astrocytes cell lines: possible role in the enhanced T cells recruitment into Central Nervous System. *Virology Journal*, 12(1):165, dec 2015.

[289] Yoshio Koyanagi, Yasuto Itoyama, Naomi Nakamura, Keita Takamatsu, Jun Ichi Kira, Teruo Iwamasa, Ikuo Goto, and Naoki Yamamoto. In Vivo Infection of Human T-Cell Leukemia Virus Type I in Non-T Cells, 1993.

[290] S E Macatonia, J K Cruickshank, P Rudge, and S C Knight. Dendritic cells from patients with tropical spastic paraparesis are infected with HTLV-1 and stimulate autologous lymphocyte proliferation. *AIDS research and human retroviruses*, 8(9):1699–1706, sep 1992.

[291] Jun-ichirou Yasunaga, Rie Furuta, Michi Miura, Kenji Sugata, Akatsuki Saito, Akari Hirofumi, Takaharu Ueno, Norihiro Takenouchi, Jun-ichi Fujisawa, Masakazu Shimizu, Fumihiko Matsuda, Anat Melamed, Charles R. M. Bangham, and Masao Matsuoka. Hematopoietic Stem Cell Infected with HTLV-1 Functions As a Viral Reservoir In Vivo. *Blood*, 128(22):1343, dec 2016.

[292] Satomi Ando, Atsuhiko Hasegawa, Yuji Murakami, Na Zeng, Natsuko Takatsuka, Yasuhiro Maeda, Takao Masuda, Youko Suehiro, and Mari Kannagi. HTLV-1 Tax-Specific CTL Epitope-Pulsed Dendritic Cell Therapy Reduces Proviral Load in Infected Rats with Immune Tolerance against Tax. *Journal of immunology (Baltimore, Md. : 1950)*, 198(3):1210–1219, feb 2017.

[293] Youko Suehiro, Atsuhiko Hasegawa, Tadafumi Iino, Amane Sasada, Nobukazu Watanabe, Masao Matsuoka, Ayako Takamori, Ryuji Tanosaki, Atae Utsunomiya, Ilseung Choi, Tetsuya Fukuda, Osamu Miura, Shigeo Takaishi, Takanori Teshima, Koichi Akashi, Mari Kannagi, Naokuni Uike, and Jun Okamura. Clinical outcomes of a novel therapeutic vaccine with Tax peptide-pulsed dendritic cells for adult T cell leukaemia/lymphoma in a pilot study. *British journal of haematology*, 169(3):356–367, may 2015.

[294] Masakatsu Hishizawa, Kazunori Imada, Toshio Kitawaki, Maki Ueda, Norimitsu Kadowaki, and Takashi Uchiyama. Depletion and impaired interferon-α-producing capacity of blood plasmacytoid dendritic cells in human T-cell leukaemia virus type I-infected individuals. *British Journal of Haematology*, 125(5):568–575, 2004.

[295] Shuichi Kinpara, Atsuhiko Hasegawa, Atae Utsunomiya, Hironori Nishitsuji, Hiroyuki Furukawa, Takao Masuda, and Mari Kannagi. Stromal cell-mediated suppression of human T-cell leukemia virus type 1 expression in vitro and in vivo by type I interferon. *Journal of virology*, 83(10):5101–5108, may 2009.

[296] Dong-Yan Jin, Kin-Hang Kok, Hei-Man V Tang, Pak-Yin Lui, and Chi-Ping Chan. Suppression of type I interferon production by human T-cell leukemia virus type 1 oncoprotein Tax. *Retrovirology*, 11(S1), 2014.

[297] Chloé Journo and Renaud Mahieux. HTLV-1 and innate immunity, aug 2011.

[298] Zainab Saeed, Aileen Rowan, Claire Greiller, Graham P. Taylor, and Katrina M. Pollock. Enhanced T-Cell Maturation and Monocyte Aggregation Are Features of Cellular Inflammation in Human T-Lymphotropic Virus Type 1–Associated Myelopathy. *Clinical Infectious Diseases*, 70(7):1326–1335, mar 2020.

[299] Ryuji Kubota, Taketo Kawanishi, Hidetoshi Matsubara, Angela Manns, and Steven Jacobson. HTLV-I specific IFN-γ+ CD8+ lymphocytes correlate with the proviral load in peripheral blood of infected individuals. *Journal of Neuroimmunology*, 102(2):208–215, 2000.

[300] Peter K.C. Goon, Emmanuel Hanon, Tadahiko Igakura, Yuetsu Tanaka, Jonathan N Weber, Graham P Taylor, and Charles R.M. Bangham. High frequencies of Th1-type CD4+ T cells specific to HTLV-1 Env and Tax proteins in patients with HTLV-1-associated myelopathy/tropical spastic paraparesis. *Blood*, 99(9):3335–3341, 2002.

[301] Peter K. C. Goon, Tadahiko Igakura, Emmanuel Hanon, Angelina J. Mosley, Anna Barfield, Amanda L. Barnard, Lambrini Kaftantzi, Yuetsu Tanaka, Graham P. Taylor, Jonathan N. Weber, and Charles R. M. Bangham. Human T Cell Lymphotropic Virus Type I (HTLV-I)-Specific CD4 + T Cells: Immunodominance Hierarchy and Preferential Infection with HTLV-I . *The Journal of Immunology*, 172(3):1735–1743, 2004.

[302] M Higuchi, K Nagasawa, T Horiuchi, M Oike, Y Ito, M Yasukawa, and Y Niho. Membrane tumor necrosis factor-alpha (TNF-alpha) expressed on HTLV-I-infected T cells mediates a costimulatory signal for B cell activation–characterization of membrane TNF-alpha. *Clinical immunology and immunopathology*, 82(2):133–140, feb 1997.

[303] Yoshihiro Nishiura, Tatsufumi Nakamura, Katsuhiro Ichinose, Susumu Shirabe, Akira Tsujino, Hirofumi Goto, Takafumi Furuya, and Shigenobu Nagataki. Increased production of inflammatory cytokines in cultured CD4 + cells from patients with HTLV-I-associated myelopathy, 1996.

[304] Yorifumi Satou, Atae Utsunomiya, Junko Tanabe, Masanori Nakagawa, Kisato Nosaka, and Masao Matsuoka. HTLV-1 modulates the frequency and phenotype of FoxP3+CD4+ T cells in virus-infected individuals. *Retrovirology*, 9:46, may 2012.

[305] Frederic Toulza, Adrian Heaps, Yuetsu Tanaka, Graham P. Taylor, and Charles R.M. Bangham. High frequency of CD4+FoxP3+ cells in HTLV-1 infection: Inverse correlation with HTLV-l-specific CTL response. *Blood*, 111(10):5047–5053, may 2008.

[306] Frederic Toulza, Kisato Nosaka, Yuetsu Tanaka, Tiziana Schioppa, Frances Balkwill, Graham P. Taylor, and Charles R. M. Bangham. Human T-Lymphotropic Virus Type 1-Induced CC Chemokine Ligand 22 Maintains a High Frequency of Functional FoxP3+ Regulatory T Cells. *The Journal of Immunology*, 185(1):183–189, 2010.

[307] Yoshimi Enose-Akahata, Anna Abrams, Raya Massoud, Izabela Bialuk, Kory R. Johnson, Patrick L. Green, Elizabeth M. Maloney, and Steven Jacobson. Humoral immune response to HTLV-1 basic leucine zipper factor (HBZ) in HTLV-1-infected individuals. *Retrovirology*, 10(1):1–13, 2013.

[308] Peter K.C. Goon, Alix Biancardi, Noam Fast, Tadahilco Igakura, Emmanuel Hanon, Angelina J. Mosley, Becca Asquith, Keith G. Gouldl, Sara Marshall, Graham P. Taylor, and Charles R.M. Bangham. Human T Cell Lymphotropic Virus (HTLV) type-1-specific CD8+ T cells: Frequency and immunodominance hierarchy. *Journal of Infectious Diseases*, 189(12):2294–2298, jun 2004.

[309] Aidan MacNamara, Aileen Rowan, Silva Hilburn, Ulrich Kadolsky, Hiroshi Fujiwara, Koichiro Suemori, Masaki Yasukawa, Graham Taylor, Charles R.M. Bangham, and Becca Asquith. HLA class I binding of HBZ determines outcome in HTLV-1 infection. *PLoS Pathogens*, 6(9), sep 2010.

[310] Kenji Sugata, Jun Ichirou Yasunaga, Yuichi Mitobe, Michi Miura, Paola Miyazato, Michinori Kohara, and Masao Matsuoka. Protective effect of cytotoxic T lymphocytes targeting HTLV-1 bZIP factor. *Blood*, 126(9):1095–1105, 2015.

[311] Silva Hilburn, Aileen Rowan, Maria Antonietta Demontis, Aidan MacNamara, Becca Asquith, Charles R.M. Bangham, and Graham P. Taylor. In vivo expression of human T-lymphotropic virus type 1 basic leucine-zipper protein generates specific CD8+ and CD4+ T-lymphocyte responses that correlate with clinical outcome. *Journal of Infectious Diseases*, 203(4):529–536, 2011.

[312] S Ugolini, C Arpin, N Anfossi, T Walzer, A Cambiaggi, R Förster, M Lipp, R E Toes, C J Melief, J Marvel, and E Vivier. Involvement of inhibitory NKRs in the survival of a subset of memory-phenotype CD8+ T cells. *Nature immunology*, 2(5):430–435, may 2001.

[313] Yoshihisa Yamano, Masahiro Nagai, Meghan Brennan, Carlos A. Mora, Samantha S. Soldan, Utano Tomaru, Norihiro Takenouchi, Shuji Izumo, Mitsuhiro Osame, and Steven Jacobson. Correlation of human T-cell lymphotropic virus type 1 (HTLV-1) mRNA with proviral DNA load, virus-specific CD8+ T cells, and disease severity in HTLV-1-associated myelopathy (HAM/TSP). *Blood*, 99(1):88–94, 2002.

[314] Franziska Lechner, David K.H. Wong, P. Rod Dunbar, Roger Chapman, Raymond T. Chung, Paul Dohrenwend, Gregory Robbins, Rodney Phillips, Paul Klenerman, and Bruce D. Walker. Analysis of successful immune responses in persons infected with hepatitis C virus. *Journal of Experimental Medicine*, 191(9):1499–1512, may 2000.

[315] Barbara Rehermann. Pathogenesis of chronic viral hepatitis: Differential roles of T cells and NK cells. *Nature Medicine*, 19(7):859–868, jul 2013.

[316] Antigoni Morou, Elsa Brunet-Ratnasingham, Mathieu Dubé, Roxanne Charlebois, Eloi Mercier, Sam Darko, Nathalie Brassard, Krystelle Nganou-Makamdop, Sahaana Arumugam, Gabrielle Gendron-Lepage, Lifei Yang, Julia Niessl, Amy E. Baxter, James M. Billingsley, Premeela A. Rajakumar, François Lefebvre, R. Paul Johnson, Cécile Tremblay, Jean Pierre Routy, Richard T. Wyatt, Andrés Finzi, Daniel C. Douek, and Daniel E. Kaufmann. Altered differentiation is central to HIV-specific CD4+ T cell dysfunction in progressive disease. *Nature Immunology*, 20(8):1059–1070, aug 2019.

[317] Filippos Porichis and Daniel E. Kaufmann. HIV-specific CD4 T cells and immune control of viral replication. *Current Opinion in HIV and AIDS*, 6(3):174–180, may 2011.

[318] S. Ranasinghe, M. Flanders, S. Cutler, D. Z. Soghoian, M. Ghebremichael, I. Davis, M. Lindqvist, F. Pereyra, B. D. Walker, D. Heckerman, and H. Streeck. HIV-Specific CD4 T Cell Responses to Different Viral Proteins Have Discordant Associations with Viral Load and Clinical Outcome. *Journal of Virology*, 86(1):277–283, jan 2012.

[319] Laura A. Vella, Ramin S. Herati, and E. John Wherry. CD4+ T Cell Differentiation in Chronic Viral Infections: The Tfh Perspective. *Cell Press Reviews: Trends in Molecular Medicine*, 23(12):1072–1087, dec 2017.

[320] Petra Bacher, Elisa Rosati, Daniela Esser, Gabriela Rios Martini, Carina Saggau, Esther Schiminsky, Justina Dargvainiene, Ina Schröder, Imke Wieters, Yascha Khodamoradi, Fabian Eberhardt, Maria J.G.T. Vehreschild, Holger Neb, Michael Sonntagbauer, Claudio Conrad, Florian Tran, Philip Rosenstiel, Robert Markewitz, Klaus Peter Wandinger, Max Augustin, Jan Rybniker, Matthias Kochanek, Frank Leypoldt, Oliver A. Cornely, Philipp Koehler, Andre Franke, and Alexander Scheffold. Low-Avidity CD4+ T Cell Responses to SARS-CoV-2 in Unexposed Individuals and Humans with Severe COVID-19. *Immunity*, 53(6):1258–1271.e5, 2020.

[321] Alison Crawford, Jill M. Angelosanto, Charlly Kao, Travis A. Doering, Pamela M. Odorizzi, Burton E. Barnett, and E. John Wherry. Molecular and Transcriptional Basis of CD4+ T Cell Dysfunction during Chronic Infection. *Immunity*, 40(2):289–302, feb 2014.

[322] Nayan D. Bhattacharyya and Carl G. Feng. Regulation of T Helper Cell Fate by TCR Signal Strength. *Frontiers in Immunology*, 11:624, may 2020.

[323] Petra Bacher, Christian Schink, Janka Teutschbein, Olaf Kniemeyer, Mario Assenmacher, Axel A. Brakhage, and Alexander Scheffold. Antigen-Reactive T Cell Enrichment for Direct, High-Resolution Analysis of the Human Naive and Memory Th Cell Repertoire. *The Journal of Immunology*, 190(8):3967–3976, apr 2013.

[324] Marco Frentsch, Olga Arbach, Dennis Kirchhoff, Beate Moewes, Margitta Worm, Martin Rothe, Alexander Scheffold, and Andreas Thiel. Direct access to CD4+ T cells specific for defined antigens according to CD154 expression. *Nature Medicine*, 11(10):1118–1124, oct 2005.

[325] Angela Risso, Daniela Smilovich, Maria C. Capra, Isabella Baldissarro, Gu Yan, Antonio Bargellesi, and Maria E. Cosulich. CD69 in resting and activated T lymphocytes: Its association with a GTP binding protein and biochemical requirements for its expression. *Journal of Immunology*, 146(12):4105–4114, 1991.

[326] Melika Motamedi, Lai Xu, and Shokrollah Elahi. Correlation of transferrin receptor (CD71) with Ki67 expression on stimulated human and mouse T cells: The kinetics of expression of T cell activation markers. *Journal of Immunological Methods*, 437:43–52, 2016.

[327] Ning Yu, Xiaomei Li, Weiya Song, Dongmei Li, Daliang Yu, Xiaofeng Zeng, Mengtao Li, Xiaomei Leng, and Xiangpei Li. CD4(+)CD25 (+)CD127 (low/-) T cells: a more specific Treg population in human peripheral blood. *Inflammation*, 35(6):1773–1780, dec 2012.

[328] Montserrat Casamayor-Palleja, Mahmood Khan, and Ian C.M. MacLennan. A subset of CD4+ memory T cells contains preformed CD40 ligand that is rapidly but transiently expressed on their surface after activation through the T cell receptor complex. *Journal of Experimental Medicine*, 181(4):1293–1301, apr 1995.

[329] Alba Grifoni, Daniela Weiskopf, Sydney I. Ramirez, Jose Mateus, Jennifer M. Dan, Carolyn Rydyznski Moderbacher, Stephen A. Rawlings, Aaron Sutherland, Lakshmanane Premkumar, Ramesh S. Jadi, Daniel Marrama, Aravinda M. de Silva, April Frazier, Aaron F. Carlin, Jason A. Greenbaum, Bjoern Peters, Florian Krammer, Davey M. Smith, Shane Crotty, and Alessandro Sette. Targets of T Cell Responses to SARS-CoV-2 Coronavirus in Humans with COVID-19 Disease and Unexposed Individuals. *Cell*, 181(7):1489–1501.e15, 2020.

[330] Alexander Dobin, Carrie A. Davis, Felix Schlesinger, Jorg Drenkow, Chris Zaleski, Sonali Jha, Philippe Batut, Mark Chaisson, and Thomas R. Gingeras. STAR: Ultrafast universal RNA-seq aligner. *Bioinformatics*, 29(1):15–21, 2013.

[331] Rob Patro, Geet Duggal, Michael I. Love, Rafael A. Irizarry, and Carl Kingsford. Salmon provides fast and bias-aware quantification of transcript expression. *Nature Methods*, 14(4):417–419, 2017.

[332] David S. Deluca, Joshua Z. Levin, Andrey Sivachenko, Timothy Fennell, Marc Danie Nazaire, Chris Williams, Michael Reich, Wendy Winckler, and Gad Getz. RNA-SeQC: RNA-seq metrics for quality control and process optimization. *Bioinformatics*, 28(11):1530–1532, 2012.

[333] Bioconductor. genefilter: methods for filtering genes from high-throughput experiments v. R package version 1.76.0. 2021.

[334] Michael I. Love, Wolfgang Huber, and Simon Anders. Moderated estimation of fold change and dispersion for RNA-seq data with DESeq2. *Genome Biology*, 15(12):1–21, 2014.

[335] Allison K. Maher, Katie L. Burnham, Emma M. Jones, Michelle M.H. Tan, Rocel C. Saputil, Laury Baillon, Claudia Selck, Nicolas Giang, Rafael Argüello, Clio Pillay, Emma Thorley, Charlotte Eve Short, Rachael Quinlan, Wendy S. Barclay, Nichola Cooper, Graham P. Taylor, Emma E. Davenport, and Margarita Dominguez-Villar. Transcriptional reprogramming from innate immune functions to a pro-thrombotic signature by monocytes in COVID-19. *Nature Communications*, 13(1):1–17, 2022.

[336] Hai Fang, Bogdan Knezevic, Katie L. Burnham, and Julian C. Knight. XGR software for enhanced interpretation of genomic summary data, illustrated by application to immunological traits. *Genome Medicine*, 8(1):1–20, 2016.

[337] Margarita Dominguez-Villar, Clare M. Baecher-Allan, and David A. Hafler. Identification of T helper type 1-"like, Foxp3 + regulatory T cells in human autoimmune disease. *Nature Medicine*, 17(6):673–675, 2011.

[338] Daniel C. Douek, Jason M. Brenchley, Michael R. Betts, David R. Ambrozak, Brenna J. Hill, Yukari Okamoto, Joseph P. Casazza, Janaki Kuruppu, Kevin Kunstman, Steven Wolinsky, Zvi Grossman, Mark Dybul, Annette Oxenius, David A. Price, Mark Connors, and Richard A. Koup. HIV preferentially infects HIV-specific CD4+ T cells. *Nature 2002 417:6884*, 417(6884):95–98, may 2002.

[339] Kiruthika Manivannan, Aileen G. Rowan, Yuetsu Tanaka, Graham P. Taylor, and Charles R. M. Bangham. CADM1/TSLC1 Identifies HTLV-1-Infected Cells and Determines Their Susceptibility to CTL-Mediated Lysis. *PLOS Pathogens*, 12(4):e1005560, apr 2016.

[340] D J Saville. Multiple Comparison Procedures: The Practical Solution. *The American Statistician*, 44(2):174–180, mar 1990.

[341] Charles R.M. Bangham, Abelardo Araujo, Yoshihisa Yamano, and Graham P. Taylor. HTLV-1-associated myelopathy/tropical spastic paraparesis. *Nature Reviews Disease Primers*, 1:1–16, 2015.

[342] Sung S. Choi, Hong J. Lee, Inja Lim, Jun Ichi Satoh, and Seung U. Kim. Human astrocytes: Secretome profiles of cytokines and chemokines. *PLoS ONE*, 9(4), 2014.

[343] Marco Prinz, Takahiro Masuda, Michael A Wheeler, and Francisco J Quintana. Microglia and Central Nervous System-Associated Macrophages-From Origin to Disease Modulation. *Annual review of immunology*, 39:251–277, apr 2021.

[344] Aino Latva-Rasku, Miikka-Juhani Honka, Alena Stančáková, Heikki A Koistinen, Johanna Kuusisto, Li Guan, Alisa K Manning, Heather Stringham, Anna L Gloyn, Cecilia M Lindgren, Francis S Collins, Karen L Mohlke, Laura J Scott, Tomi Karjalainen, Lauri Nummenmaa, Michael Boehnke, Pirjo Nuutila, and Markku Laakso. A Partial Loss-of-Function Variant in AKT2 Is Associated With Reduced Insulin-Mediated Glucose Uptake in Multiple Insulin-Sensitive Tissues: A Genotype-Based Callback Positron Emission Tomography Study. *Diabetes*, 67(2):334–342, feb 2018.

[345] Min Yue Zhang, Tsz Kin Fung, Fang Yuan Chen, and Chor Sang Chim. Methylation profiling of SOCS1, SOCS2, SOCS3, CISH and SHP1 in Philadelphia-negative myeloproliferative neoplasm. *Journal of cellular and molecular medicine*, 17(10):1282–1290, oct 2013.

[346] Katarzyna Kowanetz, Nicola Crosetto, Kaisa Haglund, Mirko H H Schmidt, Carl-Henrik Heldin, and Ivan Dikic. Suppressors of T-cell Receptor Signaling Sts-1 and Sts-2 Bind to Cbl and Inhibit Endocytosis of Receptor Tyrosine Kinases *. *Journal of Biological Chemistry*, 279(31):32786–32795, jul 2004.

[347] Grégoire de Streel, Charlotte Bertrand, Nicolas Chalon, Stéphanie Liénart, Orian Bricard, Sara Lecomte, Julien Devreux, Mélanie Gaignage, Gitte De Boeck, Lore Mariën, Inge Van De Walle, Bas van der Woning, Michael Saunders, Hans de Haard, Elien Vermeersch, Wim Maes, Hans Deckmyn, Pierre G Coulie, Nicolas van Baren, and Sophie Lucas. Selective inhibition of TGF-β1 produced by GARP-expressing Tregs overcomes resistance to PD-1/PD-L1 blockade in cancer. *Nature Communications*, 11(1):4545, 2020.

[348] Xiang-jun Chen, Sha Liu, Dong-mei Han, De-zhi Han, Wei-jing Sun, and Xiao-chun Zhao. Regulation of melanoma malignancy by the RP11-705C15.3/miR-145-5p/NRAS/MAPK signaling axis. *Cancer Gene Therapy*, 28(10):1198–1212, 2021.

[349] Hania Kebir, Katharina Kreymborg, Igal Ifergan, Aurore Dodelet-Devillers, Romain Cayrol, Monique Bernard, Fabrizio Giuliani, Nathalie Arbour, Burkhard Becher, and Alexandre Prat. Human TH17 lymphocytes promote blood-brain barrier disruption and central nervous system inflammation. *Nature Medicine*, 13(10):1173–1175, 2007.

[350] C Weber, K S Weber, C Klier, S Gu, R Wank, R Horuk, and P J Nelson. Specialized roles of the chemokine receptors CCR1 and CCR5 in the recruitment of monocytes and T(H)1-like/CD45RO(+) T cells. *Blood*, 97(4):1144–1146, feb 2001.

[351] Tomoo Sato, Ariella Coler-Reilly, Atae Utsunomiya, Natsumi Araya, Naoko Yagishita, Hitoshi Ando, Junji Yamauchi, Eisuke Inoue, Takahiko Ueno, Yasuhiro Hasegawa, Kusuki Nishioka, Toshihiro Nakajima, Steven Jacobson, Shuji Izumo, and Yoshihisa Yamano. CSF CXCL10, CXCL9, and Neopterin as Candidate Prognostic Biomarkers for HTLV-1-Associated Myelopathy/Tropical Spastic Paraparesis. *PLOS Neglected Tropical Diseases*, 7(10):e2479, 2013.

[352] Yu Lei and Yousuke Takahama. XCL1 and XCR1 in the immune system. *Microbes and infection*, 14(3):262–267, mar 2012.

[353] Anne S. Dejean, Emeline Joulia, and Thierry Walzer. The role of Eomes in human CD4 T cell differentiation: A question of context. *European Journal of Immunology*, 49(1):38–41, jan 2019.

[354] Toru Koda, Akiko Namba, Makoto Kinoshita, Yuji Nakatsuji, Tomoyuki Sugimoto, Kaori Sakakibara, Satoru Tada, Mikito Shimizu, Kazuya Yamashita, Kazushiro Takata, Teruyuki Ishikura, Syo Murata, Shohei Beppu, Atsushi Kumanogoh, Hideki Mochizuki, and Tatsusada Okuno. Sema4A is implicated in the acceleration of Th17 cell-mediated neuroinflammation in the effector phase. *Journal of Neuroinflammation*, 17(1):1–9, mar 2020.

[355] George D. Kalliolias and Lionel B. Ivashkiv. TNF biology, pathogenic mechanisms and emerging therapeutic strategies. *Nature Reviews Rheumatology*, 12(1):49–62, 2016.

[356] Gaetana Minnone, Fabrizio De Benedetti, and Luisa Bracci-Laudiero. NGF and Its Receptors in the Regulation of Inflammatory Response. *International Journal of Molecular Sciences*, 18(5), may 2017.

[357] Drishya Diwaker, Kamla Prasad Mishra, and Lilly Ganju. Effect of modulation of unfolded protein response pathway on dengue virus infection. *Acta Biochimica et Biophysica Sinica*, 47(12):960–968, 2015.

[358] Shiu-Wan Chan. The unfolded protein response in virus infections. *Frontiers in Microbiology*, 5(September):1–2, 2014.

[359] Justin A Shyer, Richard A Flavell, and Will Bailis. Metabolic signaling in T cells. *Cell Research*, 30(8):649–659, 2020.

[360] Douglas H. Yamada, Ivan Osokine, Douglas H. Yamada, Justin Rafael De la Fuente, Heidi J. Elsaesser, and David G. Brooks. Overcoming CD4 Th1 Cell Fate Restrictions to Sustain Antiviral CD8 T Cells and Control Persistent Virus Infection. *Cell Reports*, 16(12):3286–3296, 2016.

[361] Wanqiu Hou, Hyun Seok Kang, and Byung S. Kim. Th17 cells enhance viral persistence and inhibit T cell cytotoxicity in a model of chronic virus infection. *Journal of Experimental Medicine*, 206(2):313–328, 2009.

[362] Arezoo Gowhari Shabgah, Ebrahim Fattahi, and Fatemeh Zare Shahneh. Interleukin-17 in human inflammatory diseases. *Postepy Dermatologii i Alergologii*, 31(4):256–261, 2014.

[363] Nicholas Schwab, Tilman Schneider-Hohendorf, and Heinz Wiendl. Therapeutic uses of anti-α4-integrin (anti-VLA-4) antibodies in multiple sclerosis. *International Immunology*, 27(1):47–53, 2014.

[364] Etty N. Benveniste, Maria Vidovic, R. Brian Panek, J. Gavin Norris, Alyssa T. Reddy, and Dale J. Benos. Interferon-γ-induced astrocyte class II major histocompatibility complex gene expression is associated with both protein kinase C activation and Na+ entry. *Journal of Biological Chemistry*, 266(27):18119–18126, 1991.

[365] Etty N. Benveniste, Shaun M. Sparacio, and John R. Bethea. Tumor necrosis factor-α enhances interferon-γ-mediated class II antigen expression on astrocytes. *Journal of Neuroimmunology*, 25(2-3):209–219, 1989.

[366] Jinar Rostami, Grammatiki Fotaki, Julien Sirois, Ropafadzo Mzezewa, Joakim Bergström, Magnus Essand, Luke Healy, and Anna Erlandsson. Astrocytes have the capacity to act as antigen-presenting cells in the Parkinson's disease brain. *Journal of Neuroinflammation*, 17(1):1–18, apr 2020.

[367] Dae Y. Kim, Gwan U. Hong, and Jai Y. Ro. Signal pathways in astrocytes activated by cross-talk between of astrocytes and mast cells through CD40-CD40L. *Journal of Neuroinflammation*, 8:1–16, 2011.

[368] Nahed Abdel-Haq, Hsiao Nan Hao, and William D. Lyman. Cytokine regulation of CD40 expression in fetal human astrocyte cultures. *Journal of Neuroimmunology*, 101(1):7–14, 1999.

[369] Shane A. Liddelow, Kevin A. Guttenplan, Laura E. Clarke, Frederick C. Bennett, Christopher J. Bohlen, Lucas Schirmer, Mariko L. Bennett, Alexandra E. Münch, Won Suk Chung, Todd C. Peterson, Daniel K. Wilton, Arnaud Frouin, Brooke A. Napier, Nikhil Panicker, Manoj Kumar, Marion S. Buckwalter, David H. Rowitch, Valina L. Dawson, Ted M. Dawson, Beth Stevens, and Ben A. Barres. Neurotoxic reactive astrocytes are induced by activated microglia. *Nature*, 541(7638):481–487, 2017.

[370] Guillaume Perriard, Amandine Mathias, Lukas Enz, Mathieu Canales, Myriam Schluep, Melanie Gentner, Nicole Schaeren-Wiemers, and Renaud A. Du Pasquier. Interleukin-22 is increased in multiple sclerosis patients and targets astrocytes. *Journal of Neuroinflammation*, 12(1):1–18, 2015.

[371] Stephen Sawcer, Garrett Hellenthal, Matti Pirinen, Chris C.A. Spencer, Nikolaos A. Patsopoulos, Loukas Moutsianas, Alexander Dilthey, Zhan Su, Colin Freeman, Sarah E. Hunt, Sarah Edkins, Emma Gray, David R. Booth, Simon C. Potter, An Goris, Gavin Band, Annette Bang Oturai, Amy Strange, Janna Saarela, Céline Bellenguez, Bertrand Fontaine, Matthew Gillman, Bernhard Hemmer, Rhian Gwilliam, Frauke Zipp, Alagurevathi Jayakumar, Roland Martin, Stephen Leslie, Stanley Hawkins, Eleni Giannoulatou, Sandra D'Alfonso, Hannah Blackburn, Filippo Martinelli Boneschi, Jennifer Liddle, Hanne F. Harbo, Marc L. Perez, Anne Spurkland, Matthew J. Waller, Marcin P. Mycko, Michelle Ricketts, Manuel Comabella, Naomi Hammond, Ingrid Kockum, Owen T. McCann, Maria Ban, Pamela Whittaker, Anu Kemppinen, Paul Weston, Clive Hawkins, Sara Widaa, John Zajicek, Serge Dronov, Neil Robertson, Suzannah J. Bumpstead, Lisa F. Barcellos, Rathi Ravindrarajah, Roby Abraham, Lars Alfredsson, Kristin Ardlie, Cristin Aubin, Amie Baker, Katharine Baker, Sergio E. Baranzini, Laura Bergamaschi, Roberto Bergamaschi, Allan

Bernstein, Achim Berthele, Mike Boggild, Jonathan P. Bradfield, David Brassat, Simon A. Broadley, Dorothea Buck, Helmut Butzkueven, Ruggero Capra, William M. Carroll, Paola Cavalla, Elisabeth G. Celius, Sabine Cepok, Rosetta Chiavacci, Françoise Clerget-Darpoux, Katleen Clysters, Giancarlo Comi, Mark Cossburn, Isabelle Cournu-Rebeix, Mathew B. Cox, Wendy Cozen, Bruce A.C. Cree, Anne H. Cross, Daniele Cusi, Mark J. Daly, Emma Davis, Paul I.W. De Bakker, Marc Debouverie, Marie Beatrice D'Hooghe, Katherine Dixon, Rita Dobosi, Bénédicte Dubois, David Ellinghaus, Irina Elovaara, Federica Esposito, Claire Fontenille, Simon Foote, Andre Franke, Daniela Galimberti, Angelo Ghezzi, Joseph Glessner, Refujia Gomez, Olivier Gout, Colin Graham, Struan F.A. Grant, Franca Rosa Guerini, Hakon Hakonarson, Per Hall, Anders Hamsten, Hans Peter Hartung, Rob N. Heard, Simon Heath, Jeremy Hobart, Muna Hoshi, Carmen Infante-Duarte, Gillian Ingram, Wendy Ingram, Talat Islam, Maja Jagodic, Michael Kabesch, Allan G. Kermode, Trevor J. Kilpatrick, Cecilia Kim, Norman Klopp, Keijo Koivisto, Malin Larsson, Mark Lathrop, Jeannette S. Lechner-Scott, Maurizio A. Leone, Virpi Leppä, Ulrika Liljedahl, Izaura Lima Bomfim, Robin R. Lincoln, Jenny Link, Jianjun Liu, Aslaug R. Lorentzen, Sara Lupoli, Fabio MacCiardi, Thomas MacK, Mark Marriott, Vittorio Martinelli, Deborah Mason, Jacob L. McCauley, Frank Mentch, Inger Lise Mero, Tania Mihalova, Xavier Montalban, John Mottershead, Kjell Morten Myhr, Paola Naldi, William Ollier, Alison Page, Aarno Palotie, Jean Pelletier, Laura Piccio, Trevor Pickersgill, Fredrik Piehl, Susan Pobywajlo, Hong L. Quach, Patricia P. Ramsay, Mauri Reunanen, Richard Reynolds, John D. Rioux, Mariaemma Rodegher, Sabine Roesner, Justin P. Rubio, Ina Maria Rückert, Marco Salvetti, Erika Salvi, Adam Santaniello, Catherine A. Schaefer, Stefan Schreiber, Christian Schulze, Rodney J. Scott, Finn Sellebjerg, Krzysztof W. Selmaj, David Sexton, Ling Shen, Brigid Simms-Acuna, Sheila Skidmore, Patrick M.A. Sleiman, Cathrine Smestad, Per Soelberg Sørensen, Helle Bach Søndergaard, Jim Stankovich, Richard C. Strange, Anna Maija Sulonen, Emilie Sundqvist, Ann Christine Syvänen, Francesca Taddeo, Bruce Taylor, Jenefer M. Blackwell, Pentti Tienari, Elvira Bramon, Ayman Tourbah, Matthew A. Brown, Ewa Tronczynska, Juan P. Casas, Niall Tubridy, Aiden Corvin, Jane Vickery, Janusz Jankowski, Pablo Villoslada, Hugh S. Markus, Kai Wang, Christopher G. Mathew, James Wason, Colin N.A. Palmer, Erich Wichmann, Robert Plomin, Ernest Willoughby, Anna Rautanen, Juliane Winkelmann, Michael Wittig, Richard C. Trembath, Jacqueline Yaouanq, Ananth C. Viswanathan, Haitao Zhang, Nicholas W. Wood, Rebecca Zuvich, Panos Deloukas, Cordelia Langford, Audrey Duncanson, Jorge R. Oksenberg, Margaret A. Pericak-Vance, Jonathan L. Haines, Tomas Olsson, Jan Hillert, Adrian J. Ivinson, Philip L. De Jager, Leena Peltonen, Graeme J. Stewart, David A. Hafler, Stephen L. Hauser, Gil McVean, Peter Donnelly, and Alastair Compston. Genetic risk and a primary role for cell-mediated immune mechanisms in multiple sclerosis. *Nature*, 476(7359):214–219, 2011.

[372] Ben J.E. Raveney, Shinji Oki, Hirohiko Hohjoh, Masakazu Nakamura, Wakiro Sato, Miho Murata, and Takashi Yamamura. Eomesodermin-expressing T-helper cells are essential for chronic neuroinflammation. *Nature Communications 2015 6:1*, 6(1):1–11, oct 2015.

[373] Ben J.E. Raveney, Wakiro Sato, Daiki Takewaki, Chenyang Zhang, Tomomi

Kanazawa, Youwei Lin, Tomoko Okamoto, Manabu Araki, Yukio Kimura, Noriko Sato, Terunori Sano, Yuko Saito, Shinji Oki, and Takashi Yamamura. Involvement of cytotoxic Eomes-expressing CD4+T cells in secondary progressive multiple sclerosis. *Proceedings of the National Academy of Sciences of the United States of America*, 118(11):e2021818118, mar 2021.

[374] Emeline Joulia, Michaël F. Michieletto, Arantxa Agesta, Cindy Peillex, Virginie Girault, Anne Louise Le Dorze, Romain Peroceschi, Florence Bucciarelli, Marion Szelechowski, Adeline Chaubet, Nawad Hakim, Rémi Marrocco, Emeline Lhuillier, Manuel Lebeurrier, Rafael J. Argüello, Abdelhadi Saoudi, Hicham El Costa, Veronique Adoue, Thierry Walzer, Jean Emmanuel Sarry, and Anne S. Dejean. Eomes-dependent mitochondrial regulation promotes survival of pathogenic CD4+ T cells during inflammation. *Journal of Experimental Medicine*, 221(2), 2024.

[375] Michael P Crawford, Sushmita Sinha, Pranav S Renavikar, Nicholas Borcherding, and Nitin J Karandikar. CD4 T cell-intrinsic role for the T helper 17 signature cytokine IL-17: Effector resistance to immune suppression. *Proceedings of the National Academy of Sciences*, 117(32):19408–19414, 2020.

[376] Nobuchika Suzuki, Nicole Hajicek, and Tohru Kozasa. Regulation and physiological functions of G12/13-mediated signaling pathways. *Neuro-Signals*, 17(1):55–70, 2009.

[377] Margarita Dominguez-Villar, Khadir Raddassi, Ann Caroline Danielsen, Joseph Guarnaccia, and David A. Hafler. Fingolimod modulates T cell phenotype and regulatory T cell plasticity in vivo. *Journal of Autoimmunity*, 96(May 2018):40–49, 2019.

[378] Jason G Cyster and Susan R Schwab. Sphingosine-1-Phosphate and Lymphocyte Egress from Lymphoid Organs. *Annual Review of Immunology*, 30(1):69–94, 2012.

[379] Siyi Liu, Shan Liao, Lin Liang, Jun Deng, and Yanhong Zhou. The relationship between CD4+ T cell glycolysis and their functions. *Trends in Endocrinology and Metabolism*, 34(6):345–360, 2023.

[380] Atsushi Yamashita, Yasuhiro Hayashi, Naoki Matsumoto, Yoko Nemoto-Sasaki, Saori Oka, Takashi Tanikawa, and Takayuki Sugiura. Glycerophosphate/Acylglycerophosphate acyltransferases. *Biology*, 3(4):801–830, nov 2014.

[381] Lishomwa C. Ndhlovu, Fabio E. Leal, Aaron M. Hasenkrug, Aashish R. Jha, Karina I. Carvalho, Ijeoma G. Eccles-James, Fernanda R. Bruno, Raphaella G.S. Vieira, Vanessa A. York, Glen M. Chew, R. Brad Jones, Yuetsu Tanaka, Walter K. Neto, Sabri S. Sanabani, Mario A. Ostrowski, Aluisio C. Segurado, Douglas F. Nixon, and Esper G. Kallas. HTLV-1 tax specific CD8+ T cells express low levels of Tim-3 in HTLV-1 infection: Implications for progression to neurological complications. *PLoS Neglected Tropical Diseases*, 5(4), 2011.

[382] Tatsufumi Nakamura, Yoshihiro Mishiura, Katsuhiro Ichinose, Susumu Shirabe, Akira Tsujino, Hirofumi Goto, Takafumi Furuya, and Shigenobu Nagataki. Spontaneous Proliferation of and Cytokine Production by T Cells Adherent to Human Endothelial Cells in Patients with Human T-Lymphotropic Virus Type I-Associated Myelopathy. *Internal Medicine*, 35(3):195–199, 1996.

[383] John S. Tzartos, Manuel A. Friese, Matthew J. Craner, Jackie Palace, Jia Newcombe, Margaret M. Esiri, and Lars Fugger. Interleukin-17 production in central nervous system-infiltrating T cells and glial cells is associated with active disease in multiple sclerosis. *American Journal of Pathology*, 172(1):146–155, 2008.

[384] A. Francesca Setiadi, Alexander R. Abbas, Surinder Jeet, Kit Wong, Antje Bischof, Ivan Peng, James Lee, Meire Bremer, Erica L. Eggers, Jason DeVoss, Tracy Staton, Ann Herman, H. Christian von Büdingen, and Michael J. Townsend. IL-17A is associated with the breakdown of the blood-brain barrier in relapsing-remitting multiple sclerosis. *Journal of Neuroimmunology*, 332(December 2018):147–154, 2019.

[385] E. John Wherry and Makoto Kurachi. Molecular and cellular insights into T cell exhaustion. *Nature Reviews Immunology*, 15(8):486–499, 2015.

[386] Vincenzo Ciminale, Maria Hatziyanni, Barbara K. Felber, Jenifer Bear, Angelos Hatzakis, and George N. Pavlakis. Unusual CD4+CD8+ phenotype in a Greek patient diagnosed with adult T-cell leukemia positive for human T-cell leukemia virus type I (HTLV-I). *Leukemia Research*, 24(4):353–358, 2000.

[387] Shahzad Raza, Seema Naik, Venkat P. Kancharla, Fekade Tafera, and Madhumati R. Kalavar. Dual-positive (CD4+/CD8+) acute adult T-cell leukemia/lymphoma associated with complex karyotype and refractory hypercalcemia: Case report and literature review. *Case Reports in Oncology*, 3(3):489–494, 2010.

[388] Giovanna S. Brunetto, Raya Massoud, Emily C. Leibovitch, Breanna Caruso, Kory Johnson, Joan Ohayon, Kaylan Fenton, Irene Cortese, and Steven Jacobson. Digital droplet PCR (ddPCR) for the precise quantification of human T-lymphotropic virus 1 proviral loads in peripheral blood and cerebrospinal fluid of HAM/TSP patients and identification of viral mutations. *Journal of neurovirology*, 20(4):341–351, 2014.

[389] Isao Miyoshi, Ichiro Kubonishi, Shizuo Yoshimoto, Tadaatsu Akagi, Yuji Ohtsuki, Yukimasa Shiraishi, Kinya Nagata, and Yorio Hinuma. Type C virus particles in a cord T-cell line derived by co-cultivating normal human cord leukocytes and human leukaemic T cells. *Nature*, 294(5843):770–771, 1981.

[390] Muhammad Esa Seegulam and Lee Ratner. Integrase inhibitors effective against human T-cell leukemia virus type 1. *Antimicrobial agents and chemotherapy*, 55(5):2011–2017, may 2011.

[391] Michał S Barski, Jordan J Minnell, and Goedele N Maertens. Inhibition of HTLV-1 Infection by HIV-1 First- and Second-Generation Integrase Strand Transfer Inhibitors. *Frontiers in microbiology*, 10:1877, 2019.

[392] D J Hazuda, P Felock, M Witmer, A Wolfe, K Stillmock, J A Grobler, A Espeseth, L Gabryelski, W Schleif, C Blau, and M D Miller. Inhibitors of strand transfer that prevent integration and inhibit HIV-1 replication in cells. *Science (New York, N.Y.)*, 287(5453):646–650, jan 2000.

[393] Robert T Abraham and Arthur Weiss. Jurkat T cells and development of the T-cell receptor signalling paradigm. *Nature Reviews Immunology*, 4(April 2004):1–8, 2004.

[394] Takeshi Egawa and Dan R. Littman. ThPOK acts late in specification of the helper T cell lineage and suppresses Runx-mediated commitment to the cytotoxic T cell lineage. *Nature Immunology 2008 9:10*, 9(10):1131–1139, sep 2008.

[395] Bernardo Sgarbi Reis, Aneta Rogoz, Frederico Azevedo Costa-Pinto, Ichiro Taniuchi, and Daniel Mucida. Mutual expression of the transcription factors Runx3 and ThPOK regulates intestinal CD4+ T cell immunity. *Nature Immunology 2013 14:3*, 14(3):271–280, jan 2013.

[396] Shinya Sakaguchi, Matthias Hombauer, Ivan Bilic, Yoshinori Naoe, Alexandra Schebesta, Ichiro Taniuchi, and Wilfried Ellmeier. The zinc-finger protein MAZR is part of the transcription factor network that controls the CD4 versus CD8 lineage fate of double-positive thymocytes. *Nature Immunology 2010 11:5*, 11(5):442–448, apr 2010.

[397] Chen Dong. Cytokine Regulation and Function in T Cells. *Annual review of immunology*, 39:51–76, apr 2021.

[398] Jun Wang, Andreea Ioan-Facsinay, Ellen I.H. van der Voort, Tom W.J. Huizinga, and René E.M. Toes. Transient expression of FOXP3 in human activated nonregulatory CD4+ T cells. *European Journal of Immunology*, 37(1):129–138, 2007.

[399] Sarah E. Allan, Sarah Q. Crome, Natasha K. Crellin, Laura Passerini, Theodore S. Steiner, Rosa Bacchetta, Maria G. Roncarolo, and Megan K. Levings. Activation-induced FOXP3 in human T effector cells does not suppress proliferation or cytokine production. *International Immunology*, 19(4):345–354, 2007.

[400] Shawn D Blackburn, Haina Shin, W Nicholas Haining, Tao Zou, Creg J Workman, Antonio Polley, Michael R Betts, Gordon J Freeman, Dario A A Vignali, and E John Wherry. Coregulation of CD8+ T cell exhaustion by multiple inhibitory receptors during chronic viral infection. *Nature immunology*, 10(1):29–37, jan 2009.

[401] Matthias Pierer, Kathrin Rothe, Dagmar Quandt, Anett Schulz, Manuela Rossol, Roger Scholz, Christoph Baerwald, and Ulf Wagner. Association of anticytomegalovirus seropositivity with more severe joint destruction and more frequent joint surgery in rheumatoid arthritis. *Arthritis and rheumatism*, 64(6):1740–1749, jun 2012.

[402] Gerrit Brandis, Sha Cao, Douglas L. Huseby, and Diarmaid Hughes. Having your cake and eating it-staphylococcus aureus small colony variants can evolve faster growth rate without losing their antibiotic resistance. *Microbial Cell*, 4(8):275–277, 2017.

[403] T A Yednock, C Cannon, L C Fritz, F Sanchez-Madrid, L Steinman, and N Karin. Prevention of experimental autoimmune encephalomyelitis by antibodies against alpha 4 beta 1 integrin. *Nature*, 356(6364):63–66, mar 1992.

[404] C H Kim, L Rott, E J Kunkel, M C Genovese, D P Andrew, L Wu, and E C Butcher. Rules of chemokine receptor association with T cell polarization in vivo. *The Journal of clinical investigation*, 108(9):1331–1339, nov 2001.

[405] J Yamamoto, Y Adachi, Y Onoue, Y S Adachi, Y Okabe, T Itazawa, M Toyoda, T Seki, M Morohashi, K Matsushima, and T Miyawaki. Differential expression of the chemokine receptors by the Th1- and Th2-type effector populations within circulating CD4+ T cells. *Journal of leukocyte biology*, 68(4):568–574, oct 2000.

[406] Paweł Piatek, Magdalena Namiecinska, Małgorzata Domowicz, Marek Wieczorek, Sylwia Michlewska, Mariola Matysiak, Natalia Lewkowicz, Maciej Tarkowski, and Przemysław Lewkowicz. Multiple Sclerosis CD49d(+)CD154(+) As Myelin-Specific Lymphocytes Induced During Remyelination. *Cells*, 9(1), dec 2019.

[407] A Colombatti, R Doliana, M Schiappacassi, C Argentini, E Tonutti, C Feruglio, and P Sala. Age-related persistent clonal expansions of CD28(-) cells: phenotypic and molecular TCR analysis reveals both CD4(+) and CD4(+)CD8(+) cells with identical CDR3 sequences. *Clinical immunology and immunopathology*, 89(1):61–70, oct 1998.

[408] Staley A. Brod, Meghan Purvee, Deborah Benjamin, and David A. Hafler. Frequency analysis of CD4+CD8+ T cells cloned with IL-4. *Cellular Immunology*, 125(2):426–436, 1990.

[409] Scott G Kitchen, Yael D Korin, Michael D Roth, Alan Landay, and Jerome A Zack. Costimulation of Naive CD8¡sup¿+¡/sup¿ Lymphocytes Induces CD4 Expression and Allows Human Immunodeficiency Virus Type 1 Infection. *Journal of Virology*, 72(11):9054–9060, 1998.

[410] Yvonne B Sullivan, Alan L Landay, Jerome A Zack, Scott G Kitchen, and Lena Al-Harthi. Upregulation of CD4 on CD8+ T cells: CD4dimCD8bright T cells constitute an activated phenotype of CD8+ T cells. *Immunology*, 103(3):270, 2001.

[411] Daniel Mucida, Mohammad Mushtaq Husain, Sawako Muroi, Femke Van Wijk, Ryo Shinnakasu, Yoshinori Naoe, Bernardo Sgarbi Reis, Yujun Huang, Florence Lambolez, Michael Docherty, Antoine Attinger, Jr Wen Shui, Gisen Kim, Christopher J. Lena, Shinya Sakaguchi, Chizuko Miyamoto, Peng Wang, Koji Atarashi, Yunji Park, Toshinori Nakayama, Kenya Honda, Wilfried Ellmeier, Mitchell Kronenberg, Ichiro Taniuchi, and Hilde Cheroutre. Transcriptional reprogramming of mature CD4+ helper T cells generates distinct MHC class II–restricted cytotoxic T lymphocytes. *Nature Immunology 2013 14:3*, 14(3):281–289, jan 2013.

[412] Kennosuke Karube, Ryosuke Aoki, Yasuo Sugita, Shiro Yoshida, Yuko Nomura, Kay Shimizu, Yoshizo Kimura, Keiko Hashikawa, Morishige Takeshita, Junji Suzumiya, Atae Utsunomiya, Masahiro Kikuchi, and Koichi Ohshima. The relationship of FOXP3 expression and clinicopathological characteristics in adult T-cell leukemia/lymphoma. *Modern Pathology*, 21(5):617–625, 2008.

[413] Yoon Mee Yang, Da Sol Kuen, Yeonseok Chung, Hitoshi Kurose, and Sang Geon Kim. Gα12/13 signaling in metabolic diseases. *Experimental and Molecular Medicine*, 52(6):896–910, 2020.